# Regional Precipitation-Frequency Analyses for Mid-Latitude Cyclones, Mesoscale Storms with Embedded Convection, Local Storms and Tropical Storm Remnant Storm Types in the Tennessee Valley Watershed

**Prepared for:**

Tennessee Valley Authority

**Prepared by:**

Schaefer M, Barker B, Carney S, Day J, Gibson W, Martin D, Parzybok T, Taylor G

MGS Engineering Consultants, Inc.

RIVERSIDE
global science solutions

ACS Applied Climate Services

METSTAT

**Abstract:** This report provides descriptions of the methodologies employed and the findings obtained from regional precipitation-frequency analyses conducted for point precipitation for locations within the Tennessee Valley watershed. This study is Phase 1 of a three-phase program for developing precipitation-frequency relationships and scalable storm templates for watersheds in the Tennessee Valley. The ultimate goal is to conduct stochastic modeling for floods generated by the various storm types and to develop hydrologic hazard curves for dams and nuclear plants operated by the Tennessee Valley Authority (TVA).

The Tennessee Valley Study Area (TVSA) included the Tennessee Valley watershed and bordering areas in the states of Alabama, Georgia, Kentucky, Mississippi, North Carolina, South Carolina, Virginia, and West Virginia. Thirteen climatic regions were defined to assist in the regional analyses for depicting the spatial variation of precipitation maxima in the complex topographic study area.

A major component of the study was the development of precipitation data series that were comprised of precipitation maxima produced by specific storm types. This was accomplished by using meteorological criteria to identify the storm type for each rainy day in the period from 1881 through mid-2014 and using this database in assembling precipitation annual maxima data series for precipitation stations for each of four storm types. The storm types included Local Storms (LS), Mesoscale Storms with Embedded Convection (MEC), and synoptic-scale Mid-Latitude Cyclones (MLC) and Tropical Storm Remnants (TSR). There were 1,250 precipitation measurement stations and 60,096 station-years of record available for the synoptic-scale MLC and TSR storm types, 393 stations and 13,516 station-years of record for the MEC storm type, and 221 stations and 9,160 station-years of record for the LS storm type.

Separate regional precipitation-frequency analyses were conducted for precipitation annual maxima data series for key durations for each of the four storm types. The key durations were 48-hours for the synoptic scale MLC and TSR storm types, 6-hours for the mesoscale MEC storm type, and 1-hour for the LS storm type. Findings from the regional analyses provided for spatial mapping of statistical measures used to develop the point precipitation-frequency relationships. This included spatial mapping of the at-site means, regional L-moment ratio statistics L-Cv and L-Skewness, and identification of the regional probability distribution. This information provided for development of point precipitation-frequency relationships for locations throughout the TVSA. Isopluvial maps were prepared for point precipitation maxima for annual exceedance probabilities of 10-1, 10-2, 10-3, 10-4 and 10-5 for the key durations for each of the four storm types.

Equivalent Independent Record Length (EIRL) analyses were conducted for each storm type to provide a measure of the effective record length of the statistical information for the storms contained in the regional datasets. This information will be used in uncertainty analyses in Phase 3 to develop uncertainty bounds for watershed-specific precipitation-frequency relationships.

Seasonality analyses were also conducted for the four storm types that provide a probabilistic description of the likelihood for storms to occur at various times throughout the year. This information is important for stochastic modeling of floods for the four storm types.

The findings of the point precipitation-frequency analyses for the four storm types will provide a sound technical basis for development of watershed-specific precipitation-frequency relationships and for stochastic flood modeling for the various storm types.

# Contents

# List of Figures

## List of Tables

## List of Equations



## Attachments

Refer to ***Appendix A*** for a list and description of attachments

# REGIONAL PRECIPITATION-FREQUENCY ANALYSES FOR MID-LATITUDE CYCLONES, MESOSCALE STORMS WITH EMBEDDED CONVECTION, LOCAL STORMS AND TROPICAL STORM REMNANT STORM TYPES IN THE TENNESSEE VALLEY WATERSHED

## EXECUTIVE SUMMARY

This report provides descriptions of the methodologies employed and the findings obtained from regional precipitation-frequency analyses conducted for point precipitation for locations within the Tennessee Valley watershed. This study is Phase 1 of a three-phase program for developing precipitation-frequency relationships and scalable storm templates for watersheds in the Tennessee Valley. The ultimate goal is to conduct stochastic modeling for floods generated by the various storm types and to develop hydrologic hazard curves for dams and nuclear plants operated by the Tennessee Valley Authority (TVA).

The Tennessee Valley Study Area (TVSA) included the Tennessee Valley watershed and bordering areas in the states of Alabama, Georgia, Kentucky, Mississippi, North Carolina, South Carolina, Virginia, and West Virginia. Thirteen climatic regions were defined to assist in the regional analyses for depicting the spatial variation of precipitation maxima in the complex topographic study area.

A major component of the study was the development of precipitation data series that were comprised of precipitation maxima produced by specific storm types. This was accomplished by using meteorological criteria to identify the storm type for each rainy day in the period from 1881 through mid-2014 and using this database in assembling precipitation annual maxima data series for precipitation stations for each of four storm types. The storm types included Local Storms (LS), Mesoscale Storms with Embedded Convection (MEC), and synoptic-scale Mid-Latitude Cyclones (MLC) and Tropical Storm Remnants (TSR). There were 1,250 precipitation measurement stations and 60,096 station-years of record available for the synoptic-scale MLC and TSR storm types, 393 stations and 13,516 station-years of record for the MEC storm type, and 221 stations and 9,160 station-years of record for the LS storm type.

Separate regional precipitation-frequency analyses were conducted for precipitation annual maxima data series for key durations for each of the four storm types. The key durations were 48-hours for the synoptic scale MLC and TSR storm types, 6-hours for the mesoscale MEC storm type, and 1-hour for the LS storm type. Findings from the regional analyses provided for spatial mapping of statistical measures used to develop the point precipitation-frequency relationships. This included spatial mapping of the at-site means, regional L-moment ratio statistics L-Cv and L-Skewness, and identification of the regional probability distribution. This information provided for development of point precipitation-frequency relationships for locations throughout the TVSA. Isopluvial maps were prepared for point precipitation maxima for annual exceedance probabilities of $10^{-1}$, $10^{-2}$, $10^{-3}$, $10^{-4}$ and $10^{-5}$ for the key durations for each of the four storm types.

Equivalent Independent Record Length (EIRL) analyses were conducted for each storm type to provide a measure of the effective record length of the statistical information for the storms contained in the regional datasets. This information will be used in uncertainty analyses in Phase 3 to develop uncertainty bounds for watershed-specific precipitation-frequency relationships.

Seasonality analyses were also conducted for the four storm types that provide a probabilistic description of the likelihood for storms to occur at various times throughout the year. This information is important for stochastic modeling of floods for the four storm types.

The next steps in the three-phase program of study are:

- Phase 2 – Analyze historical storms and develop scalable spatial and temporal storm patterns for the four storm types; and
- Phase 3 – Develop precipitation-frequency relationships and uncertainty bounds for watersheds in the Tennessee Valley for four storm types for use in stochastic flood modeling.

The storm typing approach coupled with regional precipitation-frequency analysis is a major advancement over traditional precipitation-frequency methods. This approach provides for a direct link between watershed precipitation-frequency and the storm spatial, temporal and seasonal characteristics for each of the four storm types. This is critically important when the precipitation-frequency information is to be used for rainfall-runoff modeling for development of flood-frequency relationships.

The storm typing approach applied to the TVSA has allowed greater insight into the statistical characteristics of the various storm types. This has provided increased reliability in the precipitation-frequency relationships for the MLC, MEC and LS storm types. This occurs because the L-moment ratio statistics were found to have only minor variation across the TVSA based on very large regional datasets. In the case of the TSR storm type, the storm typing approach allowed for precipitation-frequency analysis of TSR precipitation which would not have been possible with a traditional approach. In particular, the spatial pattern and site-specific precipitation-frequency characteristics for the synoptic scale TSR storm type are quite dissimilar to the other synoptic scale MLC storm type. This is an important finding for application in modeling of floods generated by TSR events.

The findings of the point precipitation-frequency analyses for the four storm types will provide a sound technical basis for development of watershed-specific precipitation-frequency relationships and for stochastic flood modeling for the various storm types.

# 1 Purpose

This report provides a summary of the procedures employed and the findings obtained from regional precipitation-frequency analyses conducted for point precipitation for locations within the Tennessee Valley watershed. Thirteen climatic regions were defined to assist in the regional analyses for depicting the spatial variation of precipitation maxima in the complex topographic study area. A major component of the study was the development of precipitation data series that were comprised of precipitation maxima produced by specific storm types. This was accomplished by using meteorological criteria to identify the storm type for each rainy day in the period from 1881 through mid-2014 and using this database in assembling precipitation maxima for each of four storm types. The storm types included Local Storms (LSs), Mesoscale Storms with Embedded Convection (MECs), Mid-Latitude Cyclones (MLCs), and Tropical Storm Remnants (TSRs). Separate regional precipitation-frequency analyses were conducted for precipitation maxima data series for each of the four storm types.

This study is Phase 1 of a three-phase program for developing precipitation-frequency relationships and scalable storm templates for watersheds in the Tennessee Valley. The ultimate goal is to conduct stochastic modeling for floods generated by the various storm types and to develop hydrologic hazard curves for dams and nuclear plants operated by the Tennessee Valley Authority (TVA). The three phases of the program of study are:

- **Phase 1** – Develop point precipitation-frequency relationships for the Tennessee Valley watershed for four storm types
- **Phase 2** – Analyze historical storms and develop scalable spatial and temporal storm patterns for the four storm types
- **Phase 3** – Develop precipitation-frequency relationships and uncertainty bounds for watersheds in the Tennessee Valley for four storm types for use in stochastic flood modeling

***Appendix A*** contains a list of the electronic files that are included as deliverables for Phase 1. ***Appendix B*** contains a list of acronyms, and ***Appendix C*** contains a glossary of terms to assist the reader with statistical and meteorological terminology used in regional precipitation-frequency analysis and analyses of extreme precipitation.

# 2 Study Area

The study area for the regional precipitation-frequency analysis was centered on the Tennessee Valley watershed and included adjacent areas in Tennessee, southern Kentucky, western Virginia, northwestern South Carolina and North Carolina, and northern Georgia, Alabama and Mississippi. This is an area of about 138,000 $mi^2$ within the geographic rectangle from latitude 33.5°N to latitude 38.0°N and longitude 81.0°W to 89.0°W. ***Figure 1*** depicts the areal extent of the Tennessee Valley Study Area (TVSA).

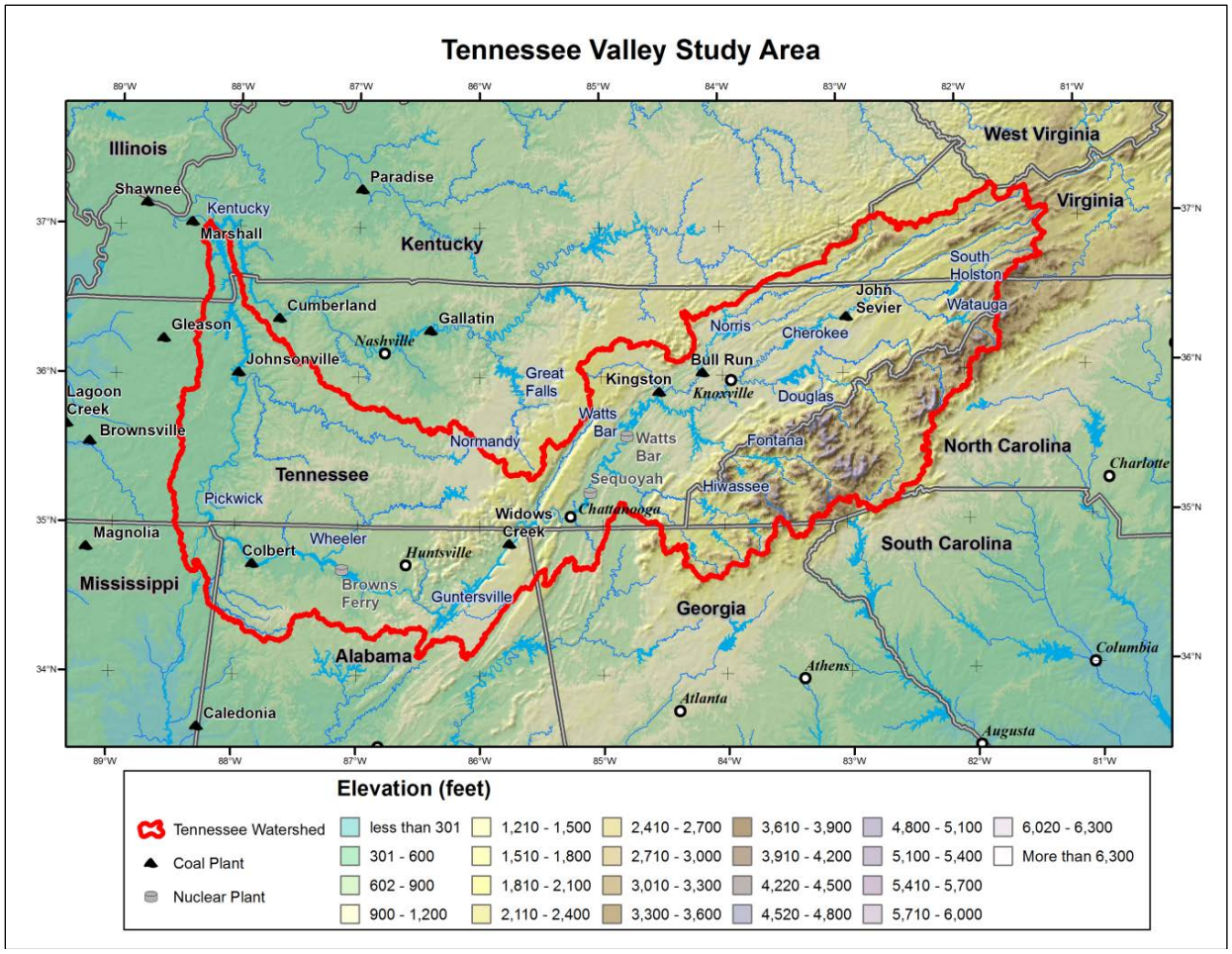


***Figure 1 - Areal Extent of the TVSA***

# 3 Storm Types of Interest

There are four storm types that impact the Tennessee Valley watershed that can produce floods with characteristics that can pose a hazard to dams and nuclear plants operated by TVA. Each of these storm types has different spatial and temporal characteristics, which in-turn produce differing flood characteristics in terms of flood peak discharge, duration and volume of runoff, and flood hydrograph shapes. TVA owns and operates dams and nuclear plants with tributary watersheds ranging in size from 60 $mi^2$ to over 30,000 $mi^2$, where one or more storm types may contribute to the flood hazard at a given project. Therefore, the precipitation-frequency relationships and spatial and temporal characteristics of each of these storm types are important considerations for a range of watershed sizes. The four storm types are described below. The Database of Daily Storm Types (DDST) developed as a part of this project lists the storm type for each rainy day in the period from 1881-2014. See ***Section*** 4 for a description of the storm typing and DDST development.

## 3.1 Mid-Latitude Cyclone (MLC)

MLCs are synoptic-scale low pressure systems with cyclonic circulation that form in the mid-latitudes. MLCs and associated frontal systems can produce precipitation for several days over very large areas. The seasonality of MLCs is depicted in ***Figure 2***, where it is seen that MLCs occur predominately in the cool season in the TVSA.

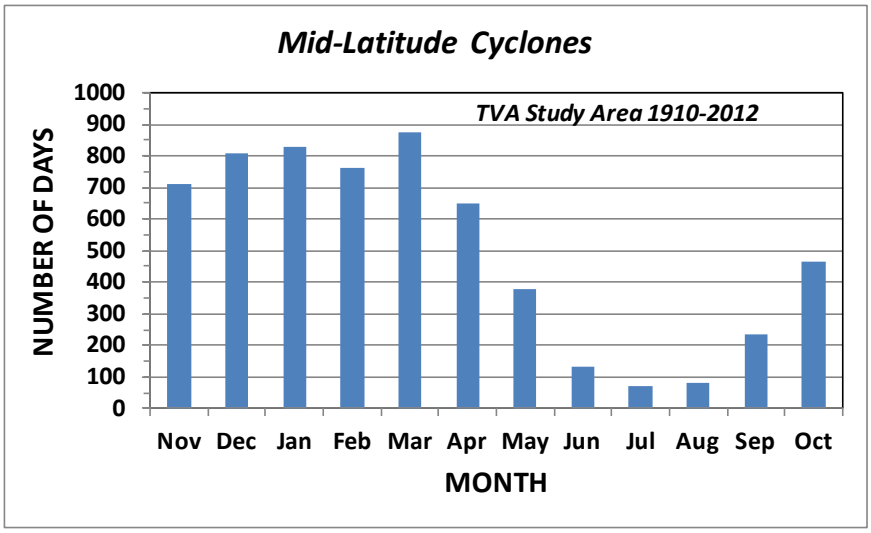


***Figure 2 - Seasonal Distribution of MLCs for 1910-2012 Period from DDST***

## 3.2 Tropical Storm Remnant (TSR)

TSR is a generic term applicable to precipitation associated with a tropical storm meteorological environment. This is a synoptic-scale storm type where precipitation is associated with an approaching or departing tropical storm or hurricane that has a storm track within roughly 200 miles of the TVSA. The number of tropical storms that affect the TVSA is highly variable from year-to-year (***Figure 3***). The seasonality of TSRs is confined to the hurricane season, June through early November, with the peak occurring in September (***Figure 4***). A review of ***Figure 2*** and ***Figure 4*** clearly shows the relatively few number of TSRs compared to the number of MLCs in a given year.

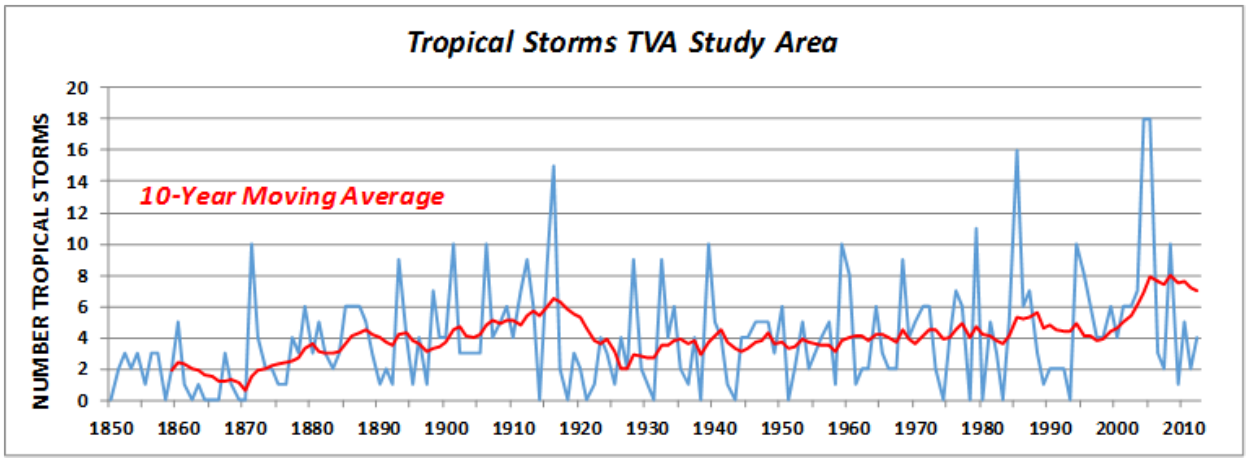


***Figure 3 - Time Series of Tropical Storms that Affected TVSA for 1910-2012 Period***

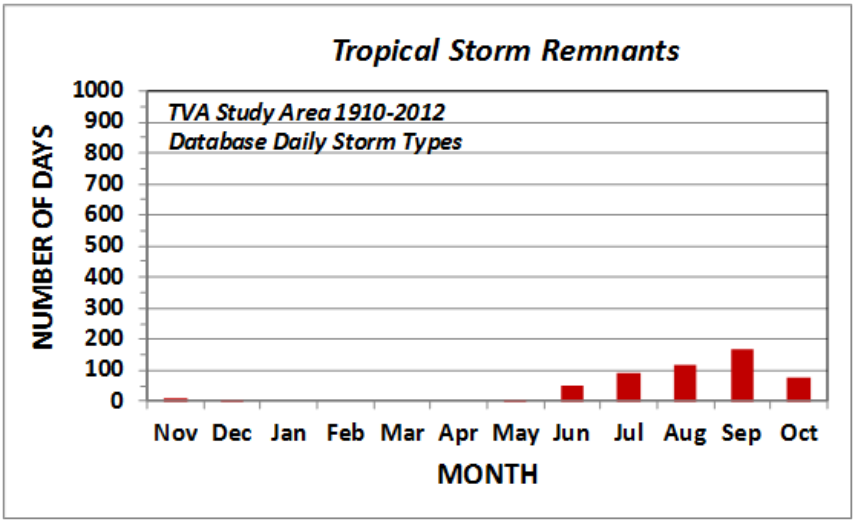


***Figure 4 - Seasonal Distribution of TSRs for 1910-2012 Period***

## 3.3 Mesoscale Storms with Embedded Convection (MEC)

MEC is a generic storm type that is intended to include Mesoscale Convective Complexes (MCCs) and other warm-season mesoscale and sub-synoptic scale storms with embedded convective cells (thunderstorms). These have storm characteristics that can cause widespread precipitation with locally high precipitation intensities that can generate high rates of runoff. This is a storm type that can produce large floods on intermediate size watersheds, generally less than about 2,000 $mi^2$. This is a warm season event occurring from April through October, with a peak storm season in July (***Figure 5***).

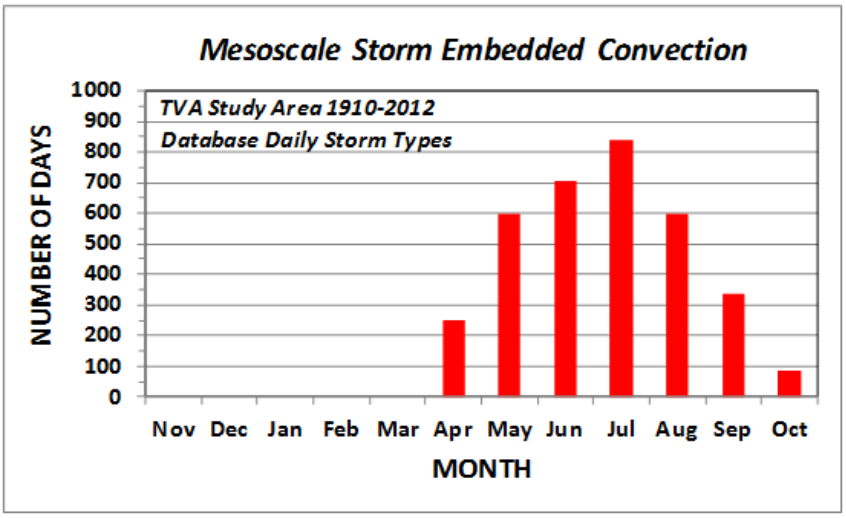


***Figure 5 - Seasonal Distribution of MECs for 1910-2012 Period from the DDST***

## 3.4 Local Storms (LS)

LS is the term given to relatively small-scale convective events (thunderstorms) which occur in the warm season in the absence of any larger scale atmospheric circulation. The areal coverage and duration of these storms are limited, typically less than a nominal 100 $mi^2$ and several hours in duration. This is a warm season event occurring from April through October, with a peak storm season in June, July and August (***Figure 6***). Comparison of the number of days of LSs (***Figure 6***) with the MLC (***Figure 2***) and MEC (***Figure 5***) storm types shows nearly double the number of days for the small-scale LSs.

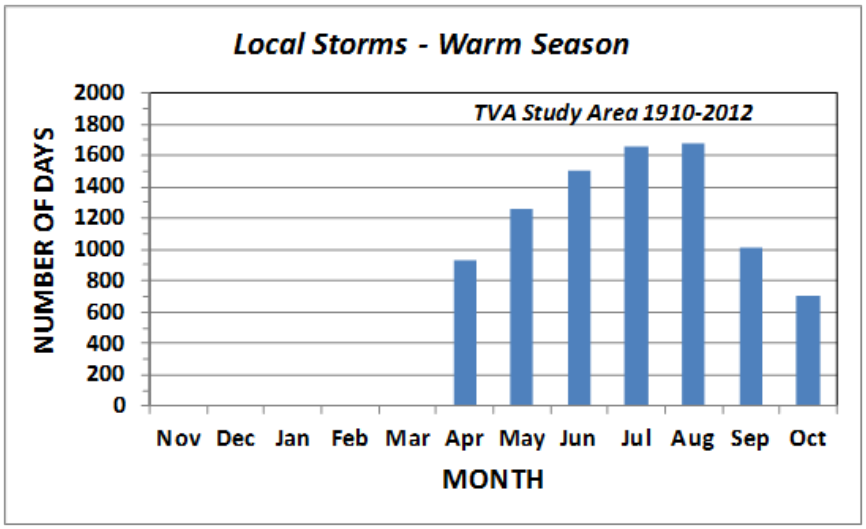


***Figure 6 - Seasonal Distribution of LSs for 1910-2012 Period from the DDST***

# 4 DDST Development

A major component of this study was the assembly of precipitation annual maxima datasets for each of the four storm types. This required a methodology for identifying the storm type that produced precipitation on a given day for a given station. The task of storm typing was accomplished by Applied Climate Services, which resulted in the creation of the DDST.

The DDST contains a listing of the storm type that is applicable for each rainy day in the period from 1881 through mid-2014. Details about development of the DDST are described in ***Appendix E***. The process of developing the DDST is summarized below.

## 4.1 Need for Automated Storm Typing

There are many thousands of rainy days in the period from 1881-2014, so it was necessary to develop automated procedures for categorizing rainy days into appropriate storm types. The methodology for creation of the DDST was accomplished in two steps. Manual methods were first used to examine the meteorological environment for over 1,100 noteworthy storm events representing all four storm types. Specifically, the all-season annual maxima databases assembled by the National Weather Service (NWS) for the National Oceanic and Atmospheric Administration (NOAA) Atlas 14 precipitation-frequency study (NWS[15]) were scanned to identify noteworthy storms at the 2-hour, 6-hour and 2-day durations. This included storms/dates where precipitation exceeded the 3-year recurrence interval at a station for the 6-hour and/or 2-day durations, and storms/dates where precipitation exceeded the 10-year recurrence interval at the 2-hour duration. These recurrence interval thresholds were chosen to obtain a reasonably large sample set of storms for local, mesoscale and synoptic-scale storms. Manual storm typing was conducted for each of the noteworthy storms, and experience gained in the manual process was used for developing criteria for automated storm typing. Automated storm typing was then conducted for the large number of rainy days that remained in the record from 1880-2014.

## 4.2 Criteria for Identification of Storm Type

Storm typing was accomplished by considering several characteristics of the precipitation and meteorological environment on a given day:

- Seasonality, time of year of storm event;
- Magnitude of areal coverage of precipitation over the study area;
- Existence of a nearby tropical storm track ;
- Magnitude of Precipitable Water (Pw); and
- Magnitude of Convective Available Potential Energy (CAPE).

These characteristics are described below.

- **Storm Seasonality** – The dates of occurrence for the 1,100 noteworthy storms included in the manual storm typing were used to establish criteria for the time of year when the various storm types are possible. The resultant seasonality for the four storm types can be seen in ***Figure 2***, ***Figure 4***, ***Figure 5***, and ***Figure 6*** for the MLC, TSR, MEC and LS storm types, respectively.

- **Areal Coverage of Precipitation** – A measure of the areal coverage of precipitation was needed to differentiate between synoptic-scale storms, mesoscale storms and local storms. This was accomplished by utilizing a network of 100 long-term, high-quality precipitation stations distributed throughout the study area. This network was given the name Century Network because of the 100 stations, and because the full network essentially came on-line over a century ago, around 1910.

  The percentage of stations active on a given day where precipitation exceeded a specified threshold was selected as the measure of storm areal coverage. The study area was divided into two zones, TVA West and TVA East, where 50 stations from the Century Network were located in each zone (***Figure 7***) to help in identifying the location and magnitude of areal coverage of the storm.

Examination of the areal coverage of precipitation for the 1,100 noteworthy storms resulted in setting the daily precipitation threshold at 0.50 inches. LSs were identified for cases where less than 20% of the stations reported daily precipitation over the 0.50-inch threshold. Conversely, mesoscale storms and synoptic-scale storms were identified when 20% or more of the active stations reported daily precipitation exceeding the 0.50-inch threshold. This measure was computed on a daily basis for both the TVA West zone and TVA East zone.

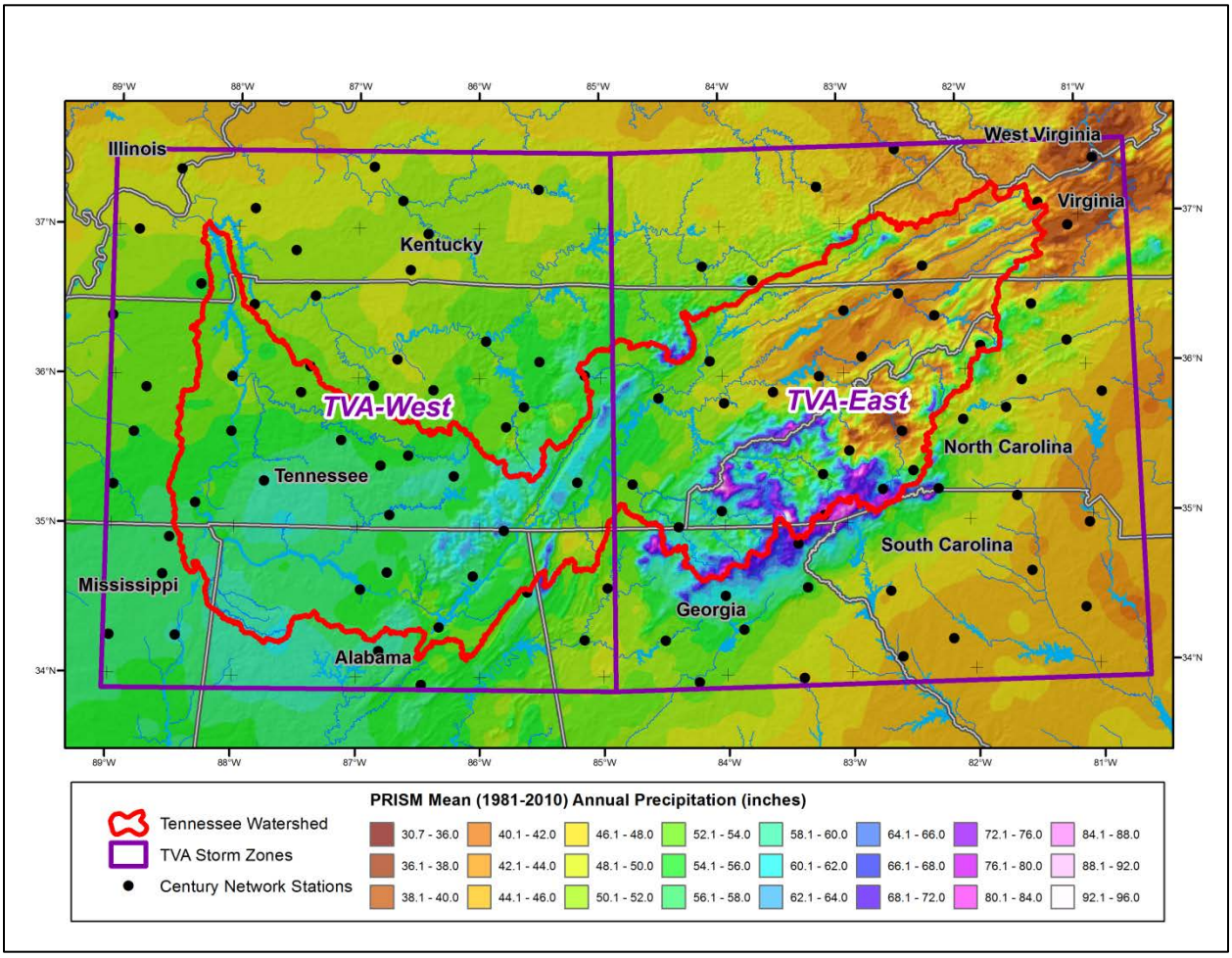


***Figure 7 - Depiction of the Century Network of 100 Daily Precipitation Stations and TVA West Zone and TVA East Zone***

- **<u>Existence of a Nearby Tropical Storm Track</u>** – Storm Typing for the rainy days associated with TSRs was accomplished using the NOAA North Atlantic tropical storm-track database (NOAA[14]) (http://www.ncdc.noaa.gov/ibtracs/). Specifically, a TSR was considered to occur when a tropical storm was in or near (within ~200 miles) of the TVSA and could have caused precipitation associated with the tropical storm meteorological environment. Based on the characteristics of several case studies across the project area, a buffer of +/- 3 days was used to capture where an approaching or departing tropical storm likely influenced the moisture driving precipitation in the TVSA.

- **<u>Precipitable Water (Pw) and Convective Potential Available Energy (CAPE)</u>** – Measures of Pw and CAPE were found to be good indicators of situations where storms contained convective cells. These measures were obtained from the NOAA-CIRES Twentieth Century Global Reanalysis Version II[14]. Applied Climate Services developed a computer tool for analysis of daily storm types.

The computer tool displayed four panels including the 500-mb and 850-mb height contour maps, Pw and CAPE maps (***Figure 8***). The timing of the Pw and CAPE measurements was for 0:00 Z (UTC) which coincides with the middle of the Century Network Day, defined as 8 AM to 8 AM local time (see description below and ***Figure 10***). Areally-average values of Pw and CAPE were computed for each day for four 2° latitude by 2° longitude grid-cells that were aligned within the TVA West and TVA East Zones (***Figure 9***). This four grid-cell format allowed further sub-division of the study area for storm typing and the corresponding AMS extraction by storm type.

Review of technical literature and examination of the Pw and CAPE measures for the 1,100 noteworthy storms provided information and data for setting storm typing criteria for Pw and CAPE. Situations where Pw exceeded 25-mm and CAPE exceeded 500 joules/kilogram were taken as indicative of conditions for convective activity associated with MEC and LS storm types. Sub-types of MLC and TSR storm types were also identified where values of Pw and CAPE exceeded the thresholds, indicative of convective activity. Storm typing was done for each of the four 2° latitude by 2° longitude grid-cells within the TVA West and TVA East Zones.

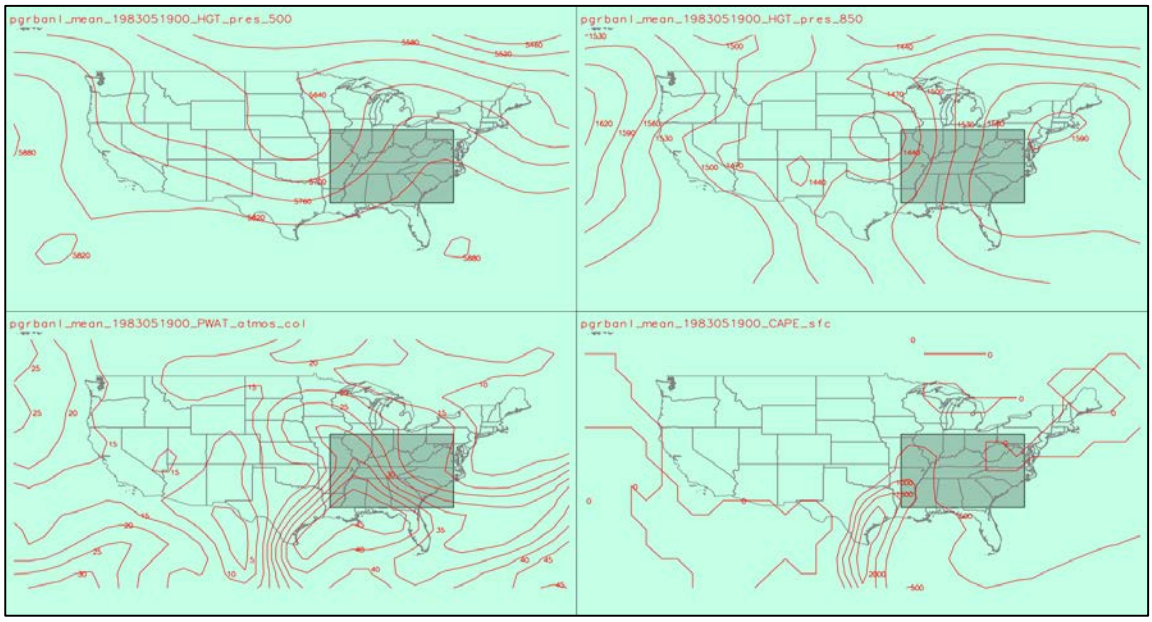


***Figure 8 - Example of Four Panel Display of 850-mb and 500-mb Contour Heights, Pw and CAPE***

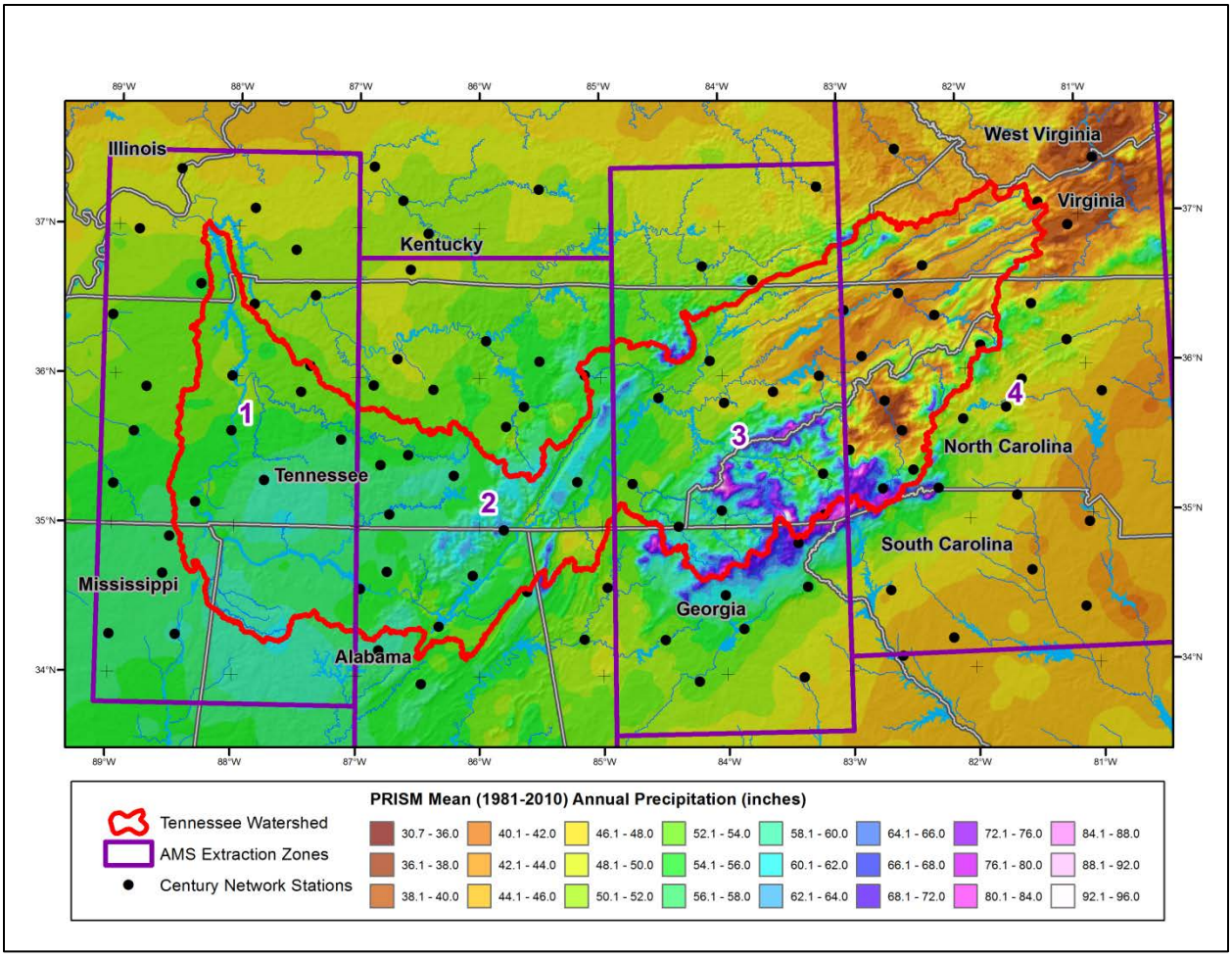


***Figure 9 - Depiction of Four Zones within the TVSA for Storm Typing***

## 4.3 DDST Example

The DDST was created by using the meteorological measures described above along with the storm typing criteria to assemble an ASCII Text database. Numerical Codes were used to designate the various storm types and sub-types as shown in ***Table 1***. Details about development of the DDST are described in ***Appendix E***).

A data field was allocated in the DDST and codes established to distinguish days which were typed by manual methods versus days that were typed by automated procedures. The following codes were used:

A – days where automated procedures were used for storm typing (Automated)
M1 – first day of date match for a 2-day noteworthy storm (Manual)
M2 – second day of date match for a 2-day noteworthy storm (Manual)
MM – part of multiple date sequence for a noteworthy storm (Manual)
MT – date match for a noteworthy Tropical Storm (Manual, Tropical)
T – storm type was set based on the NOAA tropical storm database (Tropical)

***Table 2*** depicts a sample of the DDST with numerical storm codes for the four grid-cells progressing from west to east across the TVSA. The excerpt of the DDST shows the MLC storm of May 2-3, 1984 and the MEC storm of May 7-8, 1984.

***Table 1 - Storm Types and Numerical Codes Used in Automated Storm Typing***

| STORM TYPES AND NUMERICAL CODES | | |
|---|---|---|
| **Storm Type and Sub-Type** | **Acronym** | **Numerical Code** |
| Mid-Latitude Cyclone | MLC | 10 |
| Mid-Latitude Cyclone with Embedded Convection | MLC/EC | 13 |
| Tropical Storm Remnant | TSR | 20 |
| Tropical Storm Remnant with Embedded Convection | TSR/EC | 23 |
| Mesoscale Storm with Embedded Convection | MEC | 30 |
| Mesoscale Storm without Embedded Convection | MEC/NEC | 33 |
| Local Storm | LS | 40 |
| Local Storm – cool season storm , Not of Interest | LS/NOI | 49 |
| Dry Day – No precipitation over 0.50-inch threshold reported by Century Network | DRY | 99 |

## 4.4 Timing Considerations in Application of the DDST

The long-standing system of reporting of daily precipitation created timing issues that required attention for proper application of the DDST. Specifically, the Century Network is comprised of NOAA observational-day precipitation stations reporting on a daily basis where precipitation is measured manually once per day at a fixed time. The observational time is not standard, but is typically early morning (8 AM or 9 AM) or early evening (5 PM) local time and the precipitation is for the prior 24-hour period. This situation creates ambiguity in the exact timing of precipitation both with regard to calendar dates and clock timing.

The timing of the Century Network "Day" (***Figure 10***) does not coincide with the calendar day but is set up on an 8 AM to 8 AM basis to coincide with the typical morning reporting times of the majority of daily gages in the Century Network. The timing of the Century Network Day must be considered when applying the DDST in storm typing as applied to precipitation maxima for daily, hourly and synoptic gages. Details regarding determination of the Century Network Day are addressed in ***Appendix F***.

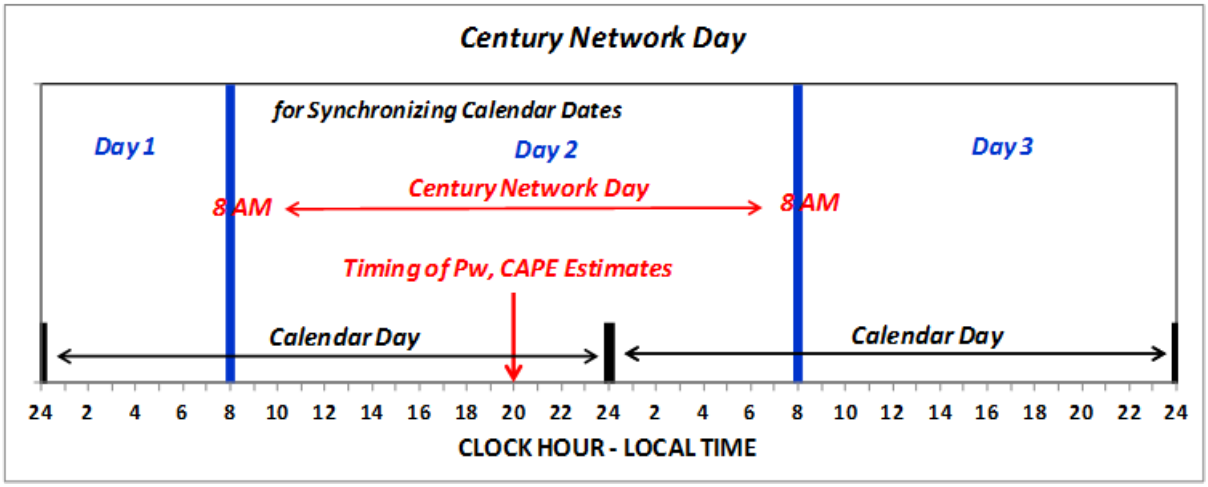


***Figure 10 - Depiction of Century Network Day for Synchronizing Timing of Precipitation Measurements from Daily, Hourly and Synoptic Gages***

***Table 2 - DDST example***

| # | CENTURY YearMoDy | NETWORK TVA-Percent Max-inch West | East | West | East | Precipitable Water (mm) Pw1 | Pw2 | Pw3 | Pw4 | Convective Energy CAPE1 | CAPE2 | CAPE3 | CAPE4 | STNC Methd Code | Genrl Envrn | AMS Extraction Zones AMS1 | AMS2 | AMS3 | AMS4 | Comments |
|---|---|---|---|---|---|---|---|---|---|---|---|---|---|---|---|---|---|---|---|---|
| 37734 | 19840424 | 0.00 | 0.00 | 0.00 | 0.00 | 16.0 | 16.5 | 15.9 | 16.0 | 45 | 37 | 39 | 60 | A | 99 | 99 | 99 | 99 | 99 | |
| 37735 | 19840425 | 0.00 | 0.00 | 0.00 | 0.00 | 19.7 | 14.8 | 11.7 | 10.9 | 0 | 3 | 11 | 11 | A | 99 | 99 | 99 | 99 | 99 | |
| 37736 | 19840426 | 0.03 | 0.00 | 0.52 | 0.00 | 23.9 | 25.3 | 23.0 | 18.3 | 96 | 34 | 9 | 7 | A | 40 | 40 | 40 | 40 | 40 | |
| 37737 | 19840427 | 0.19 | 0.14 | 2.62 | 1.25 | 30.8 | 25.4 | 25.9 | 28.5 | 357 | 252 | 420 | 483 | A | 40 | 40 | 40 | 40 | 40 | |
| 37738 | 19840428 | 0.42 | 0.14 | 3.80 | 1.45 | 38.7 | 35.1 | 30.4 | 28.4 | 1786 | 537 | 116 | 237 | A | 33 | 30 | 30 | 30 | 33 | |
| 37739 | 19840429 | 0.44 | 0.14 | 2.14 | 1.38 | 32.2 | 30.5 | 29.6 | 31.4 | 782 | 1095 | 1148 | 1055 | A | 30 | 30 | 30 | 30 | 30 | |
| 37740 | 19840430 | 0.29 | 0.05 | 2.67 | 0.85 | 43.0 | 37.6 | 31.1 | 23.7 | 50 | 12 | 10 | 9 | A | 10 | 10 | 10 | 10 | 10 | |
| 37741 | 19840501 | 0.06 | 0.07 | 1.70 | 0.94 | 9.0 | 10.1 | 14.6 | 22.3 | 0 | 0 | 4 | 83 | A | 40 | 40 | 40 | 40 | 40 | |
| 37742 | 19840502 | 0.49 | 0.14 | 2.37 | 2.01 | 24.3 | 19.4 | 14.9 | 12.5 | 0 | 0 | 0 | 0 | M1 | 10 | 10 | 10 | 10 | 10 | 2-Day |
| 37743 | 19840503 | 0.89 | 0.72 | 4.03 | 2.80 | 38.5 | 39.2 | 38.1 | 37.1 | 485 | 71 | 23 | 12 | M2 | 10 | 10 | 10 | 10 | 10 | |
| 37744 | 19840504 | 0.35 | 0.47 | 1.00 | 1.88 | 25.5 | 23.5 | 25.5 | 34.1 | 270 | 361 | 385 | 293 | A | 10 | 10 | 10 | 10 | 10 | |
| 37745 | 19840505 | 0.08 | 0.00 | 1.50 | 0.00 | 20.9 | 17.5 | 15.0 | 14.5 | 23 | 40 | 42 | 29 | A | 40 | 40 | 40 | 40 | 40 | |
| 37746 | 19840506 | 0.43 | 0.23 | 4.98 | 2.33 | 24.0 | 23.9 | 23.7 | 23.2 | 47 | 9 | 2 | 1 | A | 10 | 10 | 10 | 10 | 10 | |
| 37747 | 19840507 | 0.70 | 0.74 | 5.27 | 5.03 | 40.4 | 37.5 | 35.6 | 34.8 | 1660 | 1153 | 1013 | 960 | MM | 30 | 30 | 30 | 30 | 30 | Dup |
| 37748 | 19840508 | 0.78 | 0.70 | 4.47 | 2.75 | 42.0 | 37.6 | 34.2 | 34.6 | 946 | 1028 | 996 | 1103 | M1 | 30 | 30 | 30 | 30 | 30 | |
| 37749 | 19840509 | 0.00 | 0.02 | 0.00 | 0.85 | 13.6 | 8.4 | 5.9 | 10.8 | 0 | 0 | 0 | 14 | A | 40 | 40 | 40 | 40 | 40 | |
| 37750 | 19840510 | 0.00 | 0.00 | 0.00 | 0.00 | 10.9 | 9.8 | 11.1 | 13.4 | 0 | 4 | 16 | 44 | A | 99 | 99 | 99 | 99 | 99 | |
| 37751 | 19840511 | 0.00 | 0.00 | 0.00 | 0.00 | 21.1 | 19.5 | 15.4 | 12.5 | 11 | 0 | 0 | 0 | A | 99 | 99 | 99 | 99 | 99 | |
| 37752 | 19840512 | 0.00 | 0.00 | 0.00 | 0.00 | 27.8 | 24.0 | 21.2 | 20.5 | 273 | 101 | 21 | 2 | A | 99 | 99 | 99 | 99 | 99 | |
| 37753 | 19840513 | 0.00 | 0.00 | 0.00 | 0.00 | 31.0 | 28.4 | 26.8 | 26.8 | 281 | 205 | 238 | 240 | A | 99 | 99 | 99 | 99 | 99 | |
| 37754 | 19840514 | 0.08 | 0.00 | 0.71 | 0.00 | 42.8 | 40.5 | 37.4 | 34.5 | 1710 | 1665 | 1684 | 1584 | A | 40 | 40 | 40 | 40 | 40 | |
| 37755 | 19840515 | 0.00 | 0.00 | 0.00 | 0.00 | 11.0 | 7.5 | 7.7 | 11.5 | 0 | 0 | 0 | 1 | A | 99 | 99 | 99 | 99 | 99 | |
| 37756 | 19840516 | 0.00 | 0.00 | 0.00 | 0.00 | 13.1 | 11.8 | 10.8 | 10.2 | 0 | 0 | 0 | 3 | A | 99 | 99 | 99 | 99 | 99 | |
| 37757 | 19840517 | 0.00 | 0.00 | 0.00 | 0.00 | 11.1 | 9.3 | 8.1 | 7.5 | 0 | 0 | 0 | 0 | A | 99 | 99 | 99 | 99 | 99 | |
| 37758 | 19840518 | 0.00 | 0.00 | 0.00 | 0.00 | 14.8 | 13.8 | 13.4 | 13.7 | 0 | 0 | 0 | 0 | A | 99 | 99 | 99 | 99 | 99 | |
| 37759 | 19840519 | 0.00 | 0.00 | 0.00 | 0.00 | 17.9 | 19.0 | 19.1 | 18.8 | 1 | 4 | 1 | 0 | A | 99 | 99 | 99 | 99 | 99 | |

# 5 Precipitation Data Sources

Precipitation data were obtained from the National Climactic Data Center (NCDC) for NOAA precipitation stations and from the TVA for precipitation stations located within and near the Tennessee Valley watershed. The term “station” generically refers to a location where a variety of weather data are measured, which may include precipitation, air temperature, humidity, wind speed and direction, evaporation, and other variables. The term “precipitation gage/gauge” refers to an instrument that is used for measuring precipitation; several gage types may be present at a given station.

## 5.1 Precipitation Gages and Reporting Intervals

Precipitation data were measured by a variety of precipitation gage types and recording intervals. Precipitation is measured manually once per day at a fixed time at NOAA observational-day gages (daily gages). The observational time is not standard, but is typically early morning (8 AM or 9 AM) or early evening (5 PM) when the precipitation for the prior 24-hour period is reported. Daily gages have been operated by cooperatives since the late 1800s, and records are maintained by NCDC.

Automated precipitation gages measure precipitation on a fixed interval, with the end-of-hour time interval being the most common (hourly gages). NOAA has operated automated gages reporting on an hourly interval since approximately 1940, although electronic records are only available since 1948.

The TVA began archiving observations from automated gages throughout the Tennessee Valley in 1986 in an archive database (synoptic gages). Initially, data were archived on a 6-hour interval. The reporting interval was reduced to 1-hour in 2007, and all TVA synoptic gages are now recorded on an hourly interval. ***Table 3*** lists the number of stations and station-years of record for the various gage types.

***Table 4*** lists the number of stations and station-years of record, where co-located gages and gages for nearby locations were removed to avoid double-counting. Additional information on the number of stations and data used in analyses of the four storm types will be presented in the discussion of the findings for each storm type. ***Figure 11*** depicts the locations of the daily, hourly and synoptic gages available for the precipitation-frequency analyses.

***Table 3 - Number of Stations/Gages and Station-Years of Record for Stations/Gages with 15 or More Years of Record***

| PRECIPITATION GAGE TYPE | NUMBER OF STATIONS/GAGES | STATION-YEARS OF RECORD |
|---|---|---|
| NOAA Daily Gages | 857 | 46,580 |
| NOAA Hourly Gages | 221 | 9,160 |
| TVA Synoptic Gages | 172 | 4,356 |
| **TOTAL** | **1,250** | **60,096** |

***Table 4 - Number of Stations/Gages and Station-Years of Record for Stations/gages with 15 or More Years of Record Co-Located Gages and Gages from Nearby Stations Are Not Counted***

| PRECIPITATION GAGE TYPE | NUMBER OF STATIONS/GAGES | STATION-YEARS OF RECORD |
|---|---|---|
| NOAA Daily Gages | 758 | 43,040 |
| NOAA Hourly Gages | 91 | 3,713 |
| TVA Synoptic Gages | 135 | 3,433 |
| **TOTAL** | **984** | **50,186** |

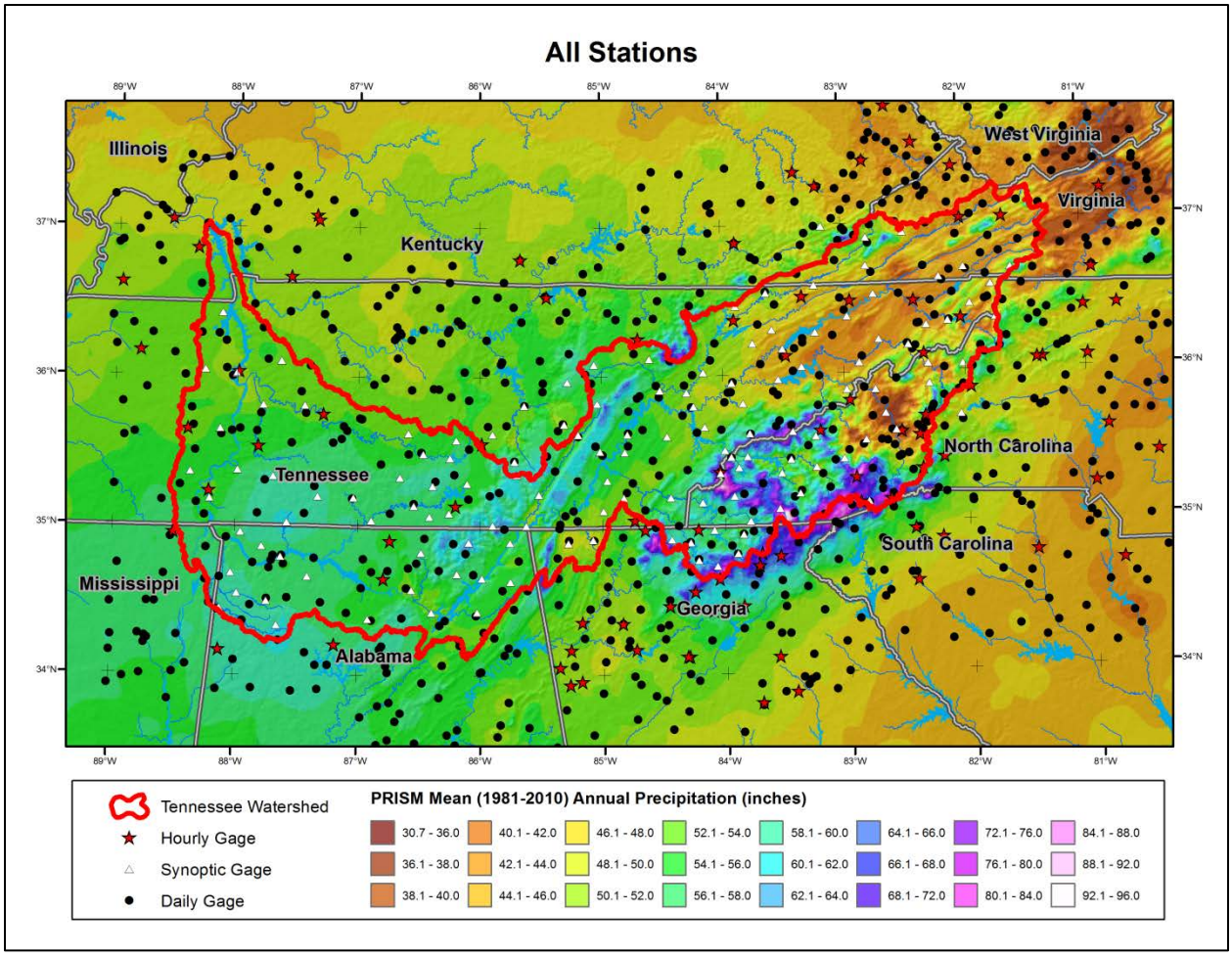


***Figure 11 - Location of Precipitation Stations with Daily, Hourly and Synoptic Gages in TVSA***

## 5.2 Key Durations for Storm Types

The temporal characteristics of the various storm types are such that a key duration can be identified that is representative of the time during which the majority of precipitation typically occurs. Synoptic-scale storms such as MLCs and TSRs are characterized by long-duration low to moderate-intensity precipitation, which can accumulate to large totals over one or more days. The key duration for these synoptic-scale storms is 48 hours (***Table 5***) where daily, hourly and synoptic gages are suitable for measurement of precipitation for these storm types.

The MEC-type storms typically occur in the afternoon through late evening, have a short life-cycle and are characterized by precipitation with moderate to high intensities over several hours. The key duration for MEC-type storms is 6 hours, where hourly and synoptic gages are suitable for measurement of precipitation for the MEC storm type.

The Local Storm, as the name implies, is more localized in areal coverage and is characterized by short-duration, high-intensity precipitation. The key duration for LSs is 1 hour, where only gages reporting on an hourly or shorter interval are suitable for measurement of precipitation for the LS storm type.

Additional durations (***Table 5***) were also analyzed for each of the four storm types to augment the analyses for the key durations and to provide additional temporal information.

***Table 5 - Key Durations used in Regional Precipitation-Frequency Analyses for Four Storm Types Listing of Additional Durations for Regional Precipitation-Frequency Analyses***

| STORM TYPE | KEY DURATION (Hours) | ADDITIONAL DURATIONS ANALYZED (Hours) |
|---|---|---|
| MLC | 48 | 24, 72 |
| TSR | 48 | 24, 72 |
| MEC | 6 | 2, 12 |
| LS | 1 | 2 |

## 5.3 Assembly of Precipitation Annual Maxima for the Four Storm Types

Separate precipitation annual maxima datasets were assembled for each of the four storm types and each of the durations of interest (***Table 5***). In this context, the term "annual maxima" refers to one precipitation maxima being selected for each precipitation gage/storm type/duration for each "climatic year" where the climatic year begins on November 1st and extends through October 31st. This seasonal timing was selected to have the start-end of the climatic-year occur at a time that is relatively dormant for the four storm types. A review of the seasonality for the four storm types (***Figure 2***, ***Figure 4***, ***Figure 5***, and ***Figure 6***) indicates the November 1st date is a practical choice for the start of the climatic year for the four storm types. It should be noted that while the terminology indicates annual maxima, three of the four storm types have limited seasonality that does not extend to a full 12-month annual period.

All precipitation annual maxima datasets are stored in the L-RAP[13] ASCII Text format and are provided as deliverables for this project.

### 5.3.1 Data Quality Checking

Extensive data quality checking was conducted to eliminate false annual maxima associated with a variety of data measurement and reporting issues/errors. In particular, incomplete reporting (missing data) and accumulations over multiple days are commonly encountered in precipitation records. Data quality-checking was accomplished by examining the completeness of the record during each climatic year and scanning records to locate anomalously small or large precipitation amounts. Data quality-checking software previously developed by MGS Engineering Consultants[18] was used to identify and then accept or reject candidate precipitation annual maxima for years where data were missing for days, weeks or months. A measure of discordancy (Hosking and Wallis[10]) was also used to identify stations whose sample statistics were markedly different from the other stations in a given climatic region. Suspicious data and stations were examined to validate the record. In general, about 3-4% of the candidate annual maxima were rejected and not included in the analyses, primarily because of missing records during the climatic year.

The largest annual maxima in the datasets for each storm type were validated by MetStat by corroboration with the precipitation amounts and timing from nearby stations. In some cases, the original Observation Forms at daily gages were examined to provide additional information for corroboration of large annual maxima. Changes made to the precipitation annual maxima datasets to address data quality are documented either in MetStat records or in the L-RAP databases.

### 5.3.2 Procedures for Assembling Precipitation Annual Maxima Datasets

A number of procedures were required for assembly of precipitation annual maxima datasets for the four storm types. These procedures were required to properly apply the DDST and address timing issues associated with the Century Network (***Figure 10***) for the four storm types.

- **Daily Gages** – Precipitation data from daily gages are applicable to the 24-hour, 48-hour and 72-hour durations for MLC and TSR storm types. Precipitation annual maxima for daily gages for these two storm types were identified in two steps. First, each day in the daily time series at a given daily gage was marked with the applicable storm type from the DDST. Next, the precipitation maximum for each climatic year was determined from those days marked with the storm type of interest.

  In the case of the 48-hour duration, each 2-day window was examined and precipitation for the given 2-day period was considered as a candidate annual maxima if either one, or both days, had

the storm type of interest. For the 72-hour duration, each 3-day window was examined and precipitation for a given 3-day period was considered as a candidate annual maxima if either two, or all three days, was marked with the storm type of interest.

- **Hourly Gages** – Precipitation data from hourly gages are applicable to all durations for all four storm types. Precipitation annual maxima for hourly gages were determined in a manner similar to that for daily gages. First, each hourly precipitation value in the hourly time series at a given hourly gage was marked with the applicable storm type with consideration given to the date and timing characteristics of the Century Network (***Figure 10***). Candidate precipitation maxima for a given climatic year were computed if 50% or more of the hours in the duration of interest were marked with the storm type of interest. Next, the precipitation annual maximum for each climatic year was determined from the candidate annual maxima.

- **TVA Synoptic Gages** – Precipitation data from TVA synoptic gages reporting on 6-hour intervals are applicable to all durations for MECs and for MLCs. The record length (1986-2014) for synoptic gages was insufficient for use with the TSR storm type because of the many years without a TSR and other years where TSR precipitation was quite small.

  Precipitation annual maxima for synoptic gages were determined in a manner similar to that for hourly gages with some additional procedures to address the 6-hour reporting interval. First, each hour in the 6-hour time series at a given precipitation gage was marked with the applicable storm type with consideration to the date and timing characteristics of the Century Network. Second, the precipitation for each 6-hour period was disaggregated equally into 1-hour values. This was done to accommodate the situation where the Century Network Day splits the second 6-hour interval in a calendar day. Candidate precipitation maxima for a given climatic year were computed if 50% or more of the hours in the duration of interest were marked with the storm type of interest. Next, the precipitation annual maximum for each climatic year was determined from the candidate annual maxima.

  Data reporting for synoptic gages was on 6-hour intervals from 1986 through 2006 and switched to hourly reporting in 2007. Procedures were implemented for computing precipitation annual maxima for the hourly reporting intervals for 2007-2014 to provide compatibility with the prior 6-hour reporting interval. Specifically, precipitation annual maxima for the 2007-2014 period were computed using the same procedures as for the hourly reporting interval as described above. An observational period adjustment (Weiss[28]) was then used to provide compatibility with the 6-hour reporting interval (***Table 6***; see discussion below).

***Table 6 - Observational Period Adjustment to Be Applied to 6-Hour Precipitation Maxima Obtained from 1-Hour Interval Reporting To Be Compatible with 6-Hour Precipitation Maxima Obtained from 6-Hour Interval Reporting***

| Observational Period Adjustments for Synoptic Gages for Years 2007-2014 | | | | | | |
|---|---|---|---|---|---|---|
| Duration (Hours) | | | | | | |
| 1 | 2 | 6 | 12 | 24 | 48 | 72 |
| n/a | n/a | 0.894 | 0.962 | 0.980 | 1.000 | 1.000 |

- **Identification of Duplicate Gages** – "Duplicate" gage is the term given to the situation where two or more gages are either co-located at a given site or closely located and have overlapping years of record. Closely located gages are considered to be gages within 5 miles of each other and within a few hundred feet of elevation. All duplicate gages are marked and documented in the L-RAP databases and are not considered in regional frequency analysis to avoid double-counting.

- **Merging of Data from Nearby Gages** – It is common for precipitation gages to be moved short distances from time to time, primarily to accommodate a change in operators/observers and to provide for a continuous long-term record. Some precipitation annual maxima datasets were formed using data from two or more gages when short distance changes in location were made. Gages less than 5 miles apart, within a few hundred feet of elevation, and having segments of non-

overlapping records were considered in merging of data. All gages involved in a data merge were marked and documented in the L-RAP databases.

- **Observational Period Adjustments** – Precipitation annual maxima for continuous durations are desired for regional precipitation-frequency analysis. This can be visualized as having continuous precipitation measurements and sliding a window of time for the desired duration through the continuous data to determine the precipitation maximum for the climatic year. However, precipitation is reported on fixed time intervals and not on a continuous basis. For example, at a daily gage where measurements are taken each day at 8 AM, it is easy to visualize situations where part of a continuous 24-hour precipitation event is reported on day 1 and the remainder on day 2. The maximum 1-day measurement underestimates the continuous 24-hour measurement. Standard practice is to use an Observational Period Adjustment (Weiss[28], NWS[15]) to adjust the sample statistics for the mean and standard deviation from fixed interval measurements to be representative of continuous measurements (***Table 7***). ***Table 8*** lists the observational period adjustments that were applied to sample at-site mean values for various precipitation gages and durations. No adjustments are needed for dimensionless sample L-Moment ratio statistics for L-Cv, L-Skewness and L-Kurtosis.

***Table 7 - Observational Period Adjustments for Number of Observational Periods***

| OBSERVATIONAL PERIOD ADJUSTMENTS | | | | | | |
|---|---|---|---|---|---|---|
| Number of Observational Periods | | | | | | |
| **1** | **2** | **3** | **4** | **5** | **6** | **7 or More** |
| 1.13 | 1.04 | 1.03 | 1.02 | 1.01 | 1.01 | 1.000 |

***Table 8 - Observational Period Adjustments for Gage Types and Durations***

| OBSERVATIONAL PERIOD ADJUSTMENTS | | | | | | | |
|---|---|---|---|---|---|---|---|
| Duration (Hours) | | | | | | | |
| **Gage Type** | **1** | **2** | **6** | **12** | **24** | **48** | **72** |
| Daily Gage | n/a | n/a | n/a | n/a | 1.13 | 1.04 | 1.03 |
| Hourly Gage | 1.13 | 1.04 | 1.01 | 1.00 | 1.00 | 1.00 | 1.00 |
| Synoptic Gage | n/a | n/a | 1.13 | 1.04 | 1.02 | 1.00 | 1.00 |

- **Listing of Storm Type in L-RAP Databases** – The L-RAP databases include a field listing the storm type for each annual precipitation maximum. For the case of precipitation annual maxima for durations of multiple days, the storm type for each day of the multi-day event is listed. The time-of-day of the start of precipitation is also listed for precipitation annual maxima recorded at hourly gages.

# 6 Heterogenous Climatic Regions

Identification of homogeneous regions is an important element of regional analysis. Experience has shown that is easiest to identify homogeneous regions/sub-regions for precipitation-frequency analysis in complex terrain by starting with heterogeneous climatic regions (Schaefer et al[17,19,20,22]). In this context, heterogeneous climatic regions are locations/areas with similar climatic and topographic characteristics where similarities would be expected in the precipitation-frequency characteristics, although the region may not be statistically homogeneous.

.

Heterogenous climatic regions were formed primarily by considering topographic features such as contiguous mountain faces, plateaus and contiguous valley bottoms. Variation of mean annual precipitation was also used in the western portion of the TVSA to differentiate climatically wetter versus drier locations in areas of lower topographic relief. The heterogeneous climatic regions used in the regional precipitation-frequency analysis are depicted in ***Figure 12*** and are described below progressing from northwest to southeast across the various mountain ranges. The non-sequential region numbering reflects changes made to climatic region definition as the study progressed.

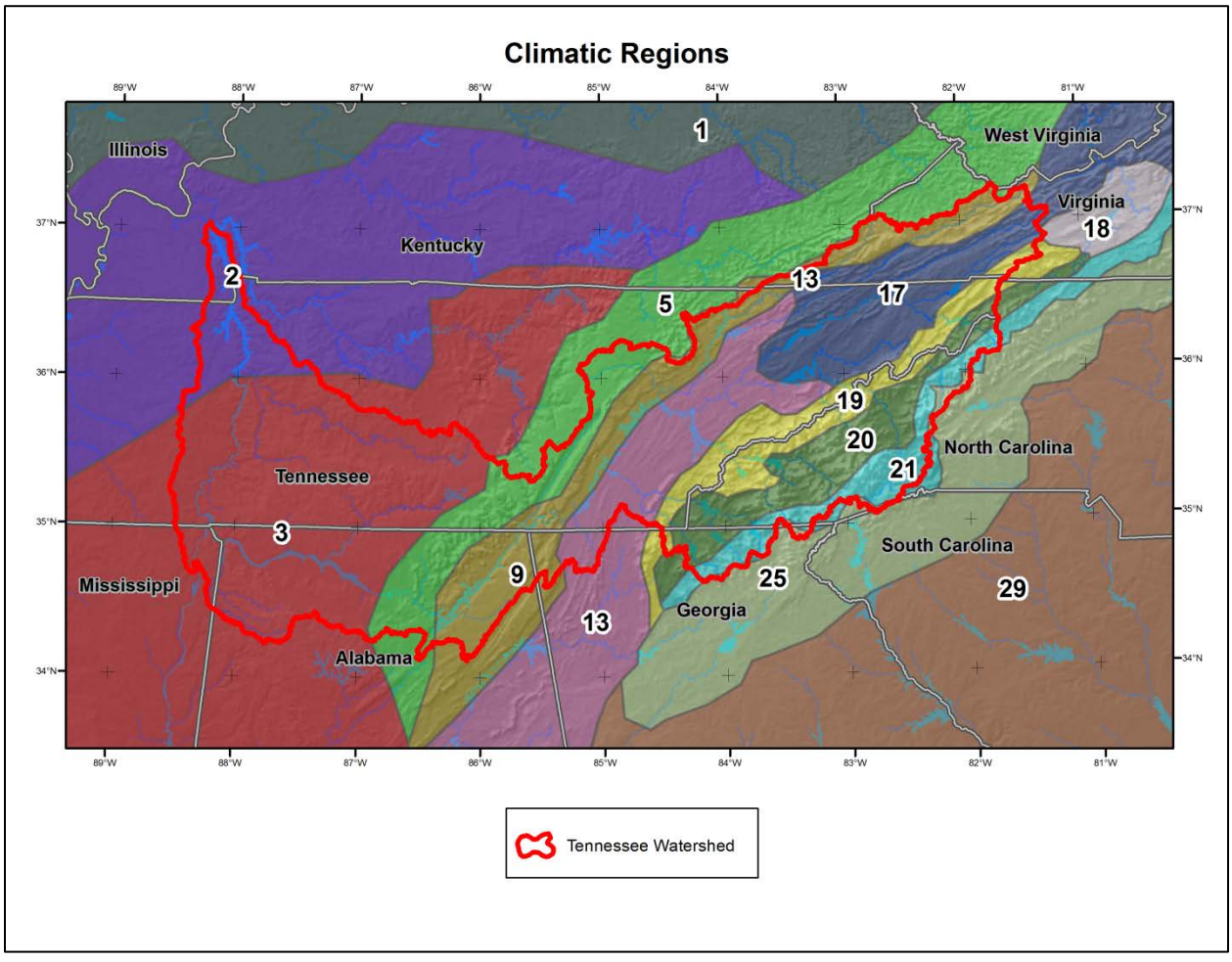


***Figure 12 - Heterogeneous Climatic Regions for TVSA***

***Region 1: Low Orographic Areas in Northern Tennessee and Southern Kentucky*** - This climatic region is comprised of low orographic areas which are northwest of the Cumberland and Allegheny

Mountains. This is an area with the lowest mean annual precipitation relative to the other low orographic areas of Climatic Regions 2 and 3.

***Region 2: Low Orographic Areas of Northwestern Tennessee and Southwestern Kentucky*** - This climatic region is comprised of low orographic areas in northwestern Tennessee and southwestern Kentucky which are to the south of Climatic Region 1. This is an area of intermediate mean annual precipitation relative to Climatic Regions 1 and 3.

***Region 3: Low Orographic Areas of Southwestern Tennessee, Northern Mississippi and Northern Alabama*** - This climatic region is comprised of low orographic areas in southwestern Tennessee and northern Mississippi and Alabama. This is an area of the highest mean annual precipitation for low orographic areas relative to Climatic Regions 1 and 2.

***Region 5: Northwest Facing Slope of Cumberland and Allegheny Mountains*** - This climatic region is comprised of the northwest face of the Cumberland and Allegheny Mountains. The northwestern boundary of this region is a generalized line drawn through the base of the mountain foothills at the intersection with the low orographic areas of Climatic Regions 1, 2 and 3. The southeastern boundary with Climatic Region 9 is a generalized line drawn through the ridgeline of mean annual precipitation near the crest of the Cumberland and Allegheny Mountains.

***Region 9: Southeast Facing Slope of Cumberland and Allegheny Mountains*** - This climatic region is comprised of the southeast face of the Cumberland and Allegheny Mountains. The southeastern boundary for this region is a generalized line drawn through the base of the mountain foothills at the intersection with the lower elevation areas in the Tennessee River valley (Climatic Regions 13 and 17).

***Region 13: Southwestern Valley Bottoms of Tennessee River*** - This climatic region is comprised of the non-orographic valley bottoms along the Tennessee River in south-central Tennessee, Georgia and Alabama.

***Region 17: Northeastern Valley Bottoms of Tennessee River*** - This climatic region is comprised of undulating elongated hills and low-orographic valley bottoms along the Holston River (a tributary of the Tennessee River) which are northeast of Climatic Region 13. The boundary between Climatic Regions 13 and 17 is a generalized line separating the undulating hills of the northeastern Tennessee Valley from the more gentle topography of the southwestern Tennessee Valley.

***Region 18: Intermountain Basin Area Northeast of Tennessee Valley*** - This climatic region is comprised of an intermountain basin northeast of Climatic Region 17 and just outside the Tennessee Valley watershed. This basin area is surrounded on three sides by the Appalachian and Blue Ridge Mountains.

***Region 19: Northwest Facing Slope and Crest Area of Appalachian Mountains*** - This climatic region is comprised of orographic areas on the northwest face and crest area of the Appalachian Mountains. The valley bottoms of the Tennessee River (Climatic Regions 13 and 17) provide the boundary to the northwest. A generalized line drawn through the crest area of the Appalachian Mountains provides the boundary to the southeast with Climatic Region 20.

***Region 20: Intermountain Areas of Appalachian and Blue Ridge Mountains*** - This climatic region is comprised of intermountain and sheltered areas between the Appalachian and Blue Ridge Mountains. This region is bounded to the northwest and southeast by the generally higher mountain ridges and crests of the Appalachian and Blue Ridge Mountains, Climatic Regions 19 and 21, respectively.

***Region 21: Crest Area of Blue Ridge Mountains*** - This climatic region is comprised of areas near the crest of the Blue Ridge Mountains. This region is bounded to the southeast by the southern face of the Blue Ridge Mountains, Climatic Region 25.

***Region 25: Southeast Facing Slope of Blue Ridge Mountains*** - This climatic region is comprised of the southeast facing slope of the Blue Ridge Mountains. This region is bounded to the southeast by a generalized line marking the transition from the steeper areas of the Blue Ridge Mountains to milder slopes of the piedmont in Georgia, North Carolina and South Carolina, (Climatic Region 29).

***Region 29: Piedmont and Coastal Plains in Alabama, Georgia, South Carolina, North Carolina and Virginia*** - This climatic region is comprised of the foothills and coastal plains of Alabama, Georgia, South Carolina, North Carolina and Virginia residing to the southeast of the Blue Ridge Mountains.

# 7 Regional Analysis Methodology

Regional analysis is a methodology for analysis of datasets comprised of measurements of the same phenomenon observed at multiple sites. The primary goal in a regional analysis is to use the collective statistical information from all measurement sites to develop magnitude-frequency relationships that can be applied throughout the study area. This approach can greatly reduce sampling variability present at any specific site and increase the reliability of magnitude-frequency estimates throughout the region, particularly at ungaged sites.

In those applications where the phenomenon of interest manifests itself spatially, such as precipitation magnitudes, spatial mapping techniques are used to expand the findings from individual sites to large geographical areas.
The following sections provide an overview of the methodologies and procedures that were used to conduct the regional precipitation-frequency analyses for each of the four storm types. In addition, methodologies are presented that were used for developing the probabilistic description of the seasonality of occurrence for the four storm types. The methodology for estimating the Equivalent Independent Record Length (EIRL) of a regional datasets is also presented. This information will be used in Phase 3 for conducting uncertainty analyses and computing uncertainty bounds for watershed-specific precipitation-frequency relationships.

## 7.1 Homogeneous Regions

A cornerstone of a regional analysis is that data from sites within a homogeneous region can be pooled to improve the reliability of the magnitude-frequency estimates for all sites. The success of a regional precipitation-frequency analysis is determined by the ability to identify homogeneous regions and to spatially map the precipitation-frequency characteristics. In this study, homogeneous sub-regions were formed as collections of stations/sites within a small range of values for selected climatic and/or location indices. The climatic indices included mean annual precipitation and mean monthly precipitation for November through March and June through August (computed from the Parameter-Elevation Regression on Independent Slopes Model (PRISM)[4,5]). Longitude was used as a location index.

## 7.2 L-Moment Statistics

L-moment statistics (Hosking and Wallis[9,10]) were used extensively to conduct the regional precipitation-frequency analyses. L-Moment methodologies were used for computing sample statistics, characterizing the shapes of probability distributions and identifying a best-fit probability distribution. L-moment statistics are a significant improvement over standard product-moment statistics and are particularly well-suited for analyses of environmental data where small sample sizes are common and the data are often highly skewed.***Appendix D*** is an excerpt of the L-RAP User's Manual[13] and is included to provide additional background information on L-Moment statistics and associated discordancy, homogeneity, and goodness-of-fit measures.

L-moment sample statistics were computed to provide dimensionless measures of variability (L-Cv), skewness (L-Skewness) and kurtosis (L-Kurtosis) for the precipitation annual maxima at each station.

L-moment heterogeneity measures H1 and H2 were used to assess the homogeneity of candidate homogeneous sub-regions. An H1 value of 1.0 was originally proposed by Hosking and Wallis[10] for determining if a proposed region/sub-region was acceptably homogeneous. That criterion was based solely on statistical considerations of the sampling characteristics for L-Cv. Oftentimes, there is additional variability in L-Cv that arises from difficulties in accurate measurement and recording of data. In addition, there may be a variety of data quality control issues associated with human intervention in collecting and managing the data. Experience indicates that an H1 value of 2.0 is a reasonable choice for distinguishing between likely homogeneous and likely heterogeneous regions (L-RAP[13]). Accordingly, values of H1 and H2 less than 2.0 were used to indicate acceptable homogeneity in these analyses. Lastly, L-moment goodness-of-fit measures were used to identify the parent regional probability distribution.

## 7.3 Regional Growth Curve

Implicit in the definition of a homogeneous region is the condition that all sites can be described by one probability distribution having common distribution parameters after the site data are rescaled by their at-site mean. This formulation is termed an Index-Flood approach, originally introduced by Dalrymple[3] for use in flood-frequency analysis. Thus, all sites within a homogeneous region have a common regional magnitude-frequency curve, termed a regional growth curve (***Figure 13***), that becomes site-specific after scaling by the at-site mean of the data from the site of interest. Thus,

$$Qi(F) = \hat{\mu}_i \; q(F) \qquad \textit{(Equation 1)}$$

where: $Q_i(F)$ is the at-site inverse Cumulative Distribution Function (CDF), $\hat{\mu}_i$ is the estimate of the population at-site mean, and $q(F)$ is the regional growth curve (i.e., regional inverse CDF).

Using the regional growth curve format, L-Cv is seen to control the slope of the precipitation-frequency relationship (***Figure 14***) and L-Skewness controls the shape of the upper tail of the precipitation-frequency relationship (***Figure 15***). L-kurtosis also has an effect on the upper tail, similar to L-Skewness. These figures will be helpful in visualizing the effect of changes in the magnitude of L-Cv and L-Skewness on precipitation-frequency relationships across the TVSA.

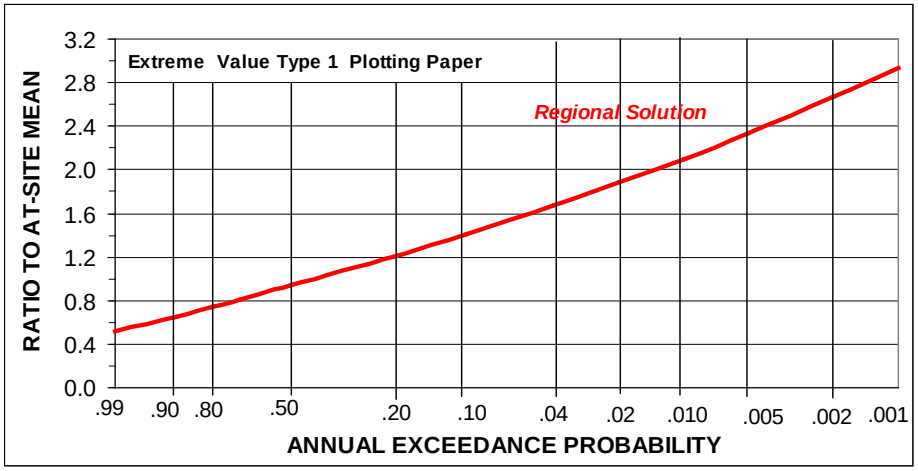


***Figure 13 - Example of a Regional Growth Curve***

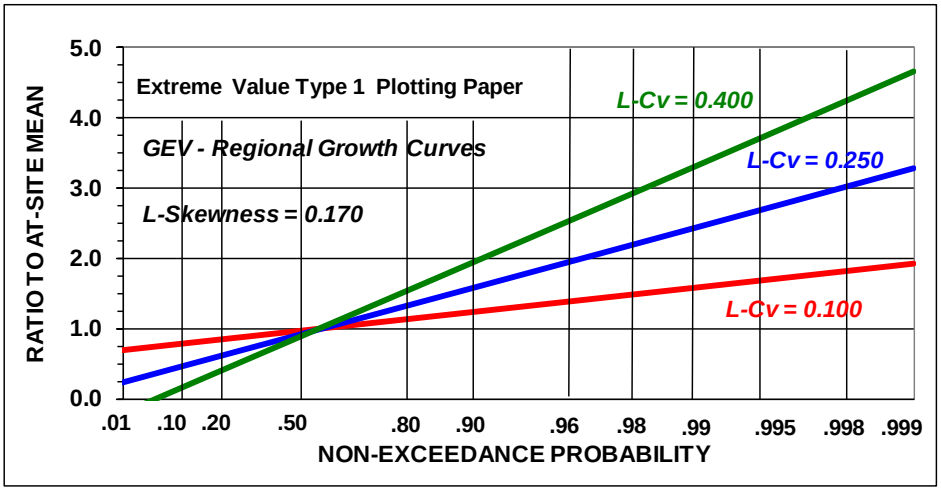


***Figure 14 - Example of Effect of Changes in L-Cv on Regional Growth Curve***

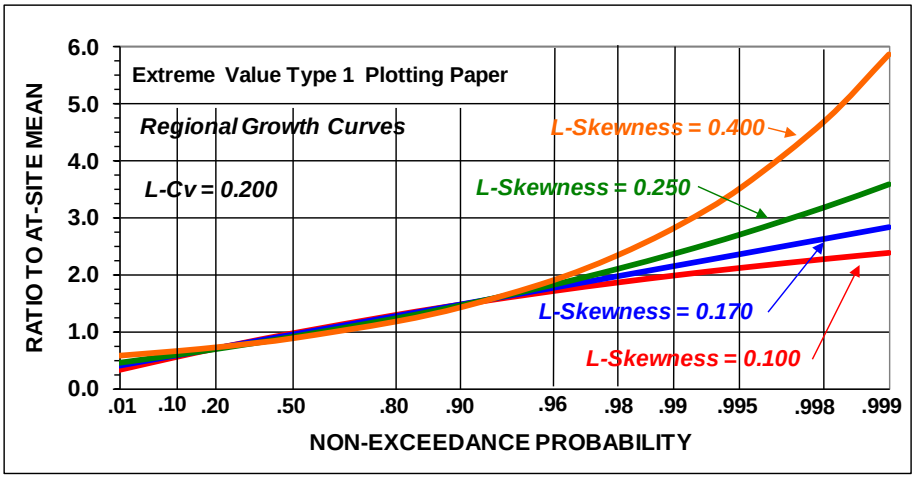


***Figure 15 - Example of Effect of Changes in L-Skewness on Regional Growth Curve***

## 7.4 Regional Probability Distribution

The L-Moment goodness-of-fit test (Hosking and Wallis[10]) was used for identifying the best-fit regional probability distribution. Experience in analysis of precipitation annual maxima for durations of several days and shorter in the United States and British Columbia (Schaefer et al[17, 19, 21, 22]) has shown the best-fit regional probability distribution to be near the Generalized Extreme Value (GEV) distribution. The 4-parameter Kappa distribution (Hosking and Wallis[10], ***Equation 2***) is a very flexible distribution capable of emulating distributions near the GEV. In particular, the 4-parameter Kappa distribution with a fixed shape parameter (*h*) has been found to provide a suitable regional probability distribution and has the added advantage of emulating alternative probability distributions, which is needed in uncertainty analyses.

Three parameter probability distributions, such as the GEV, have a fixed relationship between L-Skewness and L-Kurtosis. L-moment ratio diagrams are useful for depicting the relationship between L-Skewness and L-Kurtosis for a number of 3-parameter probability distributions (***Figure 16***). In addition, the L-moment ratio diagram provides a graphical depiction of the L-moment goodness-of-fit test by showing the nearness of regional L-Skewness and L-Kurtosis pairings to a specific 3-parameter probability distribution. ***Figure 16*** provides a graphical depiction of the L-moment goodness-of-fit test for 38 homogeneous sub-regions in the TVSA for 48-hour precipitation maxima for MLCs. The centroid of the cluster of L-Skewness and L-Kurtosis pairings is taken as the indicator of the best-estimate 3-parameter probability distribution. The scattering of data in the cluster is due to the natural sampling variability of skewness and kurtosis measures that is inherent in real-world datasets.

The quantile function for the 4-parameter Kappa distribution is:

$$q(F) = \xi + \frac{\alpha}{\kappa}\left\{1 - \left(\frac{1 - F^{h}}{h}\right)^{\kappa}\right\} \qquad \textit{(Equation 2)}$$

where: $\xi$, $\alpha$, $\kappa$, and $h$ are location, scale and two shape parameters respectively.

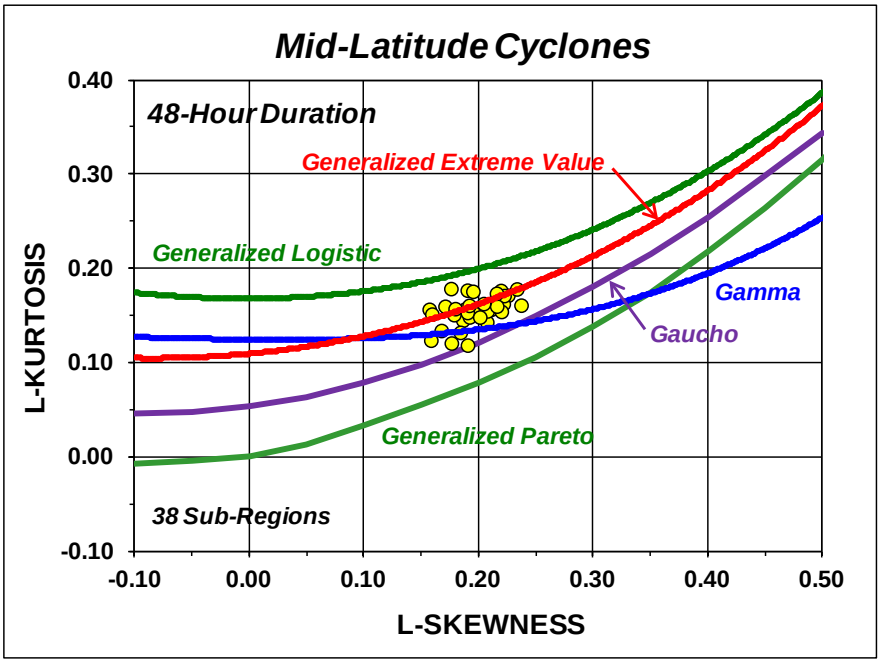


***Figure 16 - L-Moment Ratio Diagram Depicting Regional L-Skewness and L-Kurtosis Values for Homogeneous Sub-Regions for 48-Hour Precipitation Maxima for MLCs***

## 7.5 Procedures for Regional Precipitation-Frequency Analysis

The methodology employed here follows the L-moments regional analysis procedures originally developed by Hosking and Wallis[10] and modified by Schaefer et al[17, 19,20,21,22] for application in complex terrain. The methodology applied to precipitation maxima for each storm type can be summarized as follows.

**Regional Analysis Methodology for Each Storm Type and Duration*:***

1. Form a proposed homogeneous sub-region by assigning stations/gages within a climatic region or several climatic regions to groups within a small range of the climatic and/or location indices;
2. Compute L-moment sample statistics and L-moment heterogeneity measures H1 and H2 for the collection of stations/gages within the proposed homogeneous sub-region;
3. Use L-moment heterogeneity criteria to assess the heterogeneity of the proposed homogeneous sub-region and accept/reject the proposed homogeneous sub-region;
4. Repeat Steps 1-3 for all gages within the study area until homogeneous sub-regions have been identified for all locations. Record the regional L-Cv and L-Skewness values for each of the homogeneous sub-regions;
5. Conduct L-moment goodness-of-fit tests to identify a suitable probability distribution for the regional growth curve based on the collective behavior in the homogeneous sub-regions;
6. Develop a predictor equation(s) for describing the spatial behavior of at-site mean values using some combination of climatic and location indices as explanatory variables. Spatially map the at-site mean values;
7. Develop a predictor equation(s) for describing the spatial behavior of the regional values of L-Cv and L-Skewness for the collection of sub-regions using some combination of climatic and location indices. Spatially map regional L-Cv and regional L-Skewness;
8. Use the gridded values of the at-site mean, regional L-Cv, and regional L-Skewness (Steps 6-8) to solve for the distribution parameters for the regional growth curve for each grid-cell in the study area. Use ***Equation 1*** and ***Equation 2*** to compute quantile estimates for each grid-cell and create isopluvial maps for selected annual exceedance probabilities.
9. Use the datasets of precipitation annual maxima to compute an estimate of the Equivalent Independent Record Length (EIRL) for the key duration for each storm type.

10. Use the datasets of precipitation annual maxima for the key duration for each storm type to conduct a seasonality analysis to describe the seasonality of occurrence of the largest storm events for a given storm type.
11. Evaluate additional durations for each storm type to assist in characterizing the temporal storm patterns and to support the determination of the regional probability distribution for the key duration.

The following sections provide a brief summary of several of the procedures listed above. Additional details will be provided in the description of the regional precipitation-frequency analysis for each storm type.

## 7.6 Systematic Variation of L-Cv and L-Skewness across Climatic Regions

As described previously, heterogeneous climatic regions are comprised of numerous homogeneous sub-regions, where homogeneous sub-regions are comprised of a collection of stations (sites) within a small range of climatic and location indices. Each homogeneous sub-region provides an estimate of the regional values of L-Cv and L-Skewness representative of sites for the average of the climatic and location indices (weighted by record length) for the collection of stations.

Predictor equations were used to estimate the regional values of L-Cv and L-Skewness at any location and to allow for spatial mapping of L-Cv and L-Skewness throughout the study area. An example of the systematic variation of regional L-Cv with longitude for 48-hour precipitation maxima for MLCs is shown in ***Figure 17*** for 38 homogeneous sub-regions. ***Equation 3***, ***Equation 4*** and ***Equation 5*** depict examples of the type of forms of predictor equations for regional L-moment ratios, L-Cv and L-Skewness:

$$L\text{-}Cv = \alpha_0 + \alpha_1\, Longitude + \alpha_2 Longitude^2 + \alpha_3 MonthlyPrecip_{Dec\text{-}Mar} \qquad \textbf{(Equation 3)}$$

$$L3 = \alpha_4 + \alpha_5 L_2 \qquad \textbf{(Equation 4)}$$

$$L\text{-}Skewness = \alpha_6 + \alpha_7/L2 \qquad \textbf{(Equation 5)}$$

where: alpha ($\alpha_0$, $\alpha_1$, $\alpha_2$, $\alpha_3$, $\alpha_4$, $\alpha_5$, $\alpha_6$, and $\alpha_7$) are coefficients; $Longitude$ and $MonthlyPrecip_{Dec\text{-}Mar}$ are location and climatic indices, respectively; $L2$ is the second regional L-moment; and $L3$ is the third regional L-moment in the Index-Flood formulation.

It should be noted that much of the apparent scatter in the regional L-moment ratio relationships is often due to sampling variability rather than real differences in behavior. This is particularly true for measures of skewness and L-Kurtosis, which have inherently high sampling variability. Thus, very large datasets are needed to distinguish the signal (systematic trend) from the noise (sampling variability). This situation is partially addressed by using datasets with long records for computing regional L-Cv and L-Skewness. A minimum record length of 25 years was used for determining regional L-Cv, L-Skewness and L-Kurtosis for the MLC, MEC and LS storm types. A minimum record length of 36 years was used for determining regional L-moment ratios for the TSR storm type. The 36 years of record for the TSR storm type equates to 20 years of TSR values for the peaks-over-threshold approach used for TSR events.

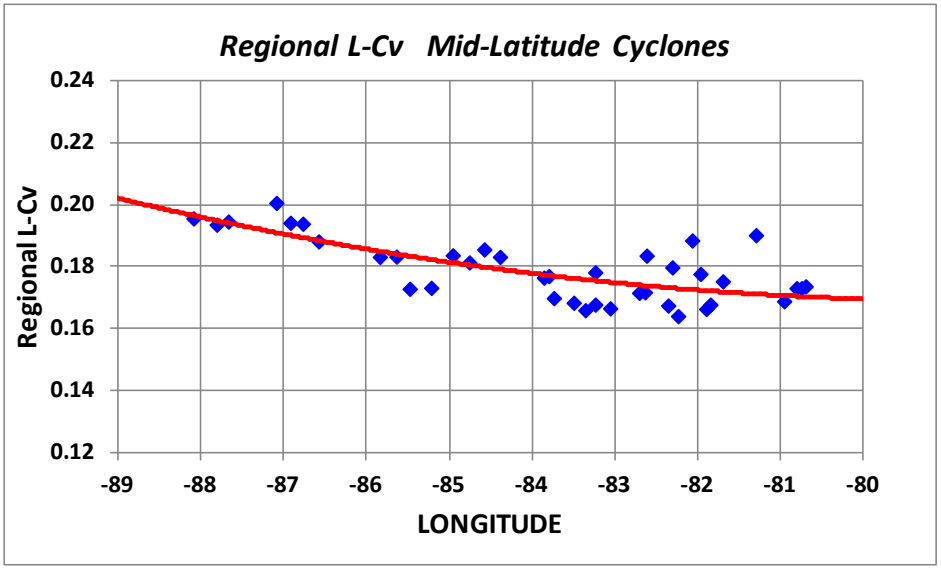


***Figure 17 - Example of Variation of Regional L-Cv with Longitude for 48-Hour MLCs***

## 7.7 Spatial Mapping of At-Site Means

Spatial mapping of at-site means for the key duration (***Table 2***) for each storm type is needed for developing isopluvial maps for selected annual exceedance probabilities and for conducting Isopercental storm analyses of historical storms. Isopercental storm analyses are used in analyzing the spatial and temporal charcaterics of historical storms, which is part of Phase 2 of the three-phase program of study.

Spatial mapping of at-site means involved a three-step process:

1. Define predictor equations for at-site means
2. Compute a weighted average of the predicted and sample at-site mean based on record length
3. Adjust the resulting at-site means to account for coherence in error residuals

Predictor equations for the at-site means are developed in a manner similar to that for regional L-Cv and regional L-Skewness as described above. For example, ***Figure 18*** depicts a scatterplot of sample estimates of 48-hour at-site means for MLCs for stations with 15 years or more of record. Review of the behavior of at-site means for selected climatic regions allowed for the grouping of at-site mean data from adjacent climatic regions to develop regression relationships for the prediction of at-site means for spatial mapping. ***Equation 6*** lists the regression relationship for MLC 48-hour at-site means ($AtSiteMean_{MLC}$) for Climatic Regions 5 and 9 in the lowlands of the Tennessee Valley watershed using both location and climatic indices as explanatory variables.

$$AtSiteMean_{MLC} = \alpha_0 + \alpha_1\, Longitude + \alpha_2 MonthlyPrecip_{Dec\text{-}Mar} \qquad \textbf{(Equation 6)}$$

The approach of using a multiple regression equation and combining of climatic regions significantly reduced the predictive error relative to that for the general relationship seen in ***Figure 18***. ***Figure 19*** depicts a comparison of predicted and observed 48-hour at-site mean values based on ***Equation 6***.

Best estimates of the 48-hour at-sites means at the stations were obtained as a weighted average of the values predicted from the regression relationship and the sample value of the station at-site mean. Greater weight was given to the sample value of the at-site mean as the record length at a station increased (Kuczera[12]). Residuals were defined as the difference between the weighted-average at-site mean and the regression-predicted at-site mean. Adjustments were then made to the predicted estimates of the at-site means to account for coherence in the spatial distribution of residuals, where the residuals in some geographic areas were not random, but rather systematically over-estimated or under-estimated the at-site mean relative to the regression prediction.

The final mapped values of the MLC 48-hour at-site means for Climatic Regions 5 and 9 are depicted in ***Figure 20***, where the root mean square error (RMSE) was 4.0% for the two climatic regions. A comparison of ***Figure 20*** with ***Figure 19*** shows a noticeable reduction in the predictive error for the mapped values of the at-site means. This is a result of accounting for both regional information (regional predictive equation) and local information (station at-site mean) and accounting for the spatial coherence of residuals. The final (mapped) values of the at-site mean are judged to be the best-estimates achievable from the collection of regional and at-site information. ***Figure 21*** depicts the final mapped value of the MLC 48-hour at-site means for the TVSA.

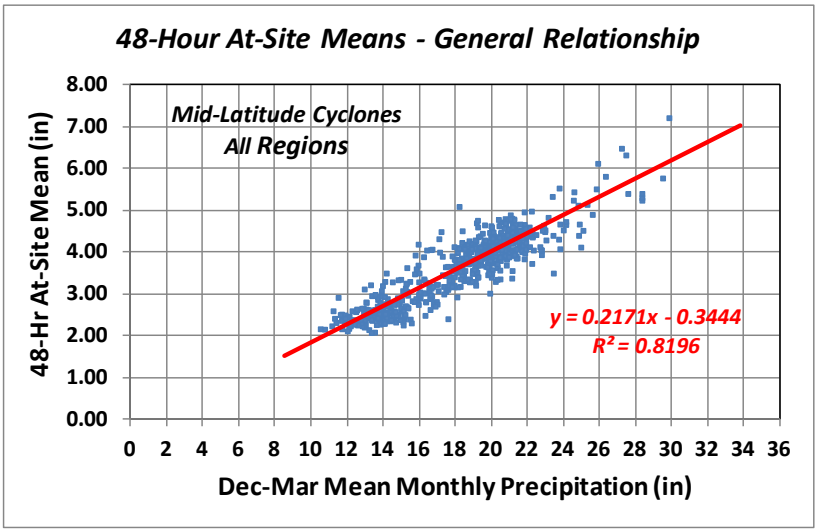


***Figure 18 - Scatterplot of Sample 48-Hour At-Site Means for MLCs for All Climatic Regions for Stations with Record lengths of 15-Years or More***

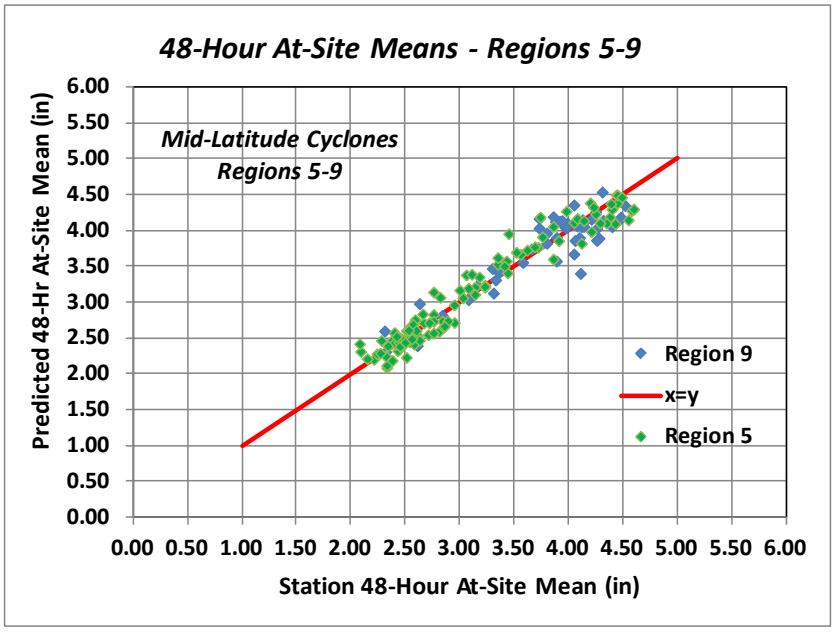


***Figure 19 - Comparison of Regression-Predicted 48-Hour At-Site Means and Sample 48-Hour At-Site Means for Climatic Regions 5 and 9 for MLCs***

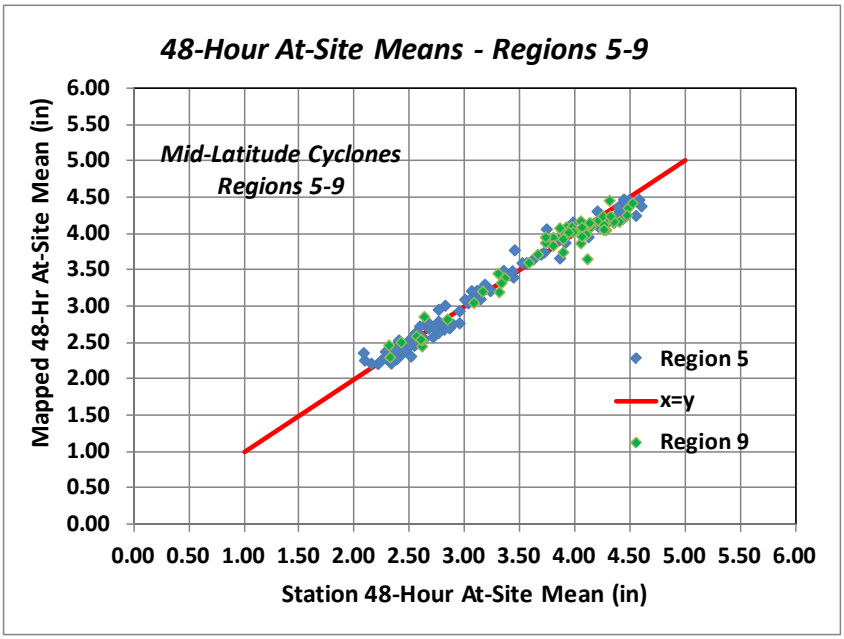


*Figure 20 - Comparison of Spatially Mapped 48-Hour At-Site Means and Sample 48-Hour At-Site Means for Climatic Regions 5 and 9 for MLCs*

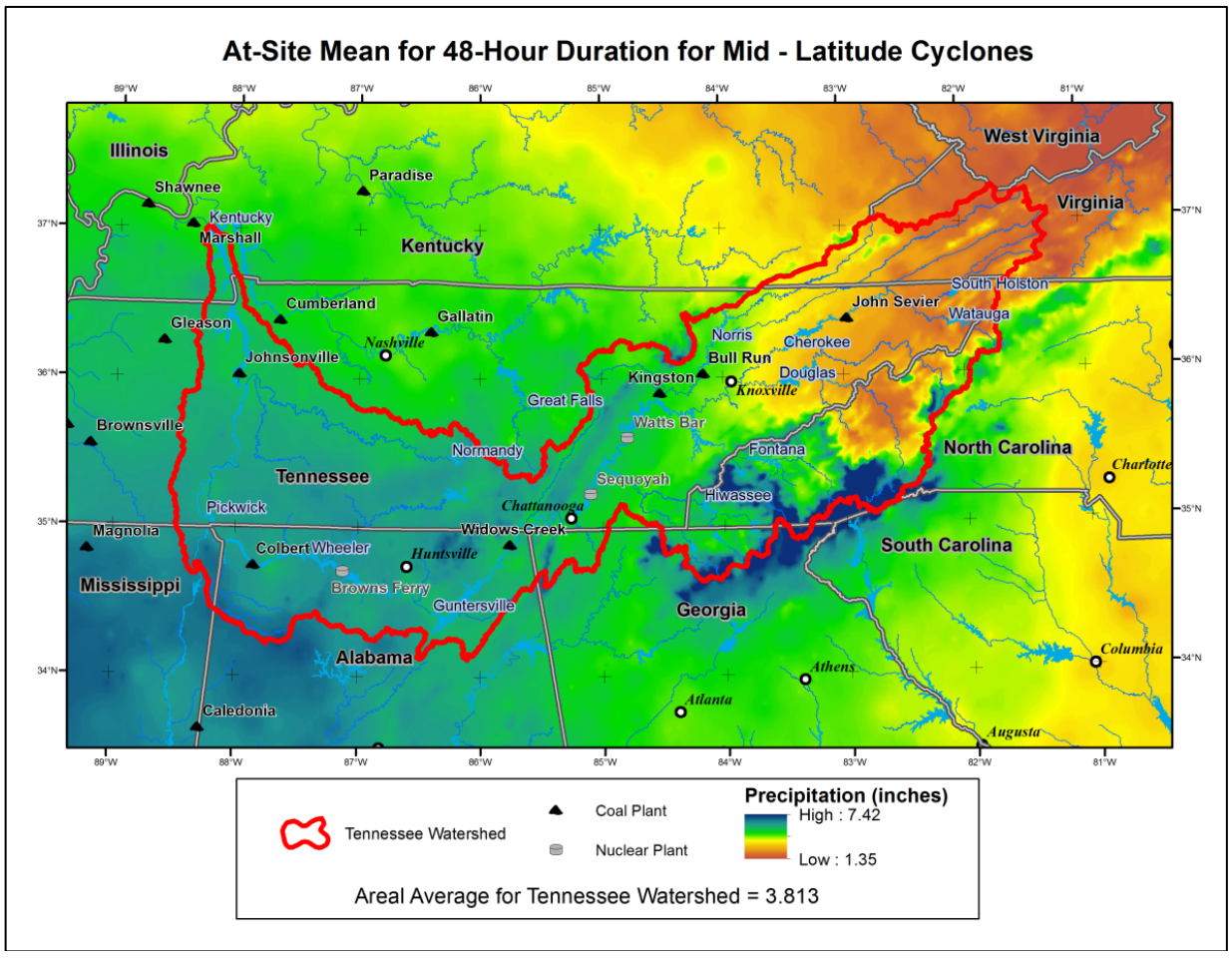


*Figure 21 - Mapping of 48-Hour At-Site Means for MLCs for TVSA*

## 7.8 Seasonality Analysis of Largest Storm Events

Information on the seasonality of occurrence of extreme storms is needed for flood modeling for the four storm types. In particular, the most extreme storms of a given storm type often have a narrower season of occurrence than the seasonality of precipitation with smaller magnitudes. Seasonality analyses have been conducted for the four storm types, and the findings are appropriate for modeling of large to extreme floods. ***Figure 22*** depicts the seasonality histogram for LSs. Details for conducting the seasonality analyses are described in ***Appendix G***, with application of the analysis to the seasonality of PMP described in a companion Technical Memorandum (Schaefer[24]). The findings of those analyses are presented later in this report for each of the four storm types.

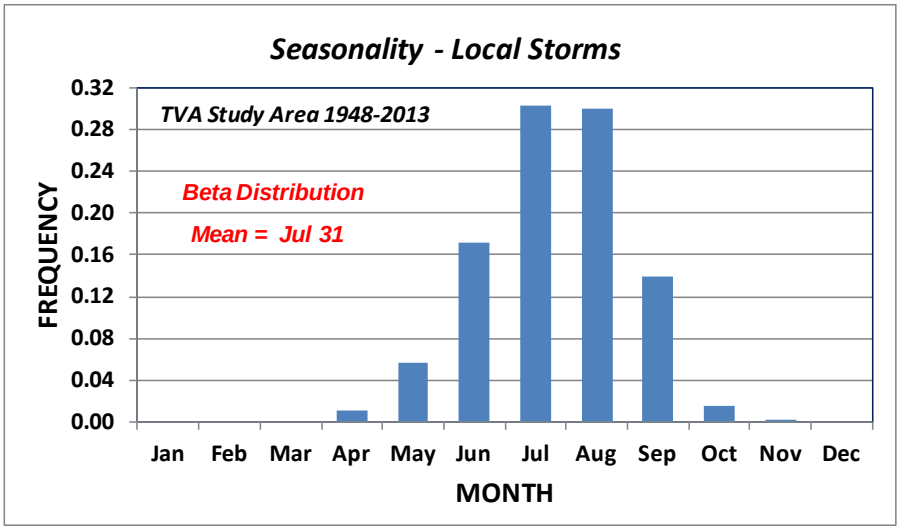


***Figure 22 - Frequency Histogram for Seasonality of 2-Hour Duration LSs***

## 7.9 Equivalent Independent Record Length (EIRL)

One of the important concepts employed in a regional precipitation-frequency analysis is the concept of trading space for time sampling. This approach takes advantage of the situation that the size of the study area is much larger than the typical storm areal coverage where precipitation annual maxima are produced. Therefore, there will be many storms in the regional dataset of storms (separate storm dates) with annual exceedance probabilities rarer than indicated by the chronological length of the sampling period. The regional dataset of precipitation annual maxima for stations therefore contains many rare storms, which are of primary interest in the precipitation-frequency analysis. In particular, the large dataset of storms can greatly reduce uncertainties in estimation of regional statistical parameters by reducing the effects of sampling variability.

EIRL is a measure of the independent information contained in a regional dataset. EIRL is a function of the size of the study area, the typical areal coverage of storms and the density of precipitation measurement stations. If the storms of interest have large areal coverage relative to the density of the station network, then the EIRL will be a small fraction of the station-years of record. This occurs because the large areal coverage of the storm would be expected to result in greater correlation (statistical dependence) amongst the gage records. Conversely, if the areal coverage of storms is small and the density of the station network is low, then the EIRL will be a large fraction of the station-years of record. The latter case is the situation for MEC and LS storm types where the cross-correlation between precipitation annual maxima at stations is low.

Two methods were used to estimate EIRL. The first method is a frequency-based method that examines the behavior of the largest 10% of storm events. ***Figure 23*** is a graphical depiction of EIRL for TSRs, where an EIRL of 1,250 years is consistent with the behavior of the number of exceedances of a given Annual

Exceedance Probability (AEP) for an independent sample size of 1,250 for 48-hour precipitation maxima. Similarly, ***Figure 24*** is a graphical depiction of EIRL for LSs with an estimated EIRL of 7,300 years for 2-hour precipitation maxima.

The second method relies on simple counting of independent storm dates for all storm events. This is accomplished using criteria for the required elapsed time between storm events and the minimum distance between stations on a given storm date for MEC and LS storm types. Both methods are described in detail in ***Appendix H***.

***Table 9*** lists the results of the EIRL analyses for the four storm types. A review of ***Table 9*** shows the percentage of EIRL relative to the station-years of record increases for Mesoscale and LS types as the areal coverage of the storms continue to decrease in size relative to the size of the study area. There are merits to both measures of EIRL, and it is reasonable to adopt a measure of EIRL that utilizes estimates from both the frequency-based and storm counting methods. A geometric mean of EIRL was computed (***Table 9***), which considers both methods to have equal merit in estimating EIRL.

The information in ***Table 9*** will be used in the uncertainty analyses for computing watershed-average precipitation-frequency relationships in Phase 3 of this project.

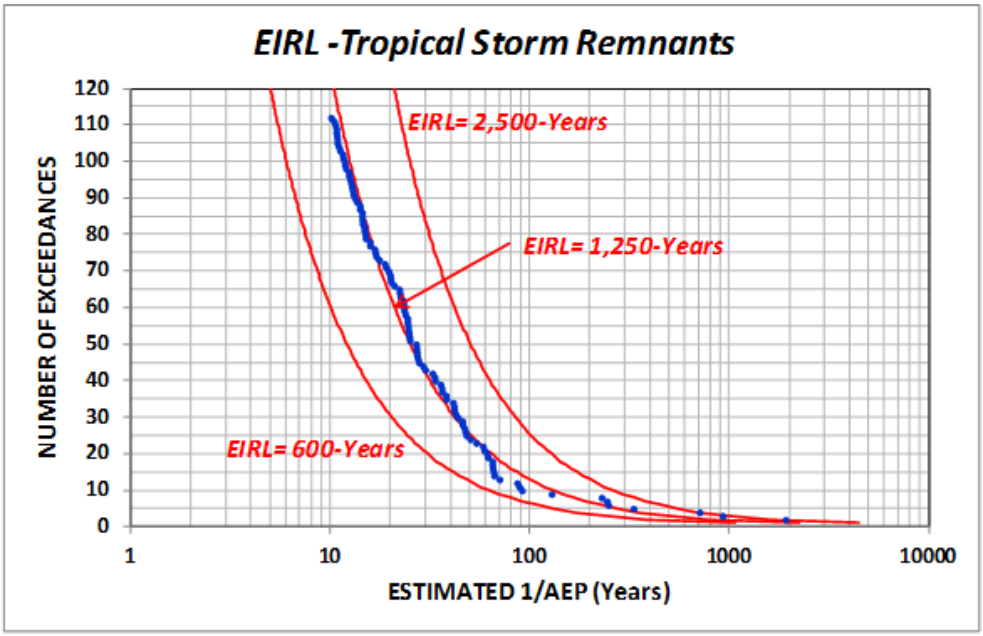


***Figure 23 - Graphical Depiction of EIRL for 48-Hour Duration TSRs for the TVSA***

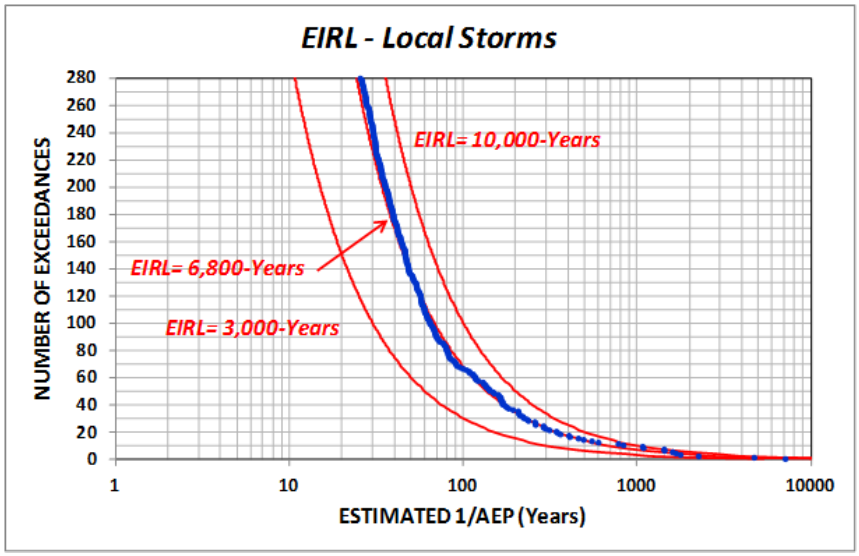


*Figure 24 - Graphical Depiction of EIRL for 2-Hour Duration for LSs for the TVSA*

*Table 9 - Estimates of EIRL for Four Storm Types*

| Storm Type | Station-Years of Record | EIRL Estimates (Years) | | | EIRL Percent of Station-Years |
|---|---|---|---|---|---|
| | | Frequency Based | Storm Count | Geometric Mean | |
| MLC | 50,281 | 5,700 | 2,760 | 3,970 | 7.9% |
| TSR | 25,862 | 1,250 | 675 | 925 | 3.6% |
| MEC | 13,611 | 5,800 | 2,690 | 3,950 | 29.0% |
| LS | 9,154 | 7,300 | 4,592 | 5,790 | 63.2% |

# 8 Mid-Latitude Cyclones - Point Precipitation-Frequency

Daily, hourly and synoptic gages were used in the regional analyses for 48-hr precipitation annual maxima for MLCs where stations with 15 years or more of record were included in the analyses (***Figure 25***). ***Table 10*** provides a listing of the number of gages and total years of record used in the analysis of MLCs, and ***Figure 26*** depicts a histogram of the number of years of record.

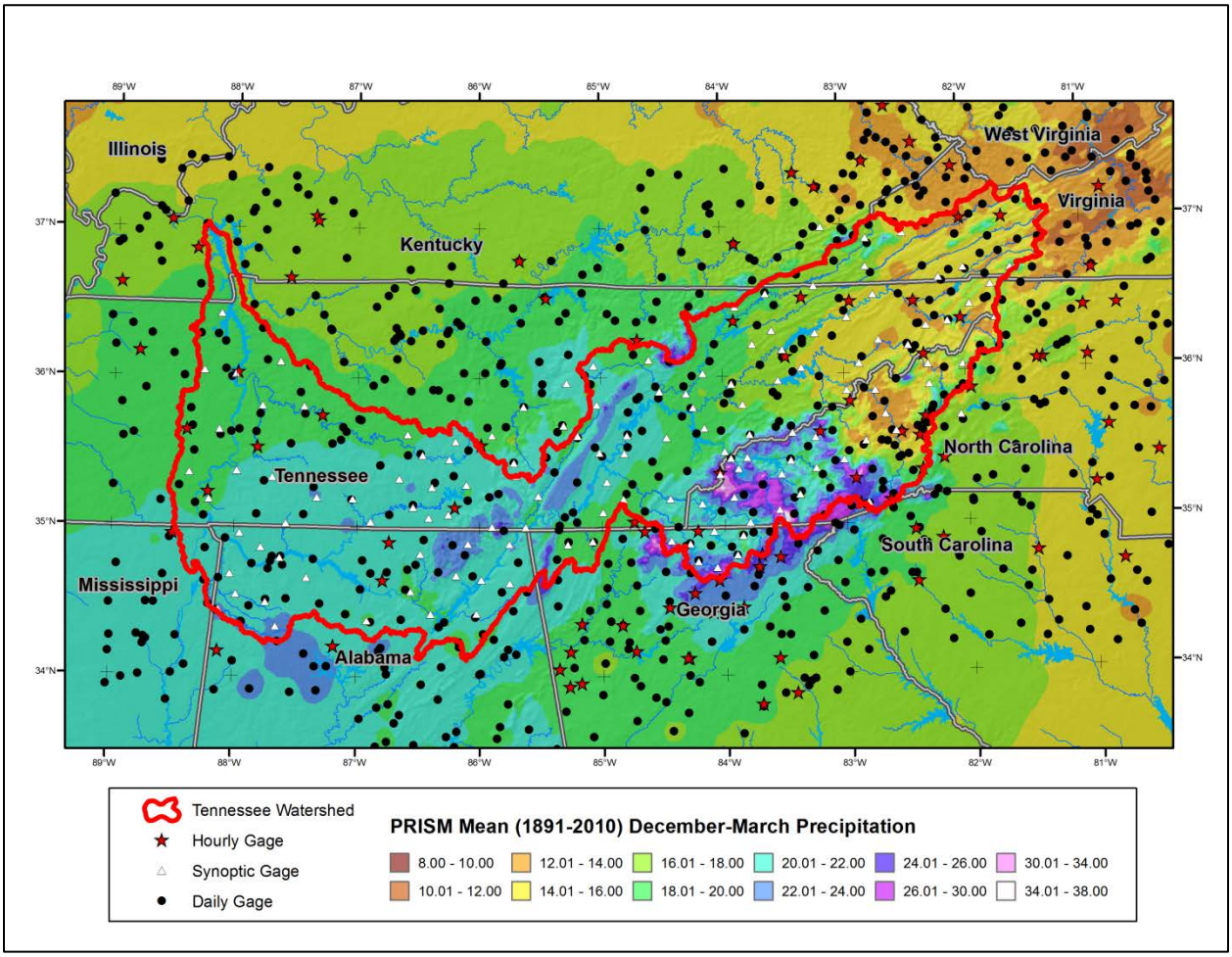


***Figure 25 - Location of Daily, Hourly and Synoptic Precipitation Gages Used in Precipitation-Frequency Analysis for MLCs***

***Table 10 - Number of Stations/Gages and Station-Years of Record for Stations/Gages with 15 or More Years of Record Used in Precipitation-Frequency Analysis for MLCs***

| PRECIPITATION GAGE TYPE | NUMBER OF STATIONS/GAGES | STATION-YEARS OF RECORD | AVERAGE STATION-YEARS |
|---|---|---|---|
| NOAA Daily Gages | 758 | 43,040 | 56.8 |
| NOAA Hourly Gages | 91 | 3,713 | 40.8 |
| TVA Synoptic Gages | 135 | 3,433 | 25.4 |
| TOTAL | 984 | 50,186 | 51.0 |

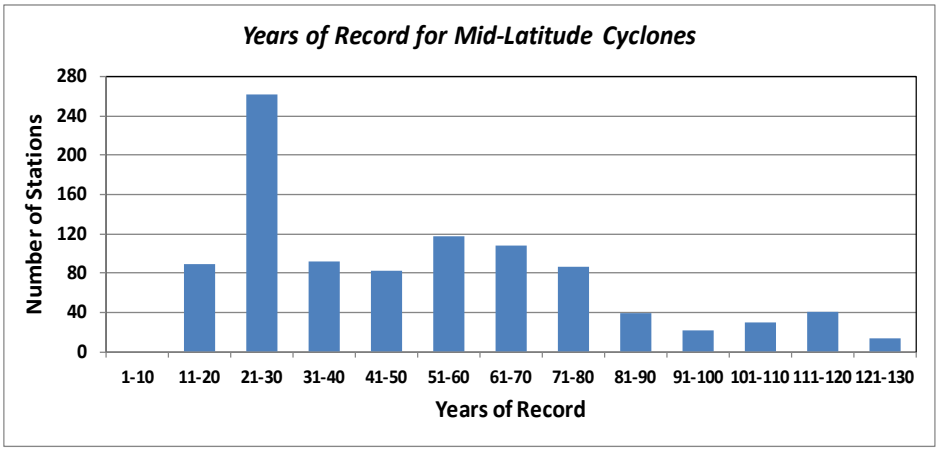


***Figure 26 - Histogram for Years of Record for Stations Used in Precipitation-Frequency Analysis for MLCs***

## 8.1 Spatial Mapping of 48-Hour At-Site Means

Spatial mapping of 48-hour at-site means for MLCs was conducted using longitude and gridded values of December through March mean monthly precipitation (PRISM[4,5]) as explanatory variables. This choice was made after reviewing the behavior of the relationship of at-site means with the December-March mean monthly precipitation (***Figure 27***). In particular, the December through March period is when the majority of MLCs occur, and it was reasonable to anticipate the at-site means would have a spatial pattern similar to the December-March precipitation (***Figure 25***).

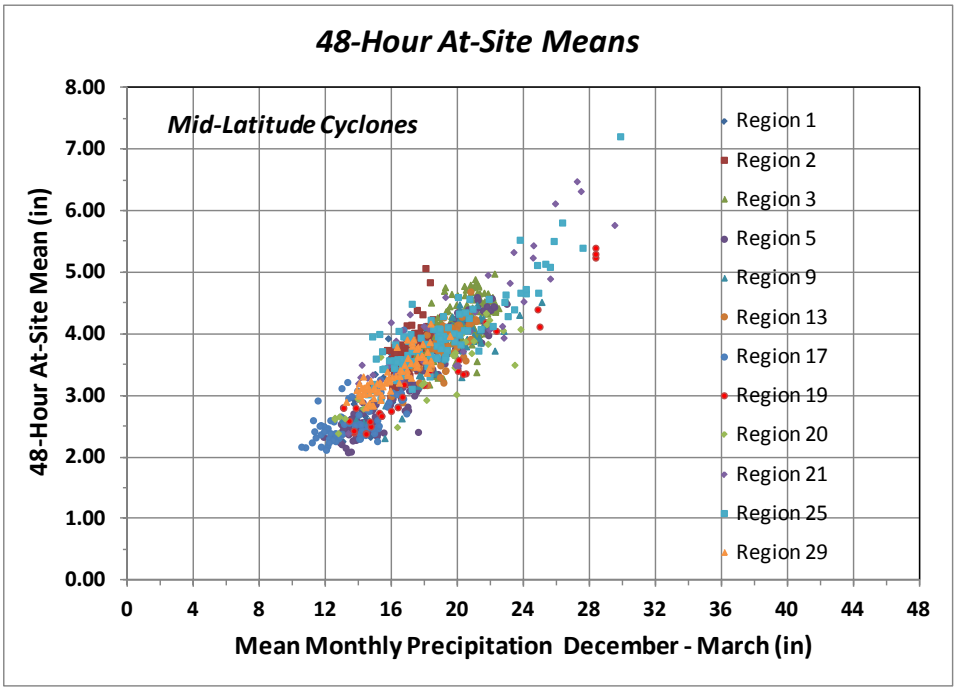


***Figure 27 - Scatterplot of Station Sample Values of 48-Hour At-Site Means for MLCs***

Collections of stations from adjacent climatic regions were grouped where they exhibited similar behavior. Multiple linear regression methods were used for the collections of stations, which resulted in the form of the mathematical relationship shown in ***Equation 5***. ***Table 11*** lists the coefficients for the multiple regression solution and the resultant RMSE for the various groupings of climatic regions. The resultant multiple linear regression equations were used to generate the mapped values of 48-hour at-site means. Minor smoothing was conducted in the vicinity of regional boundaries using a nearest neighbor approach to

provide a smooth continuum of precipitation at the boundaries. Best estimates of the at-site means were computed as a weighted-average of the station-sample values and regression-predicted values, as discussed in ***Section 7.7***. ***Figure 28*** and ***Figure 29*** depict examples of comparisons of station sample values and mapped values of the 48-hour at-site means. The mapped values of the 48-hour at-site means (***Figure 29***) are unbiased and have a RMSE of 4.4%. The spatial map of 48-hour at-site means for MLCs is shown in ***Figure 30***.

| CLIMATIC REGIONS | MULTIPLE REGRESSION COEFFICIENTS $AtSiteMean_{MLC} = \alpha_0 + \alpha_1 Longitude + \alpha_2 MonthlyPrecip_{Dec\text{-}Mar}$ | | | RMSE |
|---|---|---|---|---|
| | $\alpha_0$ | $\alpha_1$ | $\alpha_2$ | |
| 1 | -11.153 | -0.1408 | 0.1519 | 5.8% |
| 2, 3 | -9.186 | -0.1186 | 0.1496 | 6.3% |
| 5, 9 | -16.248 | -0.2083 | 0.1199 | 5.7% |
| 13,17 | -18.294 | -0.2370 | 0.1029 | 7.1% |
| 18 | 5.645 | 0.0691 | 0.2035 | 6.2% |
| 19, 20 | -13.113 | -0.1672 | 0.1399 | 8.1% |
| 21, 25, 29 | 9.031 | 0.1118 | 0.2193 | 8.0% |
| **All Regions** | **Final Mapping** | | | **4.4%** |

***Table 11 - Listing of Coefficients for Multiple Linear Regression for 48-Hour At-Site Means for MLCs and RMSE for Predictive Equations***

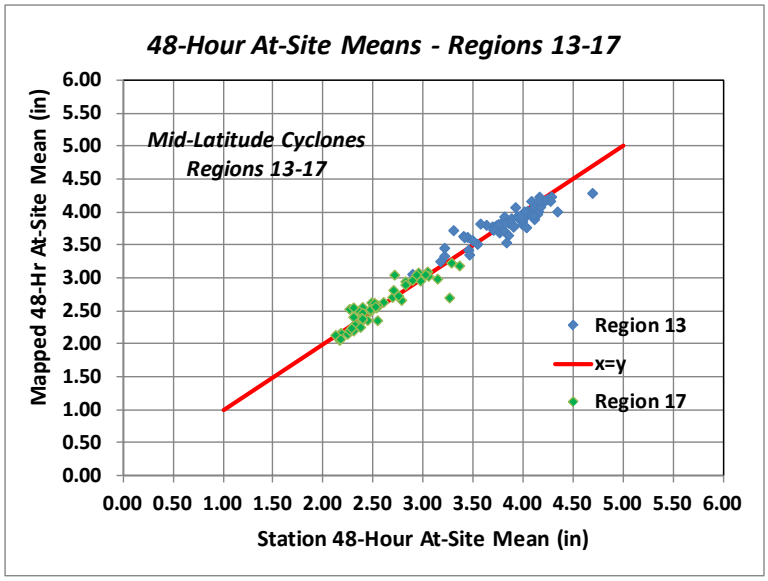


***Figure 28 - Comparison of Station Values and Mapped Values of 48-Hour At-Site Means for Tennessee Valley Lowlands (Climatic Regions 13, 17) for MLCs***

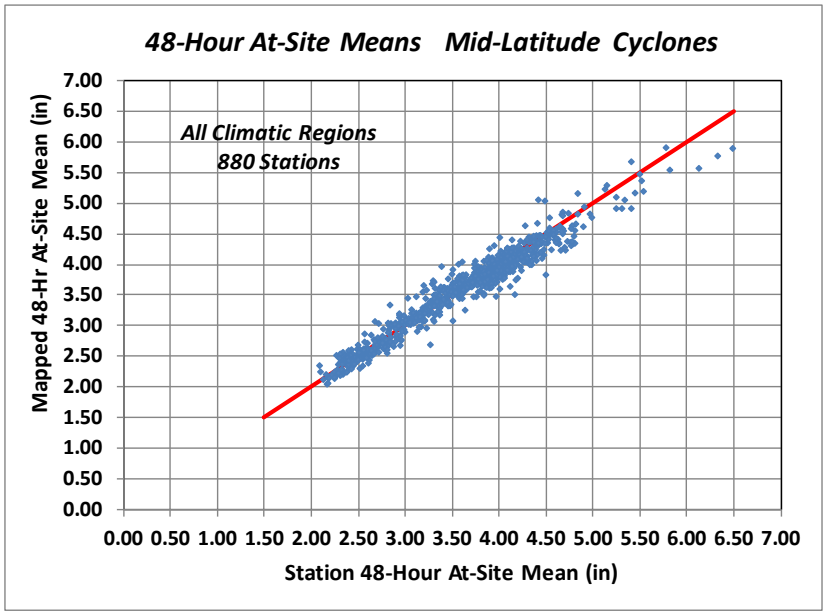


*Figure 29 - Comparison of Station Values and Mapped Values of 48-Hour At-Site Means for All Climatic Regions for MLCs*

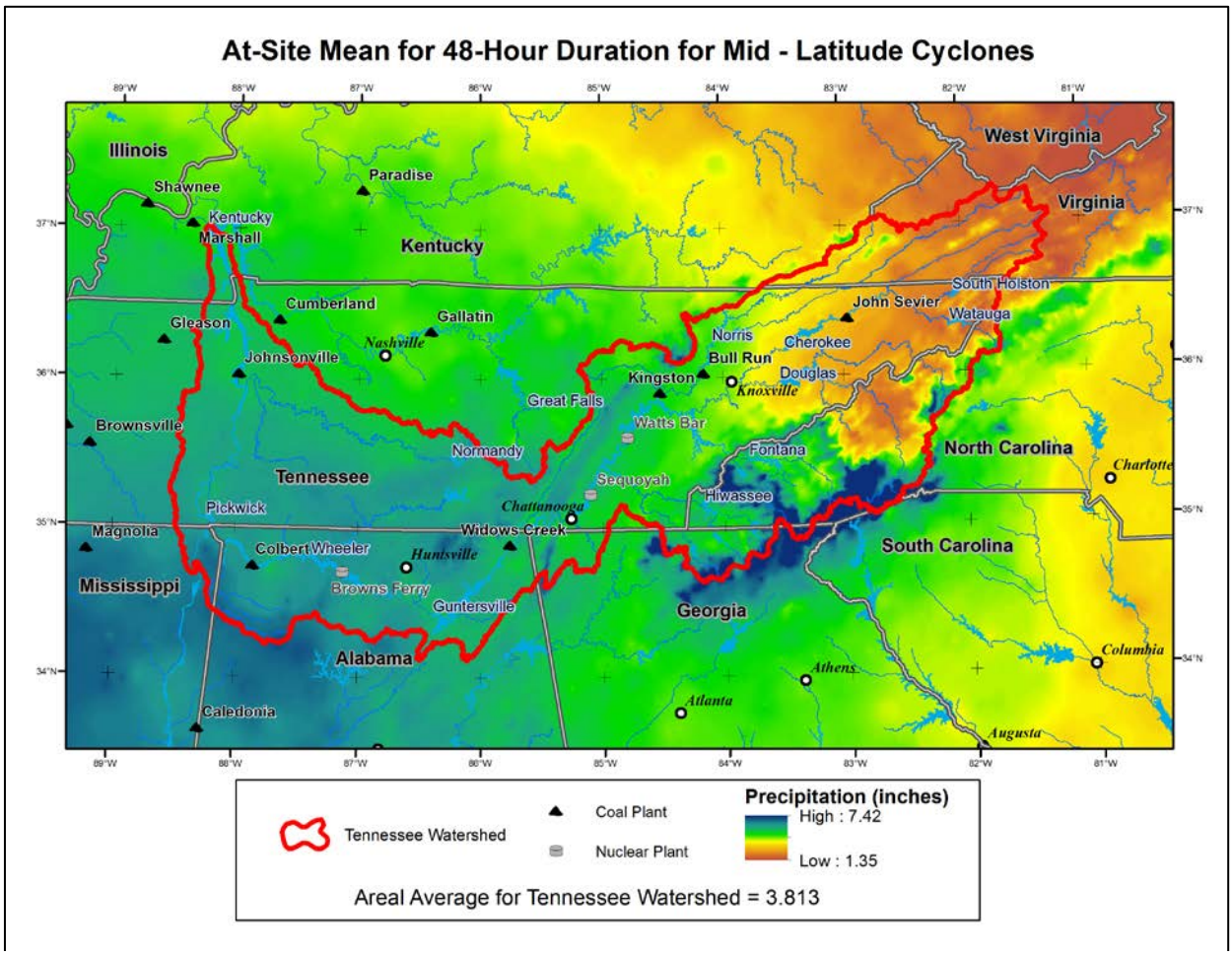


*Figure 30 - Map of At-Site Means for 48-Hour Duration for MLCs*

## 8.2 Spatial Mapping of Regional Values of L-Cv and L-Skewness

Homogeneous sub-regions were formed as groupings of stations within a limited range of longitude and December-March mean monthly precipitation for each climatic region. Stations were included that had a record length of 25 years or more. Thirty-eight sub-regions were formed in this manner, where each sub-region produced a regional L-Cv and L-Skewness value associated with a group-average longitude and group-average mean monthly December-March precipitation. All thirty-eight sub-regions were found to be acceptably homogeneous based on L-moment heterogeneity test measures.

A review of the regional L-Cv values showed a systematic variation with longitude (***Figure 31***). These thirty-eight regional values of L-Cv and L-Skewness were used in a multiple regression with longitude and December-March mean monthly precipitation as explanatory variables. ***Equation 7*** lists the form of the multiple regression for regional L-Cv, and ***Figure 32*** depicts a comparison of observed and mapped values of regional L-Cv for 48-hour precipitation annual maxima, where the RMSE for prediction of regional L-Cv was 3.6% (***Table 12***). The spatial mapping of regional L-Cv for the 48-hour duration is shown in ***Figure 33***, where regional L-Cv is seen to vary over a relatively narrow range.

$$L\text{-}Cv = 2.0656 + 0.048308Longitude + 0.0003098Longitude^2 - 0.000873MonthlyPrecip_{Dec\text{-}Mar} \quad \textit{(Equation 7)}$$

Development of a predictor equation for L-Skewness is more difficult than for L-Cv because of the naturally high sampling variability for skewness measures. The prediction of regional L-Skewness was accomplished using linear regression for regional L-moment L3 as a function of regional L-moment L2 (***Equation 8***) for the 38 homogeneous sub-regions. Use of the Index Flood methodology (Dalrymple[3]) provides for a prediction of regional L-Skewness using ***Equation 9*** because regional L-Cv is equal to regional L2 for indexed annual maxima datasets. ***Figure 34*** depicts the regression solution for regional L3, and ***Table 12*** lists the summary statistics for mapping of regional L-Skewness, where the RMSE is 9.8%. ***Figure 35*** shows the spatial mapping of regional L-Skewness, which is seen to have moderate variation across the study area.

$$L3 = -0.04171 + 0.4310*L2 \quad \textit{Equation 8}$$

$$L\text{-}Skewness = 0.4310 - 0.04171/L\text{-}Cv \quad \textit{Equation 9}$$

***Table 12 - Summary Statistics for Spatial Mapping of 48-Hour Duration Regional L-Cv and L-Skewness for MLCs***

| L-MOMENT RATIO | RANGE OF MAPPED L-MOMENT RATIO | STANDARD DEVIATION OF RESIDUALS | RMSE |
|---|---|---|---|
| Regional L-Cv | 0.1650 ≤ L-Cv ≤ 0.2000 | 0.0062 | 3.6% |
| Regional L-Skewness | 0.1782 ≤ L-Skewness ≤ 0.2225 | 0.0184 | 9.8% |

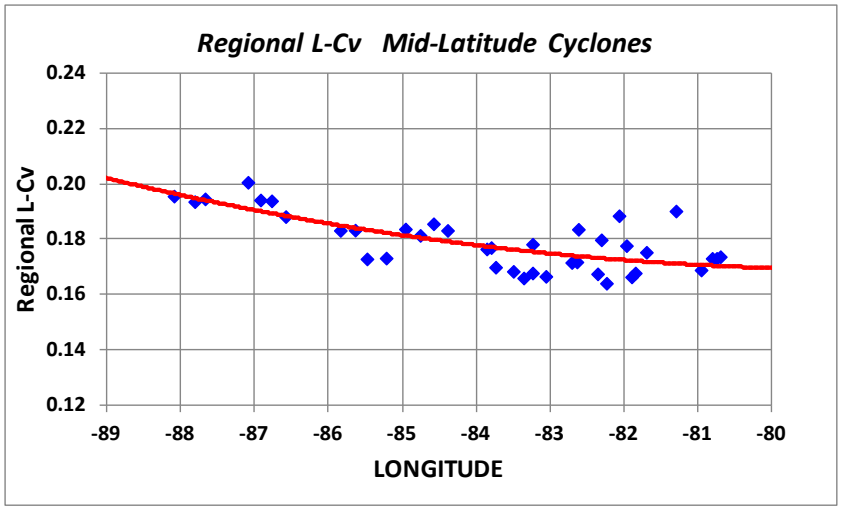


*Figure 31 - Example of Variation of Regional L-Cv with Longitude for 48-Hour Duration MLCs (Repeat of Figure 17)*

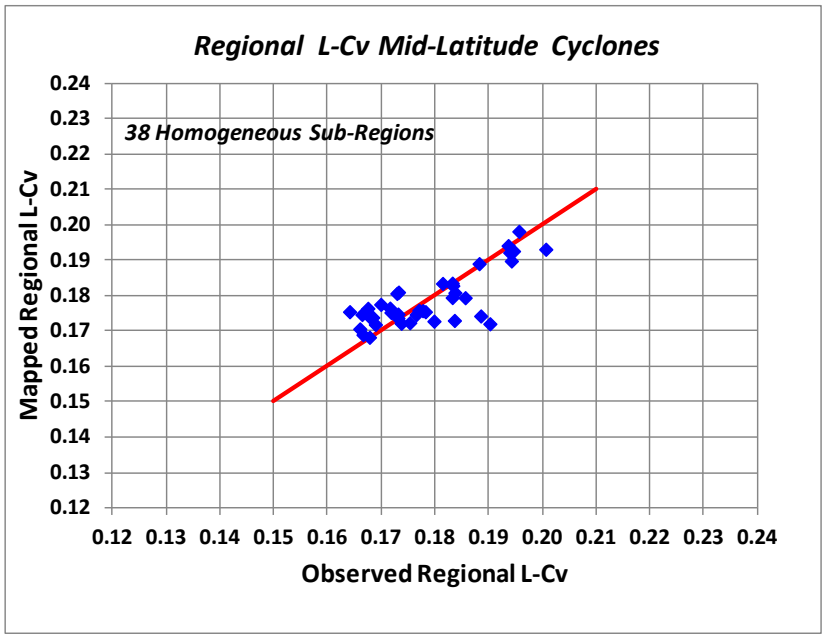


*Figure 32 -Comparison of Observed Regional L-Cv and Mapped Regional L-Cv for 48-Hour Duration for 38 Homogeneous Sub-Regions for MLCs*

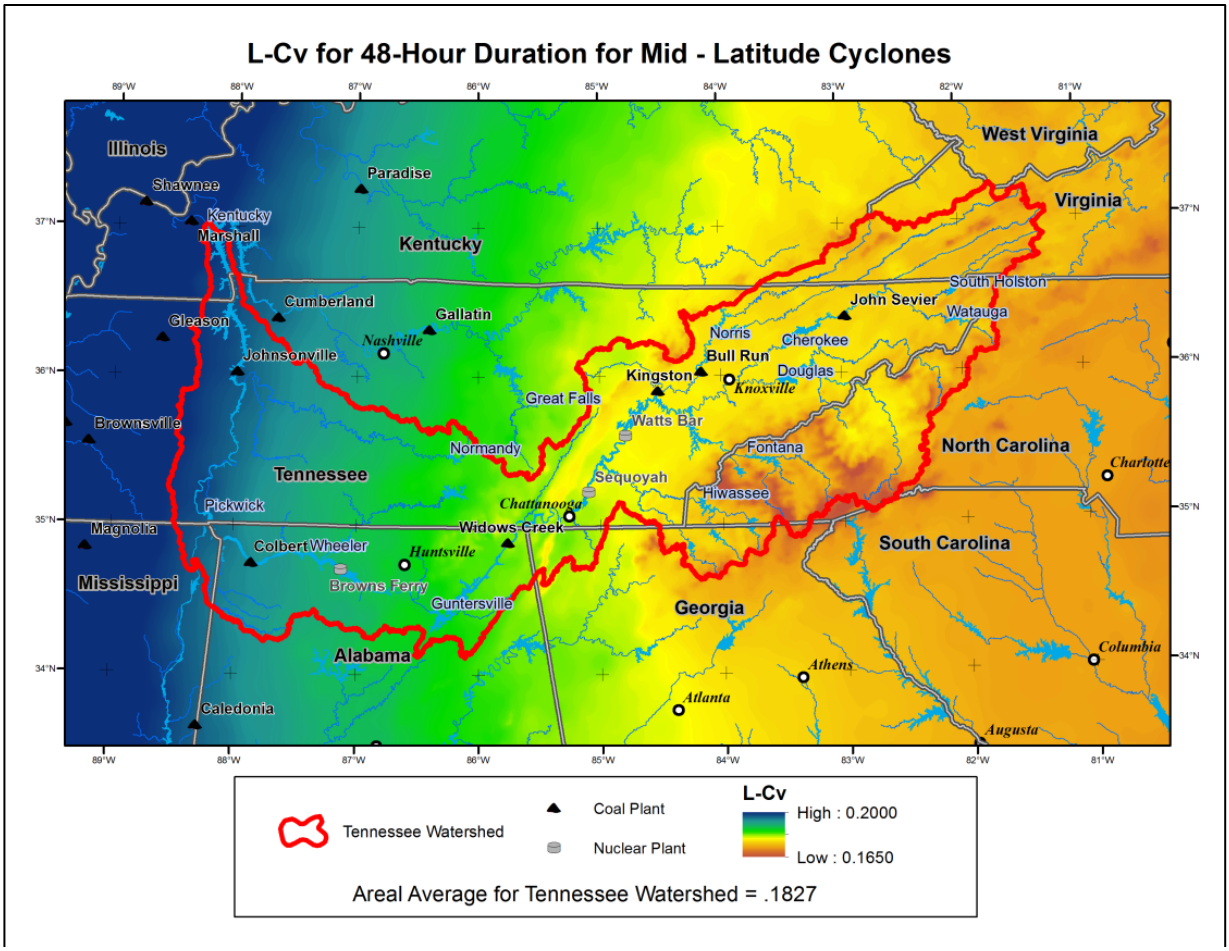


*Figure 33 -Map of Regional L-Cv for 48-Hour Duration for MLCs*

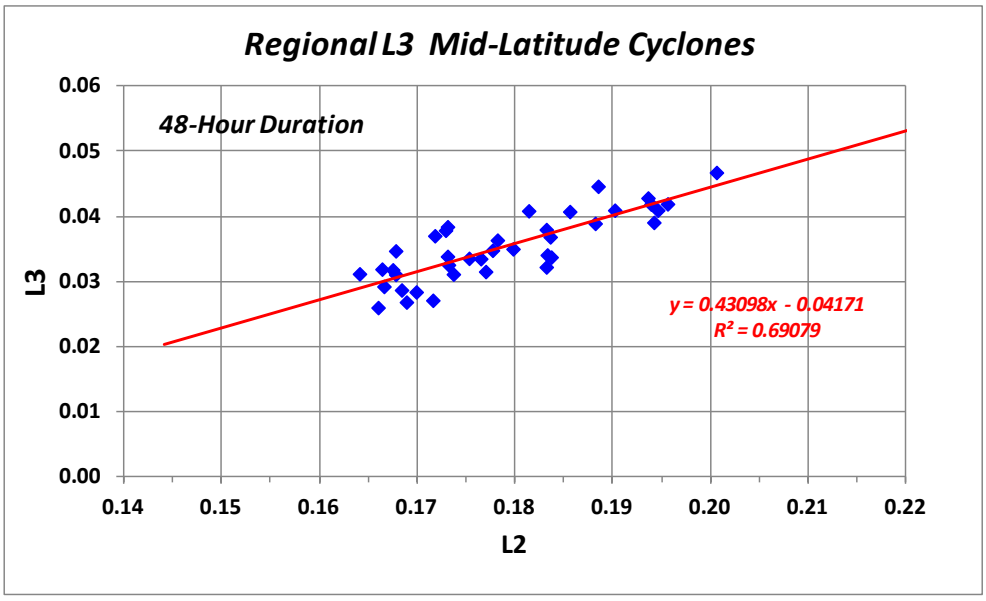


*Figure 34 - Predictor Equation for Regional L-Moment L3 as a Function of Regional L-Moment L2 for 48-Hour Duration for 38 Homogeneous Sub-Regions for MLCs*

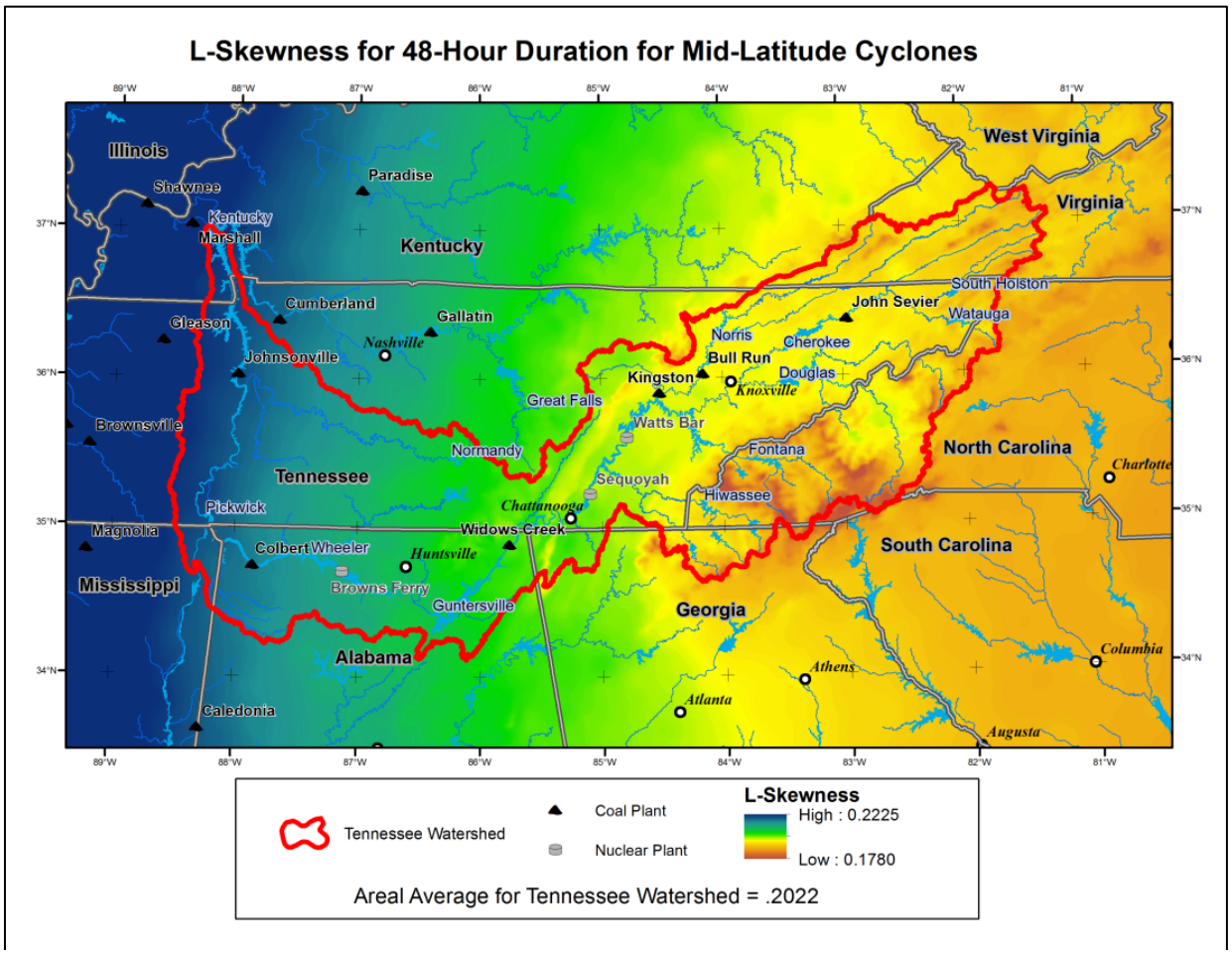


***Figure 35 -Map of Regional L-Skewness for 48-Hour Precipitation Annual Maxima for MLCs***

## 8.3 Identification of Regional Probability Distribution

L-moment goodness-of-fit tests were conducted for each of the 38 homogeneous sub-regions and the GEV distribution was identified as the best-fit 3-parameter probability distribution for the collection of sub-regions. A review of ***Figure 36*** shows the centroid of the cluster of regional L-Skewness and L-Kurtosis pairs for the 38 sub-regions to be very near the GEV distribution. As discussed previously, the 4-parameter Kappa distribution with a fixed shape parameter (*h*) emulates the GEV and near-GEV distributions and was selected for describing the point precipitation-frequency relationships for MLCs. A shape parameter (*h*) value of 0.05 (***Equation 2***) was identified as the best-fit for describing the MLC storm type.

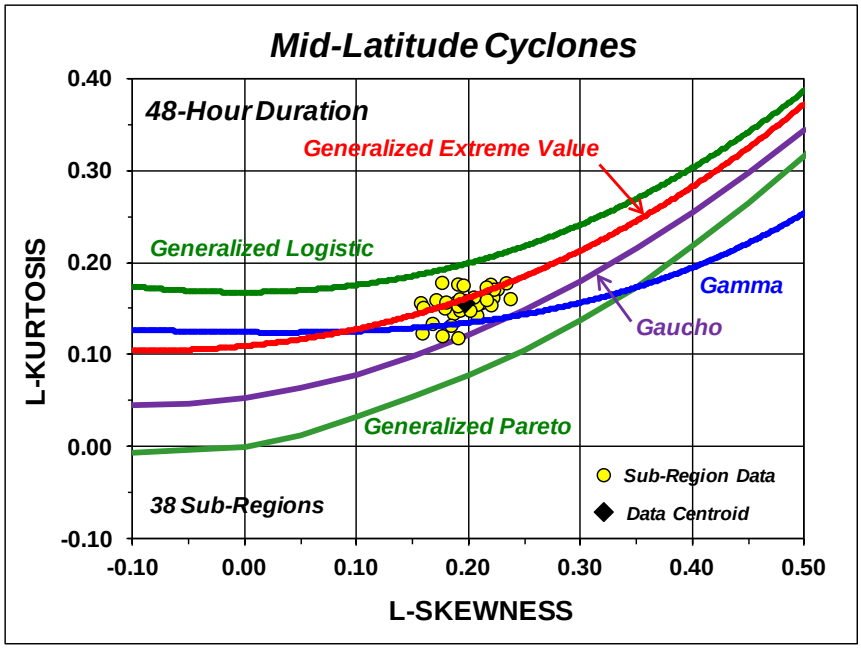


***Figure 36 - L-Moment Ratio Diagram Depicting Regional L-Skewness and L-Kurtosis Values for Homogeneous Sub-Regions for 48-Hour Duration for MLCs***

## 8.4 Isopluvial Mapping for 48-Hour Duration for Selected Annual Exceedance Probabilities

The gridded datasets for the 48-hour at-site means (***Figure 30***), regional L-Cv (***Figure 33***) and regional L-Skewness (***Figure 35***) and the 4-parameter Kappa distribution with *h*=0.05 provided the information necessary to develop gridded datasets of 48-hour precipitation for selected Annual Exceedance Probabilities (AEPs). A precipitation-frequency curve for the station at Charleston TN was developed in the manner described above and compared with a probability plot of historical data (***Figure 37***). This provides an example of the general shape of the precipitation-frequency relationship for MLC storm types.

The areal average at-site mean (***Figure 30***), regional L-Cv (***Figure 33***) and regional L-Skewness (***Figure 35***) were used to develop a representative point precipitation-frequency relationship for the Tennessee Valley watershed (***Figure 38***). Note for this calculation, the Tennessee Valley watershed included the area upstream of Great Falls Dam. This relationship provides some insight into the expected behavior of 48-hour precipitation for extreme precipitation events for MLCs.

Isopluvial gridded datasets were generated for AEPs of $10^{-1}$, $10^{-2}$, $10^{-3}$, $10^{-4}$ and $10^{-5}$ and isopluvial maps are shown in ***Appendix I***. ***Figure 39*** shows an example isopluvial map for an AEP of 1:1,000

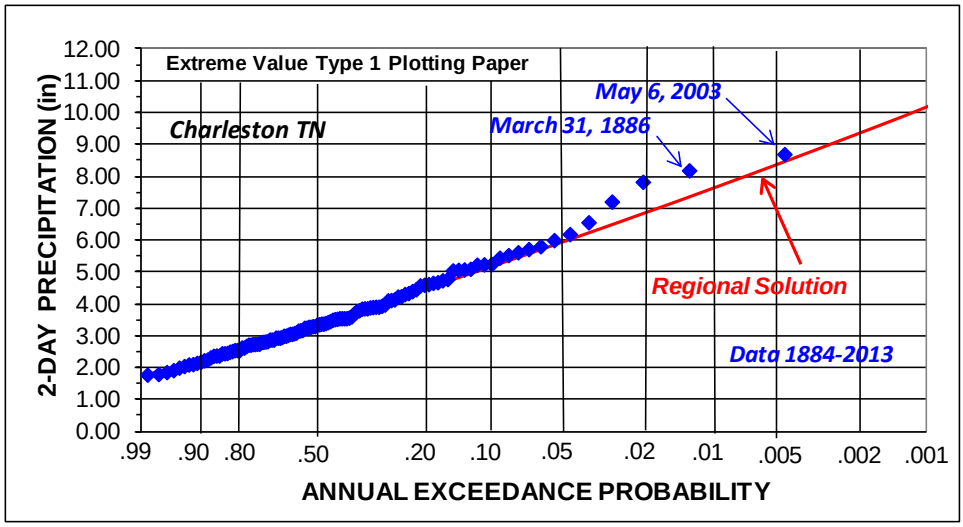


*Figure 37 - Probability plot of Historical 2-Day Precipitation Annual Maxima for MLCs for Charleston, TN and Comparison with Regional Precipitation-Frequency Curve*

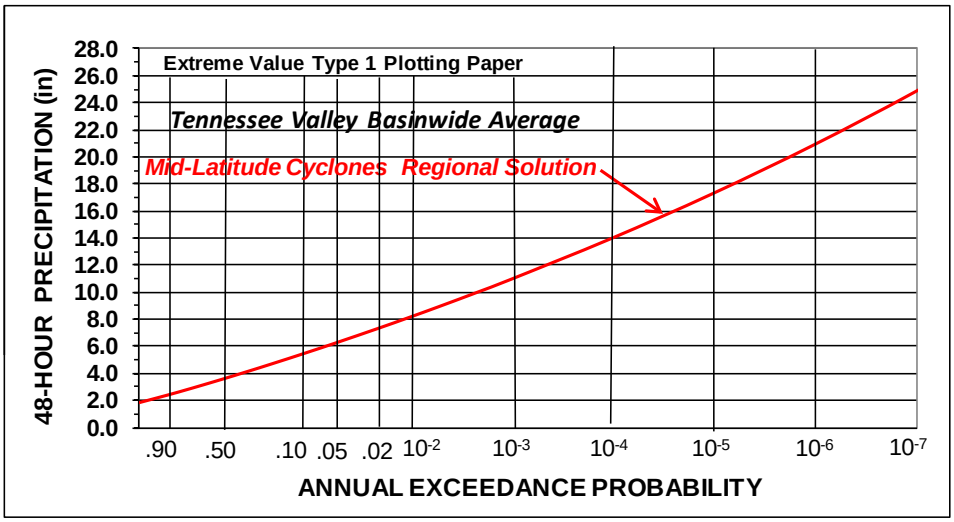


*Figure 38 - Point 48-Hour Precipitation-Frequency Relationship for Tennessee Valley Average Parameters for MLCs*

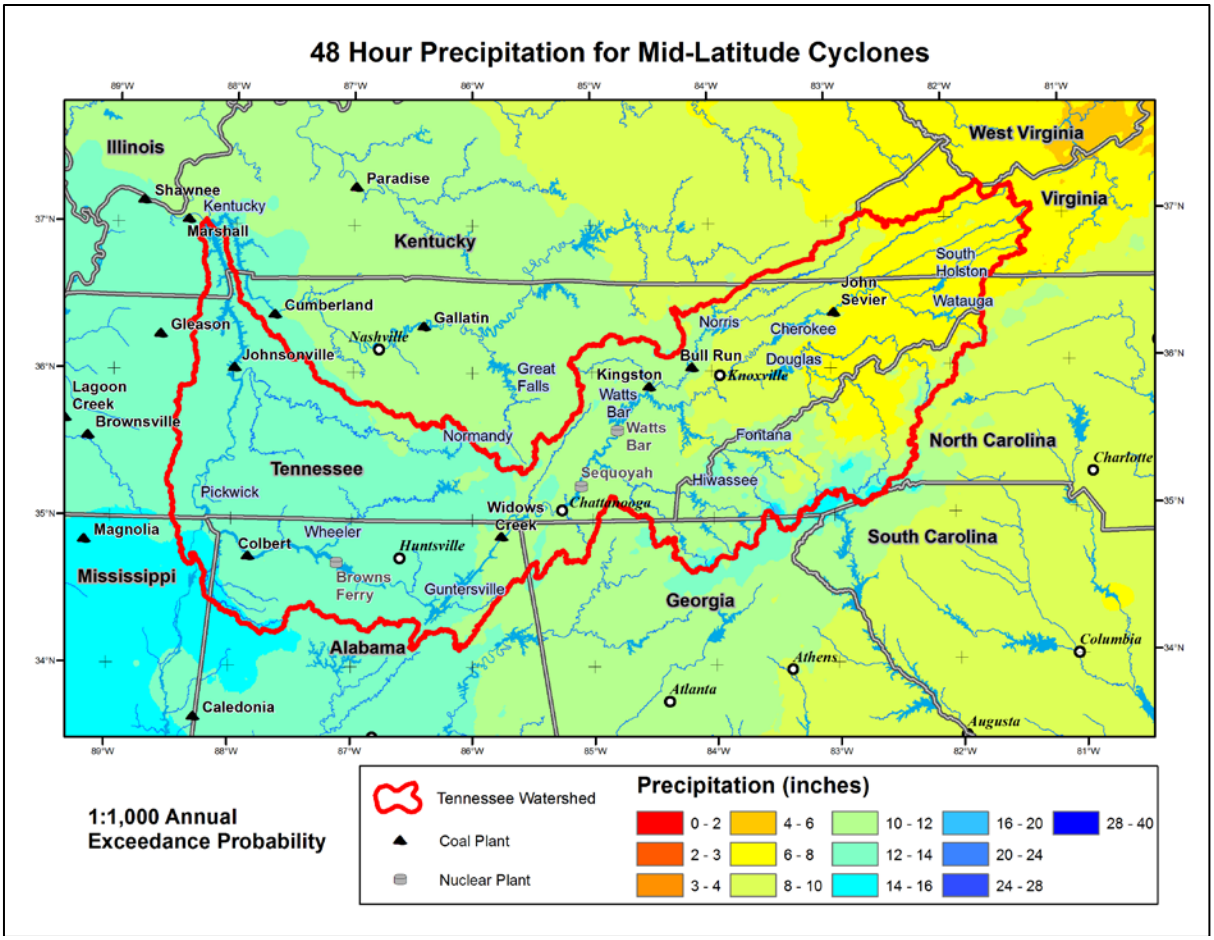


***Figure 39 -Isopluvial Map of 48-Hour Precipitation Maxima for an AEP of 1:1,000 for MLCs***

## 8.5 Seasonality of Extreme Storms for Mid-Latitude Cyclones

An initial perspective on the seasonality of MLCs was obtained by using the DDST to develop a frequency histogram of days when MLC events occurred (***Figure 40***). This frequency histogram includes many days with small precipitation totals which are smaller than the precipitation annual maxima and is therefore representative of the full range of daily precipitation.

The seasonality analysis for MLCs was conducted using 48-hour precipitation annual maxima. The focus was on the rarest storms, and a dataset of 68 noteworthy storms was assembled where 48-hour precipitation exceeded a 10-year recurrence interval at 15 or more stations. There is always a tradeoff between the desire to analyze the largest storms and the need for a dataset of sufficient size to provide a representative sample. The 10-year threshold and requirement of 15 or more stations over the threshold was judged suitable to meet the competing goals.

The calendar storm dates were converted to numerical storm dates where calendar dates were converted to numerical storm dates by expressing the day as a ratio of the total days of the month such that November 7 equates to 11.23 and March 15 equates to 15.48 to allow for frequency analysis. Computation of sample statistics resulted in a mean of January 14$^{th}$ and a standard deviation of 2.16 months. A probability plot was assembled using the 68 numerical storm dates and a 4-parameter Beta distribution was fitted to the data (***Figure 41***). The 4-parameter Beta distribution was then used to create a frequency histogram for the seasonality of Extreme 48-hour duration MLCs (***Figure 42***). A comparison of ***Figure 40*** and ***Figure 42*** shows the narrowing of the months when extreme MLC storms can be expected to occur relative to more common storm events.

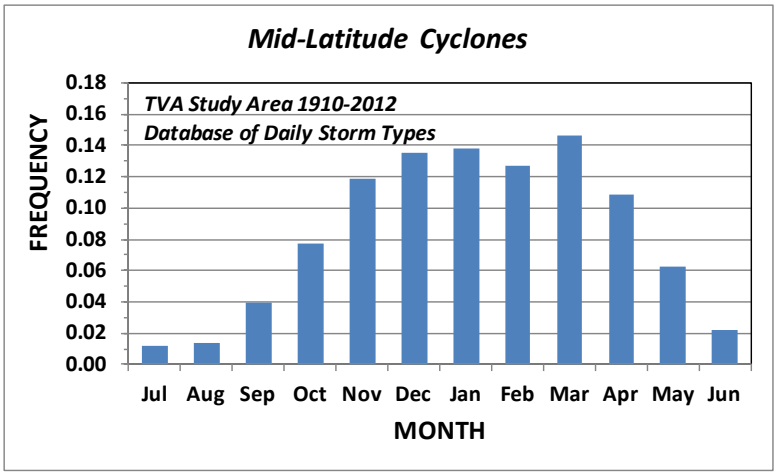


*Figure 40 -Seasonal Frequency Histogram of the Days When MLC Storm Events Have Occurred 1910-2012*

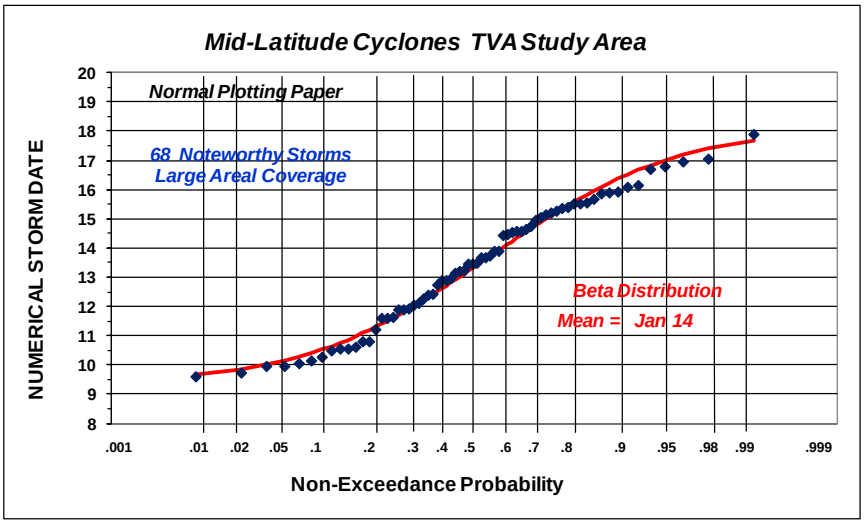


*Figure 41 - Probability plot of Numerical Storm Dates for 48-Hour Duration MLCs*

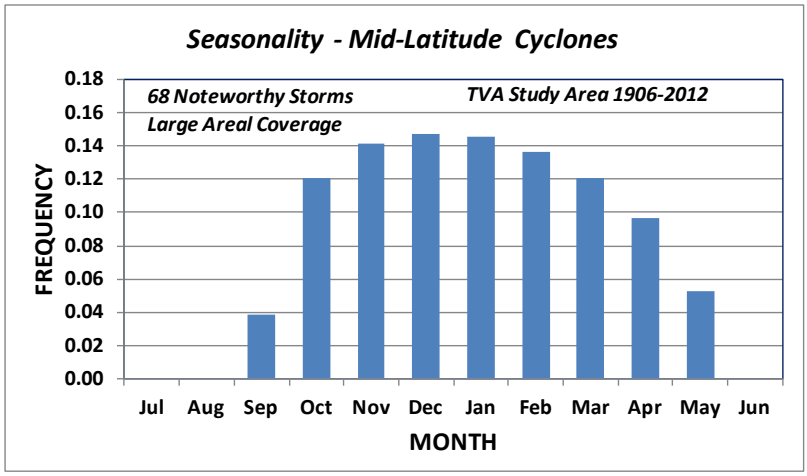


*Figure 42 - Frequency Histogram for Seasonality of Extreme 48-Hour Duration MLCs*

## 8.6 Equivalent Independent Record Length (EIRL) for Mid-Latitude Cyclones

Two methods were used to estimate EIRL. The first method was a frequency-based method using the upper 10% of 48-hour precipitation annual maxima at each station. The second method utilized counting of independent storm dates for all storm events.

The frequency-based method was conducted in the manner described in ***Appendix H***, where the upper 10% of precipitation annual maxima at the stations were examined. ***Figure 43*** shows the plotting-position representation of EIRL. The frequency-based method resulted in an estimate of 5,700 years for EIRL relative to the 50,281 station-years of record. The storm counting method resulted in an EIRL estimate of 2,760 years. The best-estimate of EIRL was taken as the geometric mean of the two estimates (***Table 13***).

***Table 13 - Estimates of EIRL for 48-Hour Duration for MLCs***

| Station-Years of Record | EIRL Estimates (Years) | | | EIRL Percent of Station-Years |
|---|---|---|---|---|
| | Frequency Based | Storm Count | Geometric Mean | |
| 50,281 | 5,700 | 2,760 | 3,970 | 7.9% |

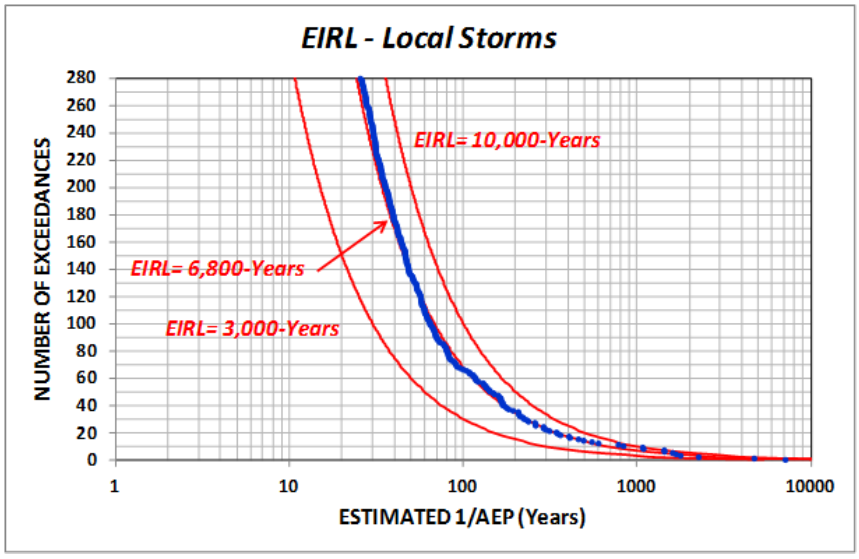


***Figure 43 -Graphical Depiction of EIRL for 48-Hour Duration MLCs***

## 8.7 24-Hour and 72-Hour Precipitation Annual Maxima for Mid-Latitude Cyclones

Precipitation annual maxima datasets were also assembled for the 24-hour and 72-hour durations for MLCs. These datasets were assembled to provide information on the variation of temporal storm characteristics across the TVSA, and to provide additional data for identification of the regional probability distribution.

### 8.7.1 Depth-Duration Ratios for 24-Hour, 48-Hour and 72-Hour At-Site Means

***Figure 44*** and ***Figure 45*** show the depth-duration ratio of observed at-site means for the 24-hour/48-hour durations for the MLC storm type and variation with longitude and elevation, respectively. Similarly, ***Figure 46*** and ***Figure 47*** shows the depth-duration ratio of observed at-site means for the 72-hour/48-hour durations for the MLC storm type and variation with longitude and elevation, respectively.

A review of ***Figure 44*** and ***Figure 46*** shows both the 24-hr/48-hr and 72-hr/48-hr depth-duration ratios do not vary with either longitude or elevation across the study area. This uniformity in behavior indicates that

storm-specific depth-duration curves for historical storms are transpositionable throughout the study area. This is an important finding for application of the spatial and temporal storm analyses conducted in Phase 2.

A depth-duration curve was prepared (***Figure 48***) to show the typical depth-duration behavior for MLC storms. This information indicates that the majority of MLC precipitation typically falls within a 24-hour to 36-hour period. Total precipitation at 72-hours is not markedly greater than 24-hour precipitation. Depth-duration curves for the collection of historical storms can naturally be expected to vary from this behavior. However, the typical (average) depth-curve for the collection of storms would be expected to be similar to that shown in ***Figure 48***.

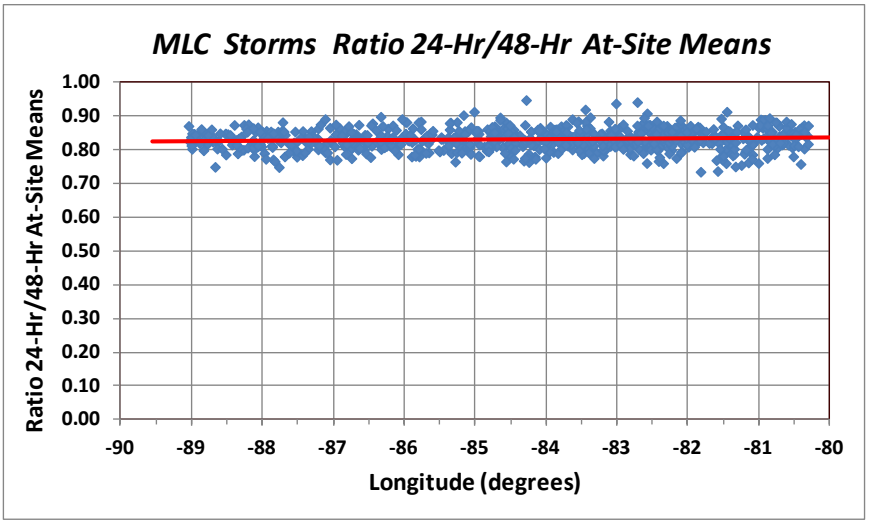


***Figure 44 -Variation with Longitude for the Ratio of 24-Hour to 48-Hour At-Site Means for MLCs***

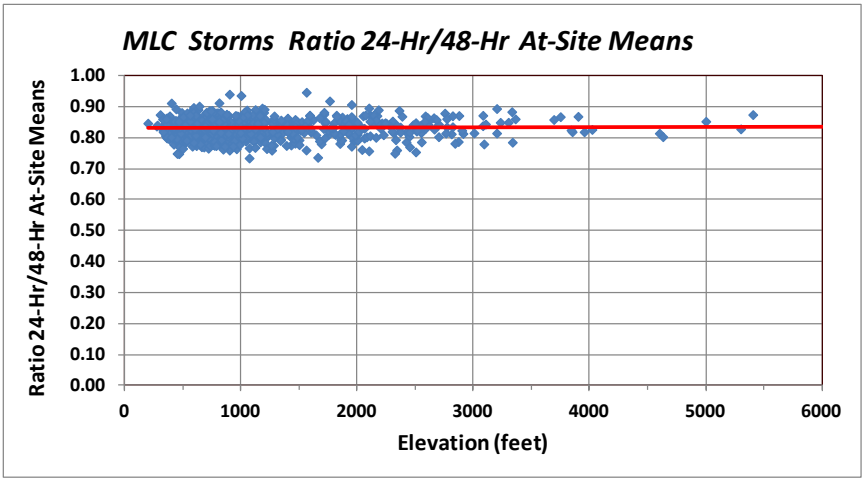


***Figure 45 -Variation with Elevation for the Ratio of 24-Hour to 48-Hour At-Site Means for MLCs***

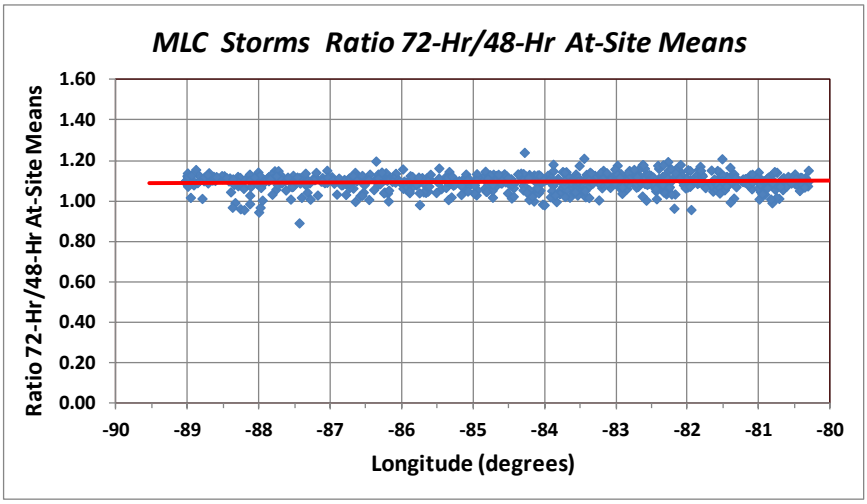


*Figure 46 -Variation with Longitude for the Ratio of 72-Hour to 48-Hour At-Site Means for MLCs*

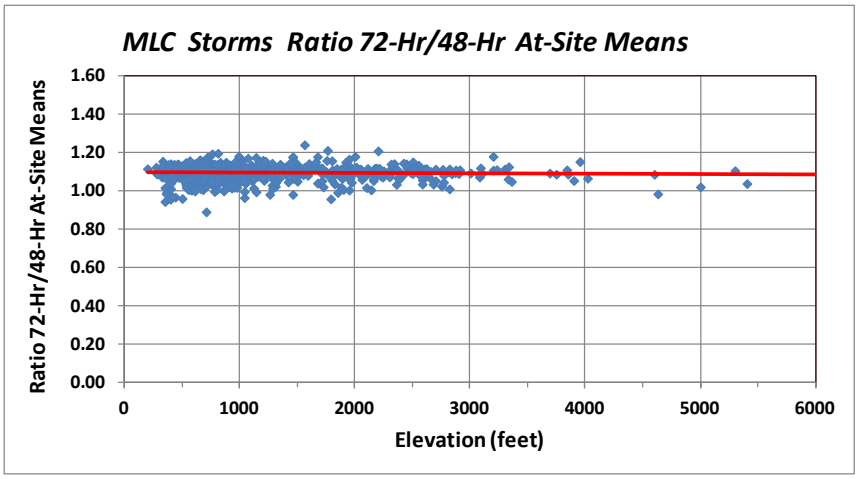


*Figure 47 -Variation with Elevation for the Ratio of 72-Hour to 48-Hour At-Site Means for MLCs*

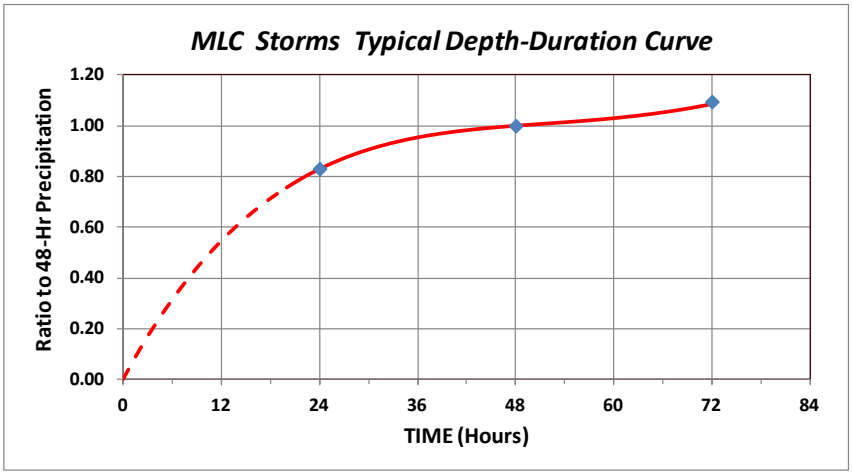


*Figure 48 -Typical Depth-Duration Curve for MLCs*

### 8.7.2 Identification of Regional Probability Distribution for 24-Hour and 72-Hour Durations

L-moment regional frequency analyses were conducted for homogeneous sub-regions for the 24-hour and 72-hour durations in the manner described previously for the 48-hour key duration. These analyses were conducted to provide regional L-Skewness and L-Kurtosis pairings for identification of the regional probability distributions for the 24-hour and 72-hour durations.

***Figure 49*** and ***Figure 50*** depict the L-Skewness and L-Kurtosis pairings for the homogeneous sub-regions for the 24-hour and 72-hour durations, respectively. For both durations, the data are clustered around the GEV distribution in a pattern similar to that seen for the 48-hour key duration (***Figure 36***). This is further demonstrated in ***Figure 51***, where the region-wide L-Skewness and L-Kurtosis pairings for the three durations (centroids of data clusters in ***Figure 36***, ***Figure 49***, and ***Figure 50***) are quite near to each other and the GEV distribution.

These findings provide additional support that the regional probability distribution for the MLC storm type is very near to the GEV distribution. Specifically, these findings support selection of the 4-parameter Kappa distribution with the 2nd shape parameter (*h*) equal to 0.05, which would lie on a curve parallel and just below the GEV curve shown in the L-moment ratio diagrams.

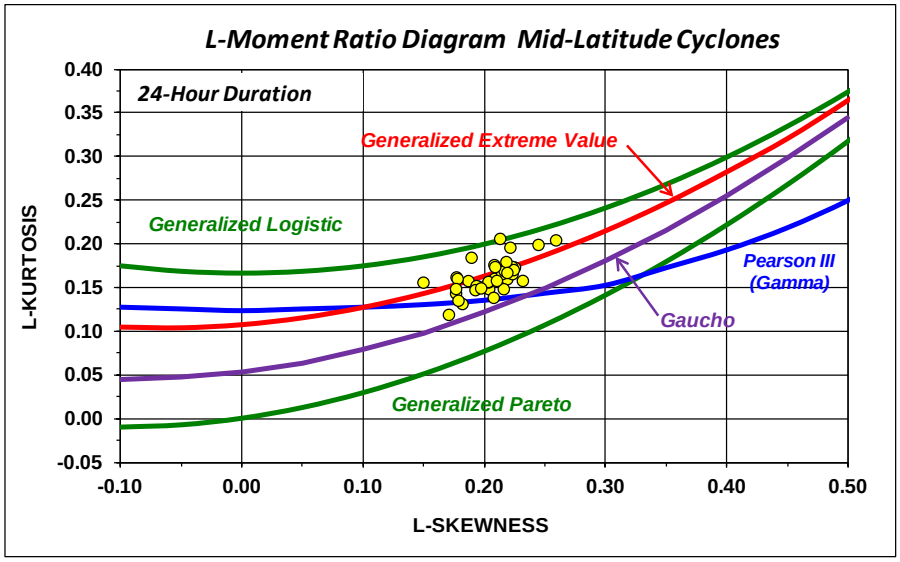


***Figure 49 - L-Moment Ratio Diagram Depicting Regional L-Skewness and L-Kurtosis Values for 38 Homogeneous Sub-Regions for the 24-Hour Duration for MLCs***

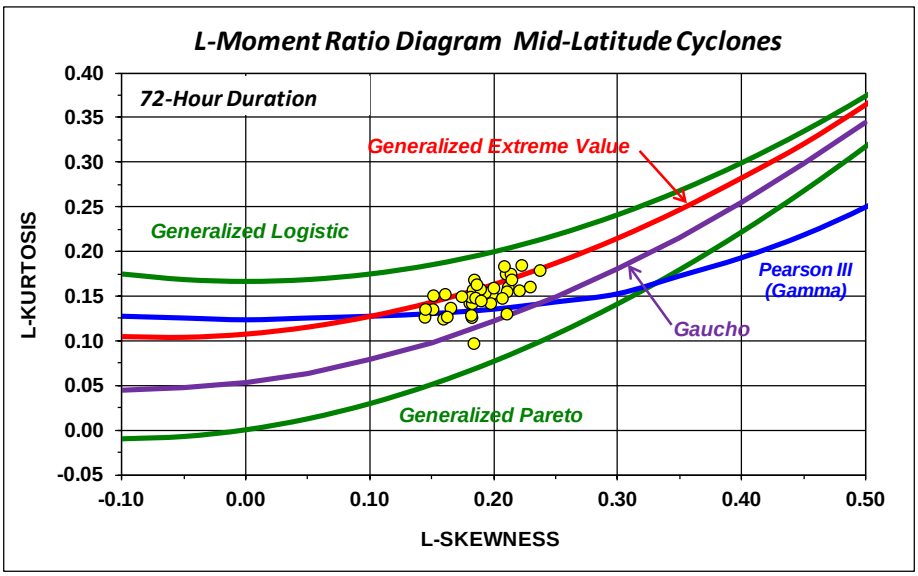


*Figure 50 - L-Moment Ratio Diagram Depicting Regional L-Skewness and L-Kurtosis Values for 38 Homogeneous Regions for the 72-Hour Duration for MLCs*

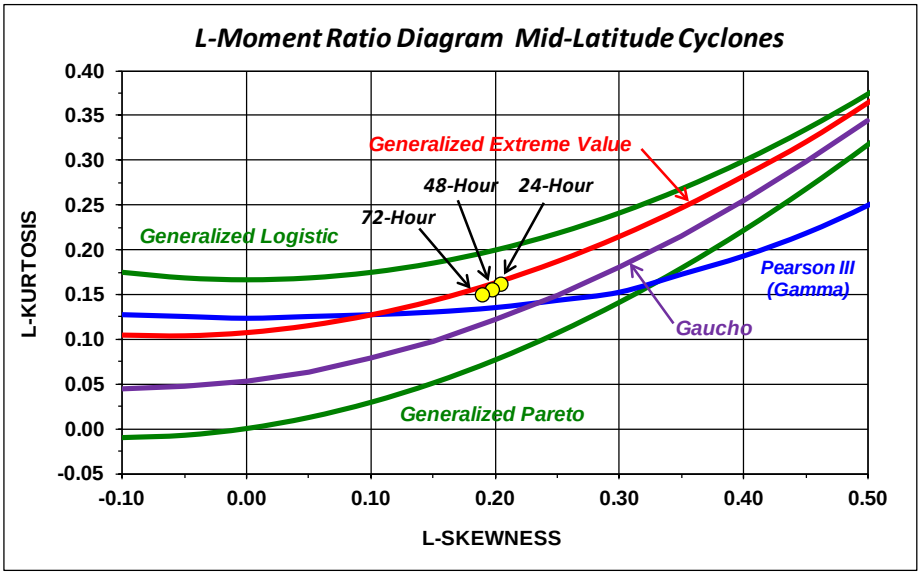


*Figure 51 - L-Moment Ratio Diagram Depicting Regionwide L-Skewness and L-Kurtosis Values for the 24-Hour, 48-Hour and 72-Hour Durations for MLCs*

# 9 Mesoscale Storms with Embedded Convection - Point Precipitation-Frequency

Hourly and synoptic gages were used in the regional analyses for 6-hour precipitation annual maxima for MECs where stations with 15 years or more of record were included in the analyses (***Figure 52***). ***Table 14*** provides a listing of the number of gages and total years of record used in the analysis of MECs, and ***Figure 53*** depicts a histogram of the number of years of record.

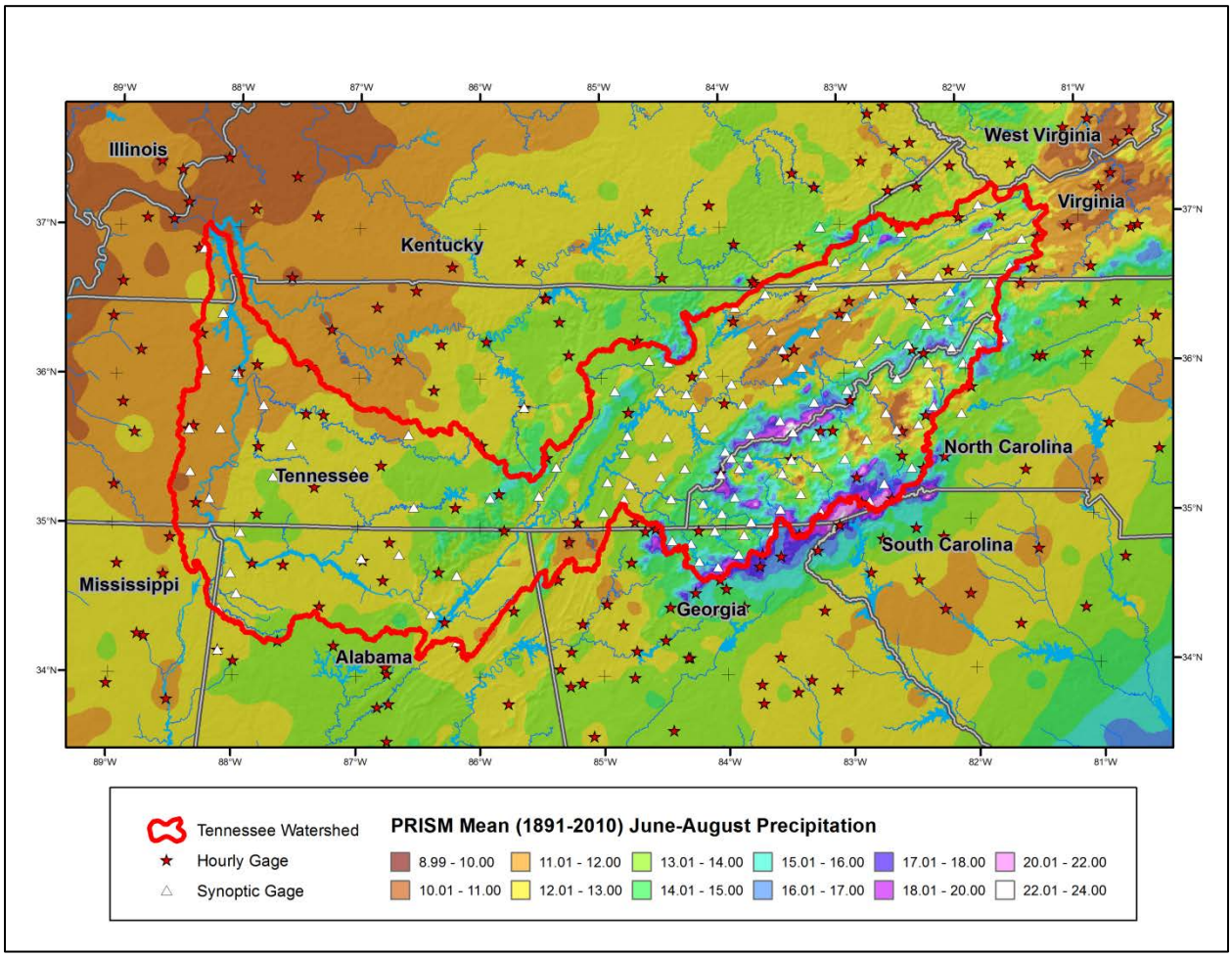


***Figure 52 - Location of Hourly and Synoptic Precipitation Gages Used in Precipitation-Frequency Analysis for MECs***

***Table 14 - Number of Stations/Gages and Station-Years of Record for Stations/Gages with 15 or More Years of Record Used in Precipitation-Frequency Analysis for MECs***

| PRECIPITATION GAGE TYPE | NUMBER OF STATIONS/GAGES | STATION-YEARS OF RECORD | AVERAGE STATION-YEARS |
|---|---|---|---|
| NOAA Hourly Gages | 210 | 8,873 | 42.3 |
| TVA Synoptic Gages | 130 | 3,166 | 24.4 |
| **TOTAL** | **340** | **12,039** | |

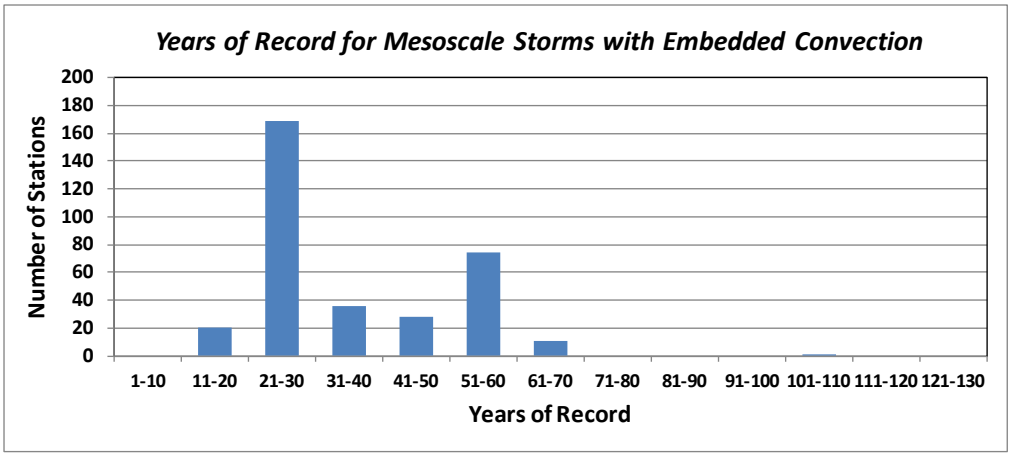


***Figure 53 -Histogram for Years of Record for Stations Used in Precipitation-Frequency Analysis for MECs***

## 9.1 Spatial Mapping of 6-Hour At-Site Means

Spatial mapping of at-site means for 6-hour precipitation annual maxima for MECs was accomplished using data from stations with 15 years or more of record. The choice of a minimum of 15-years of record was a balance between having sufficient data for a reasonable estimate of the at-site mean and the desire to have sufficient stations to capture the spatial variability of the at-site mean. Spatial mapping of 6-hour at-site means was conducted using longitude and gridded values of June through August mean monthly precipitation (PRISM[5,6]) as explanatory variables. This choice was made after reviewing the behavior of the relationship of at-site means with longitude (***Figure 54***). In addition, the June through August period is when the majority of MECs occur, so it was reasonable to anticipate the at-site means would have a spatial pattern similar to the June-August mean monthly precipitation (***Figure 52***).

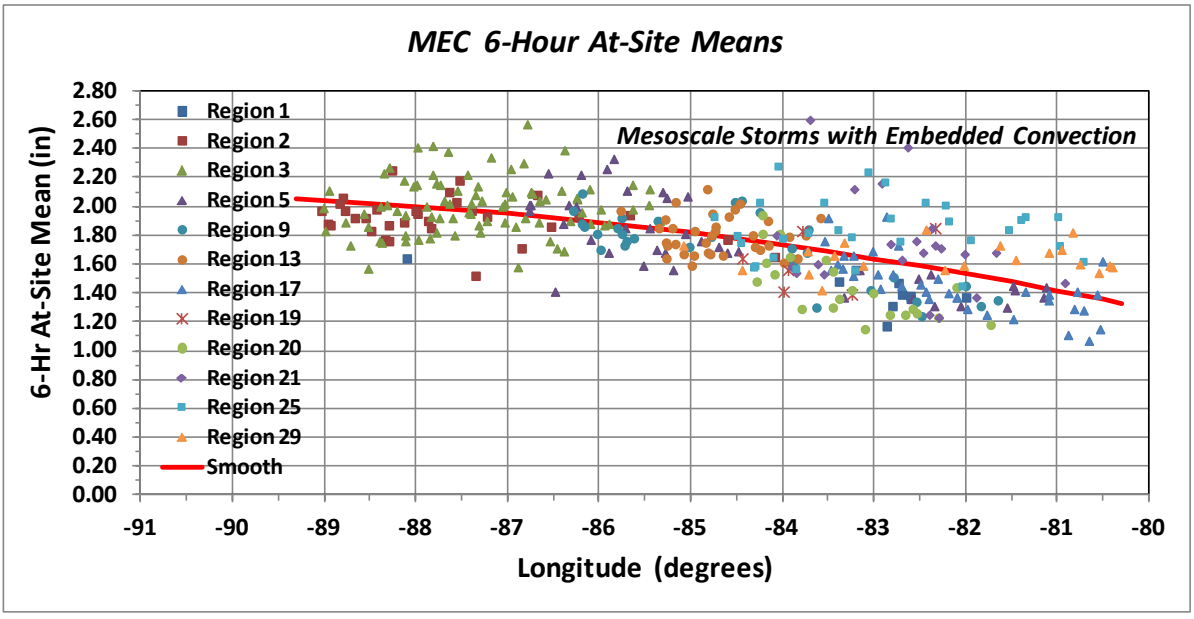


***Figure 54 -Scatterplot of Station Sample Values of 6-Hour At-Site Means for MECs***

Collections of stations from adjacent climatic regions were grouped for regional analysis where they exhibited similar behavior. Multiple linear regression methods were used for the collections of stations, which resulted in the form of the mathematical relationship shown in ***Equation 6***. ***Table 15*** lists the coefficients for the multiple regression solution and the resultant RMSE for the various groupings of climatic regions. The resultant multiple linear regression equations were used to generate the mapped values of 6-hour at-site means. Minor smoothing was conducted in the vicinity of regional boundaries to provide a

smooth continuum of precipitation. Best-estimates of the at-site means were computed as a weighted-average of the station sample values and regression predicted values, as discussed in ***Section 7.7***. ***Figure 55*** and ***Figure 56*** depict examples of comparisons of station sample values and mapped values of the 6-hour at-site means for areas within and near the Tennessee Valley lowlands. The mapped values of the 6-hour at-site means (***Figure 56***) are unbiased and have a RMSE of 6.7%. The spatial map of 6-hour at-site means for MECsis shown in ***Figure 57***.

***Table 15 - Listing of Coefficients for Multiple Linear Regression for 6-Hour At-Site Means for MECs and RMSE for Predictive Equations***

| CLIMATIC REGIONS | MULTIPLE REGRESSION COEFFICIENTS $AtSiteMean_{MEC} = \alpha_0 + \alpha_1 Longitude + \alpha_2 MonthlyPrecip_{Jun\text{-}Aug}$ | | | RMSE |
|---|---|---|---|---|
| | $\alpha_0$ | $\alpha_1$ | $\alpha_2$ | |
| 1 – 2 - 3 | -8.3508 | -0.10244 | 0.11086 | 9.4% |
| 5 – 9 – 13 – 17 -18 | -9.4444 | -0.12570 | 0.04525 | 9.7% |
| 19 – 20 - 21 | -6.2325 | -0.08062 | 0.07739 | 12.1% |
| 25 -29 | 1.5921 | 0.00904 | 0.06621 | 8.1% |
| **All Regions** | **Final Mapping** | | | **6.7%** |

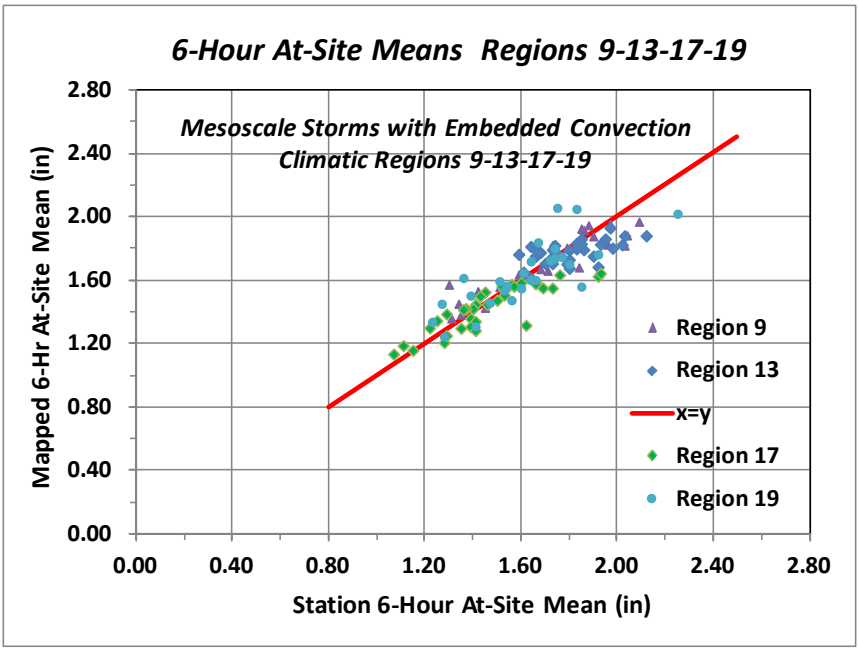


***Figure 55 - Comparison of Station Values and Mapped Values of 6-Hour At-Site Means for Tennessee Valley Lowlands (Climatic Regions 9, 13, 17, 19) for MECs***

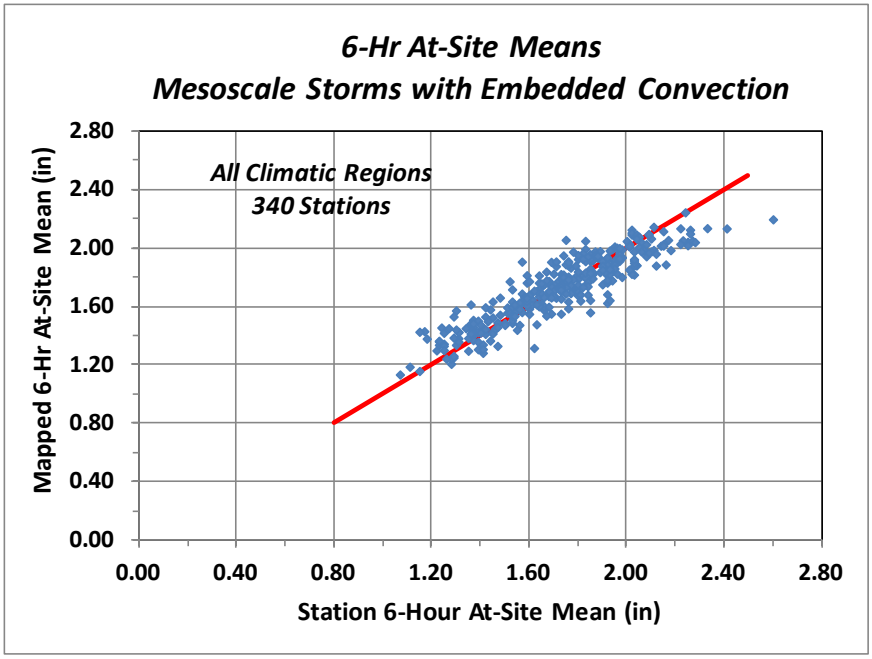


*Figure 56 - Comparison of Station Values and Mapped Values of 6-Hour At-Site Means for All Climatic Regions for MECs*

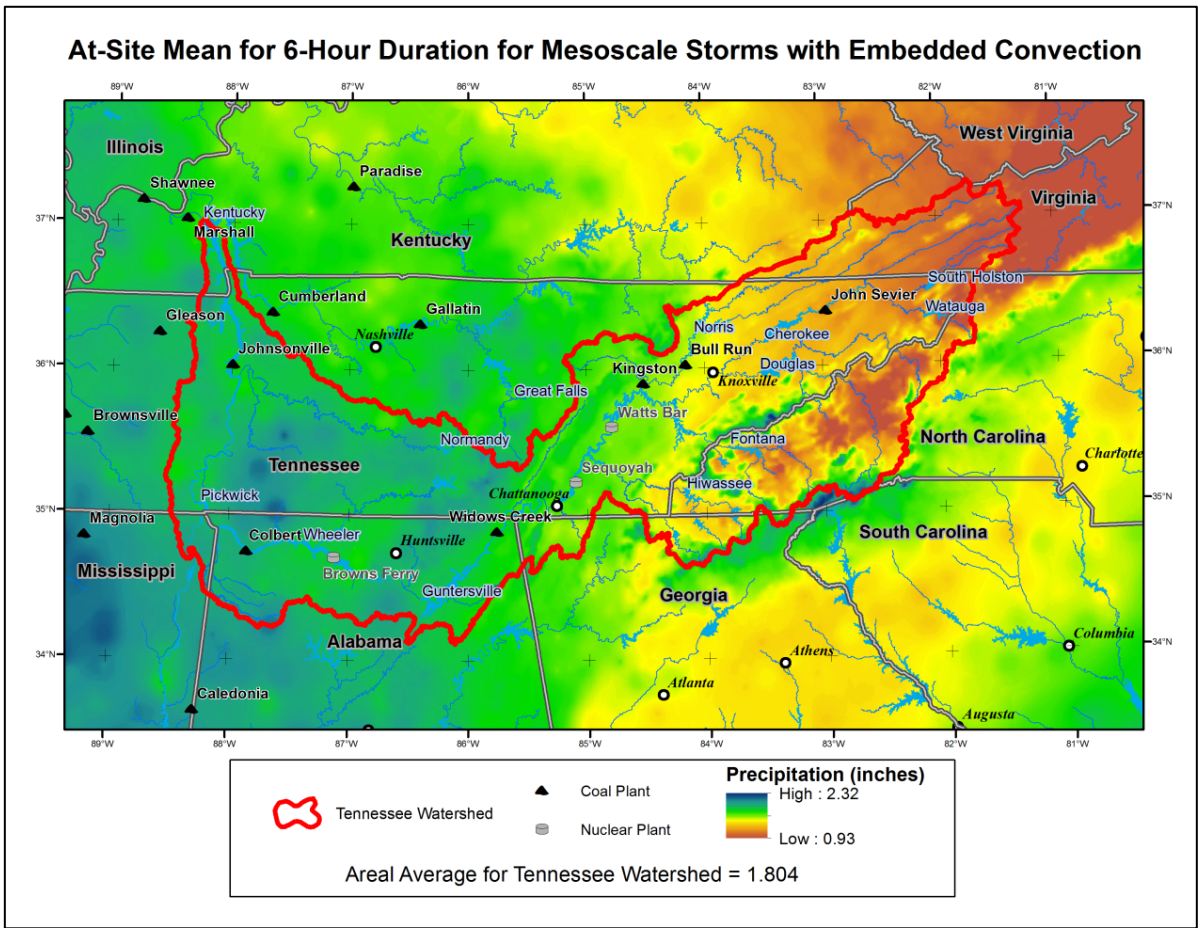


*Figure 57 - Map of At-Site Means for 6-Hour Duration for MECs*

## 9.2 Spatial Mapping of Regional Values of L-Cv and L-Skewness

Homogeneous sub-regions were formed as groupings of stations within a limited range of longitude for each climatic region. Stations were included that had a record length of 25 years or more. Eighteen sub-regions were formed in this manner, where each sub-region produced a regional L-Cv and L-Skewness value associated with a group-average longitude and group-average mean monthly June-August precipitation. All eighteen sub-regions were found to be acceptably homogeneous based on L-moment heterogeneity measures.

A review of the regional L-Cv values showed a systematic variation with longitude for groupings of stations within the Tennessee Valley watershed (***Figure 58***). Stations within the Tennessee Valley and to the northwest of the Blue Ridge Mountains (Climatic Regions 1 through 20) were grouped for analysis. Similarly, stations to the southeast of the Blue Ridge Mountains (Climatic Regions 21-29) were grouped for analysis. These eighteen regional values of L-Cv and L-Skewness were used in a multiple regression with longitude and June-August mean monthly precipitation as explanatory variables. ***Equation 10*** lists the multiple regression equation for regional L-Cv for Climatic Regions 1-20, and ***Equation 11*** lists the equation for regional L-Cv for Climatic Regions 21-29, where the RMSE for prediction of regional L-Cv was 3.7% (***Table 16***). The spatial mapping of regional L-Cv for the 6-hour duration is shown in ***Figure 59***, where regional L-Cv is seen to have moderate variation across the study area.

$$\text{L-Cv} = 2.3210 + 0.05071\text{Longitude} + 0.0003092\text{Longitude}^2 - 0.001984\text{MonthlyPrecip}_{\text{Jun-Aug}}$$

***(Equation 10)***

where: for Climatic Regions 1-20, set *Longitude* to -82.0 if *Longitude* > -82.0 and limit *L-Cv* to maximum of 0.2500; and

$$\text{L-Cv} = -10.2564 - 0.26406\text{Longitude} - 0.0001655\text{Longitude}^2 - 0.001854\text{MonthlyPrecip}_{\text{Jun-Aug}}$$

***(Equation 11)***

where: for Climatic Regions 21-29, set *Longitude* to -81.0 if *Longitude* > -81.0 and limit *L-Cv* to range of $0.2225 \leq \text{L-Cv} \leq 0.2600$.

Development of a predictor equation for L-Skewness is more difficult than for L-Cv because of the naturally high sampling variability for skewness measures. The prediction of regional L-Skewness was accomplished using linear regression for regional L-moment L3 as a function of regional L-moment L2 (***Equation 12***) for the 18 homogeneous sub-regions. Use of the Index Flood methodology provides for a prediction of regional L-Skewness using ***Equation 13*** because regional L-Cv is equal to regional L2 for indexed annual maxima datasets. ***Figure 60*** depicts the regression solution for regional L3, and ***Table 16*** lists the summary statistics for mapping of regional L-Skewness, where the RMSE is 9.9%. ***Figure 61*** shows the spatial mapping of regional L-Skewness, which is seen to have moderate variation across the study area.

$$L3 = -0.04031 + 0.40844 * L2 \qquad \textbf{(Equation 12)}$$

$$\text{L-Skewness} = 0.40844 - 0.04031/\text{L-Cv} \qquad \textbf{(Equation 13)}$$

***Table 16 - Summary Statistics for Spatial Mapping of 6-Hour Duration Regional L-Cv and L-Skewness for MECs***

| L-MOMENT RATIO | RANGE OF MAPPED L-MOMENT RATIO | STANDARD DEVIATION OF RESIDUALS | RMSE |
|---|---|---|---|
| Regional L-Cv | $0.1975 \leq \text{L-Cv} \leq 0.2600$ | 0.0082 | 3.7% |
| Regional L-Skewness | $0.2045 \leq \text{L-Skewness} \leq 0.2535$ | 0.0222 | 9.9% |

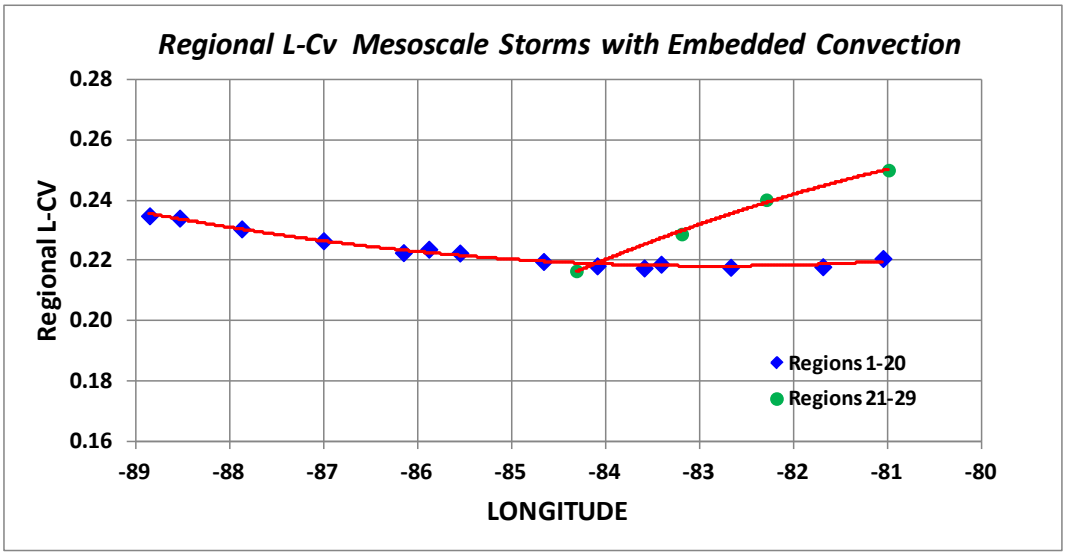


*Figure 58 - Example of Variation of Regional L-Cv with Longitude for 18 Homogeneous Sub-Regions for 6-Hour Duration MECs*

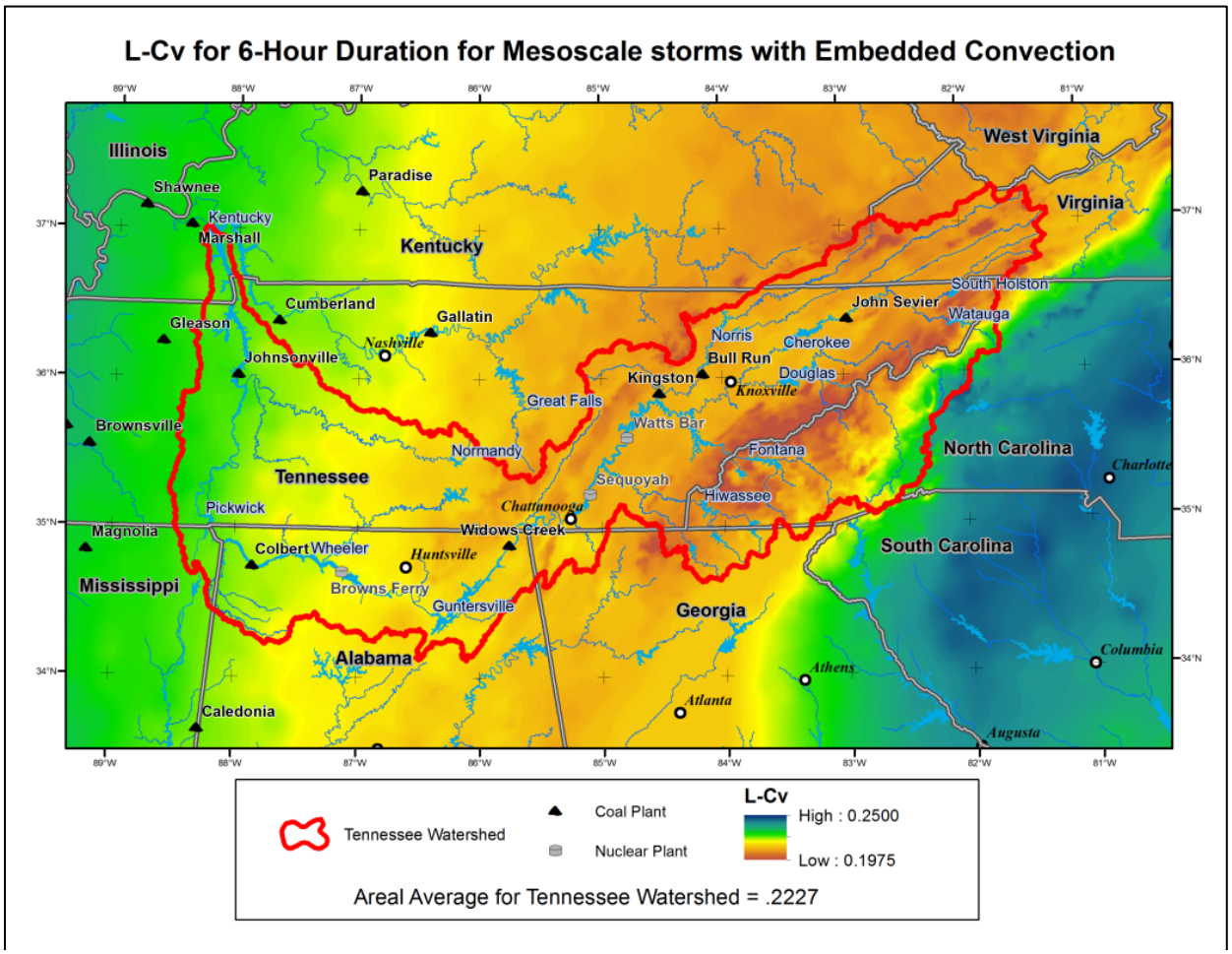


*Figure 59 - Map of Regional L-Cv for 6-Hour Duration for MECs*

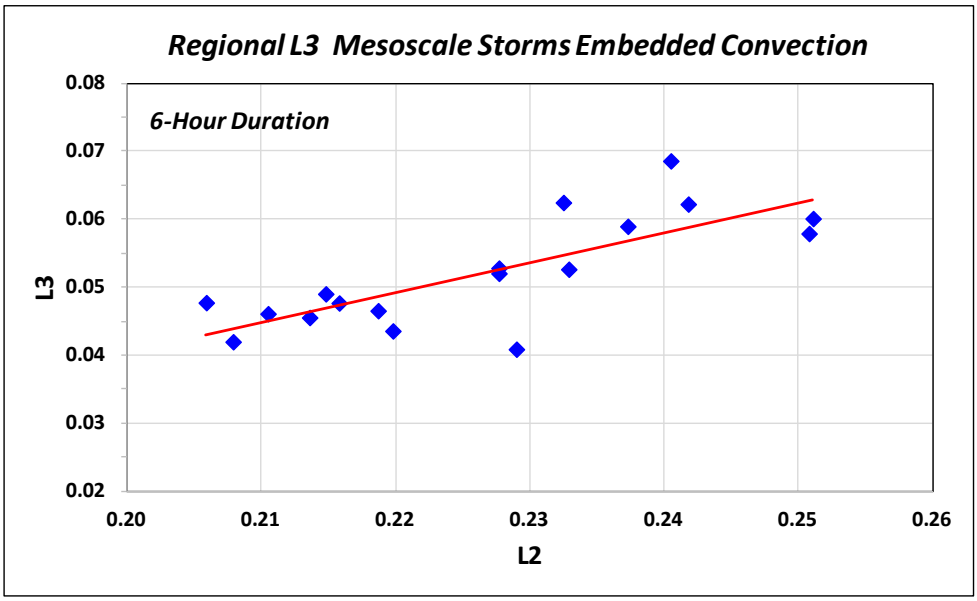


*Figure 60 - Predictor Equation for Regional L-Moment L3 as a Function of Regional L-Moment L2 for 6-Hour Duration for 16 Homogeneous Sub-Regions for MECs*

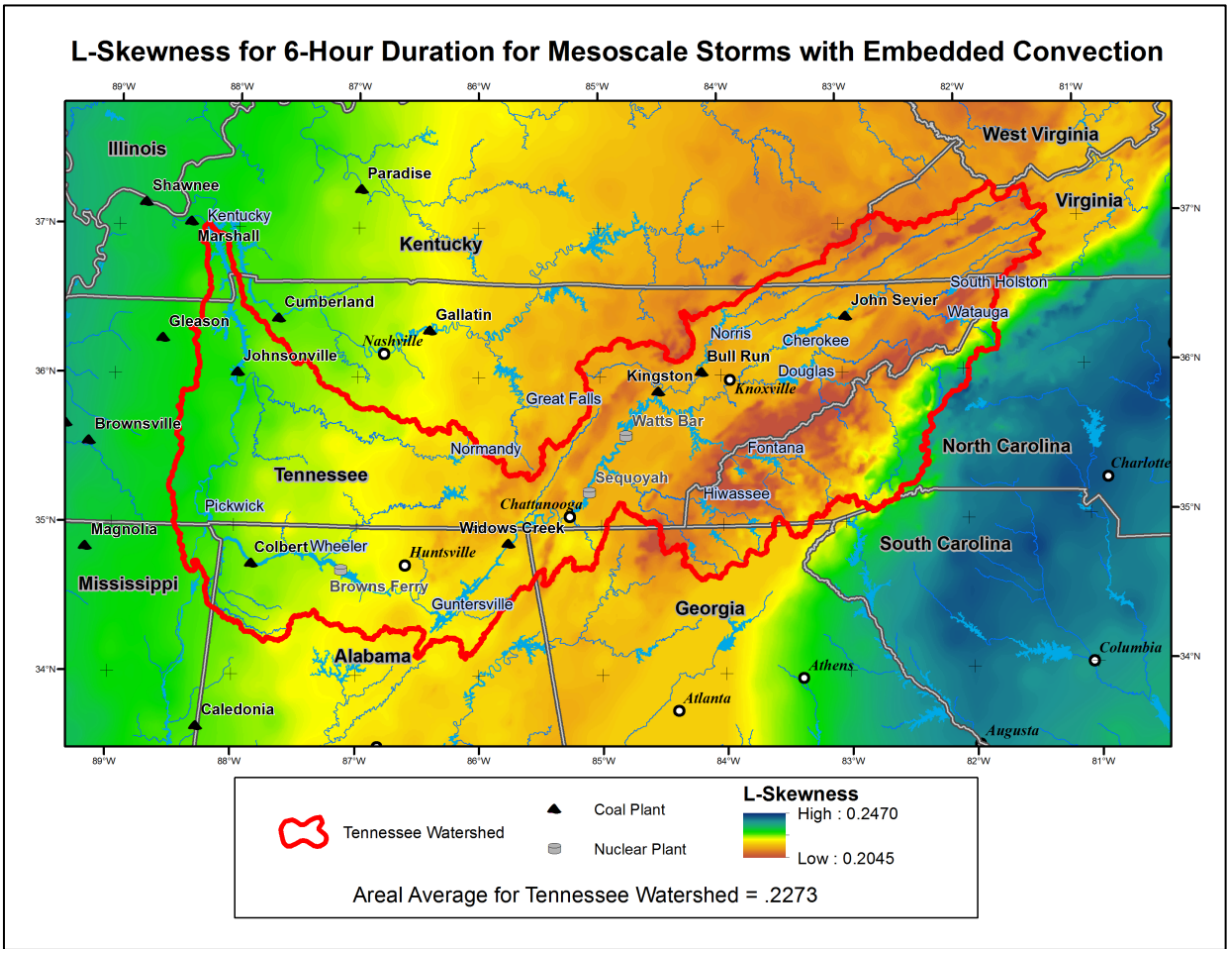


*Figure 61 - Map of Regional L-Skewness for 6-Hour Duration for MECs*

## 9.3 Identification of Regional Probability Distribution

L-moment goodness-of-fit tests were conducted for each of the 18 homogeneous sub-regions, and the GEV distribution was identified as the best-fit 3-parameter probability distribution for the collection of sub-regions. A review of ***Figure 62*** shows the centroid of the cluster of L-Skewness and L-Kurtosis pairs for the 18 sub-regions to be very near the GEV distribution. The scatter in data along the GEV curve is partially due to the spatial variation in L-Skewness as seen in Figure 61. As discussed previously, the 4-parameter Kappa distribution with a fixed shape parameter (*h*) emulates the GEV and near-GEV distributions and was selected for describing the point precipitation-frequency relationships for MECs. A shape parameter (*h*) value of 0.05 (***Equation 2***) was identified as the best-fit for describing the MEC storm type, which resides just below the GEV curve.

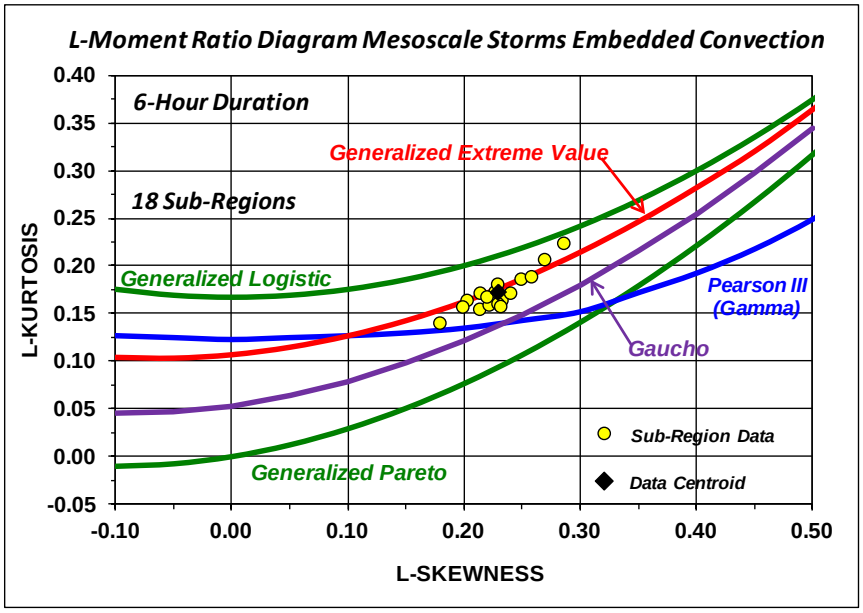


***Figure 62 - L-Moment Ratio Diagram Depicting Regional L-Skewness and L-Kurtosis Values for Homogeneous Sub-Regions for 6-Hour Duration for MECs***

## 9.4 Isopluvial Mapping for 6-Hour Duration for Selected Annual Exceedance Probabilities

The gridded datasets for the 6-hour at-site means (***Figure 57***), regional L-Cv (***Figure 59***) and regional L-Skewness (***Figure 61***) and the 4-parameter Kappa distribution with *h*=0.05 provided the information necessary to develop gridded datasets of 6-hour precipitation for selected Annual Exceedance Probabilities (AEPs). A precipitation-frequency curve for the station at McGhee Tyson Field was developed in the manner described above and compared with a probability plot of historical data (***Figure 63***). This provides an example of the general shape of the precipitation-frequency relationship for MEC storm types.

The areal average at-site mean (***Figure 57***), regional L-Cv (***Figure 59***) and regional L-Skewness (***Figure 61***) were used to develop a representative point precipitation-frequency relationship for the Tennessee Valley watershed (***Figure 64***). Note for this calculation, the Tennessee Valley watershed included the area upstream of Great Falls Dam. This relationship provides some insight into the expected behavior of 6-hour precipitation for extreme precipitation events for MECs.

Isopluvial gridded datasets were generated for AEPs of $10^{-1}$,$10^{-2}$, $10^{-3}$, $10^{-4}$ and $10^{-5}$ and isopluvial maps are shown in ***Appendix J***. ***Figure 65*** shows an example isopluvial map for an AEP of 1:1,000.

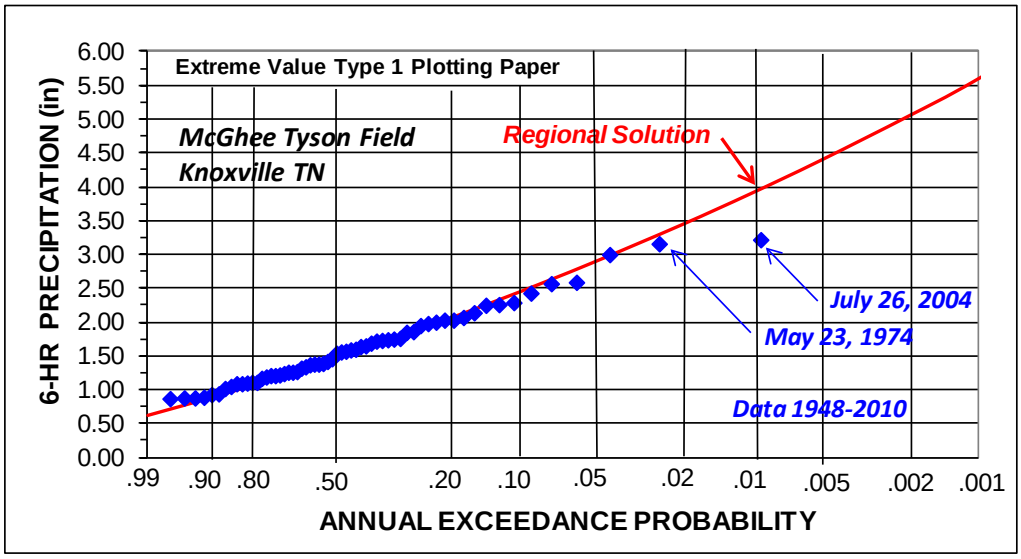


*Figure 63 - Probability plot of Historical 6-Hour Precipitation Annual Maxima for MECsfor McGhee Tyson Field Knoxville, TN and Comparison with Regional Precipitation-Frequency Curve*

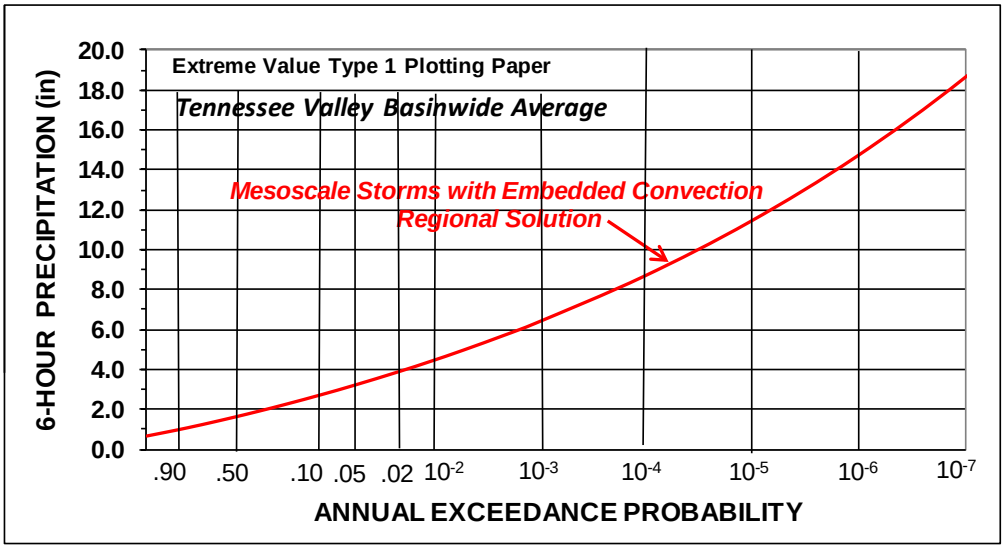


*Figure 64 - Point 6-Hour Precipitation-Frequency Relationship for Tennessee Valley Average Parameters for MECs*

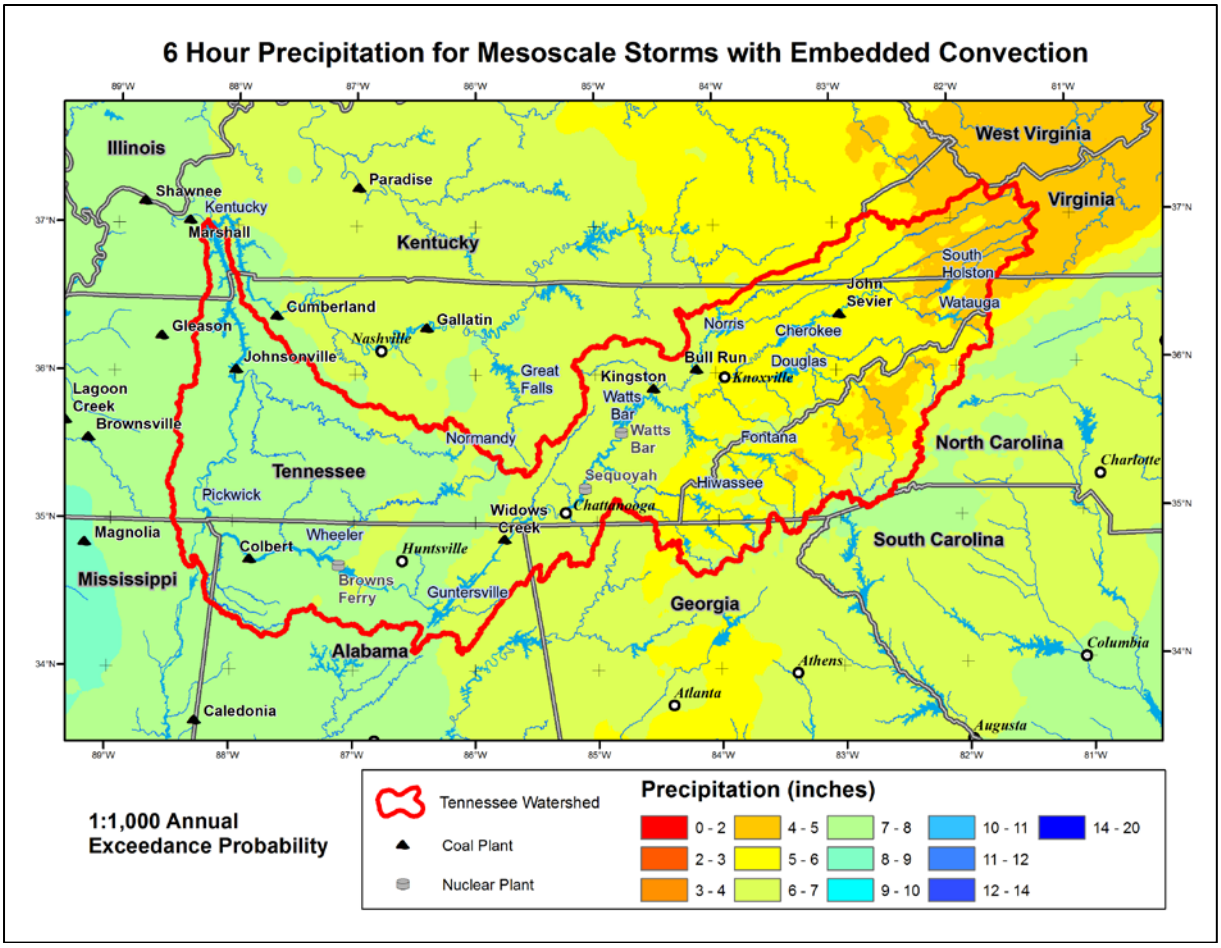


***Figure 65 - Isopluvial Map of 6-Hour Precipitation Maxima for an AEP of 1:1,000 for MECs***

## 9.5 Seasonality of Extreme Storms for Mesoscale Storms with Embedded Convection

An initial perspective on the seasonality of MECs was obtained by using the DDST to develop a frequency histogram of days when MEC events occurred (***Figure 66***). This frequency histogram includes many days with precipitation totals that are smaller than the precipitation annual maxima, and is therefore representative of the full range of daily precipitation.

The seasonality analysis for MECs was conducted using 6-hour precipitation annual maxima. The focus was on the rarest storms; a dataset of 46 noteworthy storms was assembled where 6-hour precipitation exceeded a 10-year recurrence interval at 4 or more stations.

The calendar storm dates were converted to numerical storm dates, where calendar dates were converted to numerical storm dates by expressing the day as a ratio of the total days of the month such that July 7 equates to 7.23 to allow for frequency analysis. Computation of sample statistics resulted in a mean of July 16$^{th}$ and a standard deviation of 1.71 months. A probability plot was assembled using the 46 numerical storm dates, and a 4-parameter Beta distribution was fitted to the data (***Figure 67***). The 4-parameter Beta distribution was then used to create a frequency histogram for the seasonality of extreme 6-hour duration MECs (***Figure 68***). A comparison of ***Figure 66*** and ***Figure 68*** shows the seasonality for extreme storms to more dispersed across the warm season than for common storms.

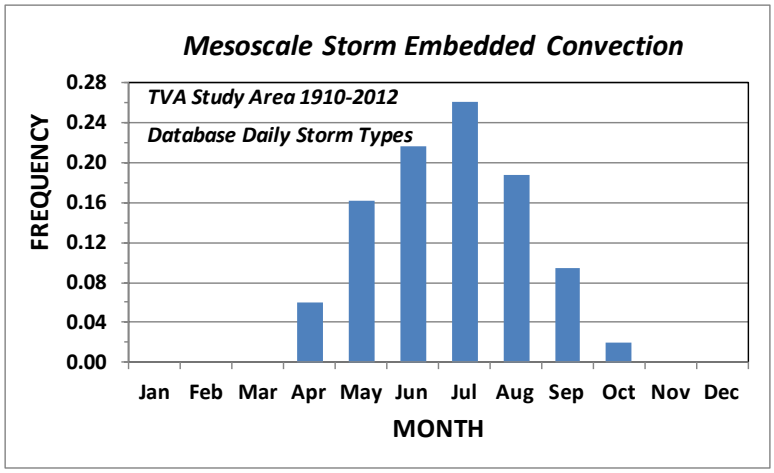


*Figure 66 - Seasonal Frequency Histogram for Days When MECsStorm Events Have Occurred 1910-2012*

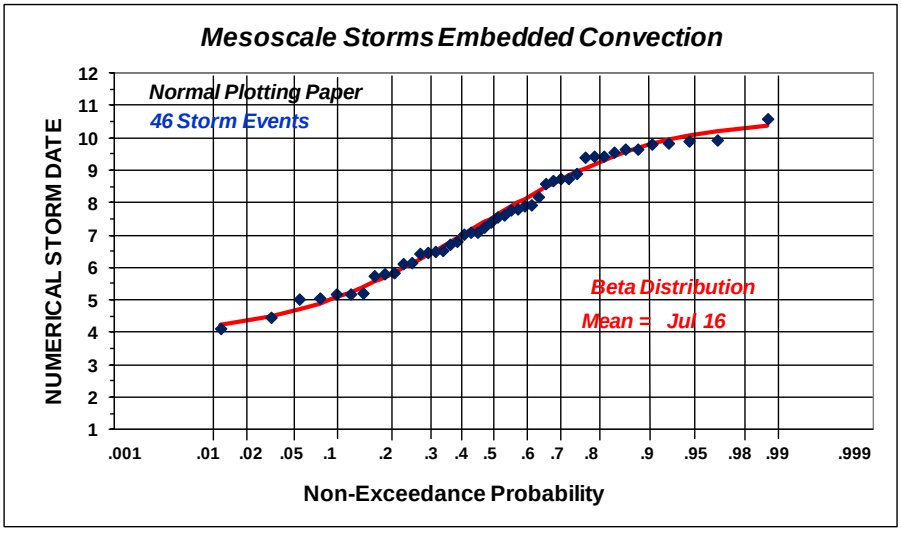


*Figure 67 - Probability plot of Numerical Storm Dates for 6-Hour Duration MECs*

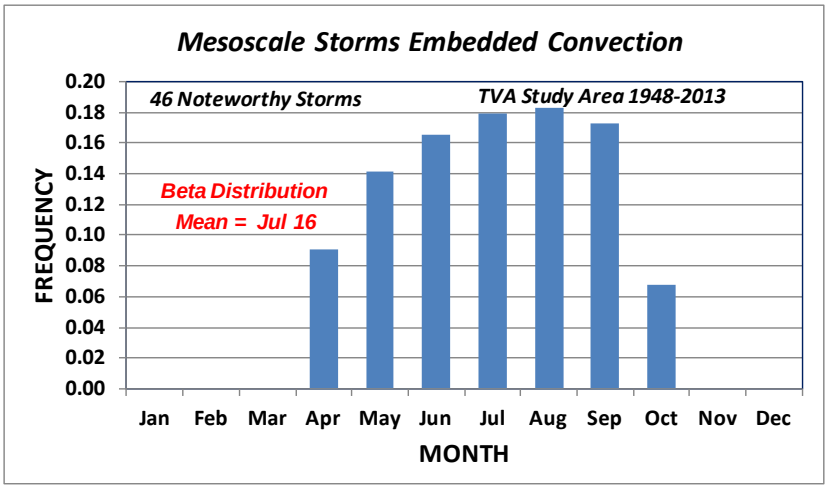


*Figure 68 - Frequency Histogram for Seasonality of Extreme 6-Hour Duration MECs*

## 9.6 Equivalent Independent Record Length (EIRL) for Mesoscale Storms Embedded Convection

Two methods were used to estimate EIRL. The first method was a frequency-based method using the upper 10% of 6-hour precipitation annual maxima at each station. The second method utilized counting of independent storm dates for all storm events.

The frequency-based method was conducted in the manner described in ***Appendix H***, where the upper 10% of precipitation annual maxima at the stations were examined. ***Figure 69*** shows the plotting-position representation of EIRL. The frequency-based method resulted in an estimate of 5,800 years for EIRL relative to the 13,611 station-years of record. The storm counting method resulted in an EIRL estimate of 2,690 years. The best estimate of EIRL was taken as the geometric mean of the two estimates (***Table 17***).

| Station-Years of Record | EIRL Estimates (Years) | | | EIRL Percent of Station-Years |
|---|---|---|---|---|
| | Frequency Based | Storm Count | Geometric Mean | |
| 13,611 | 5,800 | 2,690 | 3,950 | 29.0% |

***Table 17 - Estimates of EIRL for 6-Hour Duration for MECs***

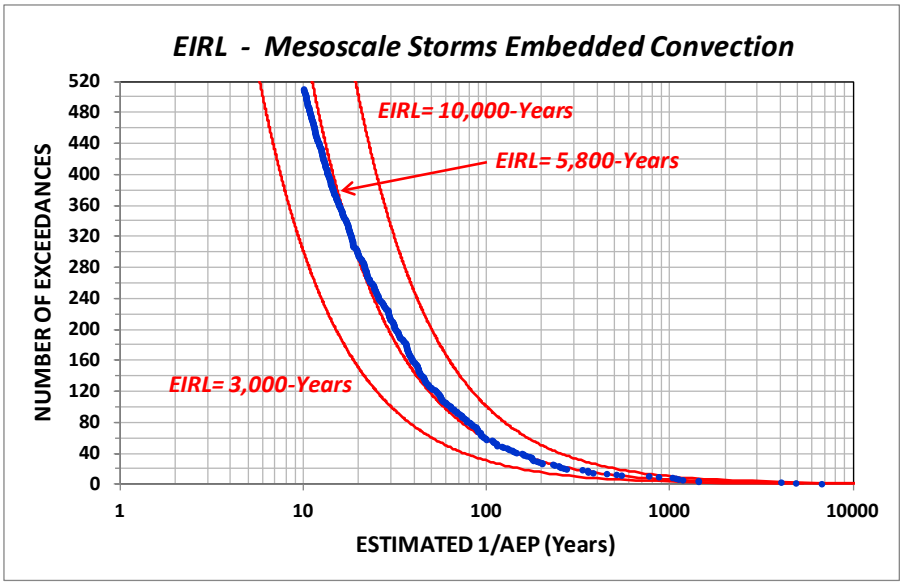


***Figure 69 - Graphical Depiction of EIRL for 6-Hour Duration MECs***

## 9.7 2-Hour and 12-Hour Precipitation Annual Maxima for Mesoscale Storms Embedded Convection

Precipitation annual maxima datasets were also assembled for the 2-hour and 12-hour durations for MECs. These datasets were assembled to provide information on the variation of temporal storm characteristics across the TVSA, and to provide additional data for identification of the regional probability distribution.

### 9.7.1 Depth-Duration Ratios for 2-Hour, 6-Hour and 12-Hour At-Site Means

***Figure 70*** and ***Figure 71*** show the depth-duration ratio of observed at-site means for the 2-hour/ 6-hour durations for the MEC storm type and variation with longitude and June-August mean monthly precipitation, respectively. Similarly, ***Figure 72*** and ***Figure 73*** shows the depth-duration ratio of observed at-site means for the 12-hour/6-hour durations for the MEC storm type and variation with longitude and June-August mean monthly precipitation, respectively.

A review of ***Figure 70*** and ***Figure 72*** shows both the 2-hr/6-hr and 12-hr/6-hr depth-duration ratios do not vary significantly with longitude across the study area. However, both ***Figure 71*** and ***Figure 73*** show a minor trend with June-August mean monthly precipitation (***Figure 52***). These trends are interpreted as having greater 6-hour and 12-hour precipitation in orographic areas that are climatologically wetter in the summer months.

Typical depth-duration curves were prepared to show the differences in depth-duration behavior between the majority of the study area and for climatologically wetter areas. A review of ***Figure 71*** shows the majority of sites to be in the range of 10-14-inches of mean monthly June-August precipitation (***Figure 52***) and the wetter sites to be near 20-inches of mean monthly June-August precipitation. ***Figure 74*** depicts the typical depth-duration curves for these two representative sites. The similarity in these depth-duration curves indicates that the storm-specific depth-duration curves for historical storms are transpositionable throughout the study area with minor adjustments to accommodate climatologically wetter areas which are usually for orographic sites. These temporal storm characteristics should be considerations in developing temporal storm patterns for the MEC storm type for hydrologic applications at locations throughout the study area.

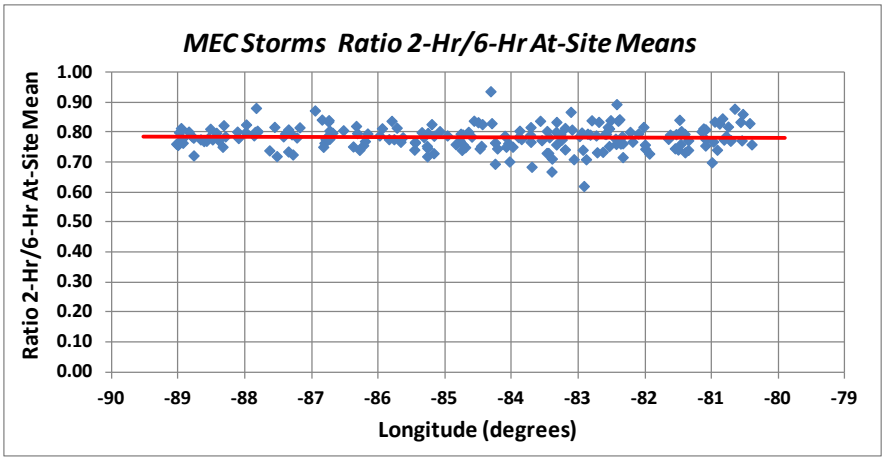


***Figure 70 - Variation with Longitude for the Ratio of 2-Hour to 6-Hour At-Site Means for MECs***

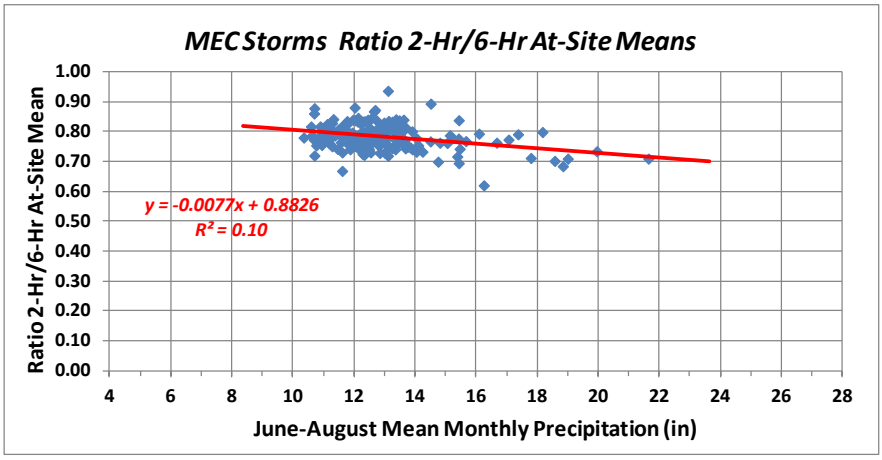


***Figure 71 - Variation with June-August Mean Monthly Precipitation for the Ratio of 2-Hour to 6-Hour At-Site Means for MECs***

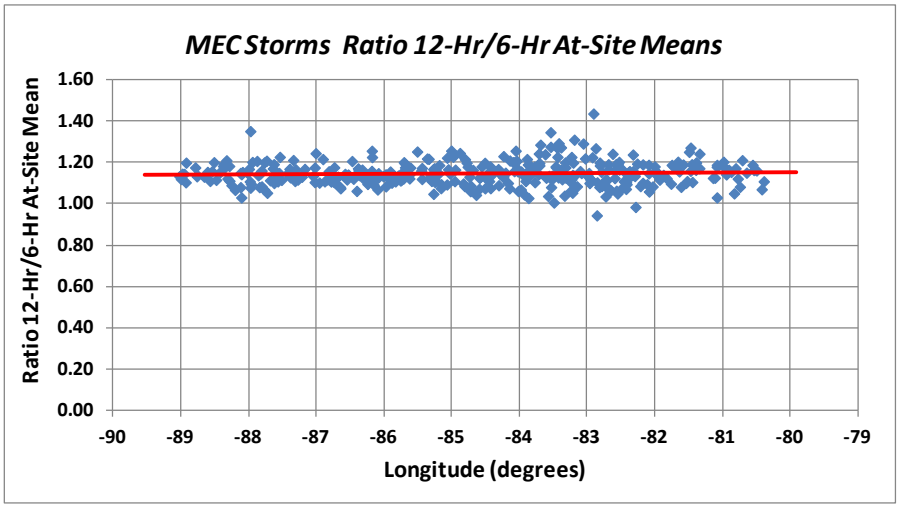


*Figure 72 - Variation with Longitude for the Ratio of 12-Hour to 6-Hour At-Site Means for MECs*

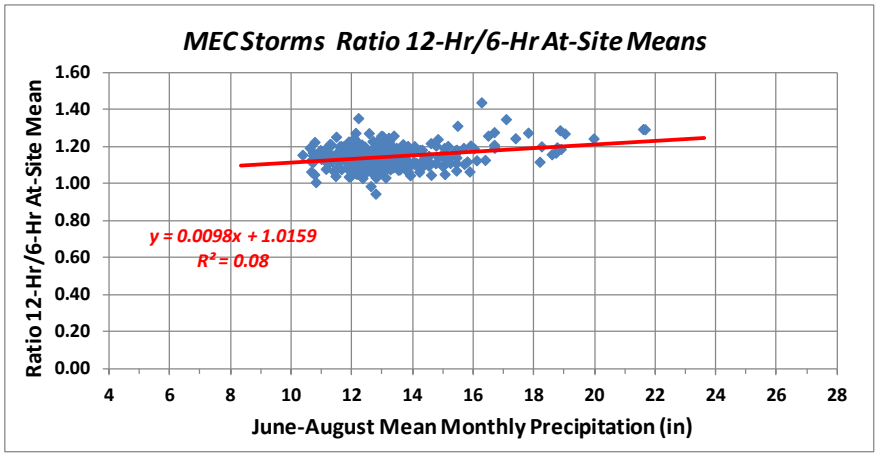


*Figure 73 - Variation with June-August Mean Monthly Precipitation for the Ratio of 12-Hour to 6-Hour At-Site Means for MECs*

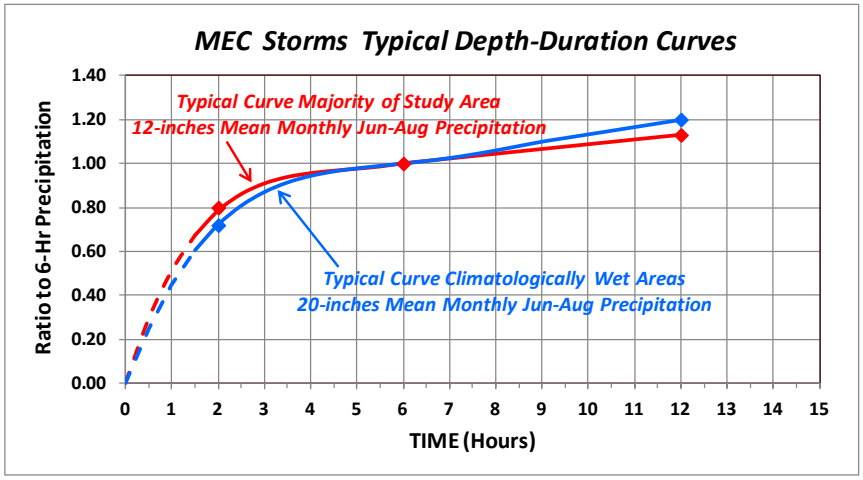


*Figure 74 - Typical Depth-Duration Curves for MECs*

### 9.7.2 Identification of Regional Probability Distribution for 2-Hour and 12-Hour Durations

L-moment regional frequency analyses were conducted for homogeneous sub-regions for the 2-hour and 12-hour durations in the manner described previously for the 6-hour key duration. These analyses were conducted to provide regional L-Skewness and L-Kurtosis pairings for identification of the regional probability distributions for the 2-hour and 12-hour durations.

***Figure 75*** and ***Figure 76*** depict the L-Skewness and L-Kurtosis pairings for the homogeneous sub-regions for the 2-hour and 12-hour durations, respectively. For both durations, the data are clustered around the GEV distribution in a pattern similar to that seen for the 6-hour key duration (***Figure 62***). This is further demonstrated in ***Figure 77***, where the region-wide L-Skewness and L-Kurtosis pairings for the three durations (centroids of data clusters in ***Figure 62***, ***Figure 75***, and ***Figure 76***) are quite near to each other and the GEV distribution.

These findings provide additional support that the regional probability distribution for the MEC storm type is very near to the GEV distribution. Specifically, these findings support selection of the 4-parameter Kappa distribution with the 2nd shape parameter (*h*) equal to 0.05, which would lie on a curve parallel and just below the GEV curve shown in the L-moment ratio diagrams.

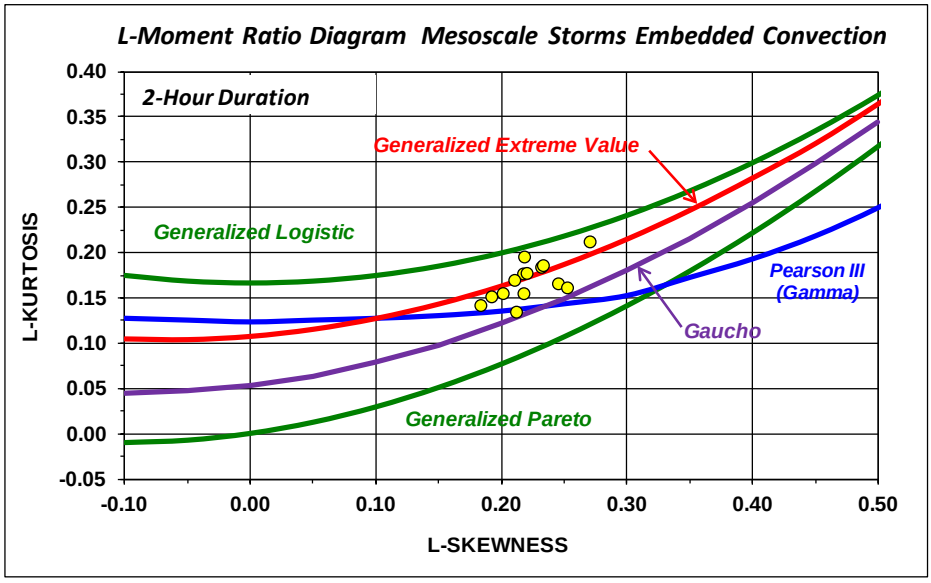


***Figure 75 - L-Moment Ratio Diagram Depicting Regional L-Skewness and L-Kurtosis Values for Homogeneous Sub-Regions for 2-Hour Duration for MECs***

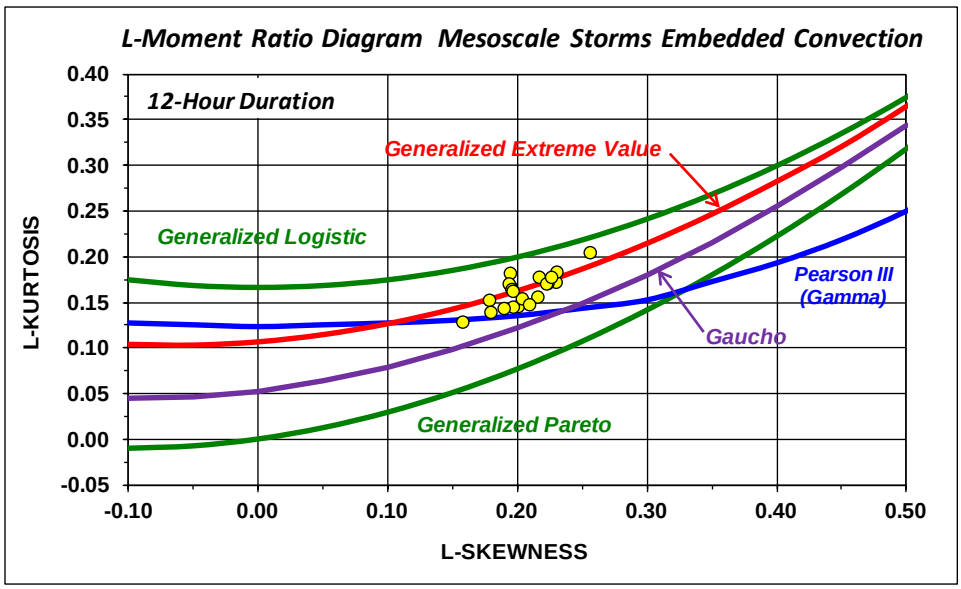


*Figure 76 -L-Moment Ratio Diagram Depicting Regional L-Skewness and L-Kurtosis Values for Homogeneous Sub-Regions for 12-Hour Duration for MECs*

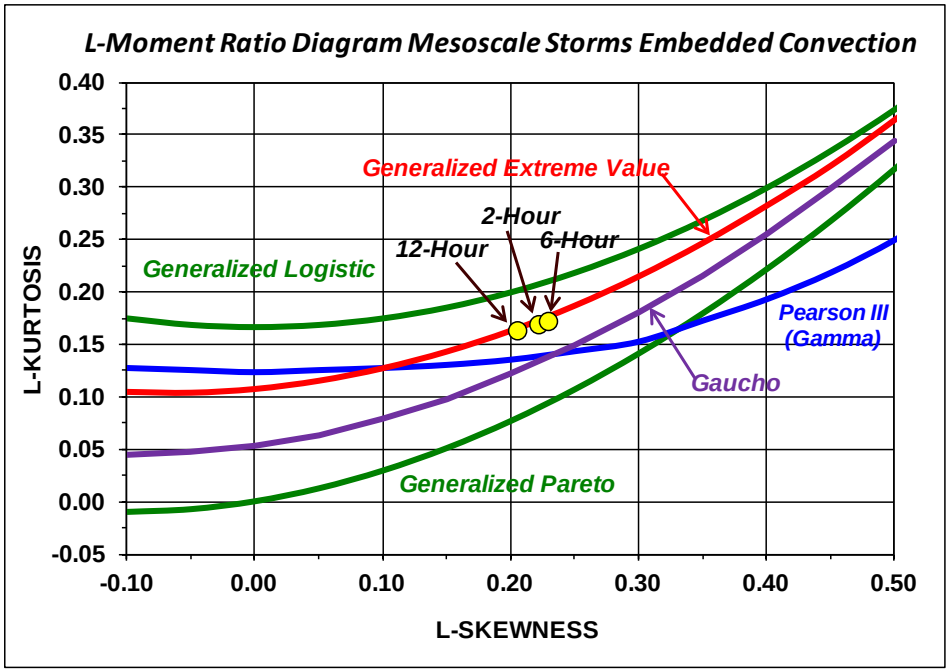


*Figure 77 - L-Moment Ratio Diagram Depicting Regionwide L-Skewness and L-Kurtosis Values for 2-Hour, 6-Hour and 12-Hour Durations for MECs*

# 10 Local Storms and Storm Types with Embedded Convection - Point Precipitation-Frequency

The primary application for short-duration high-intensity precipitation at the TVA will be in flood hazard analysis at nuclear plant sites where a thunderstorm could generate localized flooding on small, highly developed sites where there are extensive impervious surfaces. This is termed Local Intensity Precipitation (LIP) analyses in the nuclear industry.

Thunderstorm cells and associated convective storm activity can occur in a variety of meteorological environments. This situation was addressed by allowing a number of storm types and sub-types to provide candidates for 1-hour and 2-hour precipitation annual maxima. Specifically, the 1-hour and 2-hour annual maxima were obtained from the greatest precipitation amounts produced in the April 1st through October 30th time frame by any of the storm types or sub-types with convective activity within the AMS extraction zone (***Figure 11***) where the station was located. This included storm types and sub-types of LSs, MECs, and TSR/EC. This group of storm types and sub-types is termed Convective Storms in this section.

## 10.1 Precipitation Gages

Hourly gages were used in the regional analyses for 1-hour and 2-hour precipitation annual maxima for convective storms, where stations with 15 years or more of record were included in the analyses (***Figure 77***). ***Table 18*** provides a listing of the number of gages and total years of record used in the analysis of convective storms and ***Figure 78*** depicts a histogram of the number of years of record.

***Table 18 - Number of Stations/Gages and Station-Years of Record for Stations/Gages with 15 or More Years of Record Used in Precipitation-Frequency Analysis for Convective Storm Types***

| PRECIPITATION GAGE TYPE | NUMBER OF STATIONS/GAGES | STATION-YEARS OF RECORD | AVERAGE STATION-YEARS |
|---|---|---|---|
| NOAA Hourly Gages | 213 | 9,154 | 43.0 |

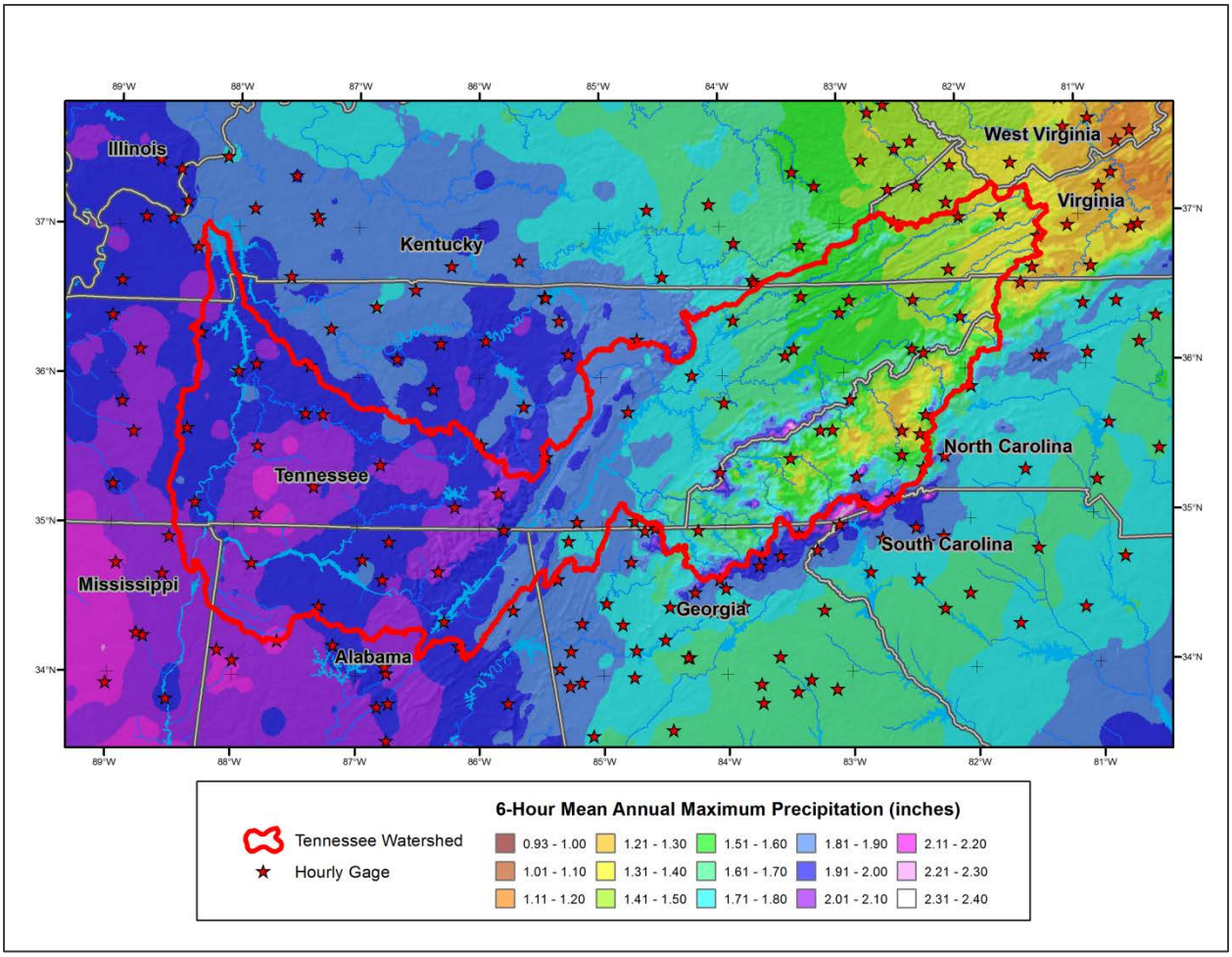


***Figure 78 - Location of Hourly Precipitation Gages Used in Precipitation-Frequency Analysis for Convective Storm Types***

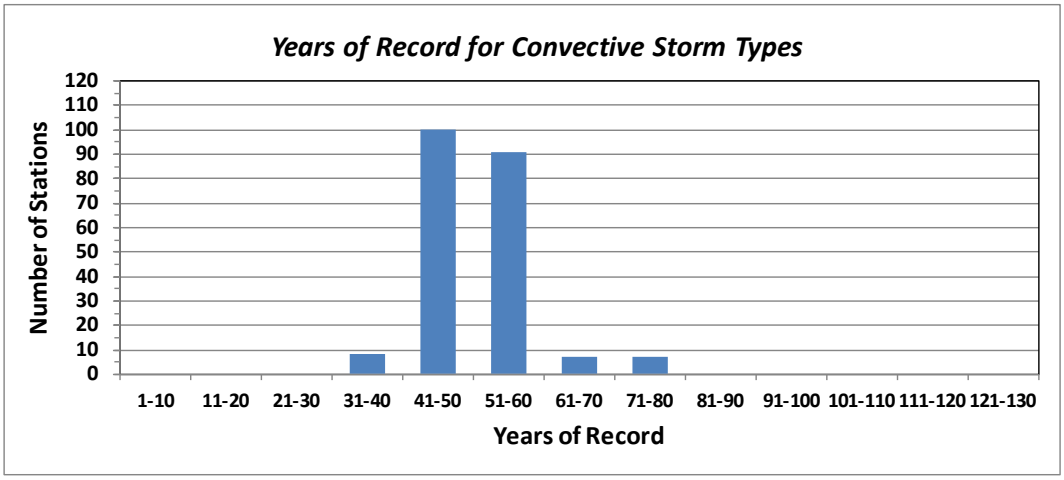


***Figure 79 - Histogram for Years of Record for Stations Used in Precipitation-Frequency Analysis for Convective Storm Types***

Spatial mapping of at-site means for 1-hour precipitation annual maxima for Convective Storm types was accomplished using data from stations with 15 years or more of record. Spatial mapping of 1-hour at-site means was conducted using the gridded dataset of 6-hour at-site means for MECs and longitude as the explanatory variables (***Figure 80***). In particular, it was reasonable to anticipate that the at-site means for

Convective Storm Types would have a similar spatial pattern to 6-hour at-site means for the MEC storm type.

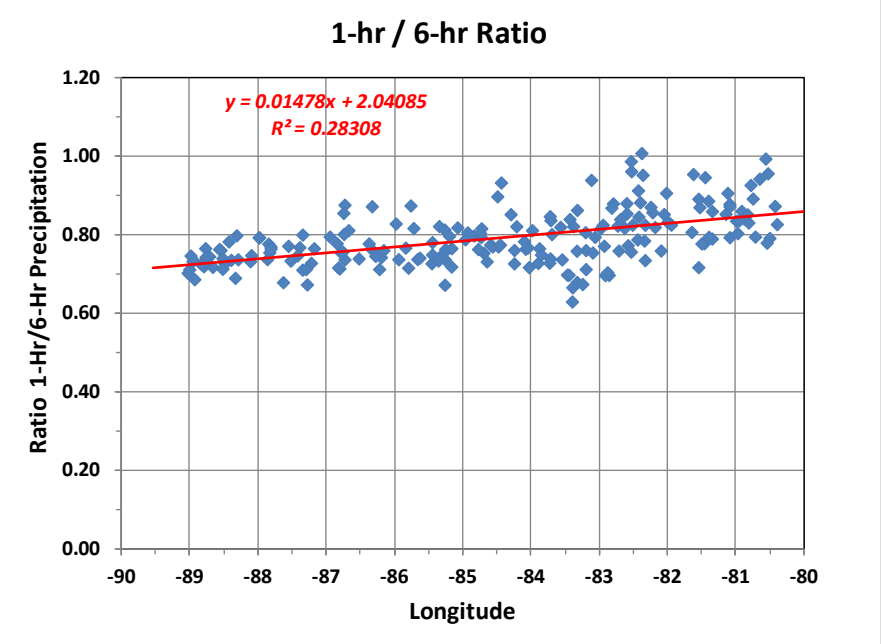


***Figure 80 - Scatterplot of Station Sample Values of the Ratio of 1-Hour Convective Storm At-Site Mean to 6-Hour MEC At-Site Mean Variation with Longitude***

The form of the multiple regression equation for prediction of the 1-hour at-site mean is listed in ***Equation 14***. The RMSE for the predictor equation was 9.5%. Best-estimates of the at-site means were computed as a weighted-average of the station sample values and regression predicted values as discussed in the prior section on mapping of at-site means. ***Figure 81*** depicts the comparison of station sample values and mapped values of the 1-hour at-site means, where the mapped values of the 1-hour at-site means are unbiased and have a RMSE of 4.0%. The spatial map of 1-hour at-site means for Convective Storms is shown in ***Figure 82***.

$$AtSiteMean_{CS1HR} = (18.775 + 0.40489 Longitude + 0.002271 Longitude^2) * AtSiteMean_{MEC6HR} \quad \textbf{(Equation 14)}$$

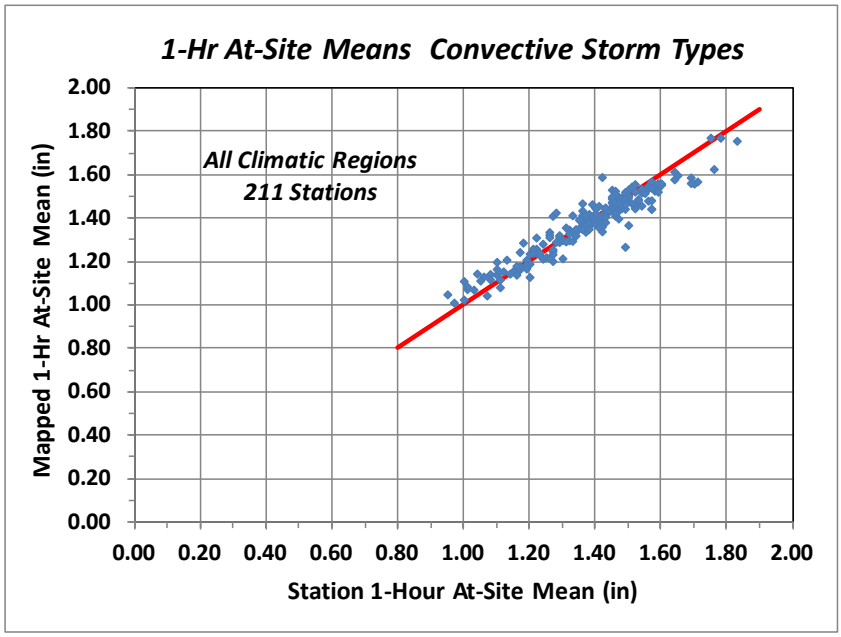


***Figure 81 - Comparison of Station Values and Mapped Values of 1-Hour At-Site Means for All Climatic Regions for Convective Storms***

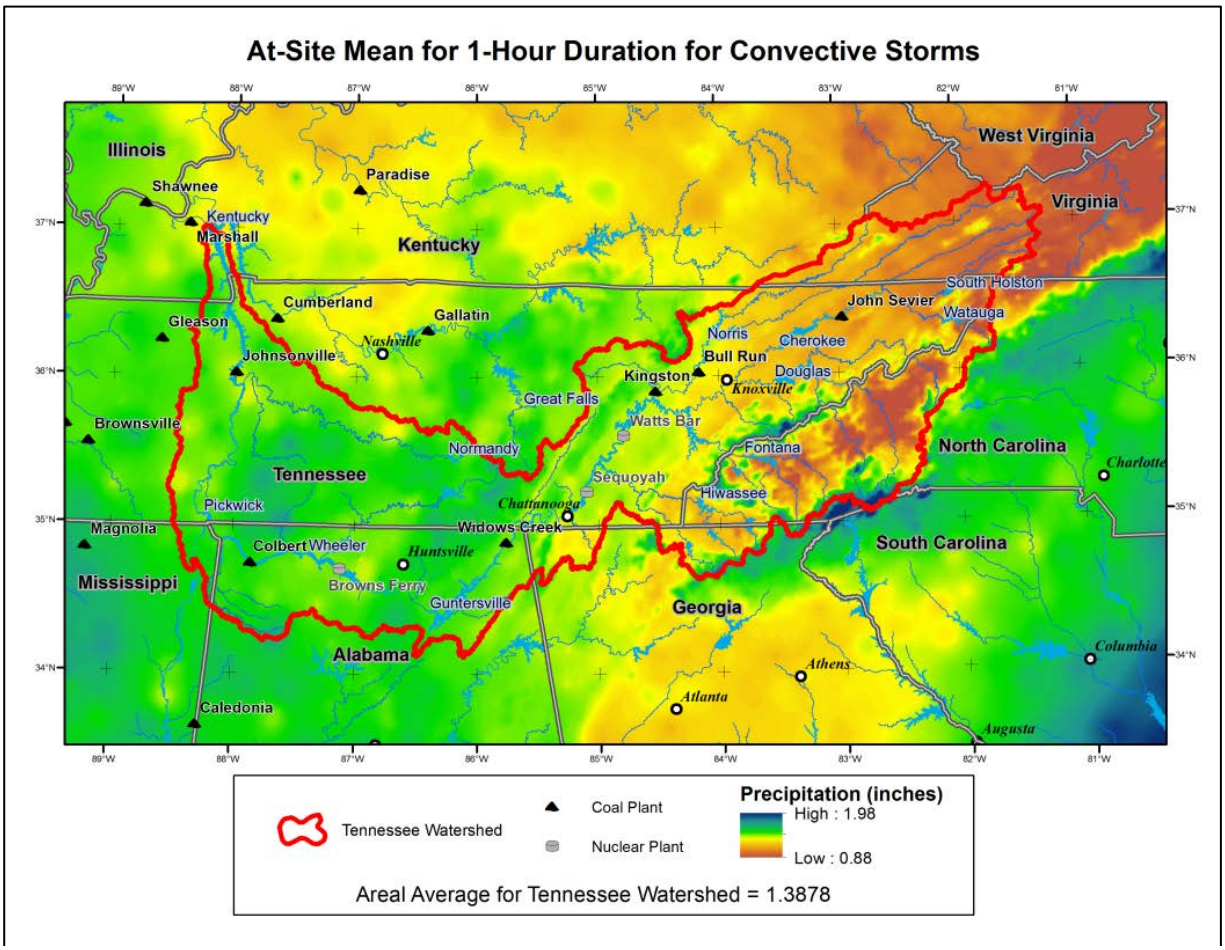


***Figure 82 - Map of At-Site Means for 1-Hour Duration for Convective Storms***

## 10.2 Considerations for Determining Regional L-Cv and Regional L-Skewness for 1-Hour Duration

The focus of this analysis is on precipitation annual maxima for the 1-hour duration. However, there are considerations in the system of measurement for 1-hour precipitation maxima that must be addressed in conducting the analysis. Specifically, hourly gages report on 1-hour intervals on the clock-hour rather than measurements taken on a continuous basis. Thus, it is common for the greatest precipitation in a continuous 60-minute period to be split between adjacent hourly reporting periods. This results in the apparent 1-hour maximum being under-reported relative to the true precipitation maximum for a continuous 60-minute period. This discrepancy is accounted for by an observational period adjustment factor (Weiss[28], ***Table 7*** and ***Table 8***), which for one observational period is an increase of 13% to the summary statistics for the mean and standard deviation. The measures of skewness and kurtosis for annual maxima obtained from one observational period are also biased and subject to greater sampling variability that are not accounted for by the adjustment factor. This situation is not highly significant when quantile estimates are of interest for more common events up to perhaps an AEP of 1:500. However, this is an important consideration when estimating very extreme AEPs.

The approach taken in this study was to use the results of the analysis of 1-hour annual maxima for estimating the 1-hour at-site mean and to use the 2-hour annual maxima for estimating the regional L-moment ratios L-Cv, L-Skewness and L-Kurtosis. Specifically, the 1-hour precipitation data constitute a time series of hourly precipitation values. The 2-hour annual maxima are computed by sliding a 2-hour window through the hourly time series and identifying the greatest total precipitation in adjacent hourly reporting periods. This procedure greatly reduces the problems that occur when precipitation is split into adjacent hourly reporting periods because the greatest precipitation amount in a continuous 1-hour period is captured within the 2-hour window. This approach is appropriate because thunderstorm precipitation is typically short-lived with the greatest intensities occurring over short periods, such that the true 2-hour annual maxima are typically not much greater than the true 1-hour annual maxima. In this description, “true” applies to the situation where precipitation measurements are made on a continuous basis where true 2-hour and 1-hour maxima would correspond to actual 120-minute and 60-minute continuous measurements, respectively. For the TVSA, the true 2-hour at-site mean is about 16% larger than the true 1-hour at-site mean. As such, the regional L-moment statistics for 2-hour annual maxima are expected to be more accurate measures of the regional statistics than regional L-moment statistics derived from 1-hour annual maxima, relative to what would be obtained for 1-hour annual maxima measured on a continuous basis.

## 10.3 Spatial Mapping of Regional Values of L-Cv and L-Skewness

Homogeneous regions were formed as groupings of stations within the thirteen Climatic Regions for determination of regional L-Cv and L-Skewness measures. Stations were included that had a record length of 25 years or more. Eleven sub-regions were formed in this manner and were found to be acceptably homogeneous based on L-moment heterogeneity tests measures.

A review of the regional L-Cv values showed a systematic variation with longitude (***Figure 83***). The regional values of L-Cv were used in a linear regression with longitude as the explanatory variable. ***Equation 15*** provides the regression equation for regional L-Cv for all sub-regions, where the RMSE for prediction of regional L-Cv was 2.1% (***Table 19***). The spatial mapping of regional L-Cv for the 1-hour duration is shown in ***Figure 84***, where regional L-Cv is seen to have only minor spatial variation across the study area.

$$L\text{-}Cv = 0.30480 + 0.001224 Longitude \qquad (\textbf{\textit{Equation 15}})$$

Examination of the spatial variability of L-Skewness found that L-Skewness could be considered a constant over the study area. ***Table 19*** lists the summary statistics for regional L-Skewness, where the RMSE is 11.0%.

***Table 19 - Summary Statistics for Spatial Mapping of 1-Hour and 2-Hour Duration Regional L-Cv and L-Skewness for Storm Types with Convection***

| L-MOMENT RATIO | RANGE OF MAPPED L-MOMENT RATIO | STANDARD DEVIATION OF RESIDUALS | RMSE |
|---|---|---|---|
| Regional L-Cv | 0.1950 ≤ L-Cv ≤ 0.2050 | 0.0042 | 2.1% |
| Regional L-Skewness | 0.2160 | 0.0234 | 11.0% |

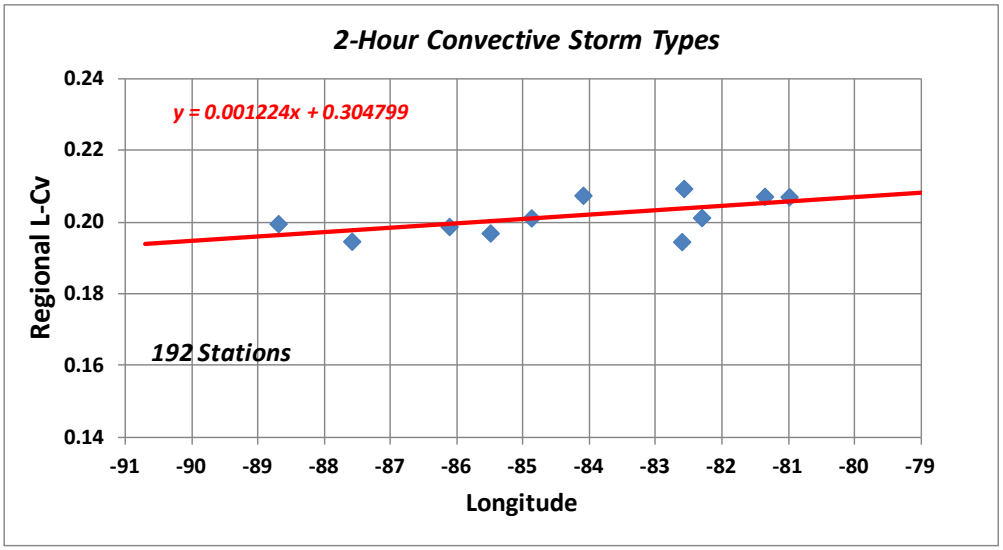


***Figure 83 - Variation of Regional L-Cv with Longitude for Climatic Regions for 2-Hour Duration for Convective Storm Types***

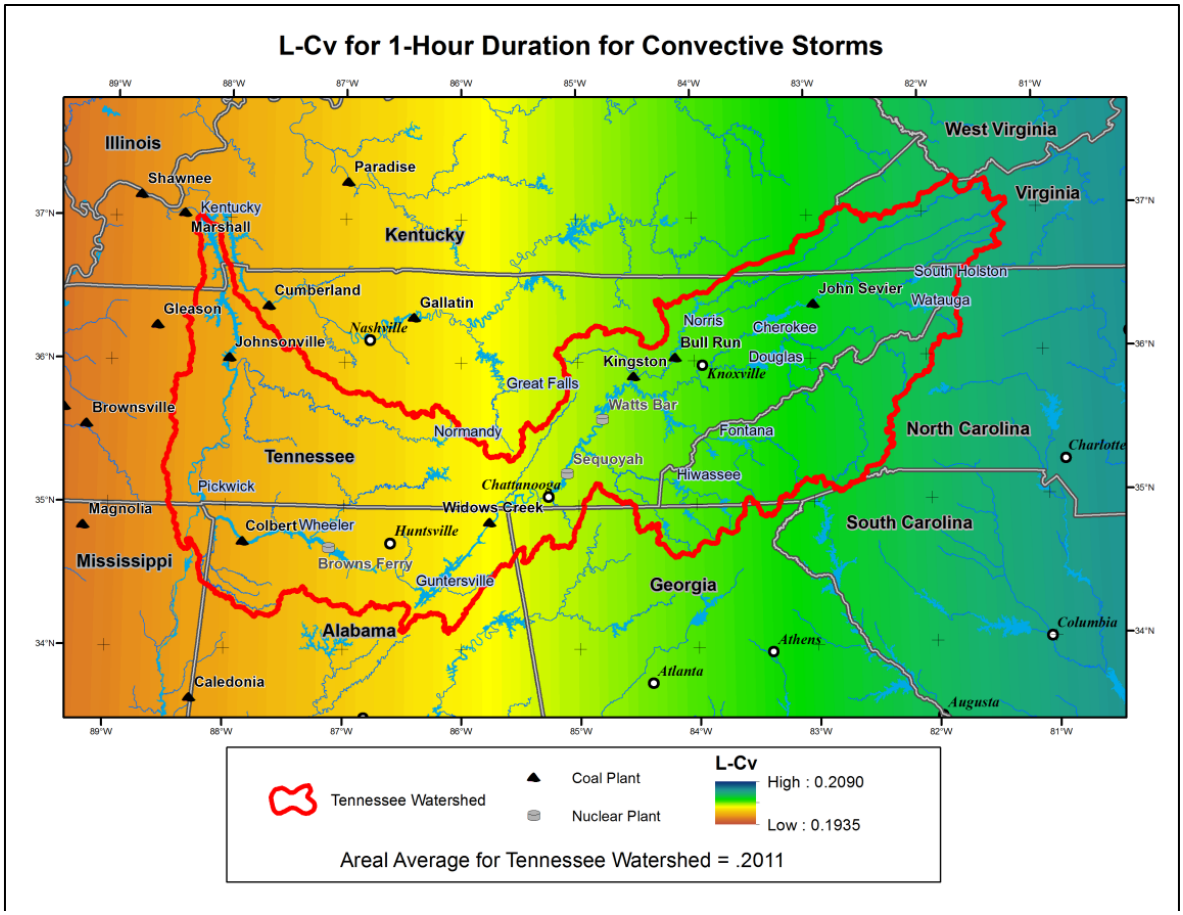


***Figure 84 - Map of Regional L-Cv for 2-Hour Duration for Convective Storm Types***

## 10.4 Identification of Regional Probability Distribution

L-moment goodness-of-fit tests were conducted for each of the 11 homogeneous sub-regions, and the GEV distribution was identified as the best-fit 3-parameter probability distribution for the collection of sub-regions. A review of ***Figure 85*** shows the centroid of the cluster of L-Skewness and L-Kurtosis pairs for the 11 sub-regions to be very near the GEV distribution. The 4-parameter Kappa distribution with a fixed shape parameter (*h*) emulates the GEV and near-GEV distributions and was selected for describing the point precipitation-frequency relationships for Convective Storms. A shape parameter (*h*) value of 0.05 (***Equation 2***) was identified as the best fit for describing Convective Storms, which resides just below the GEV curve.

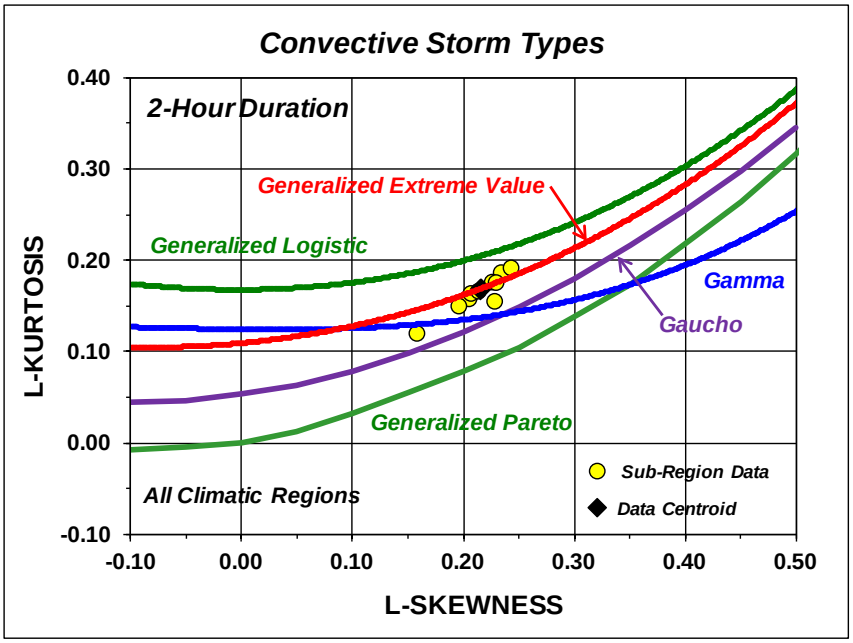


***Figure 85 - L-Moment Ratio Diagram Depicting Regional L-Skewness and L-Kurtosis Values for Homogeneous Regions for 2-Hour Duration for Convective Storm Types***

## 10.5 Isopluvial Mapping for 1-Hour Duration for Selected Annual Exceedance Probabilities

The gridded datasets for the 1-hour at-site means (***Figure 82***) and regional L-Cv (***Figure 84***), the fixed regional L-Skewness value (***Table 19***) and the 4-parameter Kappa distribution with *h*=0.05 provided the information necessary to develop gridded datasets of 1-hour precipitation for selected AEPs. A precipitation-frequency curve for the station at McGhee Tyson Field was developed in the manner described above and compared with a probability plot of historical data (***Figure 86***). This provides an example of the general shape of the precipitation-frequency relationship for Convective storm types.

The areal average at-site mean (***Figure 82***), regional L-Cv (***Figure 84***) and a regional L-Skewness value of 0.2160 were used to develop a representative point precipitation-frequency relationship for the Tennessee Valley watershed (***Figure 87***). Note for this calculation, the Tennessee Valley watershed included the area upstream of Great Falls Dam. This relationship provides some insight into the expected behavior of 1-hour precipitation for extreme precipitation events for Convective Storms for application in LIP analyses.

Isopluvial gridded datasets were generated for AEPs of $10^{-1}$, $10^{-2}$, $10^{-3}$, $10^{-4}$ and $10^{-5}$; isopluvial maps are shown in ***Appendix K***. ***Figure 88*** shows an example isopluvial map for an AEP of 1:1,000

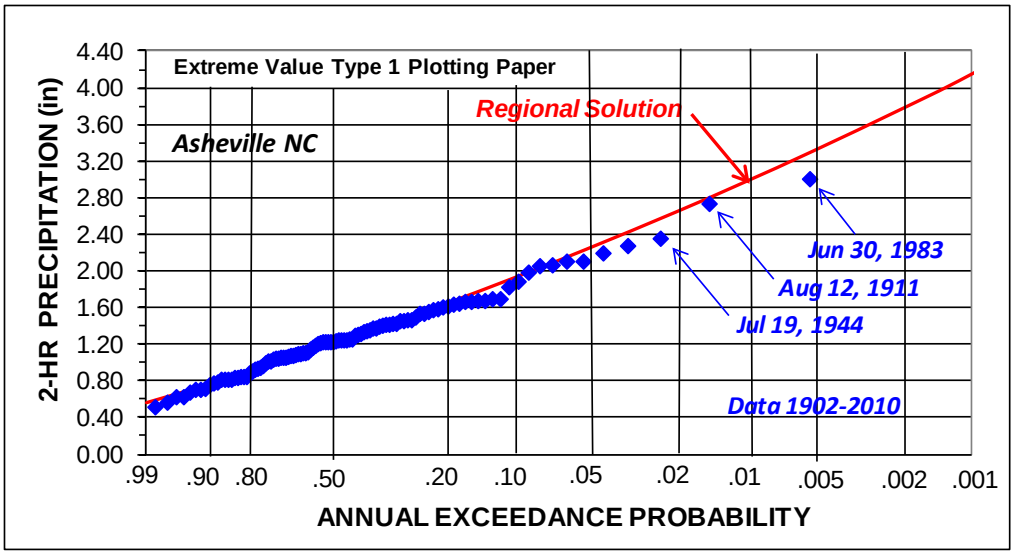


*Figure 86 - Probability plot of Historical 2-Hour Precipitation Annual Maxima for Convective Storms for Asheville, NC and Comparison with Regional Precipitation-Frequency Curve*

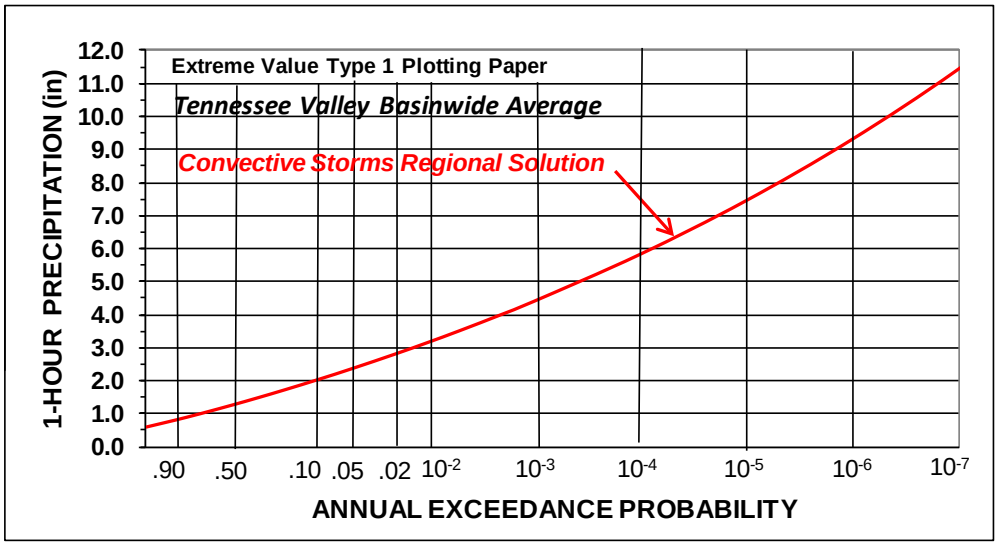


*Figure 87 - Point 1-Hour Precipitation-Frequency Relationship for Tennessee Valley Average Parameters for Convective Storms*

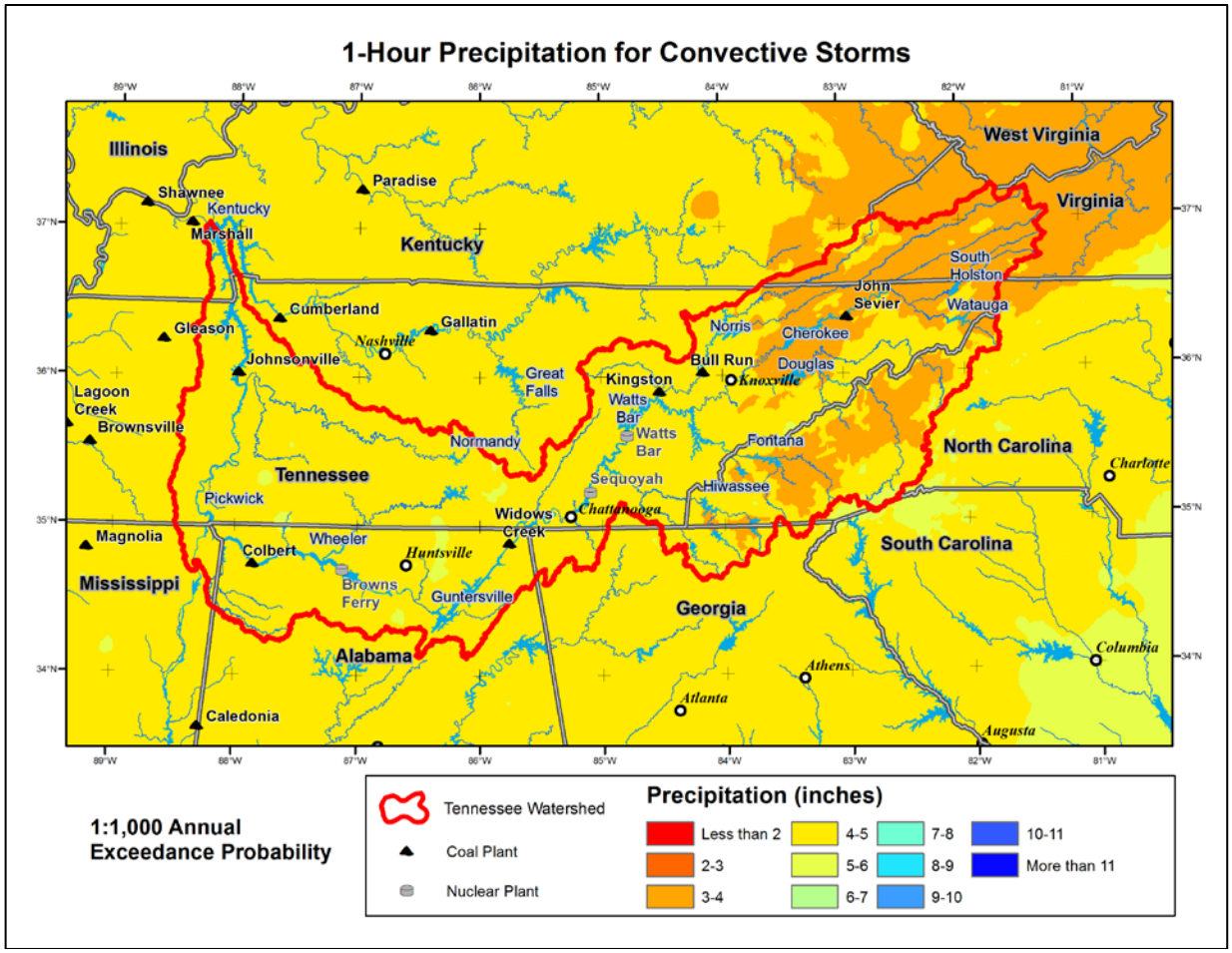


***Figure 88 - Isopluvial Map of 1-Hour Precipitation Maxima for an AEP of 1:1,000 for Convective Storms***

## 10.6 Seasonality of Extreme Storms for Convective Storms

An initial perspective on the seasonality of Convective Storms was obtained by using the DDST to develop a frequency histogram of days when convective events occurred (***Figure 89***). This frequency histogram includes many days with precipitation totals that are smaller than the precipitation annual maxima and is therefore representative of the full range of daily precipitation.

The seasonality analysis for Convective Storms was conducted using 2-hour precipitation annual maxima. The focus was on the rarest storms; a dataset of 131 noteworthy storms was assembled where 2-hour precipitation exceeded a 10-year recurrence interval at 2 or more stations. These are typically storm events where the 2-hour precipitation was twice as large or larger than the station at-site mean.

The calendar storm dates were converted to numerical storm dates dates by expressing the day as a ratio of the total days of the month such that July 7 equates to 7.23 to allow for frequency analysis. Computation of sample statistics resulted in a mean of July 26th and a standard deviation of 1.16 months. A probability plot was assembled using the 131 numerical storm dates and a 4-parameter Beta distribution was fitted to the data (***Figure 90***). The 4-parameter Beta distribution was then used to create a frequency histogram for the seasonality of extreme 2-hour duration Convective Storms (***Figure 91***). A comparison of ***Figure 89*** and ***Figure 91*** shows the seasonality for extreme storms to occur primarily in the warmest months of July and August and to be more seasonally constrained than for common storms that occur frequently throughout the months from April to October.

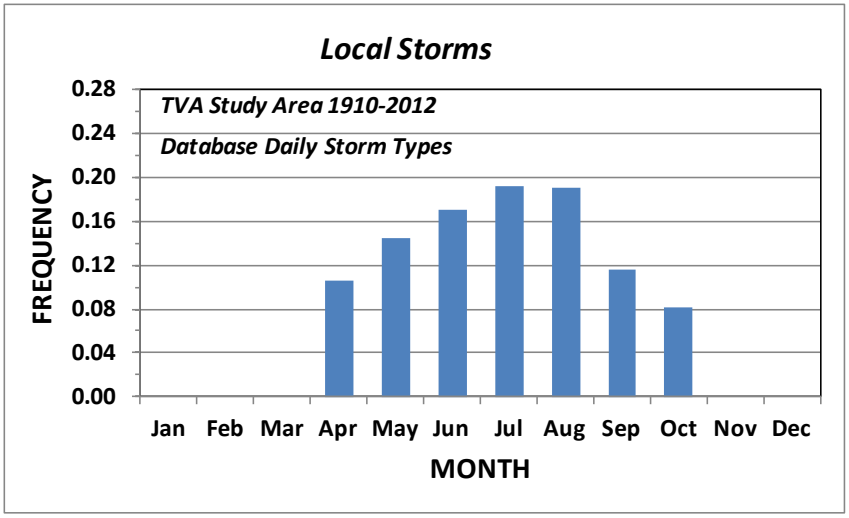


*Figure 89 - Seasonal Frequency Histogram for Days When LSs Have Occurred 1910-2012*

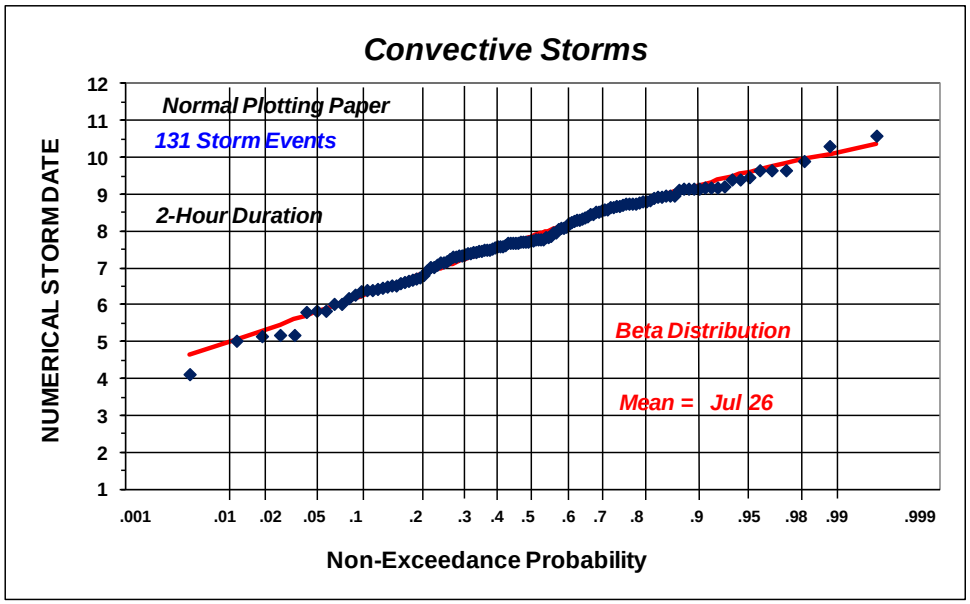


*Figure 90 - Probability plot of Numerical Storm Dates for 2-Hour Duration Convective Storms*

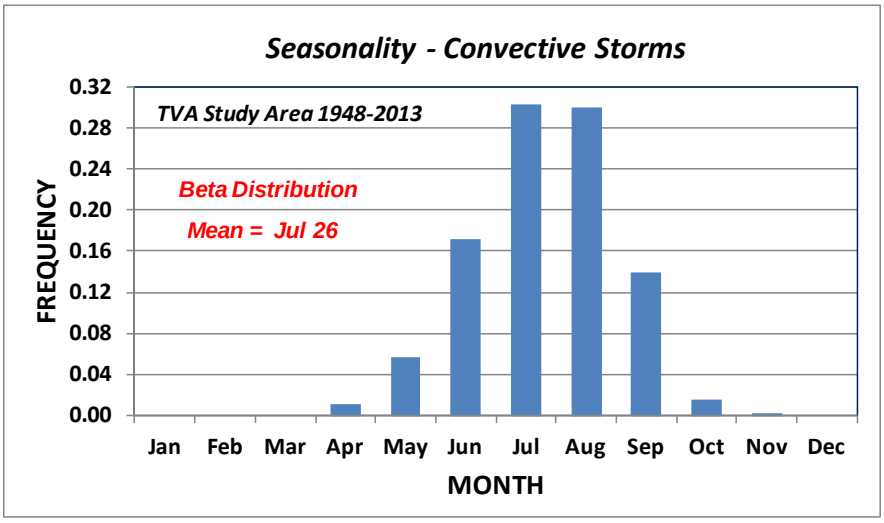


***Figure 91 - Frequency Histogram for Seasonality of Extreme 2-Hour Duration Convective Storms***

## 10.7 Equivalent Independent Record Length (EIRL) for Convective Storms

Two methods were used to estimate EIRL. The first method was a frequency-based method using the upper 10% of 2-hour precipitation annual maxima at each station. The second method utilized counting of independent storm dates for all storm events.

The frequency-based method was conducted in the manner described in ***Appendix H***, where the upper 10% of precipitation annual maxima at the stations were examined. ***Figure 92*** shows the plotting-position representation of EIRL. The frequency-based method resulted in an estimate of 6,800 years for EIRL relative to the 8,589 station-years of record. The storm counting method resulted in an EIRL estimate of 4,455 years. The best-estimate of EIRL was taken as the geometric mean of the two estimates (***Table 20***).

***Table 20 - Estimates of EIRL for 2-Hour Duration Convective Storms***

| Station-Years of Record | EIRL Estimates (Years) | | | EIRL Percent of Station-Years |
|---|---|---|---|---|
| | Frequency Based | Storm Count | Geometric Mean | |
| 8,589 | 6,800 | 4,455 | 5,500 | 64.0% |

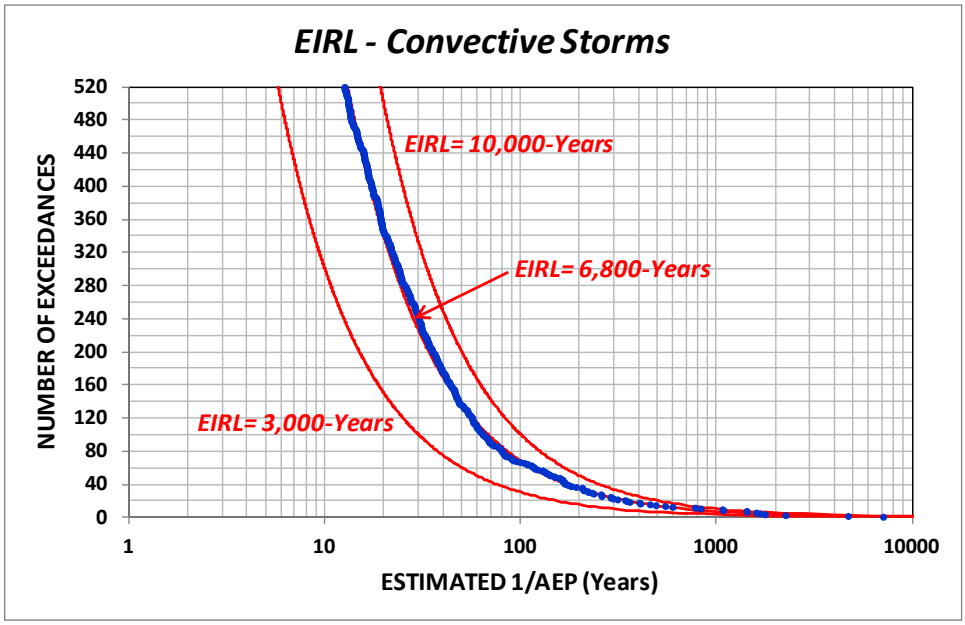


***Figure 92 - Graphical Depiction of EIRL for 2-Hour Duration Convective Storms***

## 10.8 Comparison of 1-Hour and 2-Hour Temporal Characteristics

Temporal storm characteristics for Convective Storms are of interest in conducting LIP analyses of flood hazards at nuclear sites. A comparison of at-site means for the 1-hour and 2-hour durations was made to provide information on the variation of temporal storm characteristics across the TVSA. The mapped at-site means were developed in the manner described previously for at-site means for Convective Storms.

***Figure 93*** shows the ratio of mapped at-site means for the 2-hour and 1-hour durations for Convective Storms. A review of ***Figure 93*** indicates that precipitation for the 2-hour duration is typically not much greater than for the 1-hour duration, being about 15% to 21% greater. There is also a minor trend of the 2-hour to 1-hour ratio with longitude. Sites in the southwestern portion of the study have both larger 1-hour at-site means (***Figure 82***) and larger ratios of the 2-hour to 1-hour at-site means. This is likely due to the southwestern sites being climatologically wetter and closer to more sustained sources of atmospheric moisture from the Gulf of Mexico. These temporal storm characteristics will be considerations in developing temporal patterns for LIP analyses.

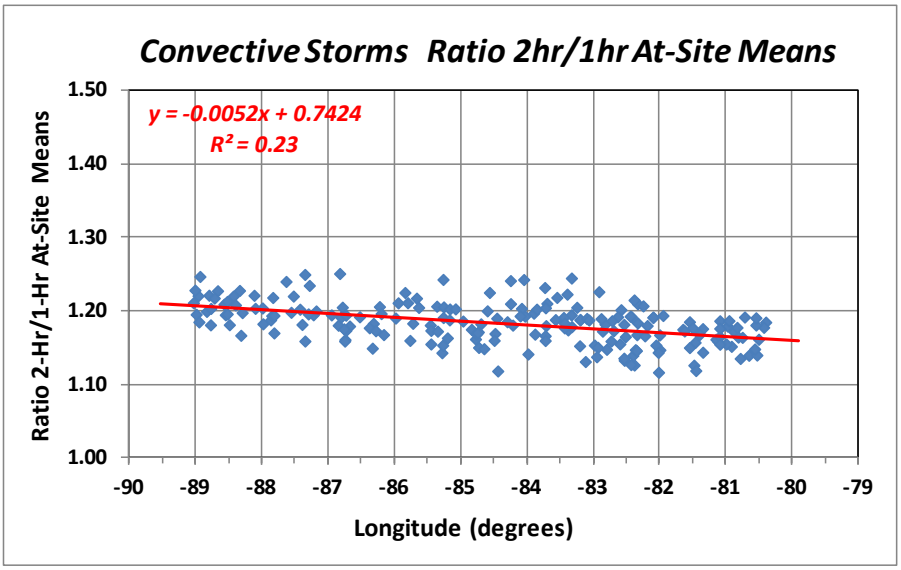


*Figure 93 - Variation with Longitude of the Ratio of 2-Hour to 1-Hour At-Site Means for Convective Storms*

# 11 Tropical Storm Remnants - Point Precipitation-Frequency

The number of storm events produced by TSRs in a given year is relatively small (***Figure 3***, ***Figure 4***) compared to the number of MLC and MEC storms. In particular, there were no TSR events in about 15% of the years of record at a given station. In addition, there were many years at any given station where the magnitudes of TSR events were so small, they should not be considered in the frequency analysis for the TSR storm type. This situation required adjustments to be made in the assembly of precipitation AMS and in the approach to precipitation-frequency analysis.

## 11.1 Peaks-Over-Threshold Data Series

The precipitation AMS were initially assembled based on the TSR storm type in the manner described previously. At this point it was discovered that about 15% of the years did not have any TSR events. Further review of the datasets revealed there were many years where the 2-day or 48-hour annual maxima were quite small, typically less than a daily amount of 0.50-inch. It is unreasonable to consider these smallish precipitation events characteristic of TSR storms suitable for precipitation-frequency analysis. The solution was to use a peaks-over-threshold approach and to use a threshold in selecting the annual maxima for frequency analysis.

A frequency threshold was chosen rather than a numerical threshold, which is consistent with the homogeneity concepts in a regional analysis. Numerous annual maxima datasets were examined, and a frequency threshold of 45% was chosen, wherein the lower 45% of data are years with no TSRs or years where the TSRs are too small to be considered. The upper 55% of precipitation maxima are considered representative of TSR storms and are included in the frequency analysis. This approach generally resulted in the smallest 2-day and 48-hour precipitation maxima included in the analysis to be in the range of 1.00 inches to 1.50 inches. This magnitude is generally consistent with the smallest precipitation maxima for the analysis of MLC storms, so the adopted approach was judged to produce a reasonable threshold.

## 11.2 Mixed Distribution Needed

A mixed distribution is required to describe the precipitation-frequency relationship for the TSR storm type to account for the situation where there are no TSR events in some years and that TSR events are quite small in other years. The mixed distribution for the TSR storm type has a construct where in any given year at a station there is a 45% chance that a TSR event occurs where the 48-hour precipitation is below the threshold. In this case, a probability distribution is fit to the upper 55% of the data over the threshold, and adjustments are made to the exceedance probabilities to account for the 45% of years of non-events (***Equation 16***).

The mixed distribution for the TSR storm type takes the form:

$$F(x) = \theta + (1 - \theta)\, G(x), \qquad x \geq \text{threshold} \qquad \textit{Equation 16}$$

where: $F(x)$ is the cumulative distribution function (CDF) for the mixed distribution for the TSR storm type,
$\theta$ is the mixing parameter ($\theta$=0.45) that defines the fraction of values below the threshold; and
$G(x)$ is the cumulative distribution function for the non-zero values (values above the threshold).

When computing quantile estimates for a mixed distribution, the non-exceedance probability for the non-zero values over the threshold $G(x)$ is expressed in terms of the non-exceedance probability for the complete mixed distribution $F(x)$ as:

$$G(x) = \frac{(F(x)-\theta)}{(1-\theta)} \qquad \textit{Equation 17}$$

## 11.3 Precipitation Gages and Datasets

Daily and hourly gages were used in the regional analyses for 48-hr precipitation annual maxima for TSRs. Data from synoptic gages were not used because there was insufficient record (1986-2013) to provide adequate record length when the 45% of non-events was considered. Stations with 30 years or more of total record were included in the analyses (***Figure 94***) which yielded 17 years of record over the 45% frequency threshold. ***Table 21*** provides a listing of the number of gages and total years of record used in the analysis of TSRs, and ***Figure 95*** depicts a histogram of the number of years of record.

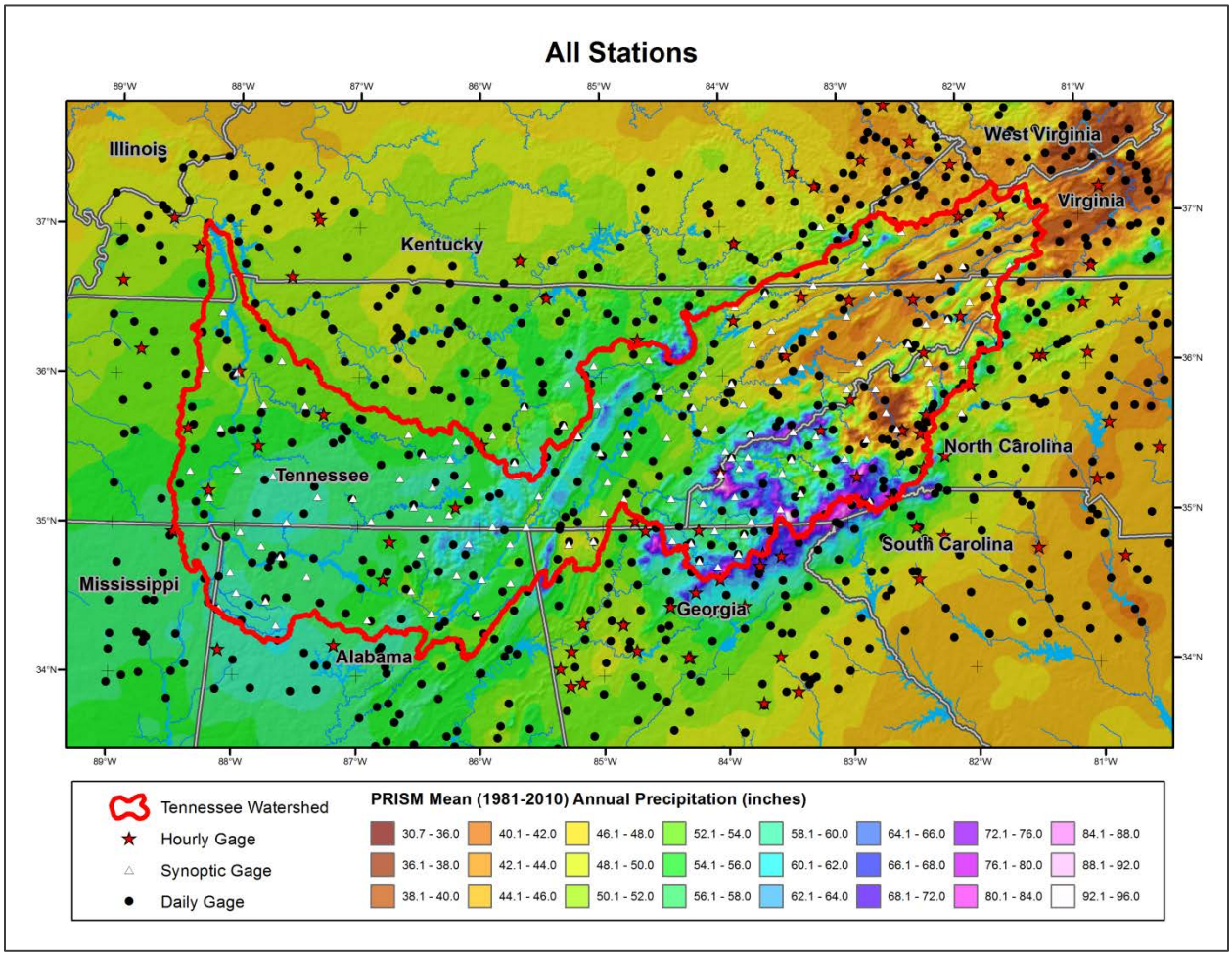


***Figure 94 - Location of Daily and Hourly Precipitation Gages Used in Precipitation-Frequency Analysis for TSRs***

***Table 21 - Number of Stations/Gages and Station-Years of Record for Stations/Gages with 17 or More Years of Record over the Frequency Threshold Used in Precipitation-Frequency Analysis for TSRs***

| PRECIPITATION GAGE TYPE | NUMBER OF STATIONS/GAGES | STATION-YEARS OF RECORD | AVERAGE STATION-YEARS |
|---|---|---|---|
| NOAA Daily Gages | 547 | 20,296 | 37.1 |
| NOAA Hourly Gages | 46 | 1,253 | 27.2 |
| **TOTAL** | **593** | **21,549** | **36.3** |

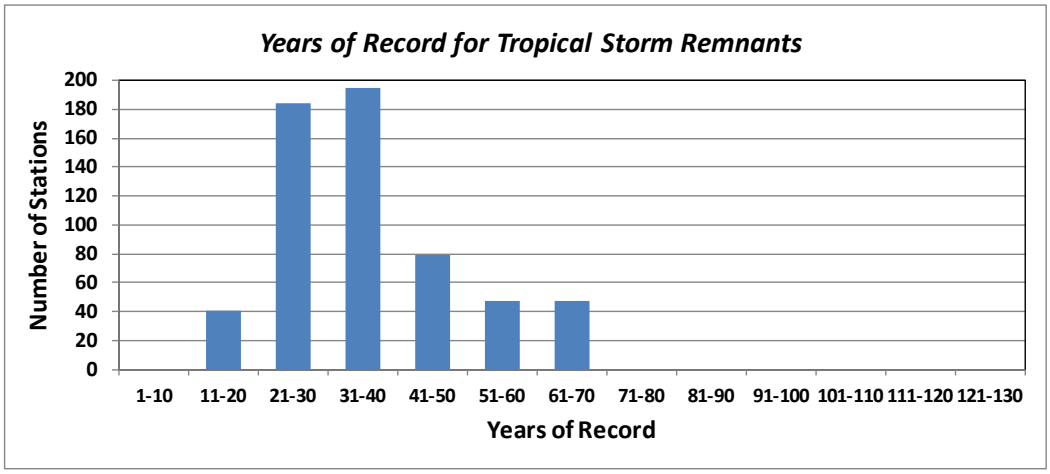


***Figure 95 - Histogram for Years of Record over the Frequency Threshold for Stations Used in Precipitation-Frequency Analysis for TSRs***

## 11.4 Spatial Mapping of 48-Hour At-Site Means

Spatial mapping of 48-hour at-site means for TSRs was conducted using longitude and gridded values of mean annual precipitation (PRISM[5,6]) as explanatory variables. This choice was made after reviewing the behavior of the relationship of at-site means with longitude and mean annual precipitation (***Figure 96*** and ***Figure 97***).

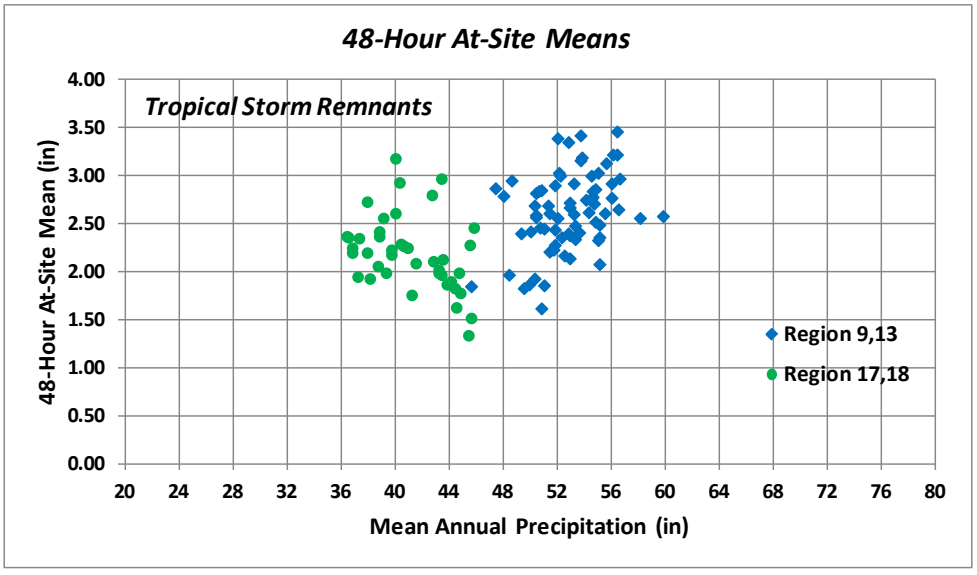


***Figure 96 - Scatterplot of Station Sample Values of 48-Hour At-Site Means for TSRs in Climatic Regions 9, 13, 17, 18 Variation with Mean Annual Precipitation***

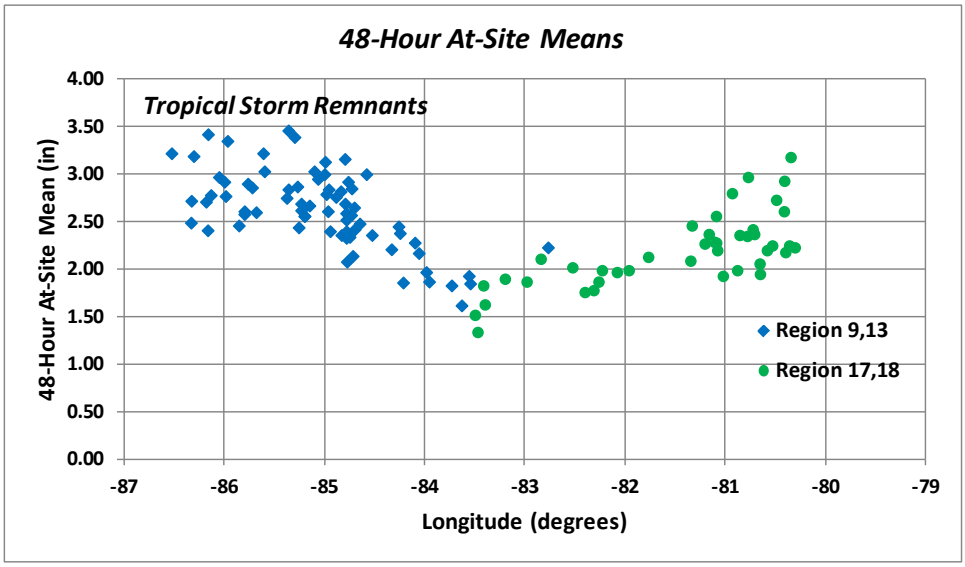


***Figure 97 - Scatterplot of Station Sample Values of 48-Hour At-Site Means for TSRs in Climatic Regions 9, 13,17,18 Variation with Longitude***

Collections of stations from adjacent climatic regions were grouped where they exhibited similar behavior. Multiple linear regression methods were used for the collections of stations which resulted in a form similar to the mathematical relationship shown in ***Equation 6***. The difference being that the second explanatory variable was mean annual precipitation. ***Table 22*** lists the coefficients for the multiple regression solution and the resultant RMSE for the various groupings of climatic regions. The resultant multiple linear regression equations were used to generate the mapped values of 48-hour at-site means. Minor smoothing was conducted in the vicinity of regional boundaries using a nearest neighbor approach to provide a smooth continuum of precipitation.

Best estimates of the at-site means were computed as a weighted-average of the station-sample values and regression-predicted values, as discussed in ***Section 7.7***. ***Figure 98*** and ***Figure 99*** depict examples of comparisons of station sample values and mapped values of the 48-hour at-site means. The mapped values of the 48-hour at-site means (***Figure 99***) are unbiased and have a RMSE of 6.2%. The spatial map of 48-hour at-site means for TSRs is shown in ***Figure 100***.

| CLIMATIC REGIONS | MULTIPLE REGRESSION COEFFICIENTS $AtSiteMean_{TSR} = \alpha_0 + \alpha_1 Longitude + \alpha_2 AnnualPrecip$ | | | RMSE |
|---|---|---|---|---|
| | $\alpha_0$ | $\alpha_1$ | $\alpha_2$ | |
| 1 – 2 – 3 - 5 | -2.0881 | -0.02278 | 0.04758 | 10.6% |
| 9 - 13 | -26.2083 | -0.33405 | 0.00799 | 11.8% |
| 17 - 18 | 29.5146 | 0.35475 | 0.03830 | 11.0% |
| 19 - 20 | 3.2693 | 0.00399 | -0.00890 | 15.8% |
| 21 – 25 - 29 | 29.3583 | 0.35486 | 0.06917 | 10.6% |
| **All Regions** | **Final Mapping** | | | **6.2%** |

***Table 22 - Listing of Coefficients for Multiple Linear Regression for 48-Hour At-Site Means for TSRs and RMSE for Predictive Equations***

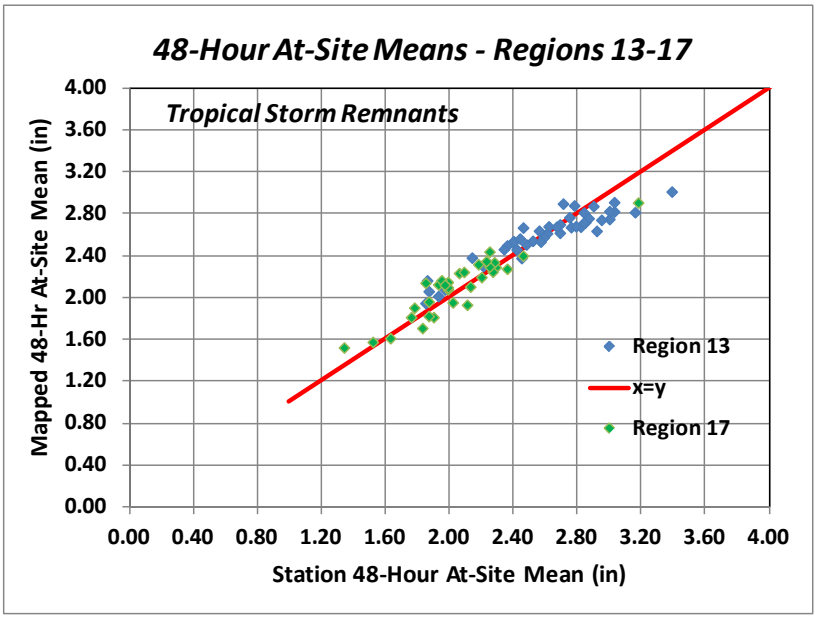


*Figure 98 - Comparison of Station Values and Mapped Values of 48-Hour At-Site Means for Tennessee Valley Lowlands (Climatic Regions 13, 17) for TSRs*

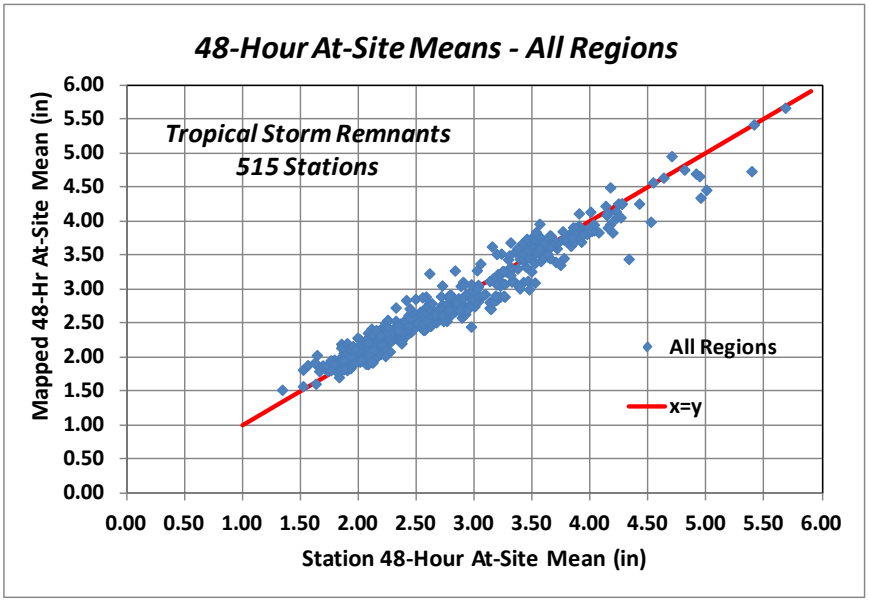


*Figure 99 - Comparison of Station Values and Mapped Values of 48-Hour At-Site Means for All Climatic Regions for TSRs*

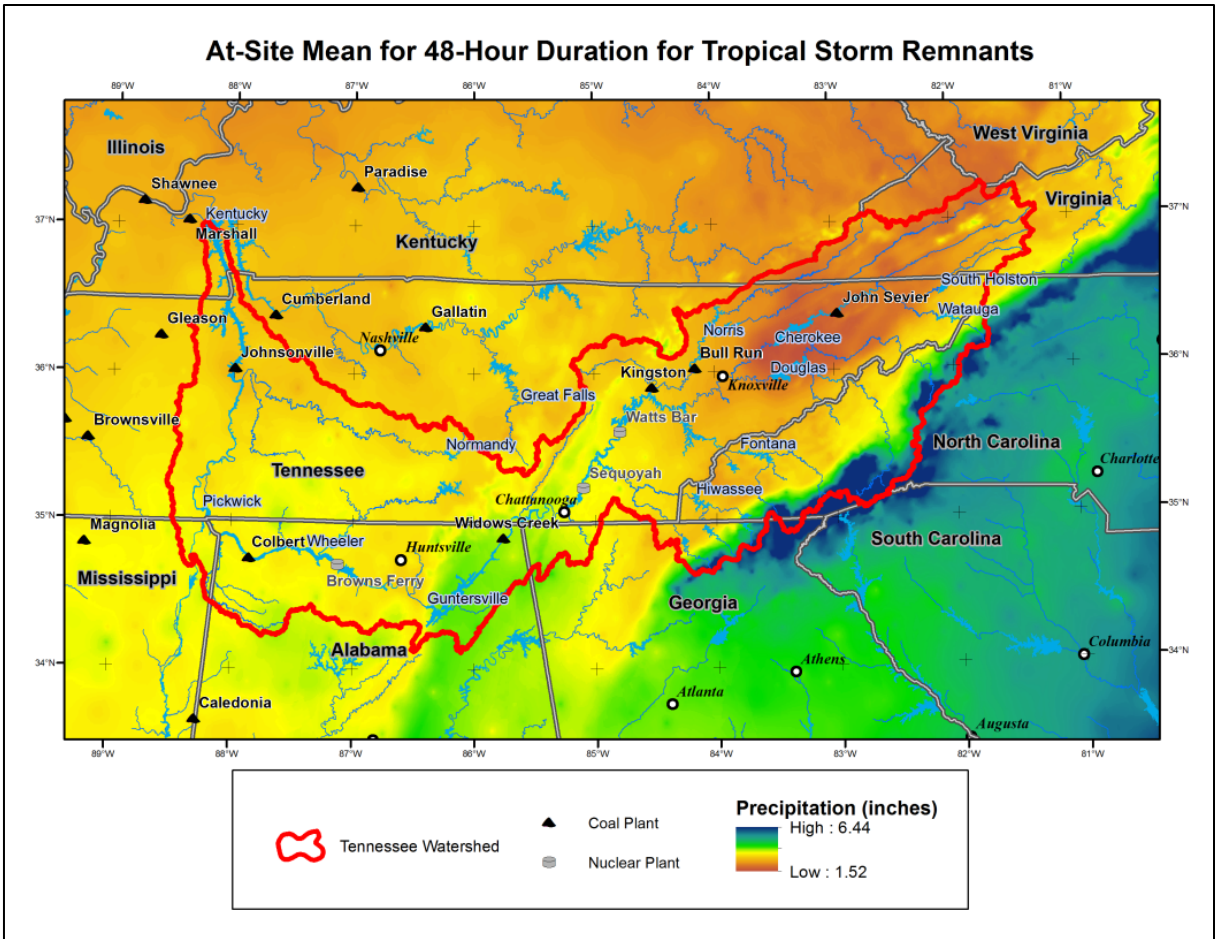


***Figure 100 - Map of At-Site Means for 48-Hour Duration for TSRs***

## 11.5 Spatial Mapping of Regional Values of L-Cv and L-Skewness

Homogeneous sub-regions were formed as groupings of stations within a limited range of longitude for groupings of climatic regions. Stations were included that had a record length of 36 years, which yielded 20 years above the 45% frequency threshold. Twenty-seven sub-regions were formed in this manner where each sub-region produced a regional L-Cv and L-Skewness value associated with a group average longitude. The collection of twenty-seven sub-regions was found to be acceptably homogeneous based on L-moment heterogeneity measures.

A review of the regional L-Cv values showed a systematic variation with longitude. The twenty-seven regional values of L-Cv were visually fit by hand to accommodate the spatial behavior posed by blocking of precipitation by the Blue Ridge and Appalachian Mountains (***Figure 101*** and ***Figure 102***). The RMSE for prediction of regional L-Cv was 3.8% (***Table 23***). The spatial mapping of regional L-Cv for the 48-hour duration is shown in ***Figure 103***. Regional L-Cv has low variability in western Tennessee and on the coastal areas windward of the Blue Ridge Mountains. Variability increases markedly in the leeward areas northeast of the Appalachian Mountains.

The prediction of regional L-Skewness was accomplished using linear regression for regional L-moment L3 as a function of regional L-moment L2 (***Equation 18***) for the 38 homogeneous sub-regions. Use of the Index Flood methodology provides for a prediction of regional L-Skewness using ***Equation 19*** because regional L-Cv is equal to regional L2 for indexed datasets. ***Figure 104*** depicts the regression solution for regional L3 and ***Table 23*** lists the summary statistics for mapping of regional L-Skewness where the RMSE

is 10.9%. ***Figure 105*** shows the spatial mapping of regional L-Skewness, which reflects the variability in regional L-Cv across the study area.

$$L3 = -0.0750 + 0.5981*L2 \quad \textit{(Equation 18)}$$

$$L\text{-}Skewness = 0.5981 - 0.0750/L\text{-}Cv \quad \textit{(Equation 19)}$$

***Table 23 - Summary Statistics for Spatial Mapping of 48-Hour Duration Regional L-Cv and L-Skewness for TSRs***

| L-MOMENT RATIO | RANGE OF MAPPED L-MOMENT RATIO | STANDARD DEVIATION OF RESIDUALS | RMSE |
|---|---|---|---|
| Regional L-Cv | 0.2100 ≤ L-Cv ≤ 0.2700 | 0.0079 | 3.8% |
| Regional L-Skewness | 0.2410 ≤ L-Skewness ≤ 0.3205 | 0.0299 | 10.9% |

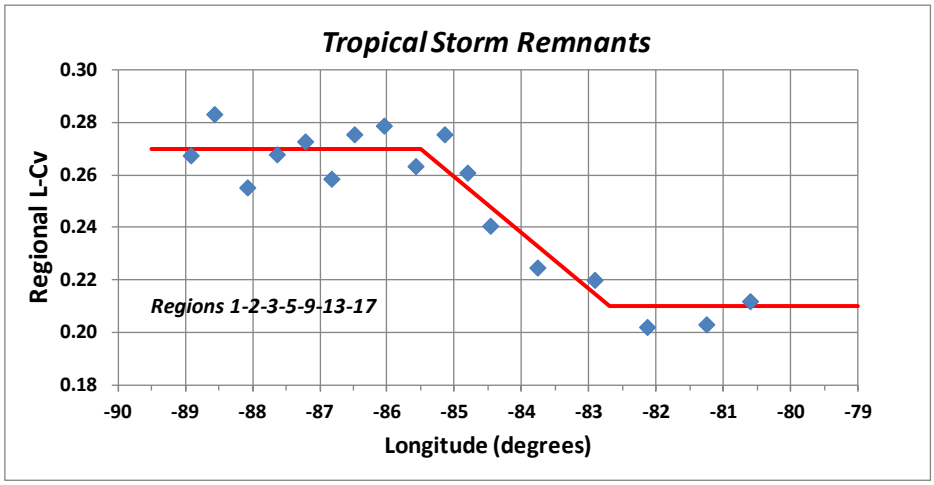


***Figure 101 - Example of Variation of Regional L-Cv with Longitude for 48-Hour Duration TSRs Climatic Regions 1-2-3-5-9-13-17-18***

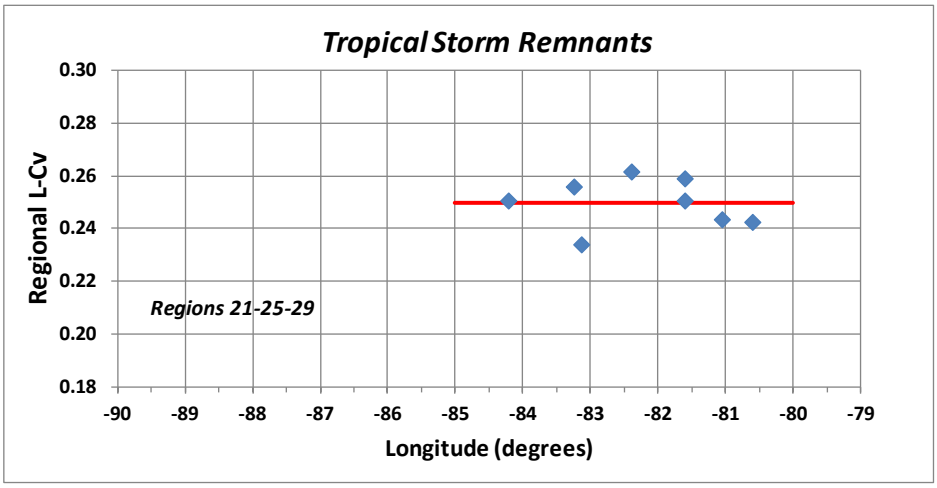


***Figure 102 - Example of Variation of Regional L-Cv with Longitude for 48-Hour Duration TSRs Climatic Regions 21-25-29***

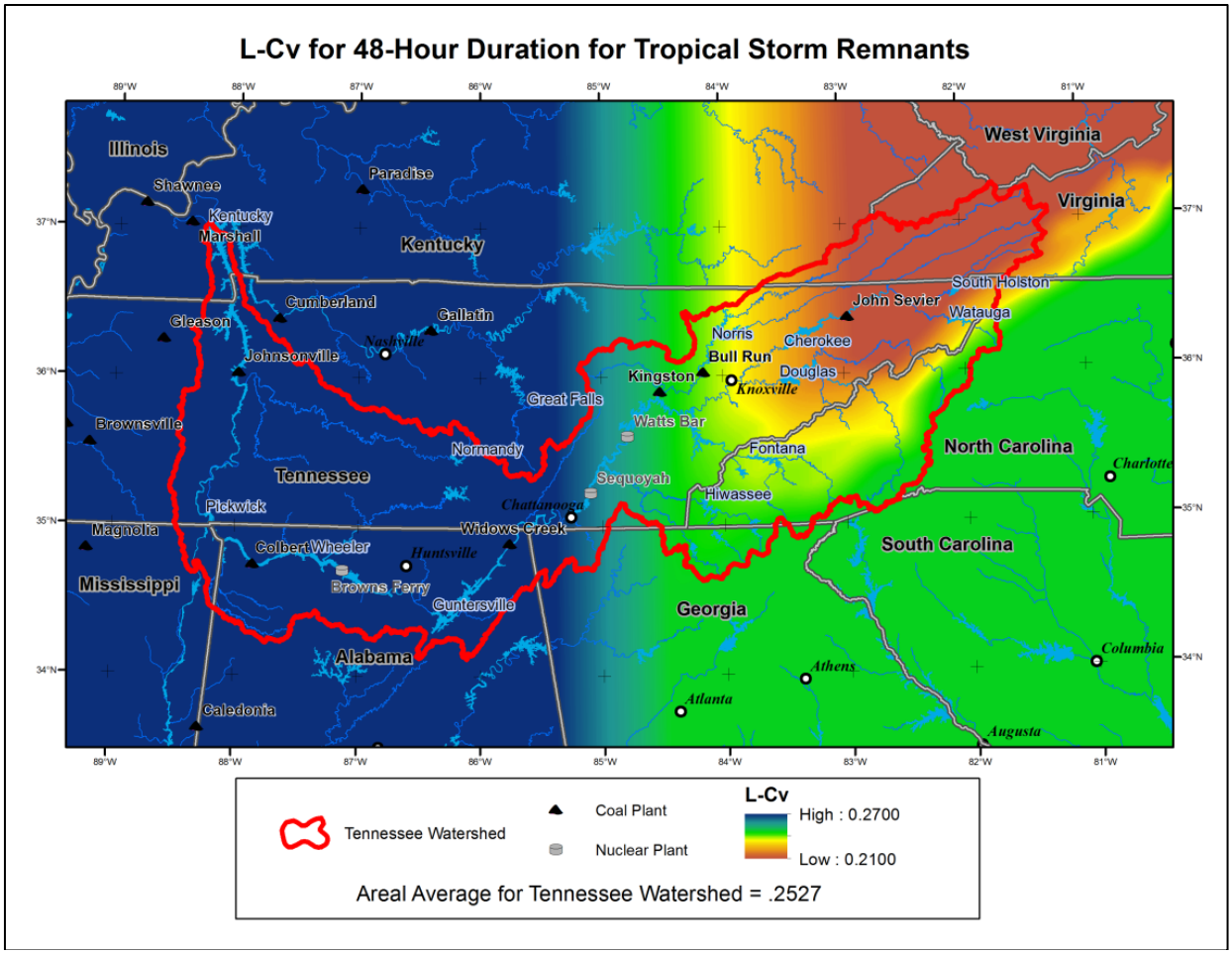


*Figure 103 - Map of Regional L-Cv for 48-Hour Duration for TSRs*

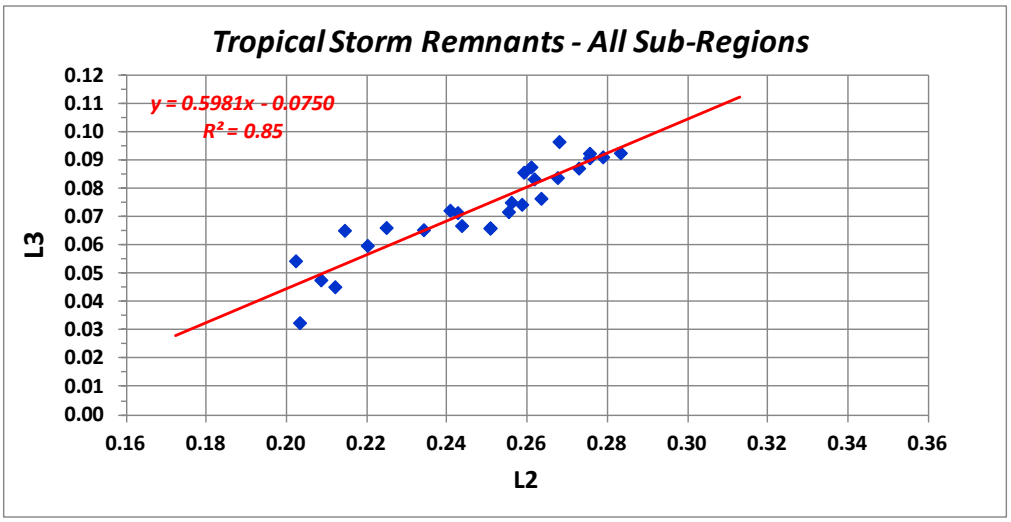


*Figure 104 - Predictor Equation for Regional L-Moment L3 as a Function of Regional L-Moment L2 for 48-Hour Duration for 38 Homogeneous Sub-Regions for TSRs*

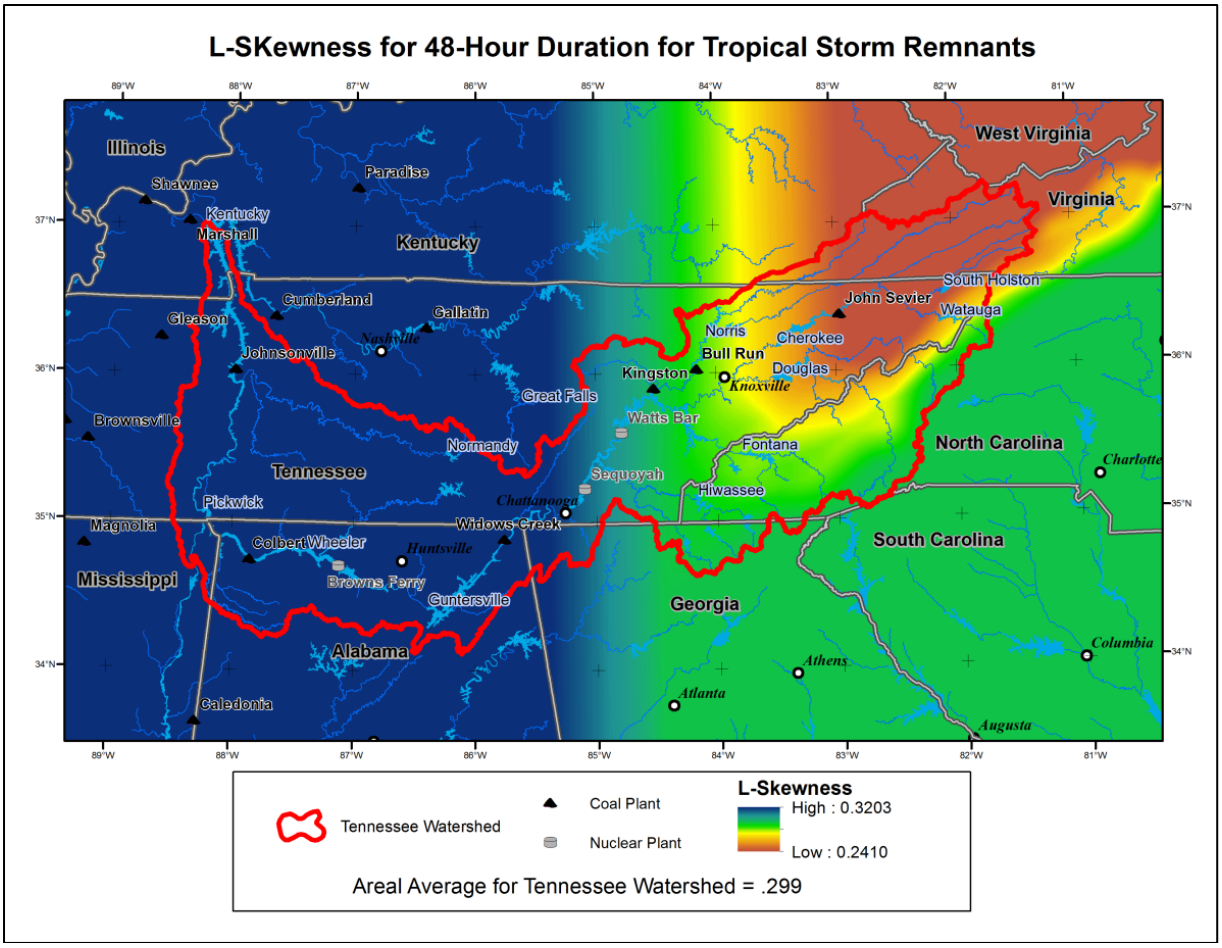


***Figure 105 - Map of Regional L-Skewness for 48-Hour Precipitation Annual Maxima for TSRs Remnants***

## 11.6 Identification of Regional Probability Distribution

L-moment goodness-of-fit tests were conducted for each of the 27 homogeneous sub-regions to identify the best-fit probability distribution. The study area is quite complex with regard to the behavior of TSR precipitation due to the influences of the Blue Ridge and Appalachian Mountains. It was discovered that the study area had markedly different behavior in western Tennessee, in the coastal areas windward of the Blue Ridge Mountains and in the leeward sheltered areas to the northeast of the Appalachian Mountains.

The 4-parameter Kappa distribution was chosen to model this complex spatial behavior. As background, the 4-parameter Kappa distribution varies within the space in the L-Moment Ratio Diagram (***Figure 106***) occupied by the Generalized Logistic ($h$= -1.00), GEV ($h$=0.00), Gaucho ($h$=0.50) and the Generalized Pareto ($h$=1.00) distributions.

L-Skewness and L-Kurtosis pairs for the sub-regions in western Tennessee, western Kentucky and northern Alabama (western Climatic Regions 1, 2 and 3) were found to be clustered between the Gaucho and Generalized Pareto distributions (***Figure 106***) with a centroid value of 0.85 for the second shape parameter ($h$) (***Table 24***). It was further found that the cluster of L-Skewness and L-Kurtosis pairs for sub-regions to the south of the crest of the Blue Ridge Mountains (Climatic regions 25 and 29) were described by the Generalized Pareto distribution (***Figure 107***) with the second shape parameter ($h$) equal to 1.00. This is a windward area where TSR precipitation is enhanced by orographic uplift on the southeast facing slopes of the Blue Ridge Mountains.

Lastly, L-Skewness and L-Kurtosis pairs for sub-regions in the Tennessee Valley to the leeward (north) of the Appalachian Mountains (Climatic Regions 5, 9, 13, 17) are clustered in the space between the Gaucho

and Generalized Pareto distributions (***Figure 108***) with the second shape parameter equal to 0.65. Transition zones exist in the intervening areas which included areas of Climatic Regions 18, 19, 20 and 21. The complex spatial behavior for L-Cv, L-Skewness and the second shape parameter *h* is seen in ***Figure 103***, ***Figure 105*** and ***Figure 109***, respectively.

***Table 24 - Values of the 2nd Shape Parameter for 4-Parameter Kappa Distribution for the TSR Storm Type***

| GEOGRAPHIC AREA | CLIMATIC REGIONS | 2nd SHAPE PARAMETER (*h*) |
|---|---|---|
| Western Tennessee and Northern Alabama | 1, 2, 3, 5, 9, 13 west of Longitude 85.5°N | 0.85 |
| Tennessee Valley North of Appalachian Mountains | 5, 9,13,17 | 0.65 |
| Coastal Areas South of Blue Ridge Mountains | 25, 29 | 1.00 |

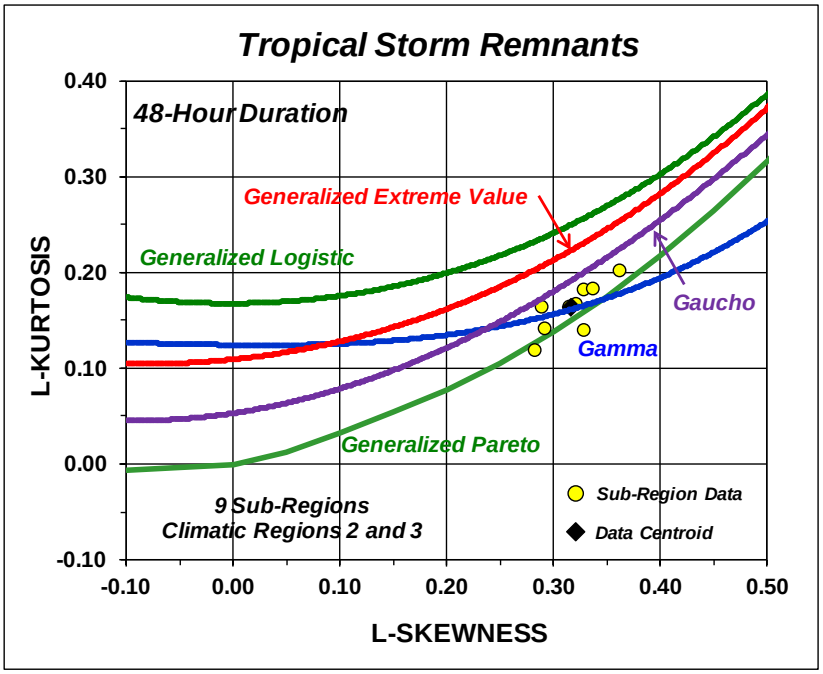


***Figure 106 - L-Moment Ratio Diagram Depicting Regional L-Skewness and L-Kurtosis Values for Homogeneous Sub-Regions within Climatic Regions 2 and 3 in Western Tennessee and Northern Alabama for the 48-Hour Duration for TSRs***

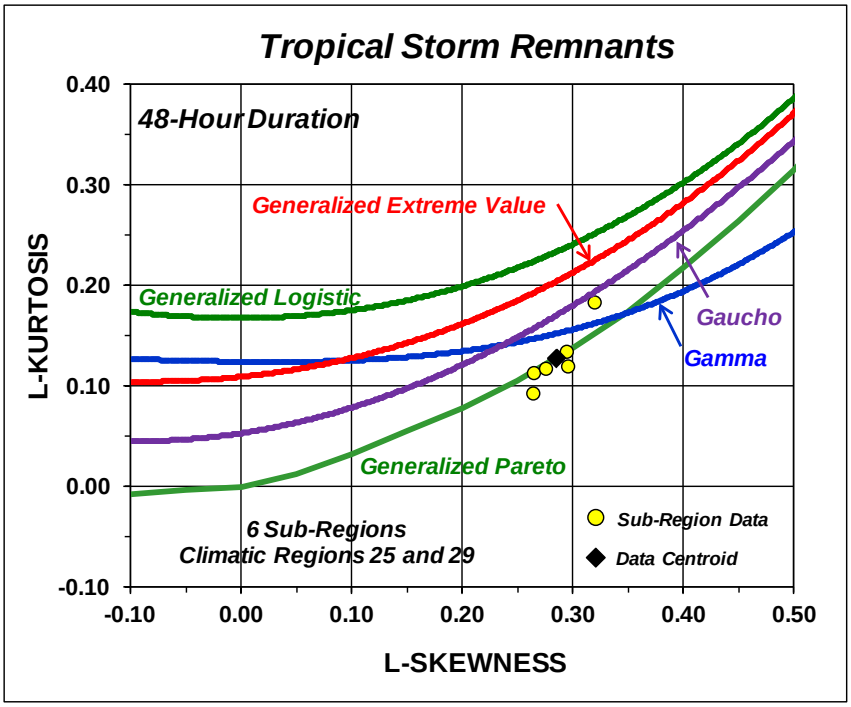


*Figure 107 - L-Moment Ratio Diagram Depicting Regional L-Skewness and L-Kurtosis Values for Homogeneous Sub-Regions within Climatic Regions 25 and 29 to the Southeast of the Blue Ridge Mountains for the 48-Hour Duration for Tropical St*

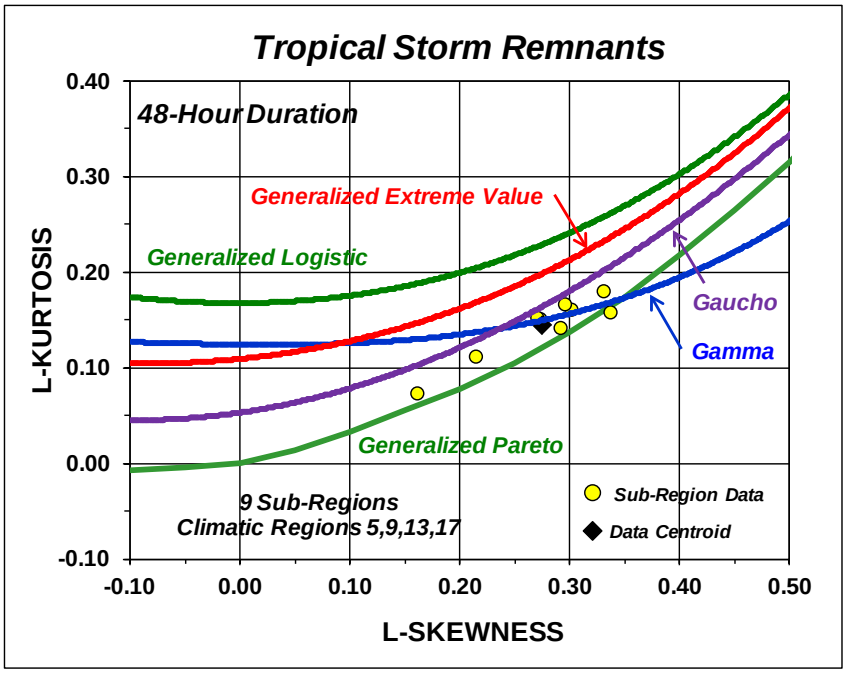


*Figure 108 - L-Moment Ratio Diagram Depicting Regional L-Skewness and L-Kurtosis Values for Homogeneous Sub-Regions within Climatic Regions 5, 9, 13 and 17 in the Tennessee Valley to the North of the Appalachian Mountains for the 48-Hour Duration for Tropical Storm*

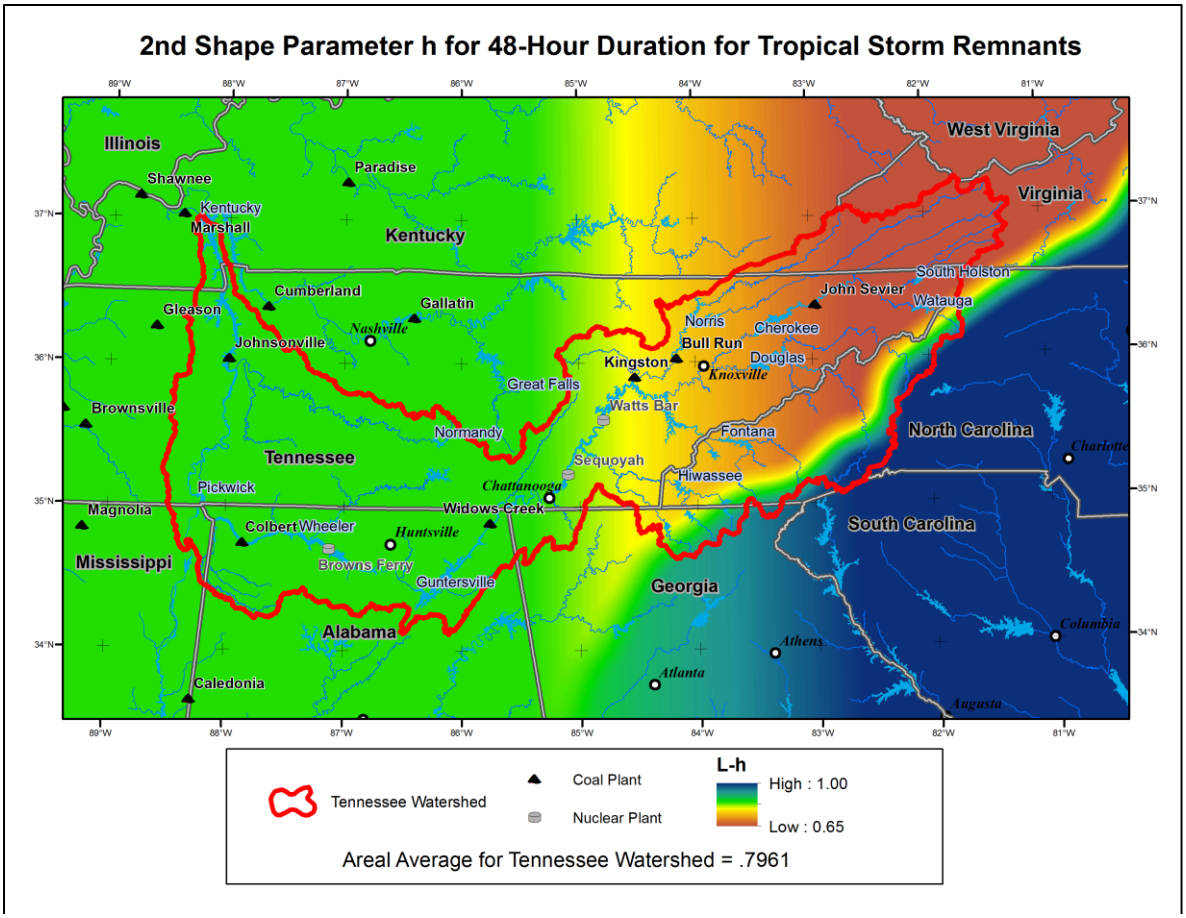


***Figure 109 - Map of Regional Shape Parameter h for Kappa Distribution for 48-Hour Precipitation Annual Maxima for TSRs***

## 11.7 Isopluvial Mapping for 48-Hour Duration for Selected Annual Exceedance Probabilities

The gridded datasets for the 48-hour at-site means (***Figure 100***), regional L-Cv (***Figure 103***), regional L-Skewness (***Figure 105***), regional shape parameter h (***Figure 109***) and the 4-parameter Kappa distribution provided the information necessary to develop gridded datasets of 48-hour precipitation for selected AEPs. A precipitation-frequency curve for the station at Kingston, TN was developed in the manner described above and compared with a probability plot of historical data (***Figure 110***). This provides an example of the general shape of the precipitation-frequency relationship for TSR storm types over the frequency threshold. ***Figure 111*** depicts the probability-plot for Kingston TN using the mixed distribution which accounts for the situation that in 45% of the years, a TSR does not occur or is too small in magnitude to exceed the threshold.

Isopluvial gridded datasets were generated for AEPs of $10^{-1}$, $10^{-2}$, $10^{-3}$, $10^{-4}$ and $10^{-5}$ and isopluvial maps are shown in ***Appendix L***. ***Figure 112*** shows an example isopluvial map for an AEP of 1:1,000.

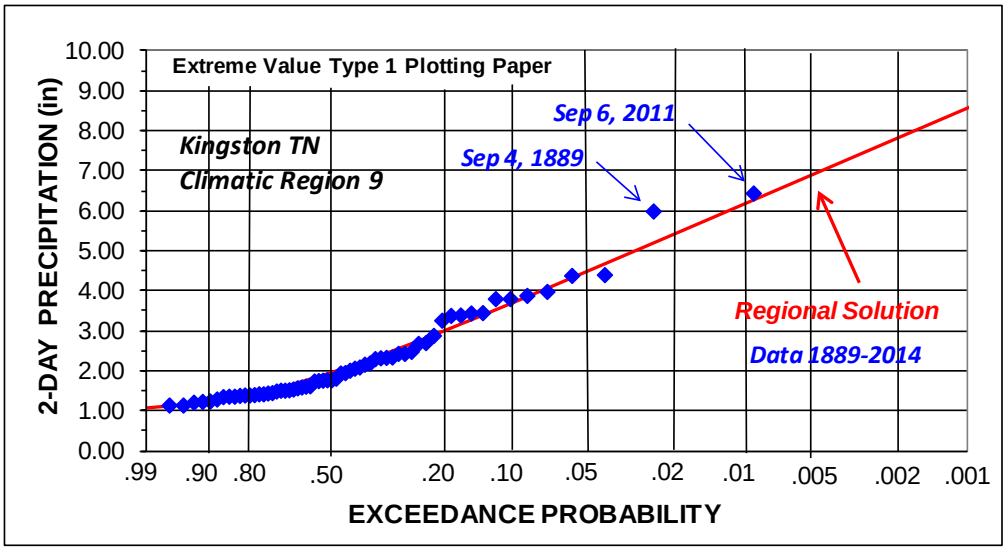


*Figure 110 - Probability plot of Historical 2-Day Precipitation Annual Maxima Over the Frequency Threshold for TSRs for Kingston, TN and Comparison with Regional Precipitation-Frequency Curve*

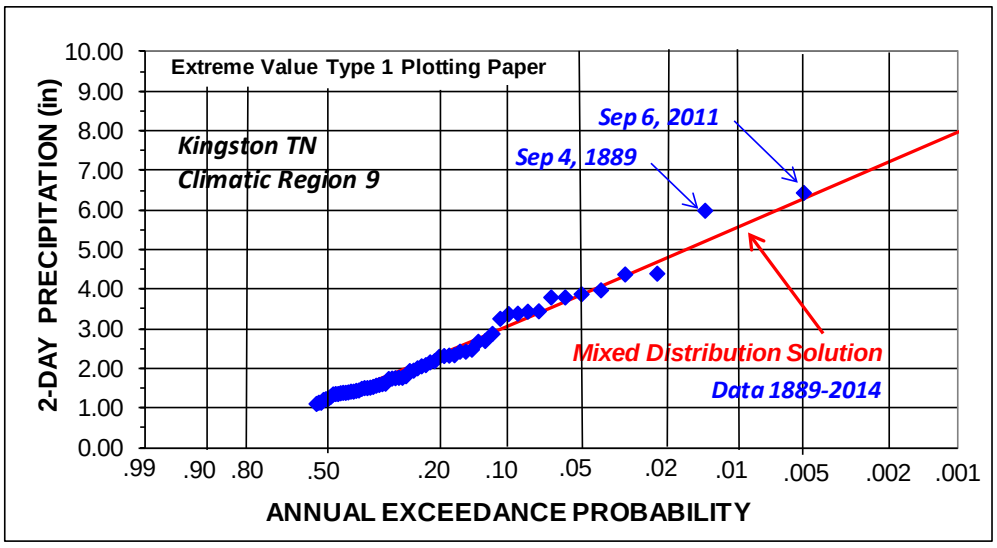


*Figure 111 - Probability plot of Historical 2-Day Precipitation Annual Maxima for TSRs for Kingston, TN and Comparison with Mixed Distribution Regional Precipitation-Frequency Curve*

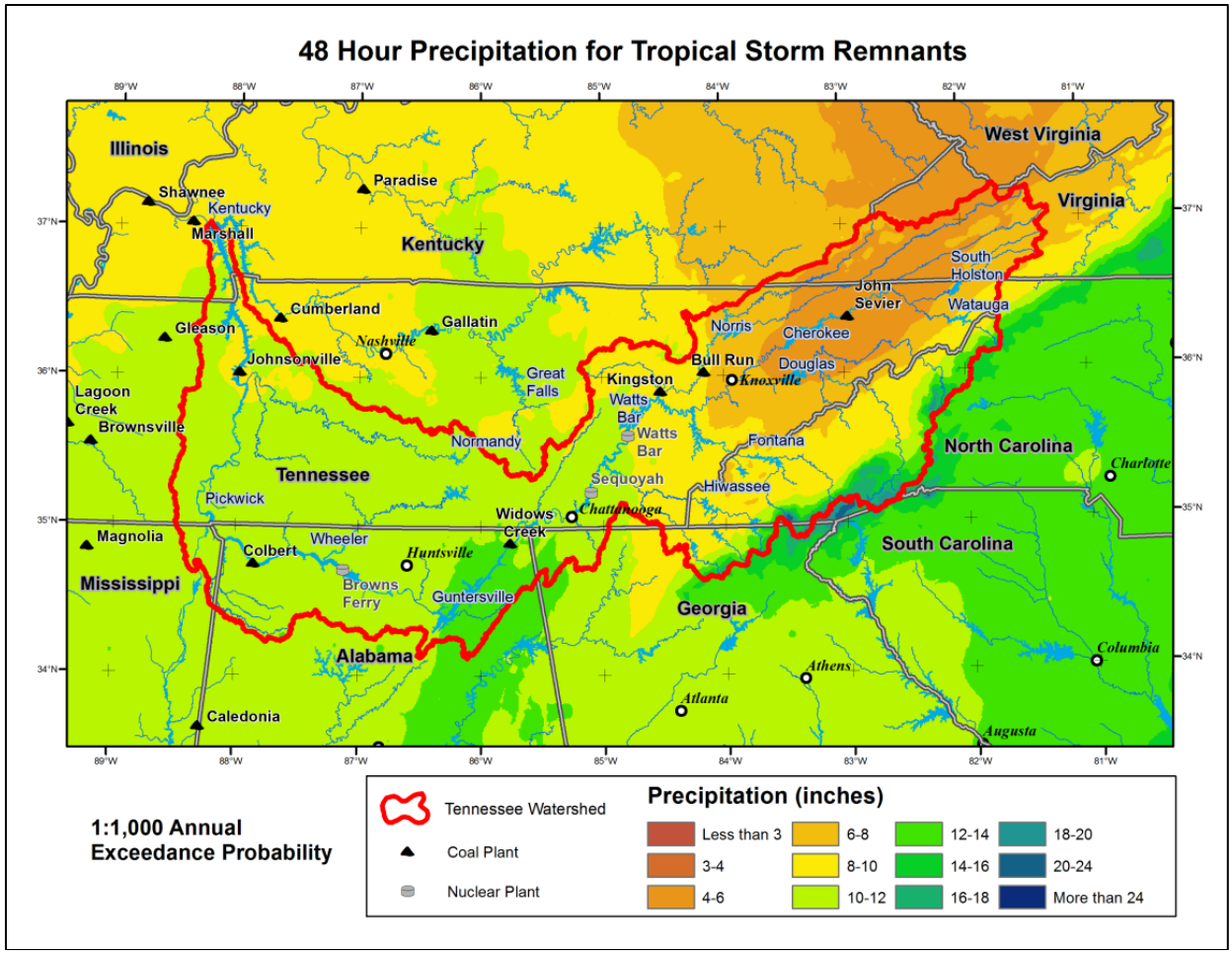


***Figure 112 - Isopluvial Map of 48-Hour Precipitation Maxima for an AEP of 1:1,000 for TSRs***

## 11.8 Seasonality of Extreme Storms for Tropical Storm Remnants

An initial perspective on the seasonality of TSRs was obtained by using the DDST to develop a frequency histogram of days when TSR events occurred (***Figure 113***). This frequency histogram includes many days with precipitation totals that are smaller than the precipitation annual maxima and is therefore representative of the full range of daily precipitation.

The seasonality analysis for TSRs was conducted using 48-hour precipitation annual maxima. The focus was on the rarest storms; for this purpose, a dataset of 61 noteworthy storms was assembled where 48-hour precipitation exceeded a 10-year recurrence interval at 14 or more stations. There is always a tradeoff between the desire to analyze the largest storms and the need for a dataset of sufficient size to provide a representative sample. The 10-year threshold and requirement of 14 or more stations over the threshold was judged suitable to meet the competing goals.

The calendar storm dates were converted to numerical storm dates by expressing the day as a ratio of the total days of the month such that November 7 equates to 11.23 to allow for frequency analysis. Computation of sample statistics resulted in a mean of August 30$^{th}$ and a standard deviation of 1.16 months. A probability plot was assembled using the 61 numerical storm dates, and a 4-parameter Beta distribution was fitted to the data (***Figure 114***). The 4-parameter Beta distribution was then used to create a frequency histogram for the seasonality of extreme 48-hour duration TSRs (***Figure 115***). A comparison of ***Figure 113*** and ***Figure 115*** shows a similar seasonality for both common and extreme TSRs.

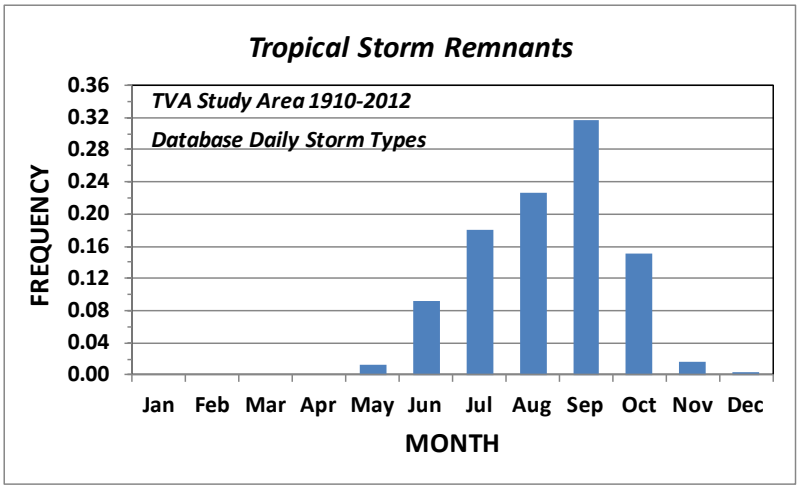


*Figure 113 - Seasonal Frequency Histogram of the Days When TSR Storm Events Have Occurred 1910-2012*

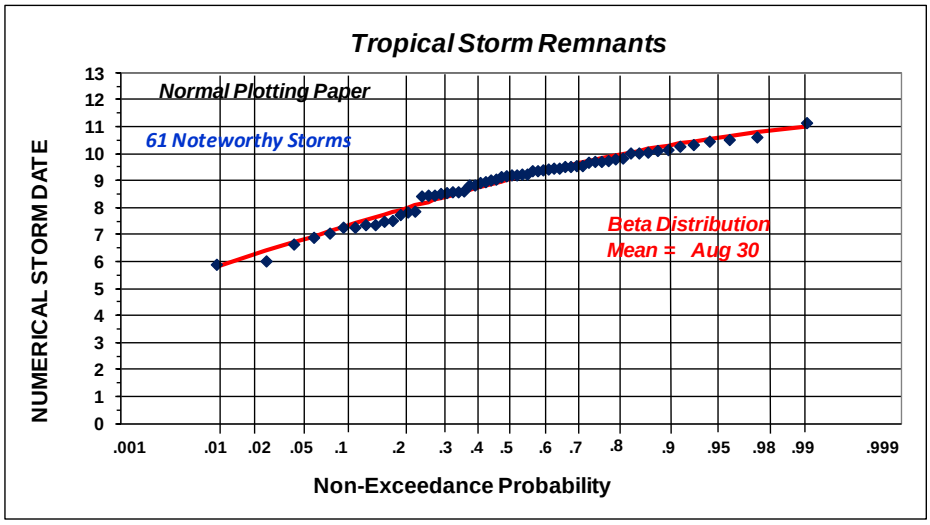


*Figure 114 - Probability plot of Numerical Storm Dates for 48-Hour Duration TSRs*

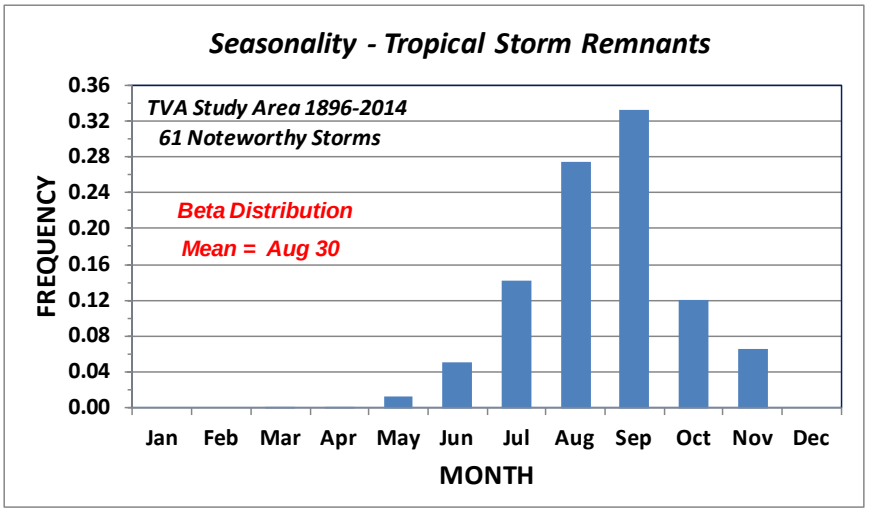


***Figure 115 - Frequency Histogram for Seasonality of Extreme 48-Hour Duration TSRs***

## 11.9 Equivalent Independent Record Length (EIRL) for Tropical Storm Remnants (TSRs)

Two methods were used to estimate EIRL. The first method was a frequency-based method using the upper 10% of 48-hour precipitation annual maxima at each station. The second method utilized counting of independent storm dates for all storm events.

The frequency-based method was conducted in the manner described in ***Appendix H***, where the upper 10% of precipitation annual maxima at the stations were examined. ***Figure 116*** shows the plotting-position representation of EIRL. The frequency-based method resulted in an estimate of 1,250 years for EIRL relative to the 25,862 station-years of record. The storm counting method resulted in an EIRL estimate of 675 years. The best-estimate of EIRL was taken as the geometric mean of the two estimates (***Table 25***).

***Table 25 - Estimates of EIRL for 48-Hour Duration for TSRs***

| Station-Years of Record | EIRL Estimates (Years) | | | EIRL Percent of Station-Years |
|---|---|---|---|---|
| | Frequency Based | Storm Count | Geometric Mean | |
| 25,862 | 1,250 | 675 | 925 | 3.6% |

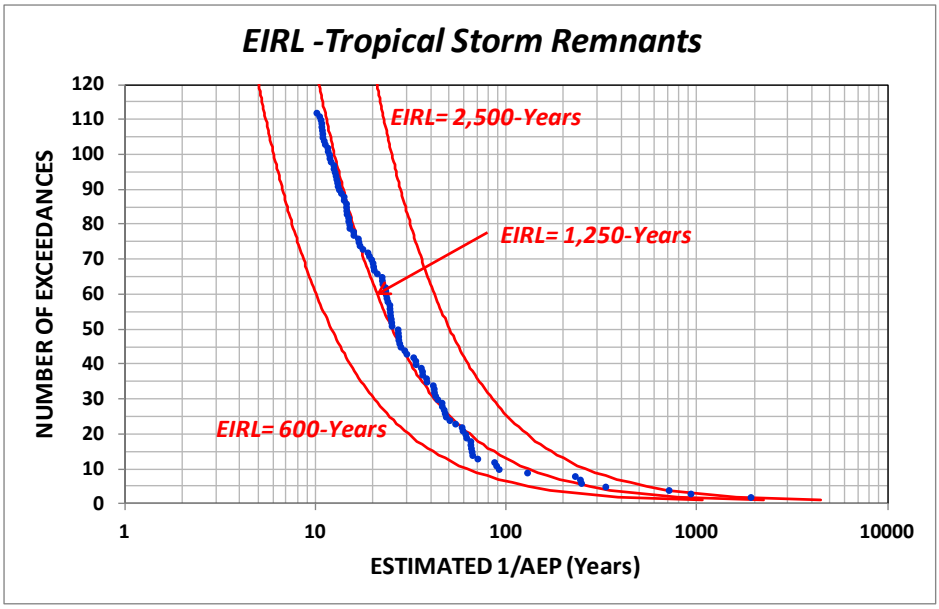


***Figure 116 - Graphical Depiction of EIRL for 48-Hour Duration TSRs***

## 11.10 24-Hour and 72-Hour Precipitation Annual Maxima for Tropical Storm Remnants (TSRs)

Precipitation annual maxima datasets were also assembled for the 24-hour and 72-hour durations for TSRs. These datasets were assembled to provide information on the variation of temporal storm characteristics across the TVSA and to provide information on regional L-Skewness and identification of the regional probability distribution.

### 11.10.1 Depth-Duration Ratios for 24-Hour, 48-Hour and 72-Hour At-Site Means

***Figure 117*** – ***Figure 120*** show the depth-duration ratio of observed at-site means for the 24-hour/48-hour durations for the TSR storm type and variation with longitude and mean annual precipitation, respectively. Similarly, ***Figure 121*** – ***Figure 124*** show the depth-duration ratio of observed at-site means for the 72-hour/48-hour durations for the TSR storm type and variation with longitude and mean annual precipitation, respectively, for three different regions.

A review of ***Figure 117***, ***Figure 118***, ***Figure 121*** and ***Figure 122*** shows both the 24-hr/48-hr and 72-hr/48-hr depth-duration ratios vary systematically with longitude, but show minor change across the study area. Similarly, ***Figure 119***, ***Figure 120***, ***Figure 123*** and ***Figure 124*** shows both the 24-hr/48-hr and 72-hr/48-hr depth-duration ratios to vary systematically with mean annual precipitation, although the variation is minor across the study area. This similarity in behavior indicates that storm-specific depth-duration curves for historical storms are transpositionable throughout the study area. In particular, storm temporal patterns would be transferable throughout the Tennessee Valley watershed.

A depth-duration curve was prepared (***Figure 125***) to show typical depth-duration behavior for TSR storms. This information indicates that the majority of TSR precipitation typically falls within a 24-hour period, and 72-hour precipitation is not markedly greater than 24-hour precipitation. Depth-duration curves for the collection of historical storms can naturally be expected to vary from this behavior. However, the average (typical) depth-curve for the collection of storms would be expected to be similar to that shown in ***Figure 125***.

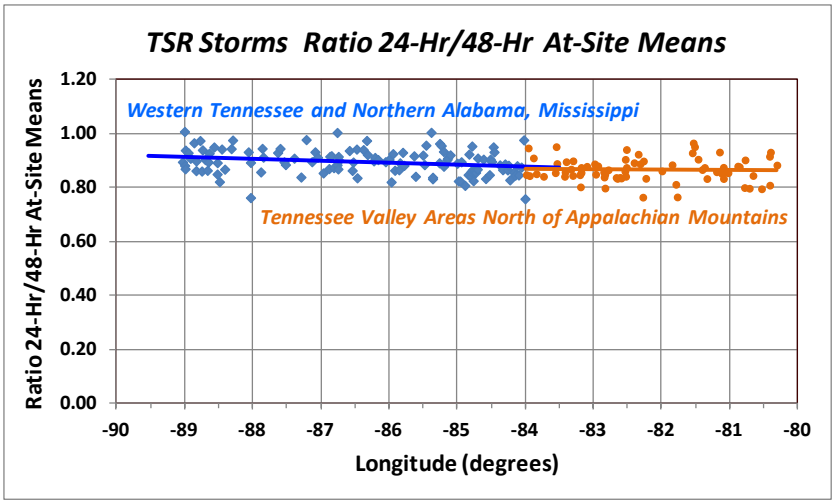


***Figure 117 - Variation with Longitude for the Ratio of 24-Hour to 48-Hour At-Site Means for the TSR Storm Type for Western Tennessee and the Tennessee Valley***

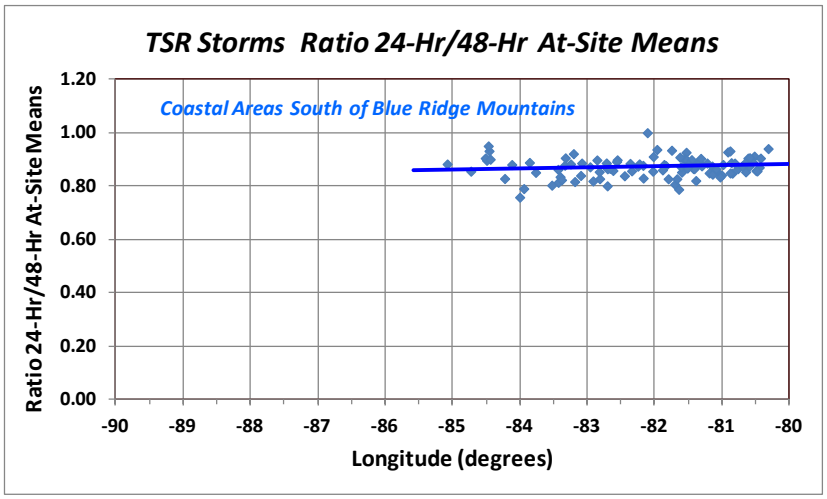


***Figure 118 - Variation with Longitude for the Ratio of 24-Hour to 48-Hour At-Site Means for the TSR Storm Type for Coastal Areas South of the Blue Ridge Mountains***

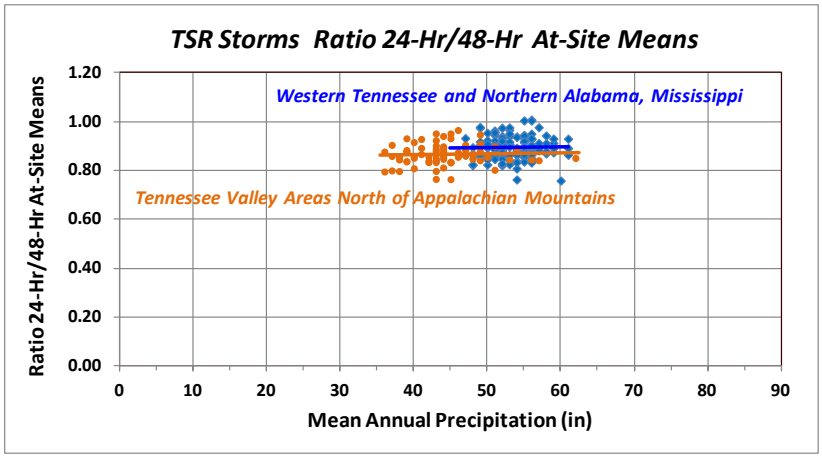


*Figure 119 - Variation with Mean Annual Precipitation for the Ratio of 24-Hour to 48-Hour At-Site Means for the TSR Storm Type for Western Tennessee and the Tennessee Valley*

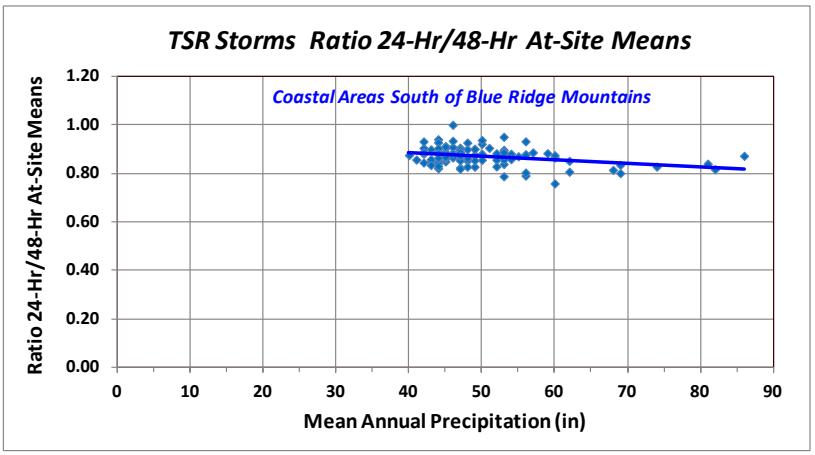


*Figure 120 - Variation with Mean Annual Precipitation for the Ratio of 24-Hour to 48-Hour At-Site Means for the TSR Storm Type for Coastal Areas South of the Blue Ridge Mountains*

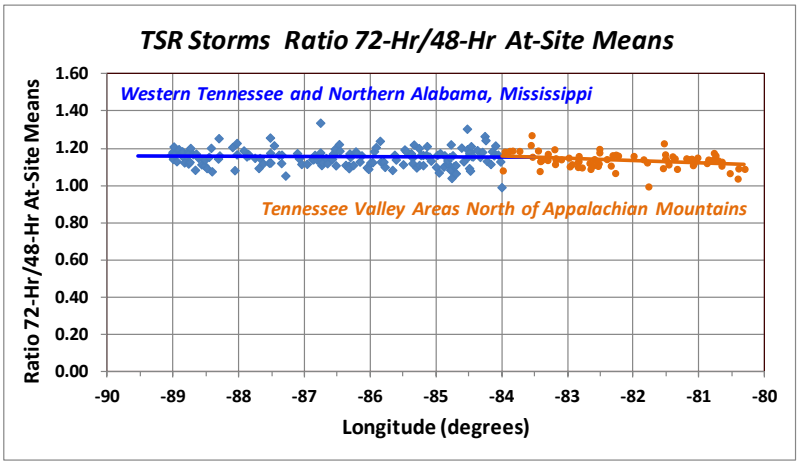


*Figure 121 - Variation with Longitude for the Ratio of 72-Hour to 48-Hour At-Site Means for the TSR Storm Type for Western Tennessee and the Tennessee Valley*

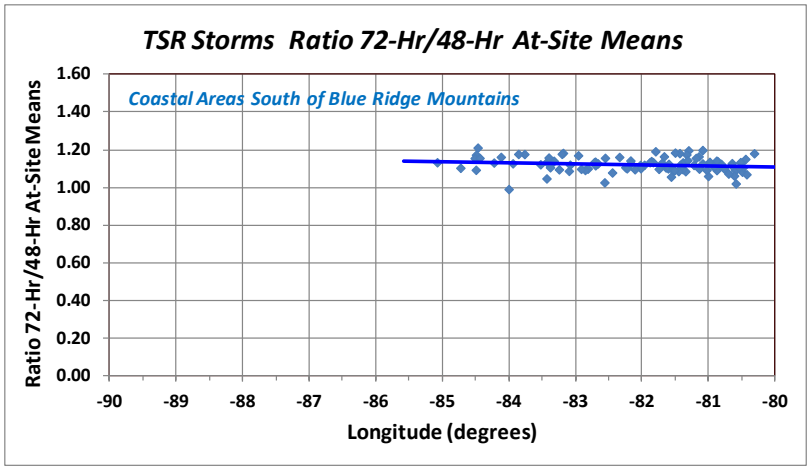


*Figure 122 - Variation with Longitude for the Ratio of 72-Hour to 48-Hour At-Site Means for the TSR Storm Type for Coastal Areas South of the Blue Ridge Mountains*

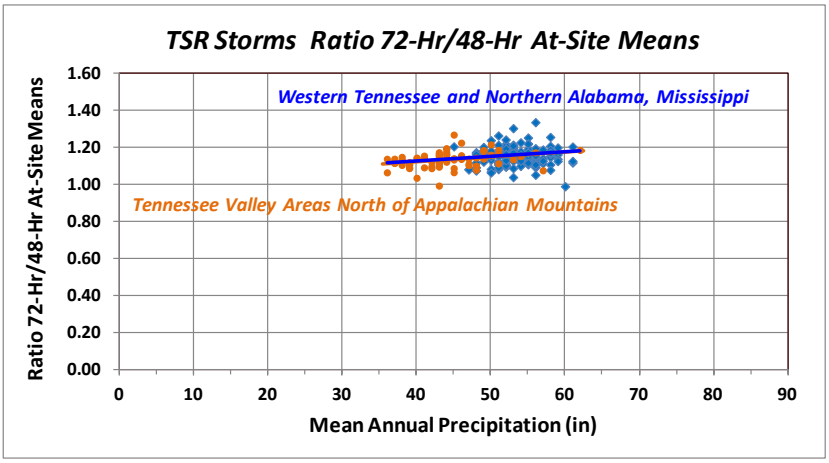


*Figure 123 - Variation with Mean Annual Precipitation for the Ratio of 72-Hour to 48-Hour At-Site Means for the TSR Storm Type for Western Tennessee and the Tennessee Valley*

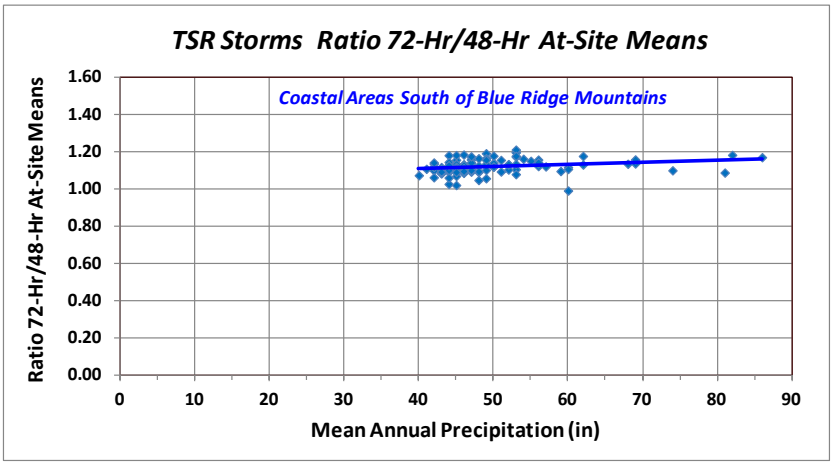


*Figure 124 - Variation with Mean Annual Precipitation for the Ratio of 72-Hour to 48-Hour At-Site Means for the TSR Storm Type for Coastal Areas South of the Blue Ridge Mountains*

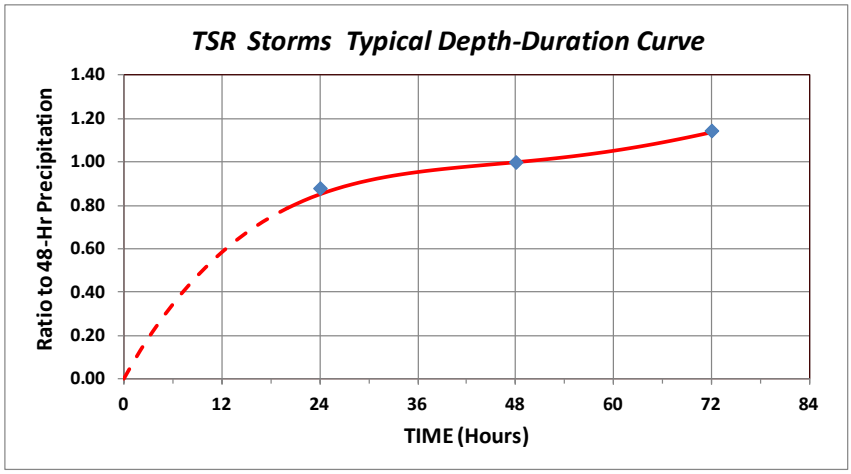


*Figure 125 - Typical Depth-Duration Curve for the TSR Storm Type*

### 11.10.2 Identification of Regional Probability Distribution for 24-Hour and 72-Hour Durations

L-moment regional frequency analyses were conducted for homogeneous sub-regions for the 24-hour and 72-hour durations in the manner described previously for the 48-hour key duration. These analyses were conducted to provide regional L-Skewness and L-Kurtosis pairings for identification of the regional probability distributions for the 24-hour and 72-hour durations.

***Figure 126***, ***Figure 127*** and ***Figure 128*** depict the centroids for the L-Skewness and L-Kurtosis pairings for the 24-hour, 48-hour and 72-hour durations for western Tennessee and northern Alabama, the Tennessee Valley north of the Appalachian Mountains, and the coastal areas to the south of the Blue Ridge Mountains, respectively. The results for the 24-hour and 72-hour durations support the original selections of the values of the second shape parameters for the 48-hour duration (***Table 24***).

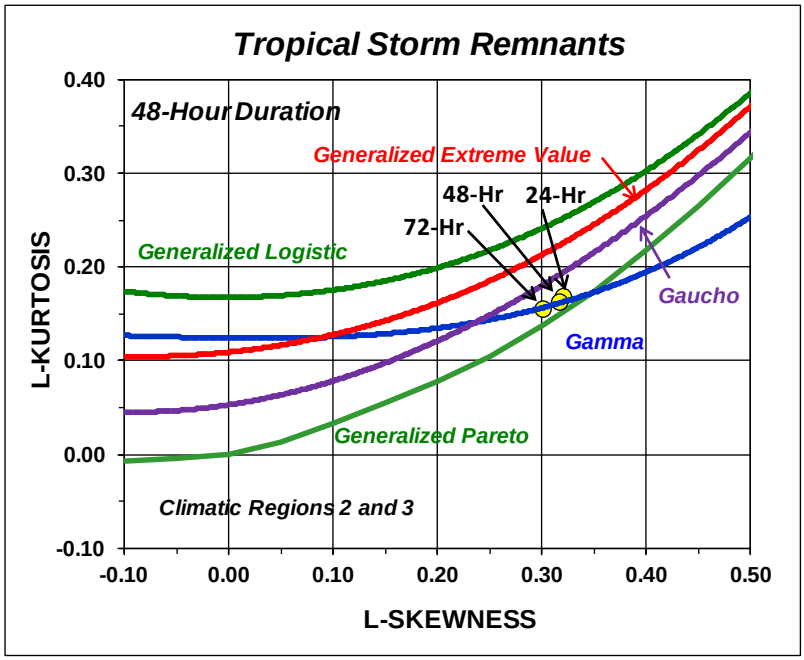


*Figure 126 - L-Moment Ratio Diagram Depicting Regionwide L-Skewness and L-Kurtosis Values for Homogeneous Sub-Regions within Climatic Regions 2 and 3 in Western Tennessee and Northern Alabama for the 24-Hour, 48-Hour and 72-Hour Durations for Tropical Storms*

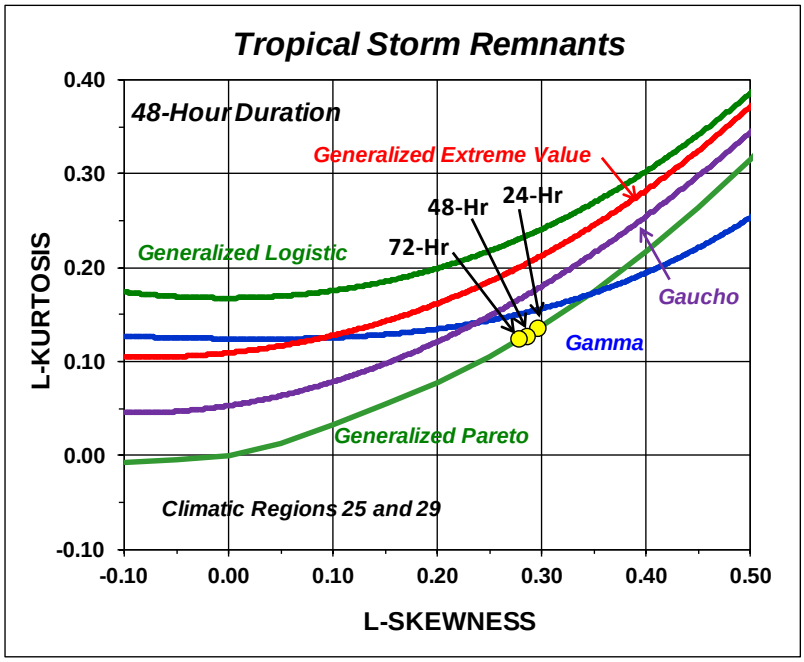


*Figure 127 - L-Moment Ratio Diagram Depicting Regionwide L-Skewness and L-Kurtosis Values for Homogeneous Sub-Regions within Climatic Regions 25 and 29 to the Southeast of the Blue Ridge Mountains the 24-Hour, 48-Hour and 72-Hour Durations for Tropical Storms*

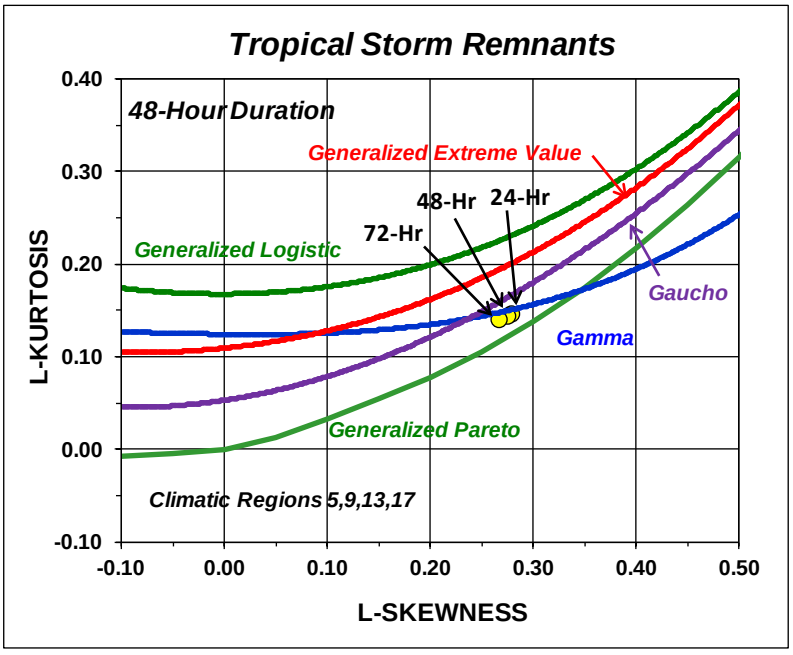


*Figure 128 - L-Moment Ratio Diagram Depicting Regional L-Skewness and L-Kurtosis Values for Homogeneous Sub-Regions within Climatic Regions 5, 9, 13 and 17 in the Tennessee Valley to the North of the Appalachian Mountains for the 24-Hour, 48-Hour and 72-Hour Durations for Tropical Storms*

# 12 Summary

This report provides descriptions of the methodologies employed and the findings obtained from regional precipitation-frequency analyses conducted for point precipitation for locations within the Tennessee Valley watershed. This study is Phase 1 of a three-phase program for developing precipitation-frequency relationships and scalable storm templates for watersheds in the Tennessee Valley. The ultimate goal is to conduct stochastic modeling for floods generated by the various storm types and to develop hydrologic hazard curves for dams and nuclear plants operated by the Tennessee Valley Authority (TVA).

The Tennessee Valley Study Area (TVSA) included the Tennessee Valley watershed and bordering areas in the states of Alabama, Georgia, Kentucky, Mississippi, North Carolina, South Carolina, Virginia, and West Virginia. Thirteen climatic regions were defined to assist in the regional analyses for depicting the spatial variation of precipitation maxima in the complex topographic study area.

A major component of the study was the development of precipitation data series that were comprised of precipitation maxima produced by specific storm types. This was accomplished by using meteorological criteria to identify the storm type for each rainy day in the period from 1881 through mid-2014 and using this database in assembling precipitation annual maxima data series for precipitation stations for each of four storm types. The storm types included Local Storms (LS), Mesoscale Storms with Embedded Convection (MEC), and synoptic-scale Mid-Latitude Cyclones (MLC) and Tropical Storm Remnants (TSR). There were 1,250 precipitation measurement stations and 60,096 station-years of record available for the synoptic-scale MLC and TSR storm types, 393 stations and 13,516 station-years of record for the MEC storm type, and 221 stations and 9,160 station-years of record for the LS storm type.

Separate regional precipitation-frequency analyses were conducted for precipitation annual maxima data series for key durations for each of the four storm types. The key durations were 48-hours for the synoptic scale MLC and TSR storm types, 6-hours for the mesoscale MEC storm type, and 1-hour for the LS storm type. Findings from the regional analyses provided for spatial mapping of statistical measures used to develop the point precipitation-frequency relationships. This included spatial mapping of the at-site means, regional L-moment ratio statistics L-Cv and L-Skewness, and identification of the regional probability distribution. This information provided for development of point precipitation-frequency relationships for locations throughout the TVSA. Isopluvial maps were prepared for point precipitation maxima for annual exceedance probabilities of $10^{-1}$, $10^{-2}$, $10^{-3}$, $10^{-4}$ and $10^{-5}$ for the key durations for each of the four storm types.

Equivalent Independent Record Length (EIRL) analyses were conducted for each storm type to provide a measure of the effective record length of the statistical information for the storms contained in the regional datasets. This information will be used in uncertainty analyses in Phase 3 to develop uncertainty bounds for watershed-specific precipitation-frequency relationships.

Seasonality analyses were also conducted for the four storm types that provide a probabilistic description of the likelihood for storms to occur at various times throughout the year. This information is important for stochastic modeling of floods for the four storm types.

The next steps in the three-phase program of study are:

- Phase 2 – Analyze historical storms and develop scalable spatial and temporal storm patterns for the four storm types; and
- Phase 3 – Develop precipitation-frequency relationships and uncertainty bounds for watersheds in the Tennessee Valley for four storm types for use in stochastic flood modeling.

## 12.1 Discussion of Findings

A number of storm types can produce floods in the Tennessee Valley for watersheds of various sizes. Each of these storm types has different spatial, temporal and seasonal characteristics, which results in a mixed population of storms and floods when frequency analysis is attempted, Traditional practice in precipitation-frequency analysis in the United States has been to only consider precipitation magnitudes for a given

duration without regard to the storm type and associated precipitation generating mechanisms. This approach can have significant shortcomings where there is a mixed population of storm types and extreme events are of interest.

The approach taken in this study was to first identify precipitation events by storm type and then conduct regional precipitation-frequency analysis for each storm type. This approach provides for a direct link between watershed precipitation-frequency and the storm spatial, temporal and seasonal characteristics. This is critically important when the precipitation-frequency information is to be used for rainfall-runoff modeling for development of flood-frequency relationships. For this reason, the storm typing approach coupled with regional precipitation-frequency analysis is a major advancement over the traditional precipitation-frequency approach.

The storm typing approach applied to the TVSA has allowed greater insight into the statistical characteristics of the various storm types. There is increased reliability in the precipitation-frequency relationships for the MLC, MEC and LS storm types. This occurs because the L-moment ratio statistics were found to have only minor variation across the TVSA based on very large regional datasets. In the case of the TSR storm type, the storm typing approach allowed for precipitation-frequency analysis of TSR precipitation, which would not have been possible with the traditional approach. The spatial pattern and site-specific precipitation-frequency characteristics for the synoptic scale TSR storm type are quite dissimilar to the other synoptic scale MLC storm type. This is an important finding for application in modeling of floods generated by TSR events.

The findings of the point precipitation-frequency analyses for the four storm types will provide a sound technical basis for development of watershed-specific precipitation-frequency relationships and for stochastic flood modeling for the various storm types.

# 13 General References


1. Cleveland WS, Computer Programs For Locally Weighted Regression (LOWESS), Bell Laboratories NJ, Dec 1985
2. Cunnane C, Unbiased Plotting Positions - A Review, Journal of Hydrology, 37, 205-222, 1978.
3. Dalrymple D, Flood Frequency Analysis, USGS, Water Supply Paper 1543-A, 1960.
4. Daly C, PRISM, Parameter-Elevation Regression on Independent Slopes Model, Oregon State University, Oregon Climate Service, 1994.
5. Daly C, Neilson RP, and Phillips DL, PRISM, A Statistical-Topographic Model for Mapping Climatological Precipitation over Mountainous Terrain, Journal of Applied Meteorology, Vol 33, pp140-158, 1994.
6. Fiorentino MS, Gabrielle S, Rossi F and Versace P, Hierarchical Approach for Regional Frequency Analysis, *Regional Frequency Analysis*, Edited by VP Singh, pp35-49, Reidel, Norwell Massachusetts, 1979.
7. Helsel DR and Hirsch RM, Statistical Methods in Water Resources, Elsevier Studies in Environmental Science 49, NY, 1992.
8. Hirsch RM, Helsel DR, Cohn TA and Gilroy EJ, Statistical Analysis of Hydrologic Data, Chapter 17, *Handbook of Hydrology*, McGraw Hill, 1992.
9. Hosking JRM, L-Moments: Analysis and Estimation of Distributions using Linear Combinations of Order Statistics, Journal Royal Statistical Society, Ser B, 52, pp105-124, 1990.
10. Hosking JRM, and Wallis JR, Regional Frequency Analysis - An Approach Based on L-Moments, Cambridge Press, 1997.
11. Jain R, The Art of Computer Systems Performance Analysis, John Wiley and Sons, 1991.
12. Kuczera G, Combining Site-Specific and Regional Information: An Empirical Bayes Approach, Water Resources Research, Volume 18, No. 2, pp306-314, April 1982.
13. L-RAP, L-Moments Regional Analysis Package, MGS Software LLC, 2009, developed by Schaefer MG and Barker BL.
14. NOAA, NOAA-CIRES Twentieth Century Global Reanalysis Version II.
15. NWS, NOAA Atlas 14 Precipitation Frequency Atlas of the United States, Volume 2 and Volume 9, NWS, Silver Spring Maryland.
16. Oregon Climate Service, Mean Annual Precipitation Maps for Western United States, PRISM Model, Corvallis Oregon, 1997.
17. Schaefer MG, Magnitude Frequency Characteristics of Precipitation Annual Maxima in Southern British Columbia, MGS Engineering Consultants, Inc., December 1997.
18. Schaefer MG, Data-Quality Checking Software for Precipitation Maxima, MGS Engineering Consultants, 1997.
19. Schaefer MG, Barker BL, Taylor GH and Wallis JR, Regional Precipitation-Frequency Analysis and Spatial Mapping for 24-Hour and 2-Hour Durations for Western Washington, MGS Engineering Consultants and Oregon Climate Service for Washington State Dept. of Transportation, March 2002.
20. Schaefer MG and Barker BL, Stochastic Modeling of Extreme Floods on the American River at Folsom Dam Flood-Frequency Curve Extension, MGS Engineering Consultants for US, US Army Corps of Engineers, Hydrologic Engineering Center, Davis CA, September 2005.
21. Schaefer MG, Barker BL, Taylor GH and Wallis JR, Regional Precipitation-Frequency Analysis and Spatial Mapping for 24-Hour and 2-Hour Durations for Eastern Washington, MGS Engineering Consultants and Oregon Climate Service for Washington State Dept. of Transportation, January 2006.
22. Schaefer MG, Barker BL, Taylor GH and Wallis JR, Regional Frequency Analysis and Spatial Mapping of 24-Hour Precipitation for Oregon, MGS Engineering Consultants and Oregon Climate Service for Oregon State Dept. of Transportation, August 2007.
23. Schaefer MG and Barker BL, Stochastic Event Flood Model – SEFM Users Manual, MGS Engineering Consultants, Inc, January 2009.
24. Schaefer MG, Technical Memorandum, Seasonality Analyses for Storm Types in the TVSA for Use in the Site-Specific PMP Study, prepared for Tennessee Valley Precipitation-Frequency Study, December 2014

25. Stedinger JR, Vogel RM, and Foufoula-Georgiou E, Frequency Analysis of Extreme Events, Chapter 18, *Handbook of Hydrology*, McGraw Hill, 1992.
26. Weiss LL, Ratio of True to Fixed Interval Maximum Rainfall, Journal Hydraulics, ASCE, 90(HY1), pp77-82, 1964.
27. Wyss GD and Jorgenson KH, A Users Guide to LHS: Sandia's Latin Hypercube Sampling Software, Sandia National Laboratories, report SAND98-0210, February 1998.

# APPENDIX A
# Listing of Electronic Datasets and Files

A number of electronic datasets and files were created in conducting the precipitation-frequency analysis for the various durations and storm types. The following list identifies electronic files and datasets which are provided as electronic deliverables for the precipitation-frequency study.

- Gridded dataset of mean annual precipitation created by PRISM[5,6] software
- Gridded dataset of mean monthly precipitation for December through March (PRISM)
- Gridded dataset of mean monthly precipitation for June through August (PRISM)
- Catalog of precipitation stations and daily, hourly and synoptic gages used in analyses
- DDST

**Local Storms (LS)**

- L-RAP database of precipitation annual maxima for all stations for 1-hr and 2-hr durations
- Listing of L-moment sample statistics for all stations for all durations
- Gridded datasets of 1-hr at-site means and regional L-Cv and regional L-Skewness
- Gridded datasets of precipitation for 1-hour duration for annual exceedance probabilities of $10^{-1}$, $10^{-2}$, $10^{-3}$, $10^{-4}$ and $10^{-5}$ for Isopluvial mapping
- Listing of largest storms used in conducting seasonality analyses for 2-hr duration
- Listing of independent storm dates, locations and annual exceedance probabilities used in conducting analyses of EIRL for 2-hour duration

**Mesoscale Storms with Embedded Convection (MEC)**

- L-RAP database of precipitation annual maxima for all stations for 2, 6 and 12-hr durations
- Listing of L-moment sample statistics for all stations for all durations
- Gridded datasets of 6-hr at-site means and regional L-Cv and regional L-Skewness
- Gridded datasets of precipitation for 6-hour duration for annual exceedance probabilities of $10^{-1}$, $10^{-2}$, $10^{-3}$, $10^{-4}$ and $10^{-5}$ for Isopluvial mapping
- Listing of largest storms used in conducting seasonality analyses for 6-hr duration
- Listing of independent storm dates, locations and annual exceedance probabilities used in conducting analyses of EIRL for 6-hour duration

**Mid-Latitude Cyclone (MLC)**

- L-RAP database of precipitation annual maxima for all stations for 24, 48 and 72-hr durations
- Listing of L-moment sample statistics for all stations for all durations
- Gridded datasets of 48-hr at-site means and regional L-Cv and regional L-Skewness
- Gridded datasets of precipitation for 48-hour duration for annual exceedance probabilities of $10^{-1}$, $10^{-2}$, $10^{-3}$, $10^{-4}$ and $10^{-5}$ for Isopluvial mapping
- Listing of largest storms used in conducting seasonality analyses for 48-hr duration
- Listing of independent storm dates, locations and annual exceedance probabilities used in conducting analyses of EIRL for 48-hour duration

**Tropical Storm Remnant (TSR)**

- L-RAP database of precipitation annual maxima for all stations for 24, 48 and 72-hr durations
- Listing of L-moment sample statistics for all stations for all durations
- Gridded datasets of 48-hr at-site means and regional L-Cv and regional L-Skewness
- Gridded datasets of precipitation for 48-hour duration for annual exceedance probabilities of $10^{-1}$, $10^{-2}$, $10^{-3}$, $10^{-4}$ and $10^{-5}$ for Isopluvial mapping
- Listing of largest storms used in conducting seasonality analyses for 48-hr duration
- Listing of independent storm dates, locations and annual exceedance probabilities used in conducting analyses of EIRL for 48-hour duration

# APPENDIX B
## List of Acronyms

| Acronym | Description |
|---|---|
| AEP | Annual Exceedance Probability |
| AMS | Annual Maxima Series |
| CAPE | Convective Available Potential Energy |
| CDF | Cumulative Distribution Function |
| DDST | Database of Daily Storm Types |
| EIRL | Equivalent Independent Record Length |
| GEV | Generalized Extreme Value |
| LIP | Local Intensity Precipitation |
| LS/NOI | Local Storm Not of Interest |
| MCC | Mesoscale Convective Complex |
| MEC | Mesoscale Storm with Embedded Convection |
| MEC/NEC | Mesoscale Storm without Embedded Convection |
| MLC | Mid-Latitude Cyclone |
| MLC/EC | Mid-Latitude Cyclone with Embedded Convection |
| NCDC | National Climatic Data Center |
| NOAA | National Oceanic and Atmospheric Administration |
| NWS | National Weather Service |
| PRISM | Parameter-Elevation Regression on Independent Slopes Model |
| Pw | Precipitable Water |
| RMSE | Root Mean Square Error |
| STNC | Storm Type Numeric Code |
| TSR | TSR |
| TSR/EC | TSR with Embedded Convection |
| TVA | Tennessee Valley Authority |
| TVSA | Tennessee Valley Study Area |

# APPENDIX C
## Glossary of Selected Terms

This glossary contains definitions for terms used in report whose definition may be unfamiliar or somewhat different than common usage or a dictionary definition.

Annual Exceedance Probability (AEP) – The probability that a random variable of interest will be equaled or exceeded in a given year.

Annual Maxima Series – A collection of data where the largest value each year is selected. For example, a 60-year period of record yields 60 annual maxima, one for each year. The annual period may be any user-defined 12-month period. This also includes the case where the maximum value in an annual period is selected from a limited number of months during the year, such as occurrence during the warm season. Also see Climatic Year.

At-Site – A term applicable to a specific location, such as at-site data or an at-site parameter. In regional frequency analysis the term at-site is used to distinguish from regional data or regional parameters. In casual conversation, at-site is often used synonymously with station.

Convective Available Potential Energy (CAPE) – A measure of the amount of energy available for convection and represents the positive bouyancy of an air parcel (Joules/Kg). It is an indicator of atmospheric instability and is associated with severe weather, particularly thunderstorm activity.

Climatic Year – A generic term for any 12-month period used in observation/measurement of various environmental phenomena. The climatic year may coincide with the calendar year, or the water year (October 1 –September 30), or any 12-month period. In precipitation-frequency analysis, the start/end of the climatic year is typically taken at a time when there is low activity in the phenomenon of interest.

Cumulative Distribution Function (CDF) – A mathematical function that describes the probability that a real-valued random variable will have a value that is less than or equal to some value (x) of interest. Notationally; $F(x)=P(X<x)$ which is read as the CDF is equal to the probability that the random variable X is less than or equal to x. F(x) is a non-exceedance probability.

Data Series – The collection of data for a site.

Deterministic Model – A model (equation, algorithm, or computer model) whose outcome(s) can be exactly determined by application of the laws of physics or other mathematical relationships.

Gage – A generic term for a variety of instruments used to measure environmental data such as precipitation, snowpack, air temperature, wind-speed, evaporation, solar radiation, streamflow, river stage, etc.

Gridded Dataset – A dataset comprised of rows and columns corresponding to the grid-cell network for a geographical area (see raster dataset).

Heterogeneous Climatic Region – A heterogeneous climatic region is a geographic area where the sites have many similar features such as climatology and topography. However, there are sufficient differences in the behavior of site data that the collection of sites within the climatic region do not meet criterion for a homogeneous region.

Homogeneous Region – A homogeneous region satisfies the condition that all sites within the region can be described by one probability distribution having common distribution parameters after the site data are rescaled by their at-site mean. Thus, all sites within a homogeneous region have a common regional magnitude-frequency curve, termed a regional growth curve. A homogeneous region may be a geographic

area delineated on a map or it may be a collection of sites having similar characteristics pertinent to the phenomenon being investigated. For the case of a homogeneous region delineated on a map, the region may be contiguous or a collection of separate areas. Also see homogeneous sub-region

Homogeneous Sub-region – Homogeneous sub-region has the same meaning as homogeneous region. The term homogeneous sub-region is often used in connection with the term heterogeneous super-region to clarify that the heterogeneous climatic region may be subdivided to produce homogeneous sub-regions.

Isopercental Method – A methodology for spatial interpolation of observed point values where the field of interest is non-linear. For the case of precipitation, it involves transformation of observed precipitation for a specific storm by division by an indexing value that reflects the average storm climatology. The transformed values are the isopercental values. This allows Inverse Distance Weighting to be used for spatial interpolation of the isopercental values in the transformed space. The isopercental field is then transformed back to the precipitation field to reflect the complex terrain features that reside between the observed point values.

Isopluvial Map – A generic term for a map showing the spatial distribution of precipitation over an area including contours (isolines) of precipitation magnitude.

Local Storm – A generic term given to relatively small scale convective events (thunderstorms) which occur in the warm season.

Observational Period – Many instrumentation systems for measuring environmental data report the measurements on fixed intervals. The fixed interval may be 5 minutes, 15 minutes, hourly, daily, etc. The observational period is the term used for the time interval of the reported measurements (i.e. 15 minutes).

Precipitable Water – The depth of water in a column of the atmosphere if all of the atmospheric moisture in the column was precipitated as rain (in, mm).

Probabilistic Method – A method using a model whose outcome(s) express the probability of an event or events occurring (not occurring), the magnitude of some item of iterest being exceeded (not-exceeded) or being within certain limits.

Quantile Estimate – The estimate from a quantile function where the quantile function was developed from observed data. For example, it would be the estimate of 48-hour precipitation for a mid-latitude cyclone for a non-exceedance probability of 0.999.

Quantile Function – The inverse of the Cumulative Distribution Function (CDF). It is a mathematical function used to compute values of a random variable associated with specified non-exceedance probabilities.

Raster Data – A data type consisting of rows and columns of cells, with each cell storing a single value. Also see gridded dataset.

Region – A generic term used in regional frequency analysis that can have many meanings. It may refer to a collection of sites. It can also refer to a geographical area and all sites within the geographic area. It can also be used conceptually, where region refers to all sites having common characteristics and that may or may not be contiguous geographically.

Regional Probability Distribution – The probability distribution that is applicable to all sites within a specified region.

Regional Value – As used in regional frequency analysis, it is a parameter that is applicable to a given region. It is computed as a weighted average of at-site (station) values where the weights are based on record length.

Site – A generic term to indicate a location of interest. It is often used for the situation where an instrument is located to measure an element of a specified phenomenon. Also see the definition for Station and At-Site.

Station – The casual use of the term station originated from First Order Weather Stations where a variety of instruments were in-place for measuring weather-related phenomenon. Streamflow gaging sites on river systems were also referred to as stations, and thus the term station has taken on the generic meaning of any site where an instrument(s) is located for measurement of some phenomenon. The terms station, site and gage are often used interchangeably, particularly in casual conversation.

Stochastic Method – an approach using a model whose outcome(s) is the result of some combination of deterministic, probabilistic and random components. The current "state" is typically expressed as a function of the past "state" of the process. In short, the future is a function of the past and random chance.

Site Meta-Data – Site meta-data (metadata) are data about the location of a specific site. This might include: the site name; site identification number; latitude; longitude; elevation; governmental jurisdiction unit; gage type (instrument for measurement); user-assigned region number; mean annual precipitation; starting and ending year of record; and anything pertinent to the phenomenon of interest.

Station Meta-Data – Same meaning as site meta-data.

Synoptic Scale – a weather system or feature recognizable at a horizontal scale of 1000 km or more, such as low pressure systems and fronts.

# APPENDIX D
# L-Moment Statistics

Note that this Appendix is excerpted directly from Chapter 3 of the L-RAP User's Manual[13].

## D.1 L-Moments

L-moment statistics are used extensively in L-RAP. L-moment statistics are used for computing sample statistics for data at individual sites; for testing for homogeneity/heterogeneity of proposed groupings of sites (regions); for conducting goodness-of-fit tests for identifying a suitable probability distribution(s); and for solving for distribution parameters for the selected probability distribution. In particular, estimation of the L-moment ratios of L-Cv and L-Skewness is a key element in determining the success of the regional frequency analysis in computing quantile estimates for selected sites.

L-moments obtain their name from their construction as linear combinations of order statistics (Hosking and Wallis[10], pp18-27). They are a dramatic improvement over conventional product moment statistics for characterizing the shape of a probability distribution and estimating the distribution parameters, particularly for environmental data where sample sizes are commonly small. Unlike product moments, the sampling properties for L-moments statistics are nearly unbiased, even in small samples, and are near Normally distributed. These properties make them well suited for characterizing environmental data that commonly exhibit moderate to high skewness.

The L-moment measure of location, and L-moment ratio measures of scale, skewness and kurtosis are:

Location, mean:

$$\text{Mean} = L_1$$

Scale, L-Cv ($t_2$):

$$t_2 = L_2/L_1$$

L-Skewness ($t_3$):

$$t_3 = L_3/L_2$$

L-Kurtosis ($t_4$):

$$t_4 = L_4/L_2$$

where: $L_1 = \beta_0$

$L_2 = 2\beta_1 - \beta_0$

$L_3 = 6\beta_2 - 6\beta_1 + \beta_0$

$L_4 = 20\beta_3 - 30\beta_2 + 12\beta_1 - \beta_0$

and, where the data ($X_{1:n}$) are first ranked in ascending order from 1 to $n$ and:

$$\beta_0 = n^{-1} \sum_{j=1}^{n} X_j$$

$$\beta_1 = n^{-1} \sum_{j=2}^{n} X_j [(j-1)/(n-1)]$$

$$\beta_2 = n^{-1} \sum_{j=3}^{n} X_j [(j-1)(j-2)]/[(n-1)(n-2)]$$

$$\beta_3 = n^{-1} \sum_{j=4}^{n} X_j [(j-1)(j-2)(j-3)]/[(n-1)(n-2)(n-3)]$$

### D.1.1 Graphical Depictions of L-Cv and L-Skewness

L-Cv is a dimensionless measure of variability. For a distribution or sample data that only has positive values, L-Cv is in the range $0 \leq L\text{-}Cv < 1$. Negative values of L-Cv are only possible if the at-site mean has a negative value. ***Table D-1*** lists some guidelines for describing the relative magnitude of L-Cv for a dataset or distribution.

L-Skewness is a dimensionless measure of asymmetry, which may take on positive or negative values. For a distribution or sample data, L-Skewness is in the range $0 \leq |\, L\text{-}Skewness \,| < 1$. ***Table D-2*** lists some guidelines for characterizing the relative magnitude of L-Skewness for a dataset or distribution.

***Table D-1 - General Descriptions of Relative Magnitude of L-Cv***

| ASSESSMENT OF THE RELATIVE MAGNITUDE OF L-Cv | |
|---|---|
| $.000 < \lvert L\text{-}C_v \rvert \leq .025$ | minimal variability – often found in controlled manufacturing processes |
| $.025 < \lvert L\text{-}C_v \rvert \leq .075$ | minor variability |
| $.075 < \lvert L\text{-}C_v \rvert \leq .150$ | moderate variability |
| $.150 < \lvert L\text{-}C_v \rvert \leq .400$ | large variability – often accompanied by large skewness |
| $.400 < \lvert L\text{-}C_v \rvert$ | very large variability – often accompanied by very large skewness |

***Table D-2 - General Descriptions of Relative Magnitude of L-Skewness***

| ASSESSMENT OF THE RELATIVE MAGNITUDE OF L-SKEWNESS | |
|---|---|
| L-skewness = 0.0 | symmetrical distribution |
| $.000 < \lvert$ L-skewness $\rvert \leq .050$ | minor skewness |
| $.050 < \lvert$ L-skewness $\rvert \leq .150$ | moderate skewness |
| $.150 < \lvert$ L-skewness $\rvert \leq .300$ | large skewness |
| $.300 < \lvert$ L-skewness $\rvert$ | very large skewness, suggestive of “volatile” or outlier prone distributions |

***Figure D-1*** through ***Figure D-6*** portray a number of frequency histograms to provide a visual depiction of how the magnitudes of L-Cv and L-Skewness relate to the shapes of sample datasets.

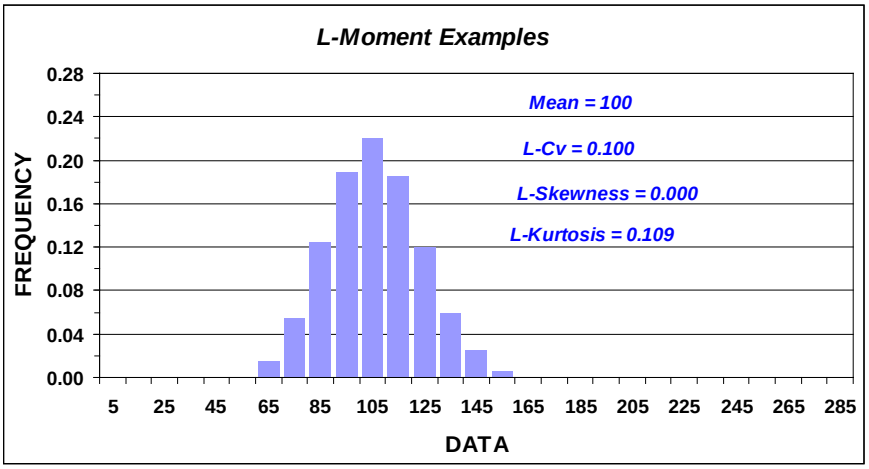


***Figure D-1 - Example Frequency Histogram for Small L-Cv for a Symmetrical Dataset***

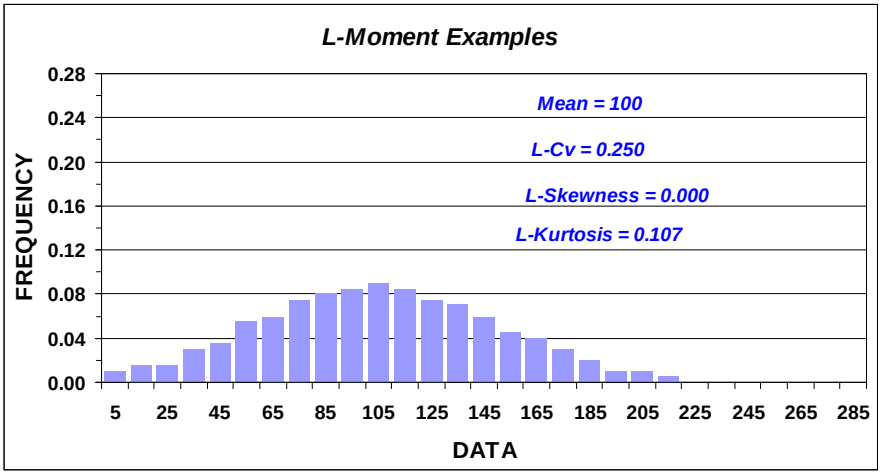


*Figure D-2 - Example Frequency Histogram for Moderate L-Cv for a Symmetrical Dataset*

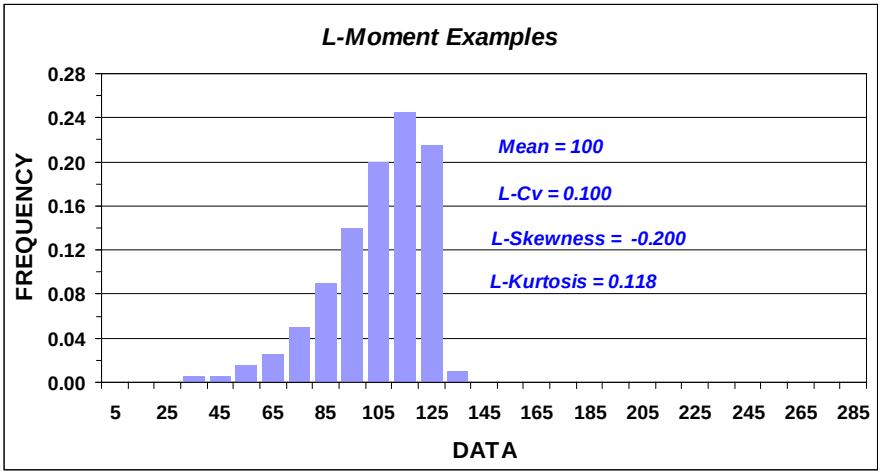


*Figure D-3 - Example Frequency Histogram for a Dataset with Moderate Negative L-Skewness*

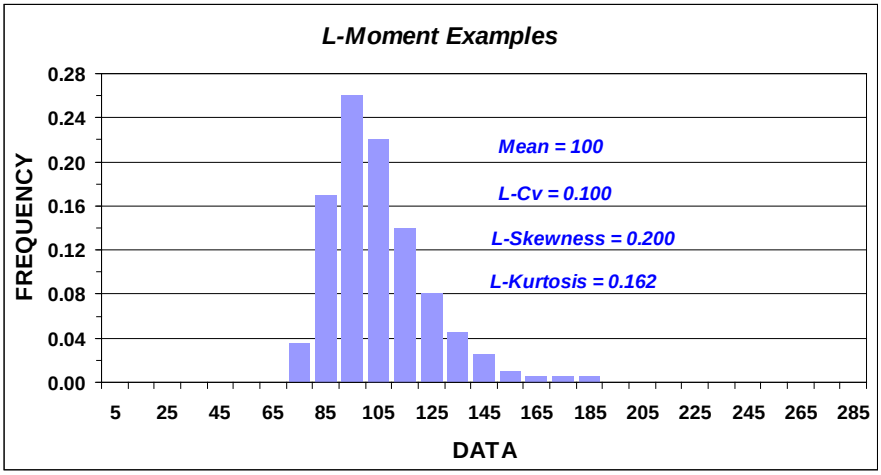


*Figure D-4 - Example Frequency Histogram for a Dataset with Moderate Positive L-Skewness*

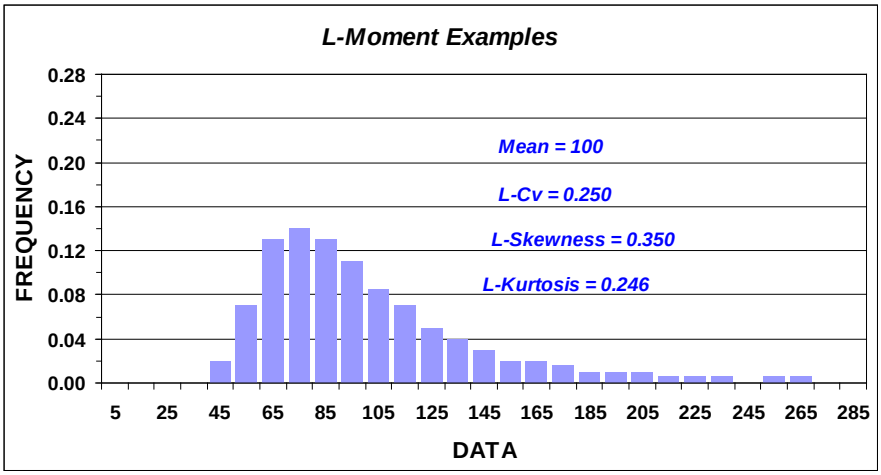


*Figure D-5 - Example Frequency Histogram for a Dataset with Moderate Positive L-Skewness*

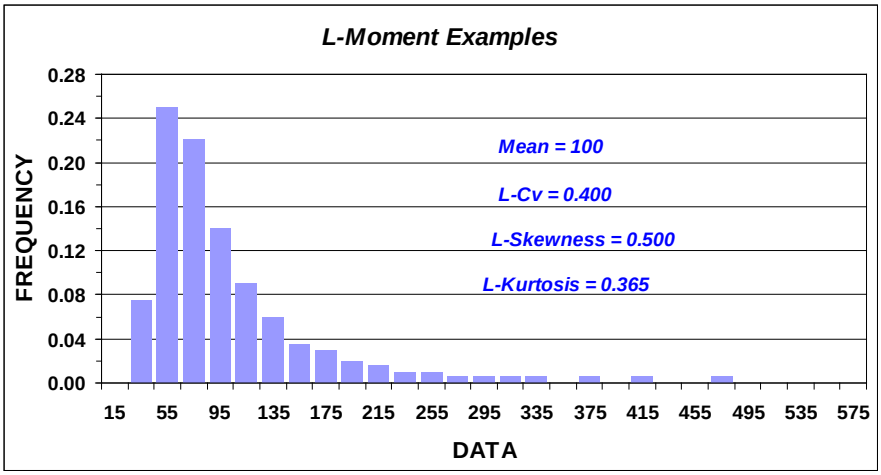


*Figure D-6 - Example Frequency Histogram for a Dataset with Very Large L-Cv and Very Large L-Skewness*

### D.1.2 Effect of Changes in L-Cv and L-Skewness on Regional Growth Curve

As described in Chapter 2 [of the L-RAP User's Manual], a homogeneous region satisfies the condition that all sites within the region can be described by one probability distribution having common distribution parameters after the site data are rescaled by their at-site mean. This rescaled non-dimensional probability distribution is termed a regional growth curve.

The conditions for a homogeneous region also equates to all sites having common values of the L-moment ratio values for L-Cv and L-Skewness. It is therefore useful to examine how changes in L-Cv and L-Skewness affect the behavior of the regional growth curve. An example was created for the GEV distribution to show the general behavior of how changes in L-Cv and L-Skewness affect the shape of the regional growth curve. Similar behavior would be seen for other 3-parameter probability distributions. Review of ***Figure D-7*** shows that if L-Cv is varied for a fixed value of L-Skewness, that changes in L-Cv affect the slope of the regional growth curve.

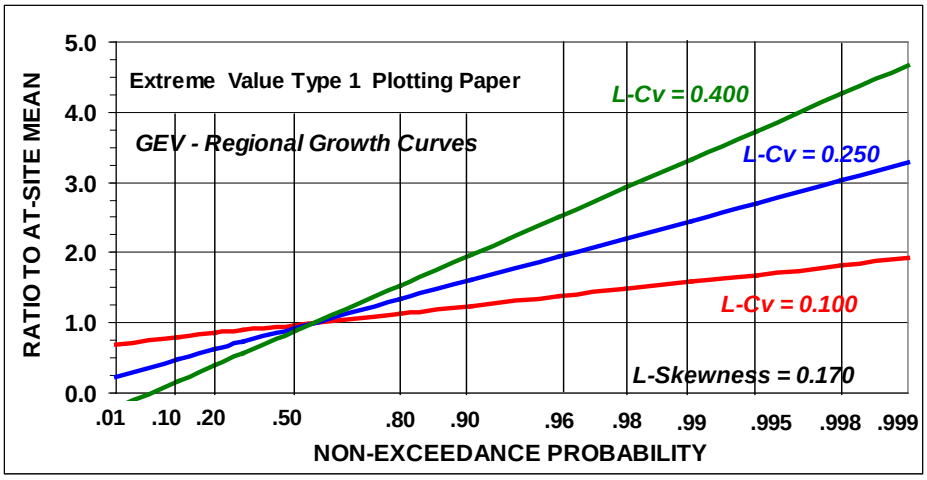


***Figure D-7 - Effect of Changes in L-Cv on Regional Growth Curve for GEV Distribution***

Review of ***Figure D-8*** shows that changes in L-Skewness affect the shape (concave-convex) of the regional growth curve. For positive L-Skewness, increases in the magnitude of L-Skewness primarily affect the upper tail of the regional growth curve. Probability distributions with large positive L-Skewness are often said to be "volatile" having large quantile values for the upper tail. For the case of negative L-Skewness, increases in the magnitude of L-Skewness primarily affect the lower tail of the regional growth curve. This behavior should be kept in mind when considering how quantile estimates are affected by changes in the magnitude of L-Cv and L-Skewness.

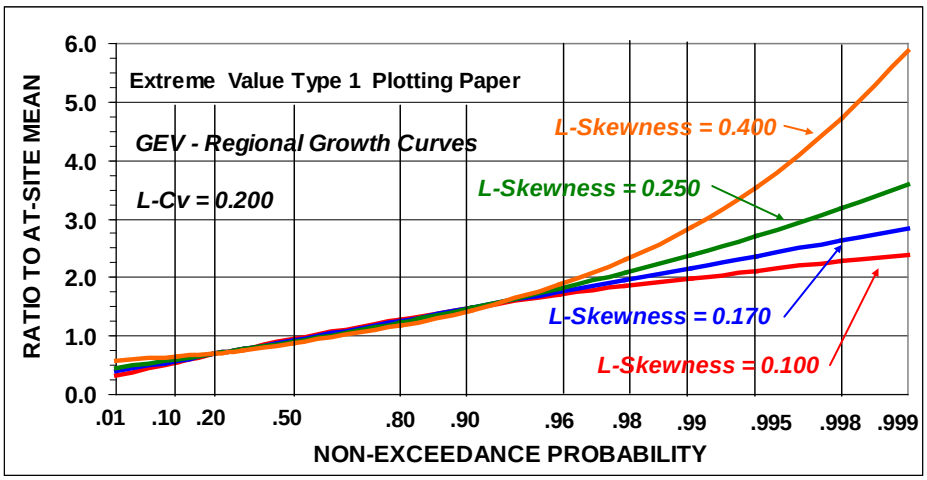


***Figure D-8 - Effect of Changes in L-Skewness to Regional Growth Curve for GEV Distribution***

## D.2 Identification of Discordant Sites Within a Group of Sites

In the process of grouping sites for proposed homogeneous regions, it is standard practice to compute a discordancy measure ($D_i$) for each site (Hosking and Wallis[10], pp45-53). The discordancy measure is used to assist in identifying those sites whose L-moment ratios are discordant (markedly different) relative to L-moment ratios for the collection of sites. Specifically, sites with a discordancy measure greater than 3 are considered discordant relative to the collective behavior for the proposed grouping of sites.

There are two applications for use of the discordancy measure. The primary application is in the data screening process where the discordancy measure is used to identify suspicious datasets (sites) where data quality problems may be responsible for the discordant behavior. The second application is in conducting a regional analysis. In this application, if the proposed region is found to be heterogeneous as indicated by a large value of the heterogeneity measure (H1), then the physical characteristics of discordant sites may be

helpful in understanding the cause of heterogeneity. This assists in determining the course of action needed to produce a homogeneous region, such as moving a site from one candidate homogeneous region to another.

### D.2.1 Discordant Sites Found in Data Screening Process

Those datasets that are flagged as discordant in the data screening process should be reviewed by examining the probability plot and time series graphics (data-screening tab) to determine if there are one or more data values whose magnitude differs markedly from the general behavior of the dataset. If discordant data values are found, the record for that site should be examined and a determination made if the data values are the result of some error in the measurement, recording or data entry process or if the values are valid. This is usually done by comparison of values with nearby sites or by using other independent information.

Identification of a discordant site or sites does not necessarily mean the site does not belong with the proposed grouping of sites. Rather, it is an indicator that additional research is needed to determine the cause of the discordancy before a decision can be made whether to keep the discordant site with the proposed group of sites; move the site to another grouping of sites; or remove the site from all analyses.

There are many possible reasons for a discordant site. ***Table D-3*** contains a partial list of possible reasons and recommended actions. In particular, it is important to note that low or high outliers should not be removed from the datasets. Low and high outliers at some sites are an expected outcome in large samples from multiple sites. The "apparent" outliers are important indicators about the natural variability of the phenomenon and the frequency of occurrence of low or high values. The real issue is the validity of the low or high values. If the data are valid - keep them. If the data are found to be erroneous, remove them.

***Table D-3 - Guidelines for Assessing and Handling of Discordant Sites During Data Screening***

| CAUSE OF DISCORDANCY | POSSIBLE ACTIONS |
|---|---|
| one or more data are suspicious, possibly due to measurement or recording errors | attempt to corroborate suspicious data from other sites or other sources of information, remove invalid data from dataset and re-compute discordancy measure |
| site dataset is generally of poor quality, numerous reasons possible | if data are found to be of poor quality, strong consideration should be given to removing the site from all analyses |
| site dataset is small and an unrepresentative sample has occurred that can be attributed to sampling variability associated with small dataset | keep this site with proposed group of sites unless there are other considerations that cause doubt about inclusion of site |
| site dataset includes one or more unusually large (small) values that can be verified as valid values, discordancy can be attributed to sampling variability | keep this site with proposed group of sites unless there are other considerations that cause doubt about inclusion of site |
| no obvious cause of discordant measure | keep this site with proposed group of sites. Delay decision until heterogeneity measure (H1) is computed during regional analyses. Conduct regional analyses with and without suspect site and compare magnitude of heterogeneity measure H1. Reassign site to another region if heterogeneity measure and other considerations indicate the site was incorrectly assigned |

### D.2.2 Discordant Sites Found in Conducting Regional Analyses

In conducting the regional frequency analysis, the heterogeneity measure (H1) is the primary indicator for accepting or rejecting a proposed region (grouping of sites). The discordancy measures for the various sites provide a secondary indicator to consider whether a discordant site should be moved to another region. ***Table D-4*** provides some rough guidelines to assist in decision-making about what action, if any, to take about a discordant site(s).

***Table D-4 - Guidelines for Handling of Discordant Sites Found During Regional Analyses***

| HETEROGENEITY MEASURE | POSSIBLE ACTIONS |
|---|---|
| H1 ≤ 2 | No compelling reason to reassign discordant site unless large magnitude of discordancy at a particular site is interpreted to mean that the site is improperly assigned |
| 2 < H1 ≤ 3 | Judgment required whether to accept as homogeneous region or to reassign discordant site(s) to another region to improve homogeneity of current grouping of sites |
| 3 < H1 | Proposed region is likely heterogeneous. Examine physical characteristics of discordant sites to assist in understanding of cause of heterogeneity relative to other sites. Consider alternative region formulation by reassigning sites to other regions. |

## D.3 Heterogeneity Measure

Heterogeneity of a proposed region is computed based on the magnitude of the site-to-site variability in the L-moment ratios relative to the level of variability expected in a homogeneous region (Hosking and Wallis[10], pp61-63). The heterogeneity measures H1, H2 and H3 are for the L-moment ratios L-Cv, L-Skewness and L-Kurtosis, respectively. In practice, the H1measure for the observed variability in L-Cv has been found to be a very useful measure. Conversely, the high level of natural variability in sample values of L-Skewness and L-Kurtosis result in the H2 and H3 measures having low discriminatory power. Therefore, the heterogeneity measure H1 for the level of variability in at-site values of L-Cv becomes the de-facto measure for assessing the relative level of heterogeneity for the proposed region.

The heterogeneity measure H1 is computed as follows. A weighted-average regional value of L-Cv ($L\text{-}CV^R$) is computed from the sample values of L-Cv for the proposed sites in the region, where the weights are based on record length. A weighted-average standard deviation is then computed for the at-site L-Cv values for the collection of sites ($V_{LCv}$). A four-parameter Kappa distribution is fitted using the weighted-average regional values of the L-moment ratios for the sites. 500 computer simulations are then conducted using the fitted 4-parameter Kappa distribution, where each simulation has the same number of sites and record lengths as that for the proposed region. The mean ($\mu_v$) and standard deviation ($\sigma_v$) are computed of the 500 samples of the standard deviation of the at-site samples of L-Cv. H1 is then computed as:

$$H1 = \frac{\left(V_{LCv} - \mu_v\right)}{\sigma_v} \qquad 3\text{-}6$$

An H1 value of zero indicates that the site-to-site variability in at-site L-Cv values for the region are the same as would be expected from a homogeneous region with the observed L-moment ratios as fitted by a four-parameter Kappa distribution. Positive values of H1 indicate the site-to-site variability of at-site L-Cv values is greater than expected for a homogeneous region, and larger values of H1 indicate possible or likely heterogeneity (see Table 3-3). Conversely, negative values of H1 indicate the site-to-site variability of at-site L-Cv values is less than expected and the proposed region would be accepted as homogeneous.

An H1 value of 1.0 was originally proposed in Hosking and Wallis[10] (pp63) for determining if the proposed region was acceptably homogeneous. That criterion was based solely on statistical considerations of the sampling characteristics for L-Cv. Oftentimes, there is additional variability in L-Cv that arises from difficulties in the accurate measurement and recording of data. In addition, there may be a variety of data quality control issues associated with human intervention in collecting and managing the data. Experience to date indicates that an H1 value of 2.0 is a reasonable choice for distinguishing between likely homogeneous and likely heterogeneous regions (Wallis[39]). Table 3-3 lists guidelines for acceptance of proposed homogeneous regions where external sources add to the variability in L-Cv beyond statistical considerations of sampling variability. Adjustment of the threshold values of H1 in ***Table D-5*** may be warranted for analyses of some phenomenon based on the magnitude of variability imparted to sample data from consideration of data accuracy and quality control considerations. Somewhat lower threshold values of H1 may be used for environmental data where there is reasonably high accuracy in data measurement and recording and where good data quality control is possible.

*Table D-5 - Guidelines for Acceptance/Rejection of Proposed Region*

| HETEROGENEITY MEASURE | DECISION ON HOMOGENEOUS REGION |
|---|---|
| H1 ≤ 2 | Proposed Region is Acceptably Homogeneous |
| 2 < H1 ≤ 3 | Marginal Heterogeneity<br>Reassignment of some sites may be beneficial |
| 3 < H1 | Proposed Region is Likely Heterogeneous<br>Reassignment of some sites is needed |

## D.4 Distribution Goodness-Of-Fit Measure

A goodness-of-fit measure (Hosking and Wallis[10], pp78-85) is used for identifying the probability distribution(s) that most closely matches the weighted-average regional L-Skewness and L-Kurtosis values for the grouping of sites for the proposed region. The test can best be visualized using the L-Moment Ratio Diagram shown in ***Figure D-9***. The test can be viewed as plotting the regional L-Skewness and L-Kurtosis values obtained from the sites for the proposed region and identifying the probability distribution(s) whose L-Kurtosis value most closely matches the regional L-Kurtosis value. The computation procedures for the goodness-of-fit measure $Z_{dist}$ are described in detail on pp79-81 of Hosking and Wallis[10].

### D.4.1 Probability Distributions Available in L-RAP

Seven probability distributions are available in L-RAP for fitting of regional data (***Figure D-9***). These seven distributions cover a wide portion of the L-Moment Ratio Diagram that has been found to be useful for describing environmental data. The seven distributions include:

- Generalized Logistic (GLO), special case of Kappa distribution with shape parameter *h = -1*
- GEV, special case of Kappa distribution with shape parameter *h = 0*
- Generalized Normal (GNO)
- Gaucho, special case of Kappa distribution with shape parameter *h = +0.5*
- Generalized Pareto (GPA), special case of Kappa distribution with shape parameter *h = +1*
- Pearson 3 (P3)
- Kappa distribution (KAP)

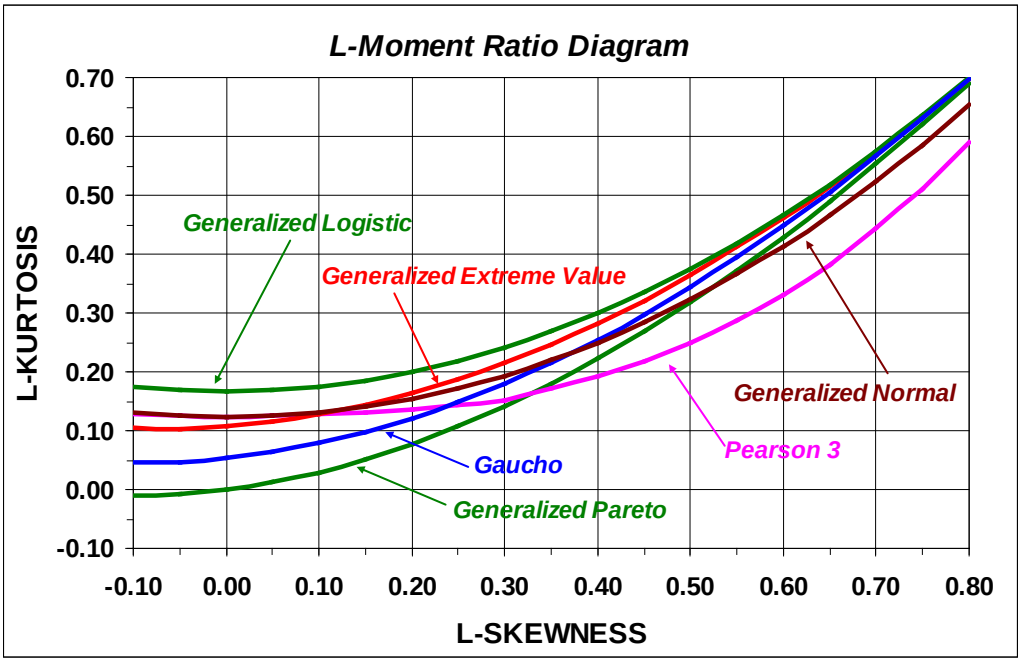


*Figure D-9 - Example L-Moment Ratio Diagram for Selecting Best-Fit Probability Distribution*

***Figure D-10*** depicts an example of regional L-Skewness and L-Kurtosis pairings for 33 regions in Eastern Oregon for 24-hour precipitation annual maxima (Schaefer et al[36]). Visually, the regional L-Skewness and L-Kurtosis pairings are seen to cluster around the curve for the GEV distribution. The centroid of the data cluster essentially lies on the GEV curve with the conclusion that the 24-hour precipitation annual maxima are well-described by GEV distribution. The numerical goodness-of-fit measures for the 33 regions confirmed the suitability of the GEV distribution.

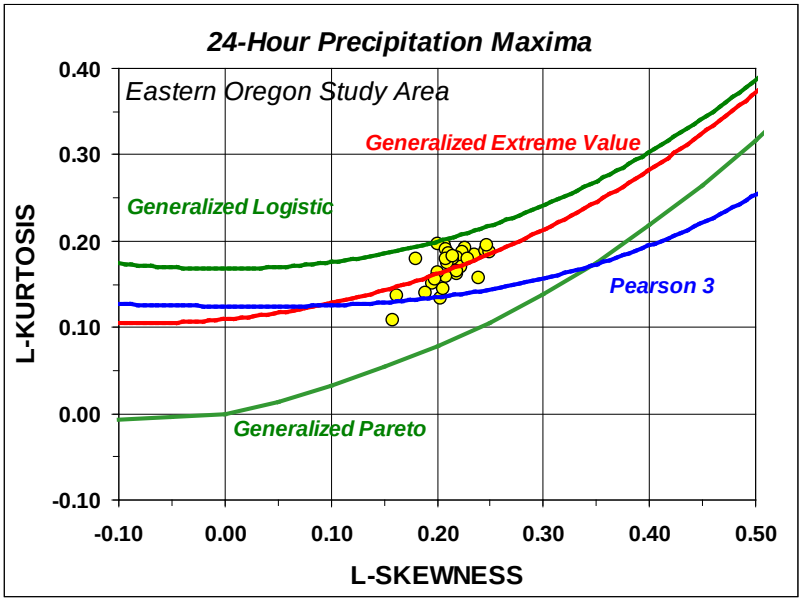


***Figure D-10 - Example L-Moment Ratio Diagram for Selecting Best-Fit Probability Distribution***

## D.4.2 Mixed Distributions

A univariate mixed distribution (mixture distribution) may generally be described as a probability distribution comprised of two or more probability distributions. This configuration is generally used in situations where one distribution is used to describe a range of magnitudes and the second distribution is used to describe another range of magnitudes where there may be some amount of overlap. For environmental data, this typically results in a CDF which is unimodal.

Some environmental data exhibit behavior that can be described by a special case of a mixed distribution. In this case, the observed data are comprised of a mixture of zero values and non-zero values. Other environmental data sets, such as water quality data, may be comprised of the number of samples below some detection threshold and non-zero values above the detection threshold. Both of these situations are best handled in a regional analysis framework by use of a mixed distribution (Hosking and Wallis[10], pp76-77).

L-RAP includes procedures that counts the number of zero values and computes the fraction of zero values. Procedures are also included in L-RAP that provides quantile estimates for the mixed distribution where the probability distribution for the non-zero values is selected from the seven distributions listed above. The mixed distribution is described in Chapter 4 and all of the procedures for applying mixed distributions are described in Chapter 6 [of the L-RAP User's Manual].

# APPENDIX E
# Creation of the DDST Using Manual and Automated Storm Typing Procedures

## E.1 Four AMS Extraction Zones for Storm Typing

Four zones were delineated in the TVA Study Area for selection of precipitation stations for use in the point precipitation-frequency study. AMS datasets were assembled from precipitation data obtained from the National Climatic Data Center's climatological databases for various storm types. These four zones (***Figure E-1***) are termed AMS Extraction Zones and generally align with four 2° latitude by 2° longitude grid-cells where daily values of Pw and CAPE have been estimated using results from computer reanalysis of atmospheric conditions from the NOAA-CIRES Twentieth Century Global Reanalysis Version II project.

## E.2 Century Station Network

MetStat assembled a collection of 100 long-term, high-quality precipitation measurement stations in the TVA-West and TVA-East Zones (***Figure E-2***) for detection of the scale of the areal coverage of precipitation. This network of stations was given the name "Century Network" and was in-place most of the 20th Century. The number of long-term stations in the Century Network increased over time and reached a relatively stable number of 50 stations in each of the TVA zones for the period from 1910 to present. AMS Extraction Zones 1 and 2 are located in what is termed the TVA-West Zone and AMS Extraction Zones 3 and 4 are located in the TVA-East Zone. A daily precipitation threshold of 0.50-inch was used as the indicator of precipitation sufficiently large to be considered as part of a "storm". Counts were made of the number of stations where the daily precipitation exceeded 0.50-inches and a count was also made for the number of stations that were active (operational) on a given day. Any stations with missing and/or accumulated precipitation values were not counted nor used in the summary statistics for the day. The "percentage of active stations over the 0.50-inch threshold" was the indicator for the scale of the areal coverage of precipitation. A separate measure was computed for the TVA-West and TVA-East zones.

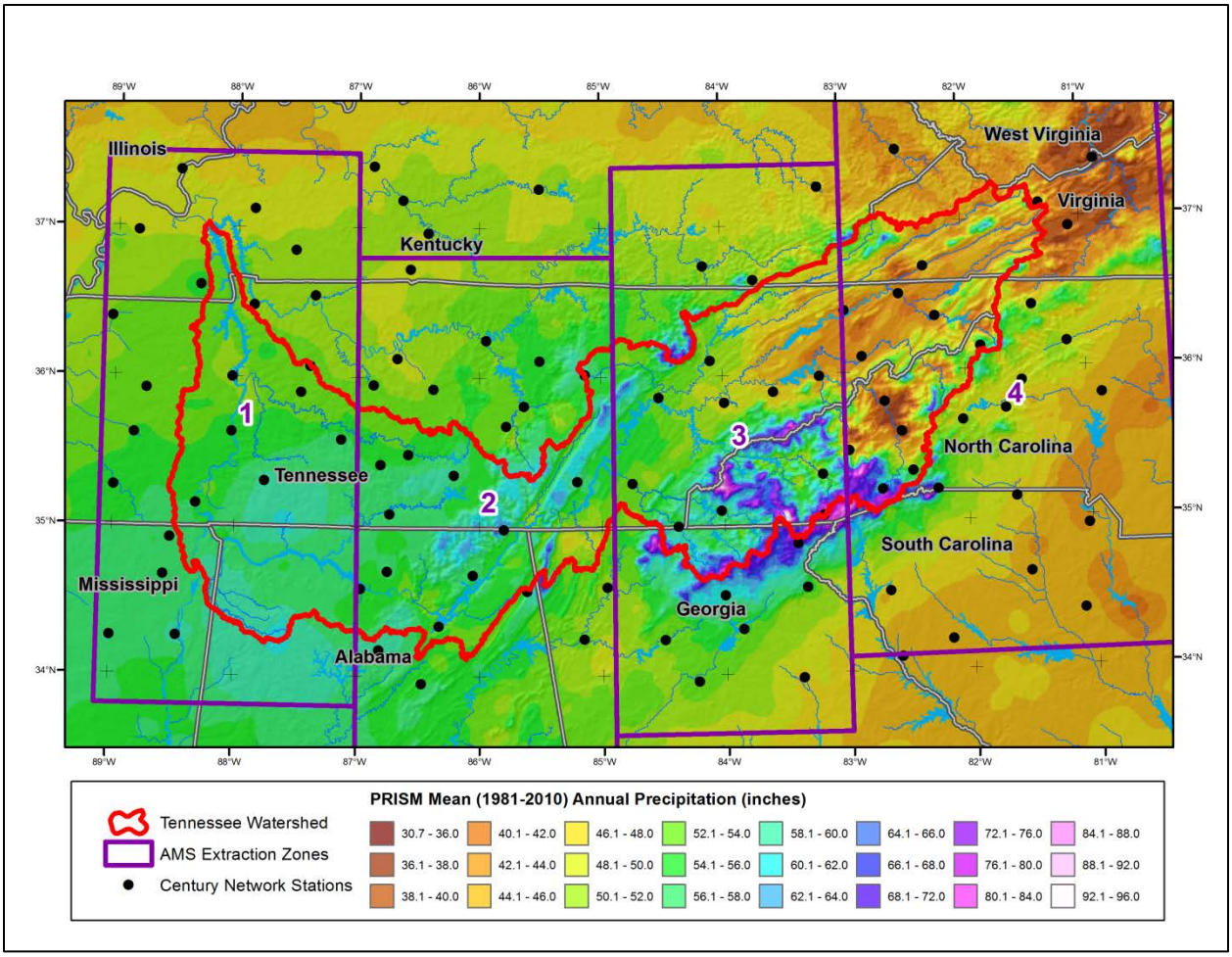


***Figure E-1 - TVA Study Area Depicting Century Network of Daily Precipitation Stations and Four AMS Extraction Zones***

## E.3 Storm Types and Numerical Codes

Four storm types with sub-types were identified for use in Storm Typing, which included:

- Mid-Latitude Cyclone (MLC)
- TSR (TSR)
- Mesoscale Storm with Embedded Convection (MEC)
- Local Storm (LS)

***Table E-1*** lists the various Storm Types, sub-types and Numerical Codes that were used in the DDST for use in Manual and Automated Storm Typing.

***Table E-1 - Storm Types and Numerical Codes Used in Manual and Automated Storm Typing***

| STORM TYPES AND NUMERICAL CODES | | |
|---|---|---|
| **Storm Type and Sub-Type** | **Acronym** | **Numerical Code** |
| Mid-Latitude Cyclone | MLC | 10 |
| Mid-Latitude Cyclone with Embedded Convection | MLC/EC | 13 |
| Tropical Storm Remnant | TSR | 20 |
| Tropical Storm Remnant with Embedded Convection | TSR/EC | 23 |
| Mesoscale Storm with Embedded Convection | MEC | 30 |
| Mesoscale Storm without Embedded Convection | MEC/NEC | 33 |
| Local Storm | LS | 40 |
| Local Storm – cool season storm , Not of Interest | LS/NOI | 49 |
| Dry Day – No precipitation over 0.50-inch threshold reported by Century Network | DRY | 99 |

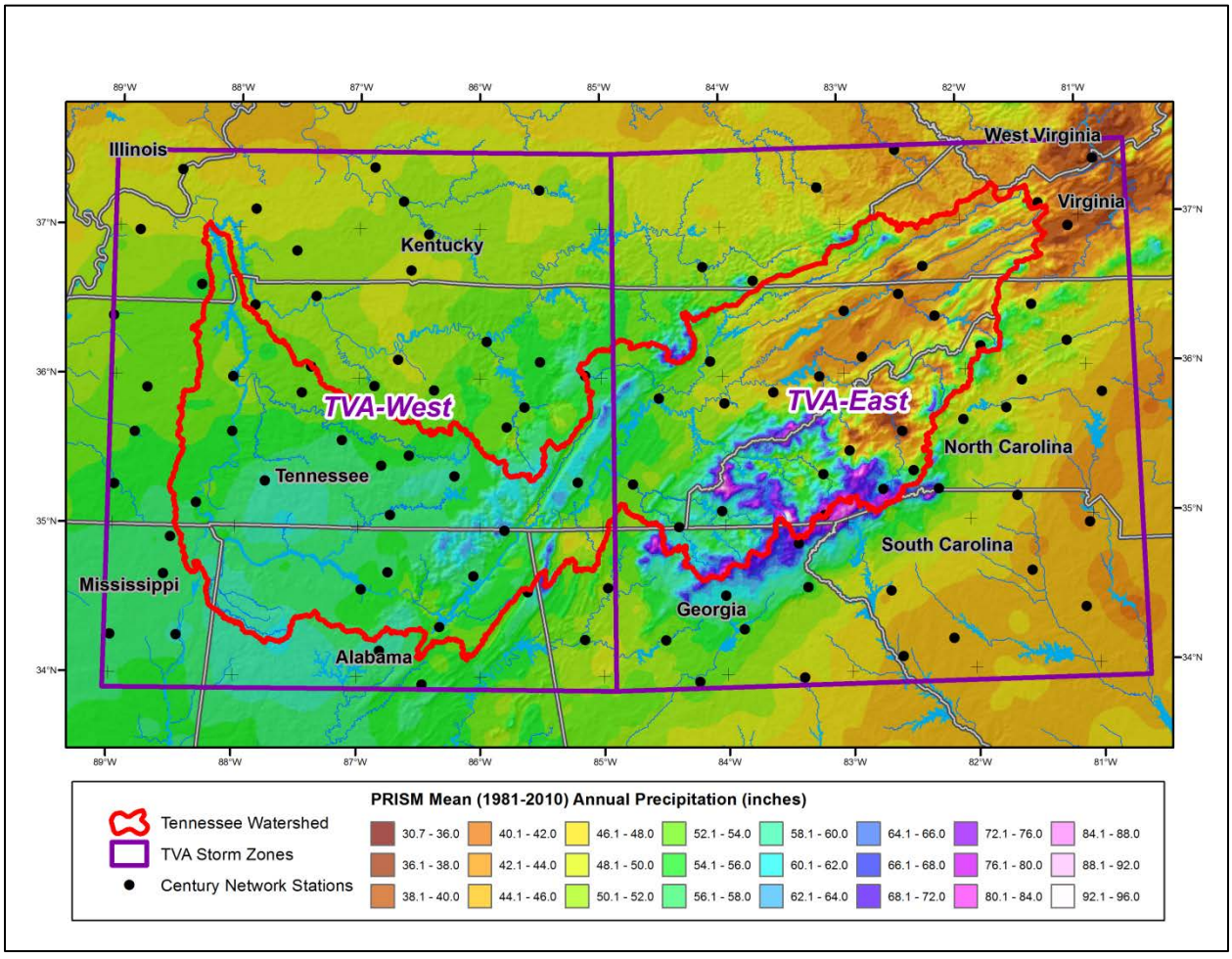


***Figure E-2 - TVA Study Area Depicting TVA West Zone and TVA East Zone***

## E.4 Manual Storm Typing Used to Develop Criteria for Automated Storm Typing

The criteria for automated storm typing was developed by examination of over 1,100 noteworthy storm events. Specifically, the all-season annual maxima databases assembled by the NWS for the NOAA Atlas 14 precipitation-frequency study were scanned to identify noteworthy storms at the 2-hour, 6-hour and 2-day durations. This included storms/dates where precipitation exceeded the 3-year recurrence interval at a station for the 6-hour and/or 2-day durations and storms/dates where precipitation exceeded the 10-year recurrence interval at the 2-hour duration. These recurrence interval thresholds were chosen to obtain a reasonably large sample set of storms for Manual storm typing.

Applied Climate Services conducted the Manual storm typing and developed a computer tool for analysis of daily storm types. The computer tool displayed four panels (***Figure E-3***) including the 500-mb and 850-mb height contour maps, Pw and CAPE maps for 0 Z (UTC). Areally-averaged values of Pw and CAPE were estimated for four 2° latitude by 2° longitude grid-cells that were aligned with the four AMS Extraction Zones (***Figure E-1***). The Pw and CAPE mapping data were obtained from the NOAA-CIRES Twentieth Century Global Reanalysis Version II.

Metstat supplied information on tropical storm influence by providing a list of days when storm tracks from tropical storms affected the TVA Study Area. This was accomplished by scanning the NOAA North Atlantic database of tropical storms and identifying when storm tracks entered a box encompassing the TVSA where the box corners were 40.0°N and 31.2°N latitude and 77.6°W and 92.0°W longitude. A buffer of 3 days on either side of the storm track entry into the box was used to include the possible influence of tropical moisture and a tropical storm meteorological environment.

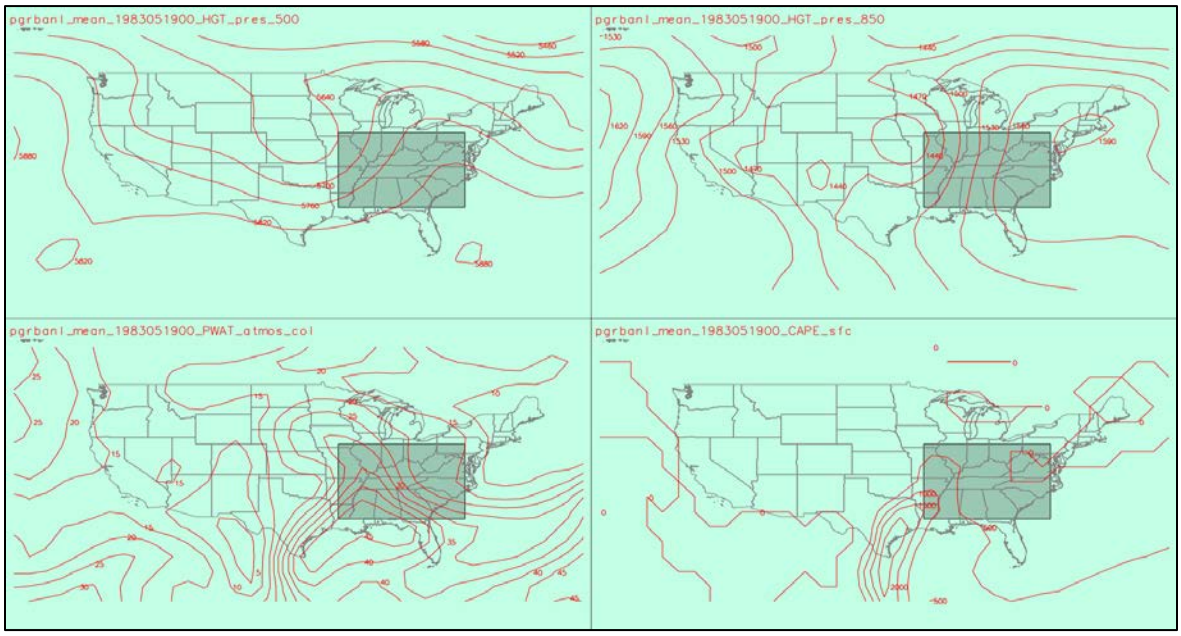


***Figure E-3 - Example of Four Panel Display of 850-mb and 500-mb Height Contour Maps, Pw and CAPE (Applied Climate Services)***

Applied Climate Services examined each of the noteworthy 1,100 storm events and assigned storm types (***Table E-1***) using the following methods and numerical measures:

- Storm seasonality, storm date may include multiple days
- 850-mb and 500-mb height contour maps and daily weather maps
- Dates of tropical storm influence from the NOAA database of tropical storm tracks
- Percentage of stations in Century Network exceeding a daily precipitation amount of 0.50-inch for the TVA-west and TVA-east zones
- Daily values of Pw and CAPE for the four AMS Extraction Zones

- Number of stations in each of the four AMS Extraction Zones that exceeded the recurrence interval thresholds for either the 2-hour, 6-hour or 2-day durations

***Table E-2*** and ***Table E-3*** list examples of storm measures for several noteworthy storms used in Manual storm typing. The MLC of March 15-17, 1973 (***Table E-2***) was an extraordinary storm that produced widespread precipitation and flooding in the Tennessee Valley, and there were 112 daily stations where the 2-day precipitation exceeded the 3-year recurrence interval threshold. A MEC occurred on May 5-7, 1984 (***Table E-3***), where 112 daily stations and 13 hourly stations exceeded the 3-year recurrence interval thresholds. The heaviest precipitation was concentrated in AMS zones 2 and 3 based on reporting from the hourly stations.

Experience gained from the Manual storm typing was used to set criteria and establish procedures for automated storm typing. A description of criteria and procedures for automated storm typing are presented in the following sections.

***Table E-2 - Storm Measures for MLC of March 15-17, 1973***

| MLC - FOR DAY OF MARCH 16, 1973 | | | | | | | | | | | | | |
|---|---|---|---|---|---|---|---|---|---|---|---|---|---|
| Century Network Percent Stations Over Threshold | | Pw (mm) | | | | CAPE (Joules/Kilogram) | | | | Number of Daily Stations Exceeding Recurrence Interval Threshold | | | |
| TVA West | TVA East | AMS Extraction Zone | | | | AMS Extraction Zone | | | | AMS Extraction Zone | | | |
| | | 1 | 2 | 3 | 4 | 1 | 2 | 3 | 4 | 1 | 2 | 3 | 4 |
| 0.91 | 0.67 | 36.3 | 36.4 | 35.6 | 35.1 | 23 | 176 | 416 | 504 | 27 | 34 | 24 | 27 |

***Table E-3 - Storm Measures for MEC of May 6-8, 1984***

| MEC- FOR DAY OF MAY 7, 1984 | | | | | | | | | | | | | |
|---|---|---|---|---|---|---|---|---|---|---|---|---|---|
| Century Network Percent Stations Over Threshold | | Pw (mm) | | | | CAPE (Joules/Kilogram) | | | | Number of Hourly Stations Exceeding Recurrence Interval Threshold | | | |
| TVA West | TVA East | AMS Extraction Zone | | | | AMS Extraction Zone | | | | AMS Extraction Zone | | | |
| | | 1 | 2 | 3 | 4 | 1 | 2 | 3 | 4 | 1 | 2 | 3 | 4 |
| 0.70 | 0.74 | 40.4 | 37.5 | 35.6 | 34.8 | 1660 | 1153 | 1013 | 960 | 1 | 5 | 6 | 1 |

## E.5 Summary of Storm Typing Criteria

The following sections summarize the specific criteria used for classifying each of the storm types.

### E.5.1 Synoptic Scale Mid-Latitude Cyclone (MLC)

**Storm Type Numerical Code: 10**

MLCs and associated fronts are essentially the only synoptic storms occurring in the cool season from Nov 1st through Mar 31st. Warm season MLCs occur less frequently as the calendar progresses from May 1st into the warm season. April and October are transition months. This storm type applies to all four AMS extraction zones on a given day. ***Table E-4*** presents the criteria used to identify MLC storms during the automated typing.

*Table E-4 - Storm Typing Criteria for MLCs*

| STORM TYPING CRITERIA FOR MLCs | | | | |
|---|---|---|---|---|
| **Seasonality** | **Century Network Active Stations Over Threshold** | **Pw (mm)** | **CAPE (Joules/Kilogram)** | **Comments** |
| Nov 1 - Mar 31 | ≥ 20% | n/a | < 500 | Dominant seasonality for MLCs |
| Apr 1 - Oct 31 | ≥ 20% | n/a | < 500 | Warm Season MLC |

## E.5.2 Synoptic Scale Mid-Latitude Cyclone with Embedded Convection (MLC/EC)

**Storm Type Numerical Code: 13**

This is a sub-type of the MLC storm type with weak embedded convection in the cool season where CAPE values are not much above the threshold value of 500. This storm type is often applicable to a few of the AMS zones where an MLC (10) is occurring in other zones. ***Table E-5*** presents the criteria used to identify MLC/EC storms during the automated typing.

*Table E-5 - Storm Typing Criteria for MLC/EC*

| STORM TYPING CRITERIA FOR MLC/EC | | | | |
|---|---|---|---|---|
| **Seasonality** | **Century Network Active Stations Over Threshold** | **Pw (mm)** | **CAPE (Joules/Kilogram)** | **Comments** |
| Nov 1 - Mar 31 | ≥ 20% | n/a | ≥ 500 | Mild embedded convection<br>Each AMS zone to be typed separately |
| Apr 1 - Oct 31 | **Mild Embedded Convection** | | **Only 1 AMS Zone Over CAPE 500 Threshold** | |
| | ≥ 20% | n/a | 500 ≤ CAPE ≤ 750 | Each AMS zone to be typed separately |

MLC/EC storms typically have mild embedded convection with CAPE values barely above the threshold value of 500, particularly in the cool season. There is a transition from MLC and MLC/EC events to MECs in April and May and then reversing in September and October (***Figure E-12***). The storm typing threshold criteria for MLC and MLC/EC storms were modified in the warm season to accommodate mild amounts of embedded convection that only affect one AMS zone. This modification was made to avoid categorization as an MEC event when CAPE values were just above the 500 threshold and where a limited portion of the study area was affected. The warm season storm typing criteria above are consistent with the criteria for the MEC events that are discussed in a later section.

A “Plus 1“ rule was adopted and applied to storm events with embedded convection. Specifically, the AMS zone or zones immediately adjacent to an AMS zone that is storm typed as MLC/EC was also typed as an MLC/EC (Storm Type Numerical Code 13). The “Plus 1” procedure provided some flexibility in storm typing by recognizing ambiguity in the timing of precipitation relative to the timing of Pw and CAPE. When this situation occurred, all other zones were typed as a MLC (Storm Type Numerical Code 10).

***Figure E-4*** and ***Figure E-5*** depict the seasonal distribution of MLCs and MLC/ECs, respectively, for the period from 1910-2012. The number of MLCs with embedded convection (MLC/EC) is small relative to the number of MLCs.

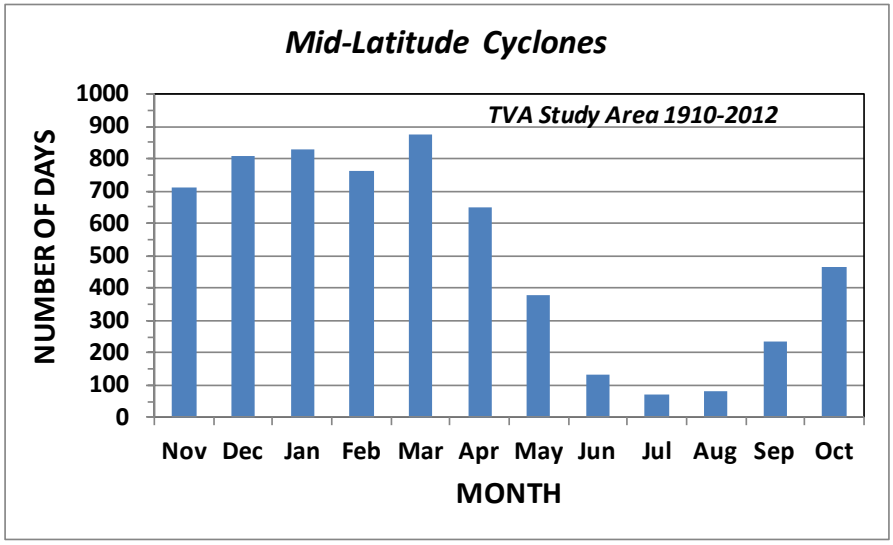


*Figure E-4 - Seasonal Distribution of MLCs for 1910-2012 Period Based on Manual and Automated Storm Typing*

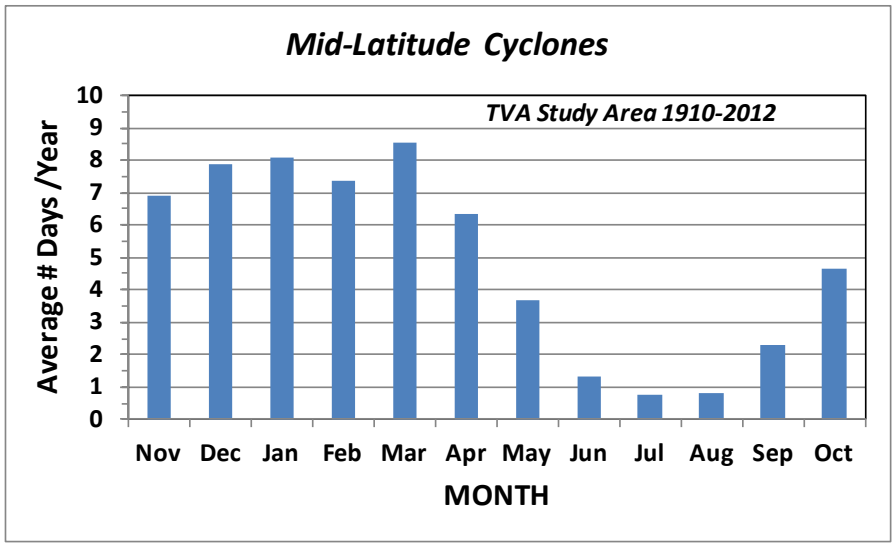


*Figure E-5 - Seasonal Distribution of MLC/EC for 1910-2012 Period Based on Manual and Automated Storm Typing*

### E.5.3 Synoptic Scale Tropical Storm Remnant (TSR)

**Storm Type Numerical Code: 20**

The NOAA North Atlantic tropical storm-track database was used to identify dates where the storm-track (http://www.ncdc.noaa.gov/ibtracs/index.php?name=ibtracs-data) from a tropical storm was in, or near, the TVSA (within ~200 miles) and could have caused precipitation associated with a tropical storm meteorological environment. Based on the characteristics of several case studies across the project area, a buffer of +/- 3 days was used to capture where an approaching or departing tropical storm likely influenced subsequent precipitation in the TVSA. Time series and seasonality graphics are depicted in ***Figure E-6*** and ***Figure E-7*** for the NOAA tropical storm tracks. ***Table E-6*** presents the criteria used to identify TSRs during the automated typing.

*Table E-6 - Storm Typing Criteria for TSRs*

| STORM TYPING CRITERIA FOR TROPICAL TSRs | | | | |
|---|---|---|---|---|
| **Seasonality** | **Century Network Active Stations Over Threshold** | **Pw (mm)** | **CAPE (Joules/Kilogram)** | **Comments** |
| May 1 - Nov 15 | n/a | n/a | < 500 | NOAA North Atlantic Storm Track Database |

### E.5.4 Synoptic Scale Tropical Storm Remnant with Embedded Convection (TSR/EC)

**Storm Type Numerical Code: 23**

This is a sub-type of the TSR storm type where there are clusters of convective cells embedded in the spatial storm footprint. Each of the four AMS zones received a separate storm typing to include TSR and TSR/EC based on the zonal values of Pw and CAPE. The "Plus 1" rule was applied for storm events with embedded convection. The AMS zone or zones immediately adjacent to an AMS zone that was storm typed as TSR/EC was also typed as TSR/EC (STNC 23). All other AMS zones were typed as TSR (STNC 20). ***Table E-7*** presents the criteria used to identify TSR/ECs during the automated typing.

*Table E-7 - Storm Typing Criteria for TSR/EC*

| STORM TYPING CRITERIA TSR/EC | | | | |
|---|---|---|---|---|
| **Seasonality** | **Century Network Active Stations Over Threshold** | **Pw (mm)** | **CAPE) (Joules/Kilogram)** | **Comments** |
| May 1 - Nov 15 | ≥ 20% | Pw ≥ 25-mm and CAPE ≥ 500 | | NWS Storm Track Tropical Storm Dates Each AMS zone to be typed separately |

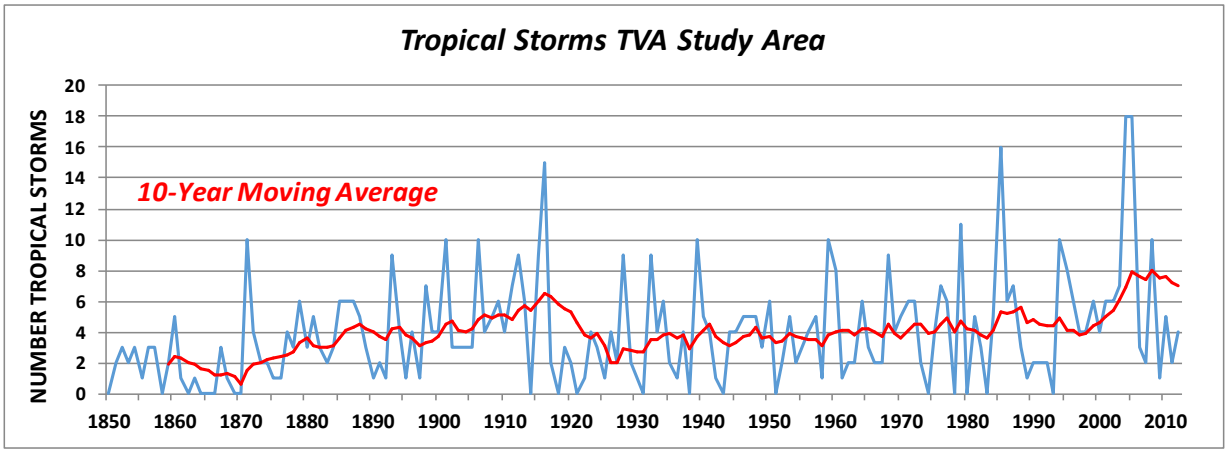


*Figure E-6 - Time series of Tropical Storms that Affected TVA Study Area*

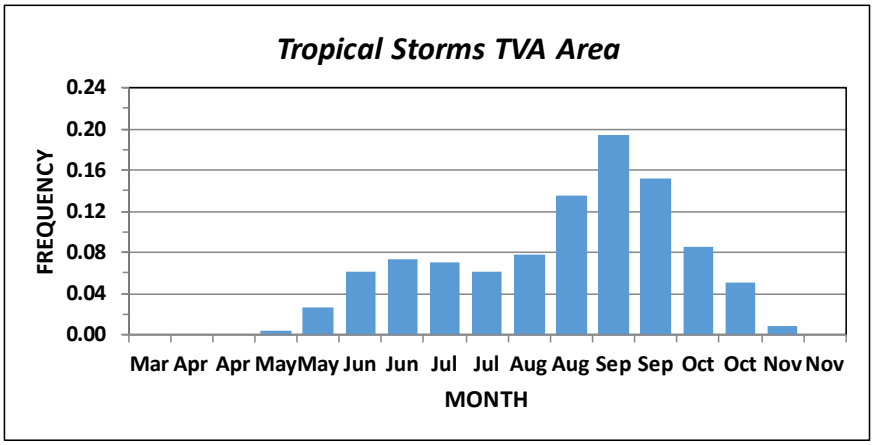


***Figure E-7 - Seasonal Distribution of Tropical Storms that Affected TVA Study Area***

There are relatively few TSR and TSR/EC storms compared to the number of MLCs and MECs. ***Figure E-8*** and ***Figure E-9*** depict the seasonal distribution of TSRs and TSR/ECs Convection for the period from 1910-2012.

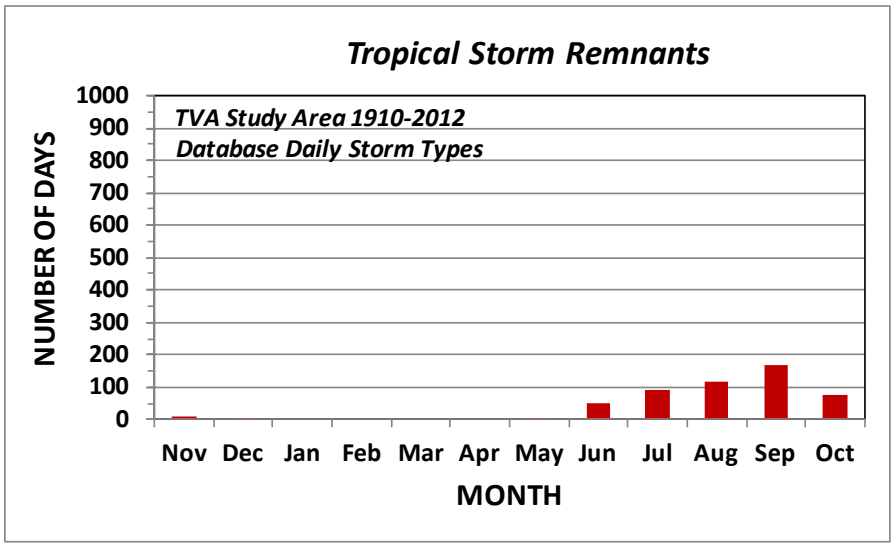


***Figure E-8 - Seasonal Distribution of TSR for 1910-2012 Period Based on Manual and Automated Storm Typing***

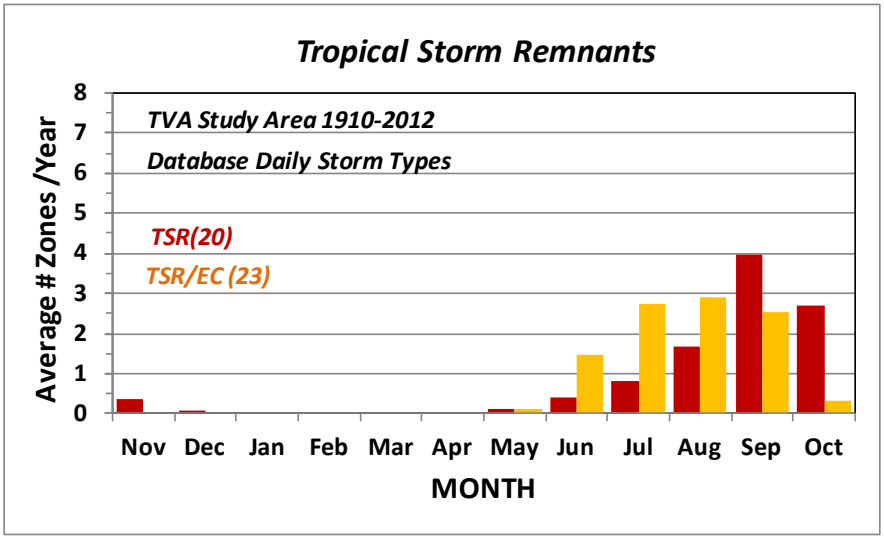


***Figure E-9 - Seasonal Distribution of TSR and TSR/EC for 1910-2012 Period Based on Manual and Automated Storm Typing***

## E.5.5 Mesoscale Storms with Embedded Convection (MEC)

**Storm Type Numerical Code: 30**

The term MEC is intended to include MCCs and other warm-season Mesoscale and sub-synoptic scale storms with embedded convective cells. These are storm characteristics that can cause widespread precipitation with locally high precipitation intensities and high rates of runoff. ***Table E-8*** presents the criteria used to identify MEC storms during the automated typing.

***Table E-8 - Storm Typing Criteria for MECs***

| STORM TYPING CRITERIA FOR MEC | | | | |
|---|---|---|---|---|
| **Seasonality** | **Century Network Active Stations Over Threshold** | **Pw (mm)** | **CAPE (Joules/Kilogram)** | **Comments** |
| Apr 1 - Oct 31 | **Only 1 AMS Zone Over Pw and CAPE Thresholds** | | | |
| | ≥ 20% | Pw ≥ 25-mm and CAPE ≥ 750 | | Each AMS zone to be typed separately |
| | **2 or More AMS Zones Over Pw and CAPE Thresholds** | | | |
| | ≥ 20% | Pw ≥ 25-mm and CAPE ≥ 500 | | Each AMS zone to be typed separately |

The "Plus 1" rule was applied for storm events with embedded convection. The AMS zone or zones cells immediately adjacent to a zone that was storm typed as MEC was also typed as MEC (STNC 30). All other zones were typed as MEC/NEC (STNC 33).

## E.5.6 Mesoscale Storms without Embedded Convection (MEC/NEC)

**Storm Type Numerical Code: 33**

This is a sub-type of the MEC storm type and allows Mesoscale and sub-synoptic storms in the warm season to have a mix of AMS zones with and without embedded convection. Storms with some AMS zones typed as MEC/NEC are considered MEC storms. In particular, if all four AMS zones were below the Pw and CAPE thresholds, then the storm would be an MLC storm type and not typed as a MEC or MEC/NEC storm. ***Table E-9*** presents the criteria used to identify MLC storms during the automated typing.

*Table E-9 - Storm Typing Criteria for Mesoscale Storms without Embedded Convection*

| STORM TYPING CRITERIA FOR MEC/NEC | | | | |
|---|---|---|---|---|
| **Seasonality** | **Century Network Active Stations Over Threshold** | **Pw (mm)** | **CAPE (Joules/Kilogram)** | **Comments** |
| Apr 1 - Oct 31 | ≥ 20% | Pw < 25-mm or CAPE < 500 | | Each AMS zone to be typed separately |

***Figure E-10*** and ***Figure E-11*** depict the seasonal distribution of MECs for the period from 1910-2012. A comparison of the seasonal distributions of MLCs and MECs is shown in ***Figure E-12***. Note the transition from MLC to MEC events in the months of April and May and the transition from MEC to MLC events in September to October.

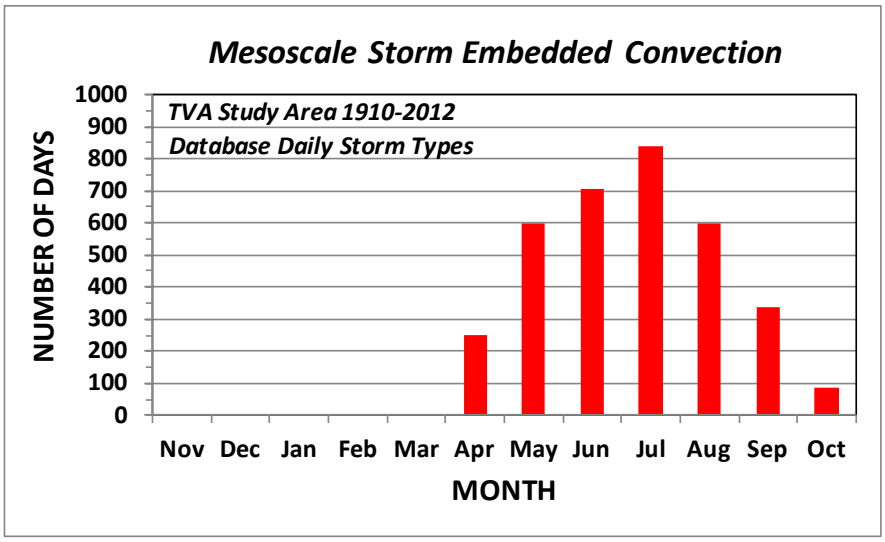


*Figure E-10 - Seasonal Distribution of MECs for 1910-2012 Period Based on Manual and Automated Storm Typing*

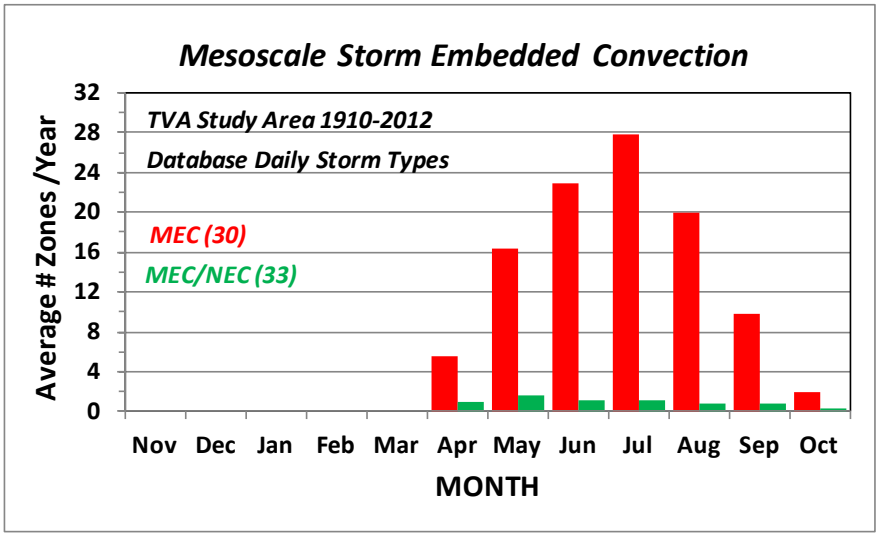


*Figure E-11 - Seasonal Distribution of MECs for 1910-2012 Period Based on Manual and Automated Storm Typing*

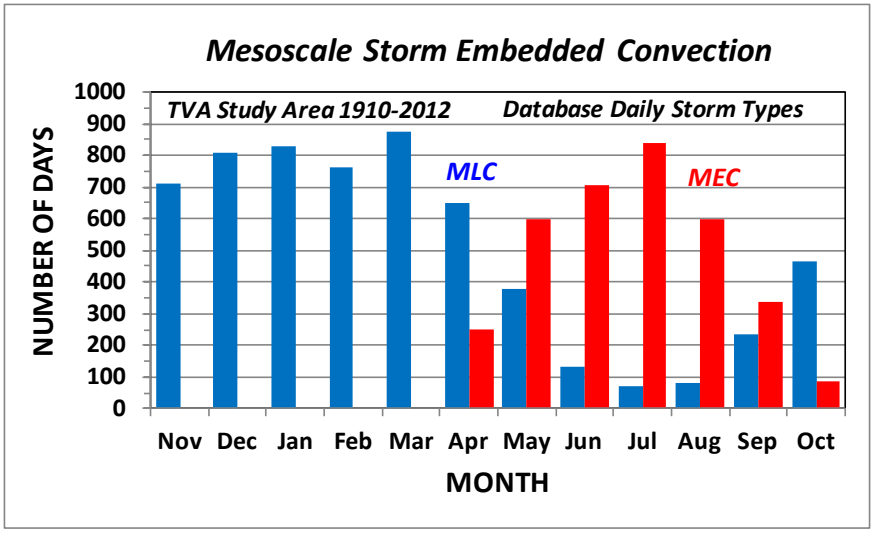


***Figure E-12 - Comparison of Seasonal Distributions of MECs and MLCs for 1910-2012 Period Based on Manual and Automated Storm Typing***

## E.5.7 Local Storms – Warm Season

**Storm Type Numerical Code: 40**

LS is the term given to relatively small scale convective events (thunderstorms) which occur in the warm season. The areal coverage and duration of these storms are limited, typically less than a nominal 100-mi2 and several hours in duration. The LS is the default warm season storm where few Century Network stations indicate precipitation over the 0.50-inch daily threshold.

The areally-averaged CAPE values for the four AMS zones are not checked against a CAPE threshold for the LSs because it is likely that the local atmospheric conditions giving rise to convection may not be detectable from the coarse 2° by 2°grid of CAPE values. ***Table E-10*** presents the criteria used to identify LSs during the automated typing.

***Table E-10 - Storm Typing Criteria for LSs***

| STORM TYPING CRITERIA FOR LSs | | | | |
|---|---|---|---|---|
| **Seasonality** | **Century Network Active Stations Over Threshold (CNASOT)** | **Pw (mm)** | **CAPE (Joules/Kilogram)** | **Comments** |
| Apr 1 - Oct 31 | 1% ≤ CNASOT < 20% | n/a | n/a | All four AMS zones will be typed the same |

All four AMS Extraction Zones are typed as LS (40). The seasonal distribution of LSs is shown in ***Figure E-13*** and ***Figure E-14***. The relatively large number of LSs is reflective of the small scale (small areal coverage) and spatial randomness of the LSs in the large TVA Study Area.

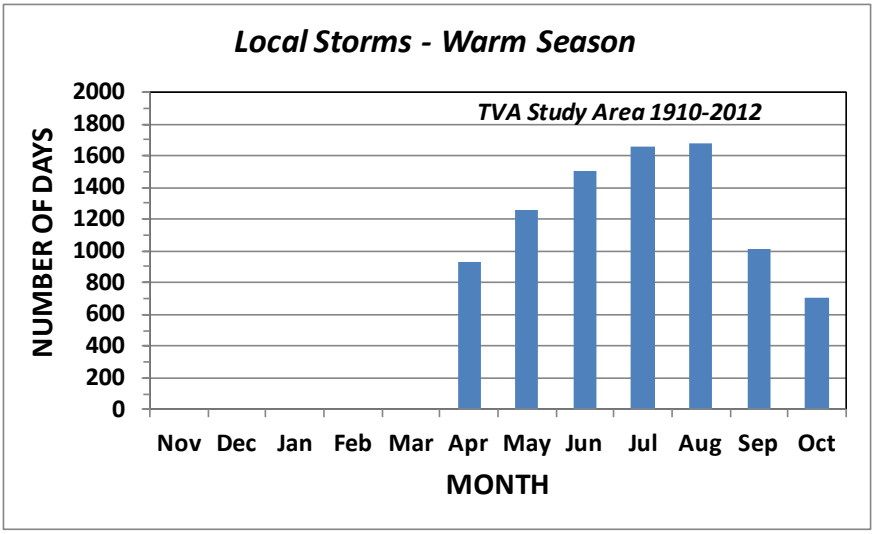


*Figure E-13 - Seasonal Distributions of LSs for 1910-2012 Period Based on Manual and Automated Storm Typing*

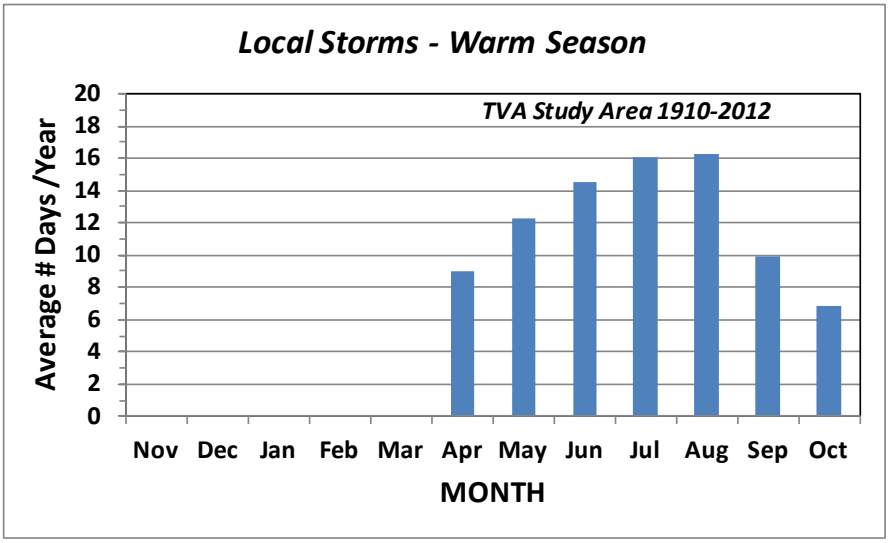


*Figure E-14 - Seasonal Distributions of LSs for 1910-2012 Period Based on Manual and Automated Storm Typing*

### E.5.8 Local Storm Not of Interest (LS/NOI) – Cool Season

**Storm Type Numerical Code: 49**

Storms with minimal areal coverage in the cool season from November 1 through March 31 are not of interest in the precipitation-frequency analysis. This conclusion is supported by the relatively low values of CAPE in the cool season and the relatively small magnitude of the cool season storms which are exceeded by the magnitude of LSs in the warm season. ***Table E-11*** presents the criteria used to identify LS/NOI events during the automated typing.

*Table E-11 - Storm Typing Criteria for LS/NOI (Cool Season)*

| STORM TYPING CRITERIA FOR LOCAL STORMS THAT ARE NOT OF INTEREST (Local Storm/NOI) | | | | |
|---|---|---|---|---|
| **Seasonality** | **Century Network Active Stations Over Threshold** | **Pw (mm)** | **CAPE (Joules/Kilogram)** | **Comments** |
| Nov 1 - Mar 31 | < 20% | n/a | n/a | Not a storm characteristic of interest |

### E.5.9 Dry Day (Dry)

**Storm Type Numerical Code: 99**

A Dry day is a day where none of the stations in the Century Network have a daily precipitation exceeding the 0.50-inch threshold (***Table E-12***). This is an indication from the Century Network that no precipitation of significance occurred. This is a catch-all category for days where no precipitation occurred or where precipitation was of small magnitude and limited areal extent.

*Table E-12 - Storm Typing Criteria for Dry Days*

| STORM TYPING CRITERIA FOR DRY DAYS (DRY) | | | | |
|---|---|---|---|---|
| **Seasonality** | **Century Network Active Stations Over Threshold** | **Pw (mm)** | **CAPE (Joules/Kilogram)** | **Comments** |
| All Months | 0% | n/a | n/a | No Century Network Stations Recording Daily Precipitation Amount over 0.50-inch |

## E.6 Procedures Employed in Automated Storm Typing and Assembling the DDST

The procedures used in implementing automated storm typing and creating the DDST are described below and a decision tree is shown in ***Figure E-18***.

### E.6.1 Timing Considerations for Daily Storm Typing for the DDST

The DDST lists storm types on a daily time-step for the period from 1881 through 2014. The “day” in the DDST is not defined on a calendar-day basis, but must be defined in terms of the timing of available measures of precipitation, Pw, CAPE, and time-of-day frequencies exhibited in the timing of various storm types. The redefined “day” is termed the Century Network Day.

The time-of-day for the end-of-the-day/start-of-new-day for the Century Network Day is important because precipitation annual maxima for multi-hour durations of interest can span the day-to-day boundary (Figure ***E-17***). This situation can result in a different storm type being associated with segments of a precipitation time series on either side of the Century Network Day boundary. This could then require a decision which storm type was associated with a segment of hourly precipitation. The time-of-day of the Century Network Day boundary is most important for short-duration precipitation annual maxima such as the 6-hour duration, typical for MECs, and the 1-hour and 2-hour durations, common for LSs. Conversely, a few hours shift in either direction for the Century Network Day boundary would not have much effect in determining the storm type for multi-day synoptic scale MLCs and TSRs.

As discussed above, the start/end timing of the Century Network Day is primarily governed by the time-of-day storm characteristics for the MEC and LS storms with consideration of the reporting times of the Century Network and the timing of the measures of Pw and CAPE. ***Figure E-15*** and ***Figure E-16*** depict the starting hour for 2-hour and 6-hour precipitation annual maxima for the months of June through August, which are in the center of the MEC and LS seasons (***Figure E-10***, ***Figure E-13***). A review of ***Figure E-15*** and ***Figure E-16*** shows a clear lull in MEC and LS activity in the morning with a maximum of storm activity in the early-afternoon and evening hours.

***Figure E-17*** depicts the selected timing of the Century Network Day where the 8 AM to 8 AM day is compatible with the predominately morning reporting of the Century Network and results in the Pw and CAPE measures being representative of the mid-point in the Century Network Day.

Note the date listed in the DDST is for precipitation which occurred in the 24-hour period ending at 8 AM on the reported date. Also note that precipitation for the Century Network is split between two calendar dates where precipitation from 8:01 (8 AM) to 24:00 (midnight) on the prior day is associated with the following calendar day for the Century Network and precipitation from 0:01 to 8:00 (8 AM) has the same calendar date as the Century Network.
Additional details on determination of the Century Network Day are discussed in ***Appendix F***.

Procedures were needed in creating the DDST for Manual and Automated Storm Typing to account for the timing issues posed by the Century Network, Pw and CAPE estimates and the timing of reporting for the precipitation stations.

In assembling the DDST, the results from the Manual Storm Typing, the Storm Type Numerical Codes (STNC), were applied as follows:

- Daily Gages, 2-Day storms – for the date listed and the following day
- Hourly Gages, 6-hour and 2-hour – for the date listed and the prior day

In applying the procedures for the Automated Storm Typing, the Storm Type Numerical Codes (STNC) were applied directly for the date listed because all measures are based on the Century Network day/date.

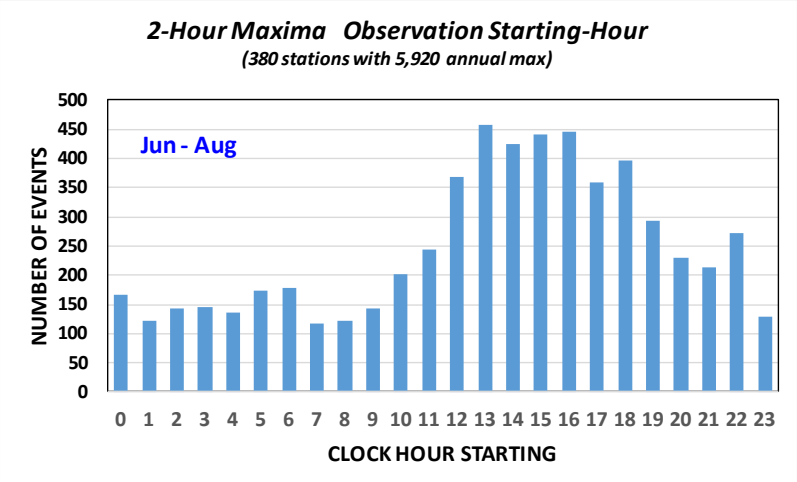


***Figure E-15 - Observed Clock-Hour Starting for 2-Hour Precipitation Maxima for TVA Study Area for the June through August Timeframe***

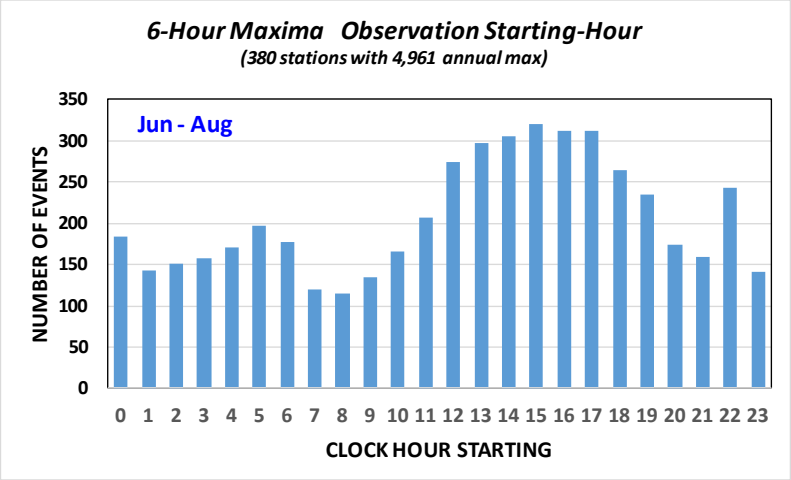


***Figure E-16 - Observed Clock-Hour Starting for 6-Hour Precipitation Maxima for TVA Study Area for the June through August Timeframe***

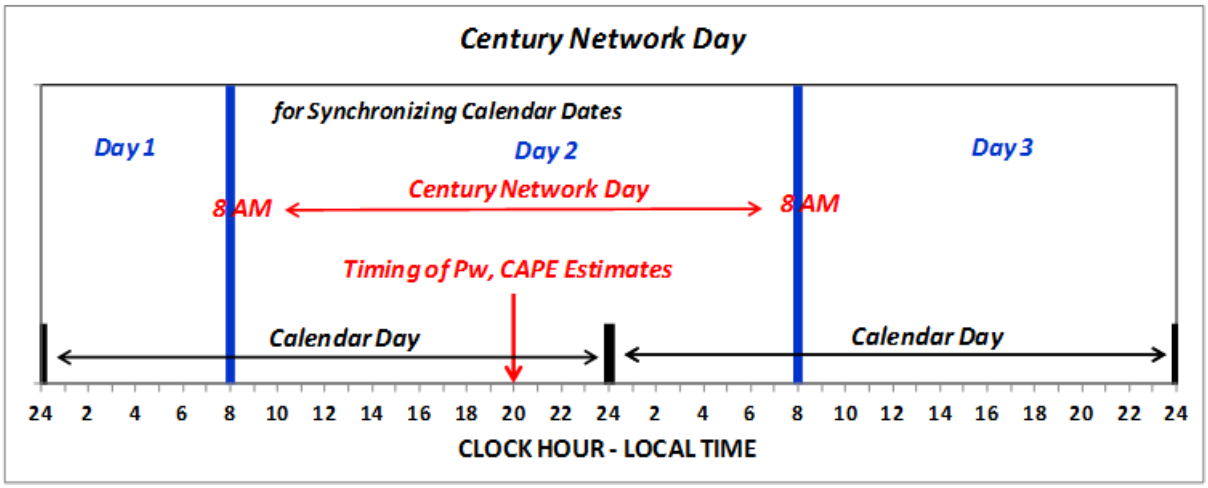


***Figure E-17 - Depiction of Century Network Day for Synchronizing Timing of Precipitation Measurements***

## E.6.2 Classifying the General Meteorological Environment

Identifying the general meteorological environment was an important first step in the process of conducting the Manual storm typing and developing the automated storm typing procedures. This can be viewed as a macro perspective for the storm type for a given day for the study area where differences in sub-types of the storm types often occurred between the four AMS zones. The adopted numeric system (***Table E-1***) was to use a two-digit numeric where the first digit was for the storm type (MLC, TSR, MEC, LS) and the second digit indicated variation in sub-types across the four AMS zones. A second digit of 0 was used to indicate no variation across the four AMS zones and a value of 3 was used to indicate variation in the sub-type across the zones. For the case of the MLC and TSR storm types, a second digit of 3 indicates that one or more of the four zones are above the convection thresholds. For the MEC storm type, a second digit of 3 indicates that one or more zones are below the convection thresholds.

As indicated above, the general meteorological environment for the TVSA was a first step in developing the storm typing procedures. The storm type applicable to a specific station on a given day is based on the storm type (***Table E-1***) for the applicable AMS zone (***Figure E-1***) where the station is located. The measure of the general meteorological environment was retained in the DDST to provide documentation of the macro meteorological conditions on a given Century Network Day.

### E.6.3 Identifying Dates where Manual versus Automated Storm Typing was Conducted

A data field was allocated in the DDST and codes established to distinguish days which were typed by Manual analysis versus days that were storm typed by automated procedures. The following codes were used:

- A – days where automated procedures were used for storm typing (Automated)
- M1 – date for larger 1-day precipitation of 2-day event for noteworthy storm (Manual)
- M2 – date for smaller 1-day precipitation of 2-day event for noteworthy storm (Manual)
- MM – part of multiple date sequence for a noteworthy storm (Manual)
- MT – date for a noteworthy Tropical Storm (Manual, Tropical)
- T – storm type was set based on the NOAA tropical storm database (Tropical)

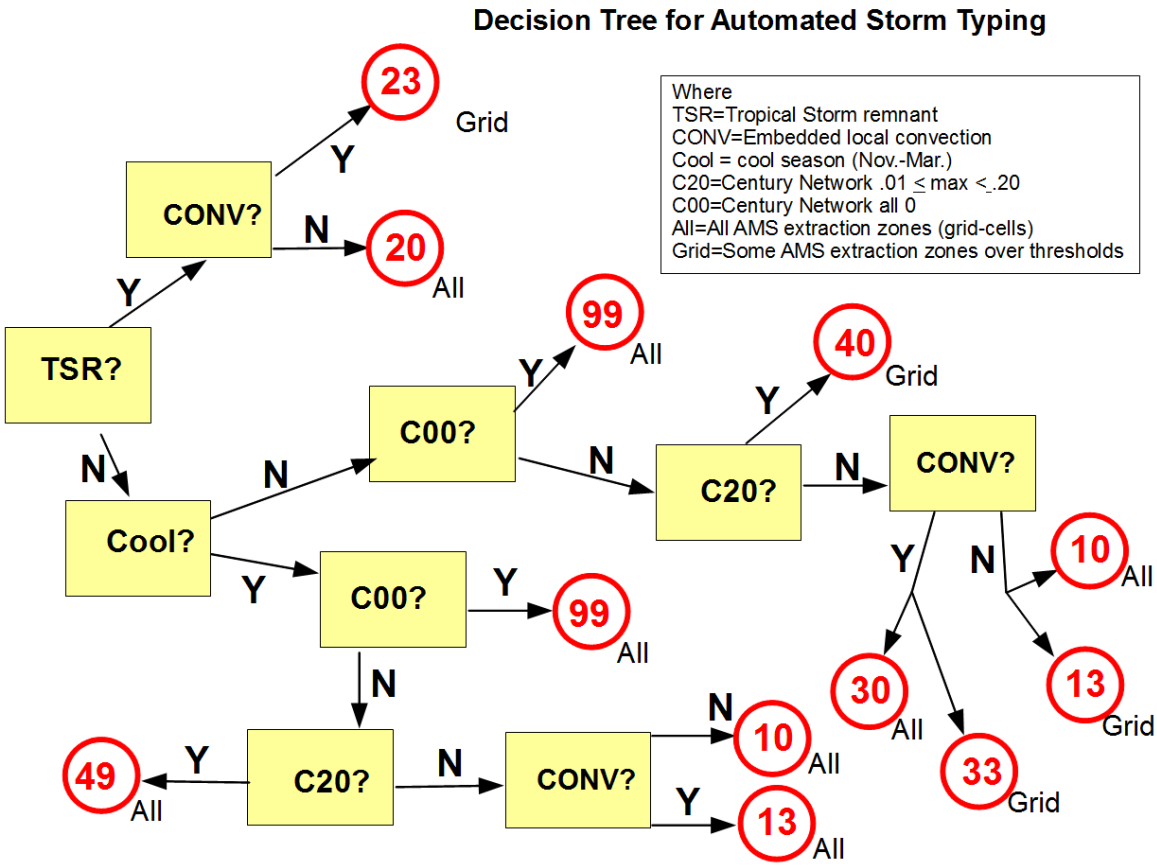


*Figure E-18 - Decision Tree for Creating DDST for Automated Storm Typing*

### E.6.4 Procedures Used for Creating the DDST Incorporating Manual and Automated Storm Typing

1. The DDST was initialized by loading a value of zero for the Storm Type Numerical Code (STNC) for all four AMS zones for each day of the 49,000+ days in the database (1881-2014). This provided a method of quality-checking to confirm that all days were typed.
2. The daily values of the Percentage of Active Century Network Stations Over 0.50-inch Threshold for the TVA-West and TVA-East zones were scanned and when both values were zero (DRY), the STNC was set to 99 for all AMS zones for the date listed.
3. The STNC was initially set to 20 (TSR) for all four AMS zones for the dates in the NOAA database of Tropical Storm Tracks that affected the TVA Study Area.
4. The STNCs from the Manual Storm Typing were transferred into the DDST as follows:
   - Daily stations – STNCs applied to the date listed and following day
   - Hourly stations – STNCs applied to the date listed and prior day
5. The procedures described in the prior sections were used to set the STNCs for automated storm type/coding of MLC, MLC/EC, TSR/EC, MEC, MEC/NEC, LS, and LS/NOI storm types. These procedures resulted in overwriting some of the STNCs for dates of TSRs where days with embedded convection occurred (TSR/EC).
6. The DDST was reviewed to confirm the initializing STNC values of zero have all been over-written with STNC values for all dates and AMS zones.
7. Summary statistics were computed for the various storm types and seasonal histograms were prepared to assess the resultant storm seasonality. These seasonality histograms are displayed in the prior sections.
8. The multi-day sequences of storm types for a large sample of the 1,100+ storms used in Manual storm typing were reviewed to confirm the reasonableness of the automated storm typing in meshing with the Manual storm typing.

***Table E-13*** lists an excerpt from the DDST. A MLC (10) with widespread precipitation is seen to occur on May 2-4, 1984. The “M1” in the Method Code column and the “2-Day” in the Comment column indicate this storm was typed by Manual methods and the 3-year recurrence interval threshold was exceeded at the 2-day duration.

A large flood was produced in the Tennessee Valley by the storm of May 6-8, 1984 which began as a MLC (10) on the first day of the storm and then transitioned into a MEC (30) on the following two days. The “Dup” in the Comment column indicates that there were multiple durations where the recurrence interval thresholds were exceeded for several durations for the given date.

***Table E-13 - Example of DDST***

| # | YearMoDy | CENTURY NETWORK TVA-Percent West | East | Max (inch) West | East | Pw (mm) Pw1 | Pw2 | Convective Energy Pw3 | Pw4 | Methd Genrl CAPE1 | CAPE2 | CAPE3 | CAPE4 | AMS Code | STNC Extraction Zones Envrn | AMS1 | AMS2 | AMS3 | AMS4 | Comments |
|---|---|---|---|---|---|---|---|---|---|---|---|---|---|---|---|---|---|---|---|---|
| . | | | | | | | | | | | | | | | | | | | | |
| . | | | | | | | | | | | | | | | | | | | | |
| . | | | | | | | | | | | | | | | | | | | | |
| . | | | | | | | | | | | | | | | | | | | | |
| 37734 | 19840424 | 0.00 | 0.00 | 0.00 | 0.00 | 16.0 | 16.5 | 15.9 | 16.0 | 45 | 37 | 39 | 60 | A | 99 | 99 | 99 | 99 | 99 | |
| 37735 | 19840425 | 0.00 | 0.00 | 0.00 | 0.00 | 19.7 | 14.8 | 11.7 | 10.9 | 0 | 3 | 11 | 11 | A | 99 | 99 | 99 | 99 | 99 | |
| 37736 | 19840426 | 0.03 | 0.00 | 0.52 | 0.00 | 23.9 | 25.3 | 23.0 | 18.3 | 96 | 34 | 9 | 7 | A | 40 | 40 | 40 | 40 | 40 | |
| 37737 | 19840427 | 0.19 | 0.14 | 2.62 | 1.25 | 30.8 | 25.4 | 25.9 | 28.5 | 357 | 252 | 420 | 483 | A | 40 | 40 | 40 | 40 | 40 | |
| 37738 | 19840428 | 0.42 | 0.14 | 3.80 | 1.45 | 38.7 | 35.1 | 30.4 | 28.4 | 1786 | 537 | 116 | 237 | A | 33 | 30 | 30 | 30 | 33 | |
| 37739 | 19840429 | 0.44 | 0.14 | 2.14 | 1.38 | 32.2 | 30.5 | 29.6 | 31.4 | 782 | 1095 | 1148 | 1055 | A | 30 | 30 | 30 | 30 | 30 | |
| 37740 | 19840430 | 0.29 | 0.05 | 2.67 | 0.85 | 43.0 | 37.6 | 31.1 | 23.7 | 50 | 12 | 10 | 9 | A | 10 | 10 | 10 | 10 | 10 | |
| 37741 | 19840501 | 0.06 | 0.07 | 1.70 | 0.94 | 9.0 | 10.1 | 14.6 | 22.3 | 0 | 0 | 4 | 83 | A | 40 | 40 | 40 | 40 | 40 | |
| 37742 | 19840502 | 0.49 | 0.14 | 2.37 | 2.01 | 24.3 | 19.4 | 14.9 | 12.5 | 0 | 0 | 0 | 0 | M1 | 10 | 10 | 10 | 10 | 10 | 2-Day |
| 37743 | 19840503 | 0.89 | 0.72 | 4.03 | 2.80 | 38.5 | 39.2 | 38.1 | 37.1 | 485 | 71 | 23 | 12 | M2 | 10 | 10 | 10 | 10 | 10 | |
| 37744 | 19840504 | 0.35 | 0.47 | 1.00 | 1.88 | 25.5 | 23.5 | 25.5 | 34.1 | 270 | 361 | 385 | 293 | A | 10 | 10 | 10 | 10 | 10 | |
| 37745 | 19840505 | 0.08 | 0.00 | 1.50 | 0.00 | 20.9 | 17.5 | 15.0 | 14.5 | 23 | 40 | 42 | 29 | A | 40 | 40 | 40 | 40 | 40 | |
| 37746 | 19840506 | 0.43 | 0.23 | 4.98 | 2.33 | 24.0 | 23.9 | 23.7 | 23.2 | 47 | 9 | 2 | 1 | A | 10 | 10 | 10 | 10 | 10 | |
| 37747 | 19840507 | 0.70 | 0.74 | 5.27 | 5.03 | 40.4 | 37.5 | 35.6 | 34.8 | 1660 | 1153 | 1013 | 960 | MM | 30 | 30 | 30 | 30 | 30 | Dup |
| 37748 | 19840508 | 0.78 | 0.70 | 4.47 | 2.75 | 42.0 | 37.6 | 34.2 | 34.6 | 946 | 1028 | 996 | 1103 | M1 | 30 | 30 | 30 | 30 | 30 | |
| 37749 | 19840509 | 0.00 | 0.02 | 0.00 | 0.85 | 13.6 | 8.4 | 5.9 | 10.8 | 0 | 0 | 0 | 14 | A | 40 | 40 | 40 | 40 | 40 | |
| 37750 | 19840510 | 0.00 | 0.00 | 0.00 | 0.00 | 10.9 | 9.8 | 11.1 | 13.4 | 0 | 4 | 16 | 44 | A | 99 | 99 | 99 | 99 | 99 | |
| 37751 | 19840511 | 0.00 | 0.00 | 0.00 | 0.00 | 21.1 | 19.5 | 15.4 | 12.5 | 11 | 0 | 0 | 0 | A | 99 | 99 | 99 | 99 | 99 | |
| 37752 | 19840512 | 0.00 | 0.00 | 0.00 | 0.00 | 27.8 | 24.0 | 21.2 | 20.5 | 273 | 101 | 21 | 2 | A | 99 | 99 | 99 | 99 | 99 | |
| 37753 | 19840513 | 0.00 | 0.00 | 0.00 | 0.00 | 31.0 | 28.4 | 26.8 | 26.8 | 281 | 205 | 238 | 240 | A | 99 | 99 | 99 | 99 | 99 | |
| 37754 | 19840514 | 0.08 | 0.00 | 0.71 | 0.00 | 42.8 | 40.5 | 37.4 | 34.5 | 1710 | 1665 | 1684 | 1584 | A | 40 | 40 | 40 | 40 | 40 | |
| 37755 | 19840515 | 0.00 | 0.00 | 0.00 | 0.00 | 11.0 | 7.5 | 7.7 | 11.5 | 0 | 0 | 0 | 1 | A | 99 | 99 | 99 | 99 | 99 | |
| 37756 | 19840516 | 0.00 | 0.00 | 0.00 | 0.00 | 13.1 | 11.8 | 10.8 | 10.2 | 0 | 0 | 0 | 3 | A | 99 | 99 | 99 | 99 | 99 | |
| 37757 | 19840517 | 0.00 | 0.00 | 0.00 | 0.00 | 11.1 | 9.3 | 8.1 | 7.5 | 0 | 0 | 0 | 0 | A | 99 | 99 | 99 | 99 | 99 | |
| 37758 | 19840518 | 0.00 | 0.00 | 0.00 | 0.00 | 14.8 | 13.8 | 13.4 | 13.7 | 0 | 0 | 0 | 0 | A | 99 | 99 | 99 | 99 | 99 | |
| 37759 | 19840519 | 0.00 | 0.00 | 0.00 | 0.00 | 17.9 | 19.0 | 19.1 | 18.8 | 1 | 4 | 1 | 0 | A | 99 | 99 | 99 | 99 | 99 | |
| . | | | | | | | | | | | | | | | | | | | | |
| . | | | | | | | | | | | | | | | | | | | | |
| . | | | | | | | | | | | | | | | | | | | | |
| . | | | | | | | | | | | | | | | | | | | | |
| . | | | | | | | | | | | | | | | | | | | | |

# APPENDIX F
# Determining Timing of the Century Network Day for Use in Storm Typing

## F.1 Overview

The DDST lists storm types on a daily time-step for the period from 1881 through 2014. The Storm Types include: MLCs, TSRs, MECs, and LSs. The “day” in the DDST is not defined on a calendar-day basis, but must be defined in terms of the timing of available measures of precipitation, Pw, CAPE, and time-of-day frequencies exhibited in the timing of various storm types. The redefined “day” is termed the Century Network Day. The name Century Network arises from the collection of long-term high quality 100 precipitation measurement stations that were in-place most of the 20th Century that provide spatial measures of daily precipitation used in creating the DDST.

The time-of-day for the end-of-the-day/start-of-new-day for the Century Network Day is important because precipitation annual maxima for multi-hour durations of interest can span the day-to-day boundary (***Figure F-9***). This situation can result in a different storm type being associated with segments of a precipitation time series on either side of the Century Network Day boundary. This could then require a decision which storm type was associated with a segment of hourly precipitation. The time-of-day of the Century Network Day boundary is most important for short-duration precipitation annual maxima such as the 6-hour duration, typical for MECs, and the 1-hour and 2-hour durations, common for LSs. Conversely, a few hours shift in either direction for the Century Network Day boundary would not have much effect in determining the storm type for multi-day synoptic scale MLCs and TSRs.

Considerations in determining the time-of-day of the end-of-the-day/start-of-new-day for the Century Network Day are discussed in the following sections.

## F.2 Time-of-Day Frequencies in MECs and LSs

As discussed above, the time-of-day of the end-of-the-day/start-of-new-day for the Century Network Day is most important for the MECs and for LSs. The seasonality of occurrence for these two storm types is strongest in the June through August timeframe (***Figure F-1***, ***Figure F-2***) when they are the dominant storm types with relatively few warm season MLCs (***Figure F-3***). TSRs, while primarily warm season events, are also infrequent by comparison (***Figure F-4***).

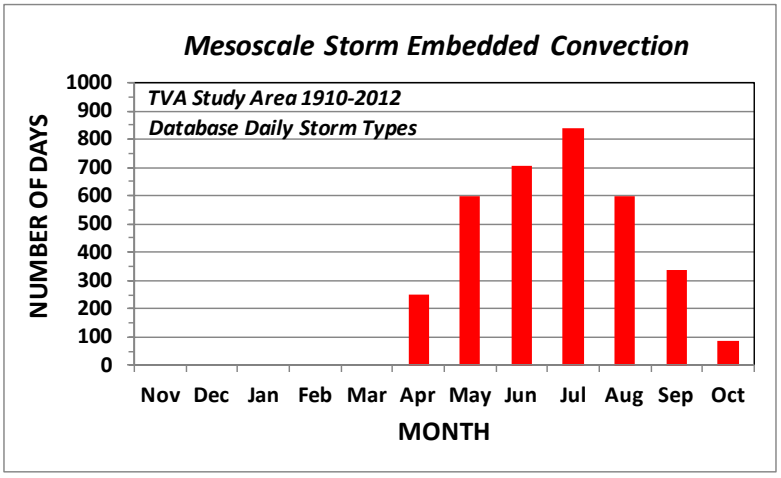


***Figure F-1 - Seasonal Distribution of MECs for 1910-2012 Period Based on Manual and Automated Storm Typing***

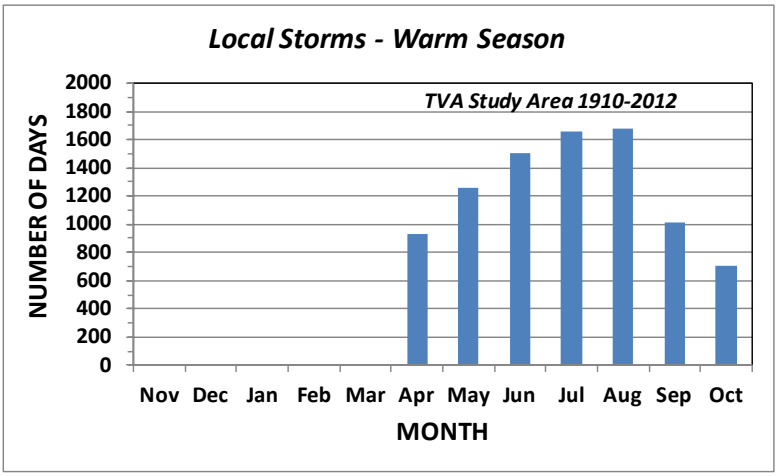


*Figure F-2 - Seasonal Distribution of LSs for 1910-2012 Period Based on Manual and Automated Storm Typing*

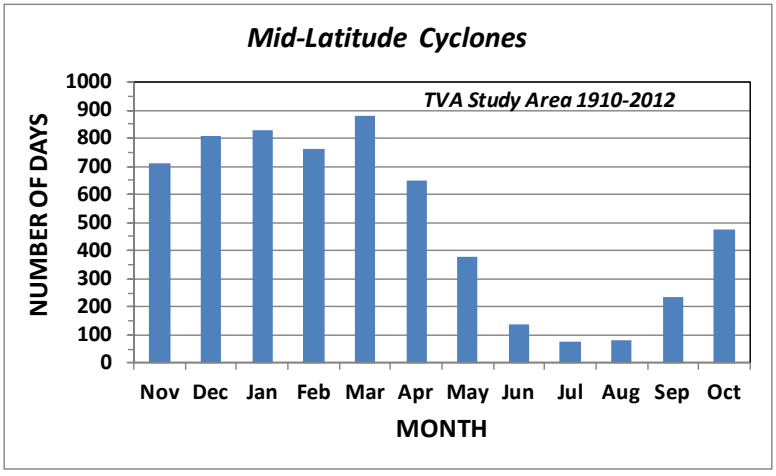


*Figure F-3 - Seasonal Distribution of MLCss for 1910-2012 Period Based on Manual and Automated Storm Typing*

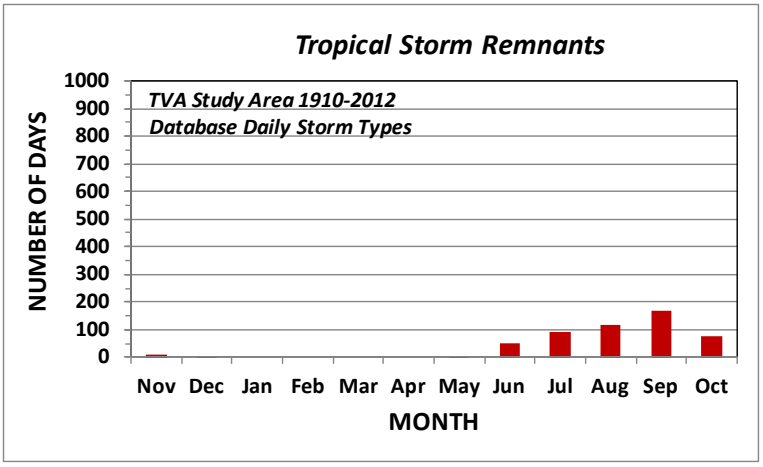


*Figure F-4 - Seasonal Distribution of TSRs for 1910-2012 Period Based on Manual and Automated Storm Typing*

A time-of-day storm analysis was conducted for the precipitation annual maxima at the 2-hour and 6-hour durations using AMS data for the TVA Study Area. ***Figure F-5*** and ***Figure F-6*** depict the starting-hour for 2-

hour and 6-hour precipitation annual maxima for the months of June, July and August. The MEC and LS storm types are characterized by convective cells (thunderstorms) that are associated with day-time heating and commonly develop in the early-afternoon and evening hours. In particular, MCCs are a subset of the MEC storm type that develop in this timeframe and often produce high precipitation intensities very late in the evening and during the night in the warm season.

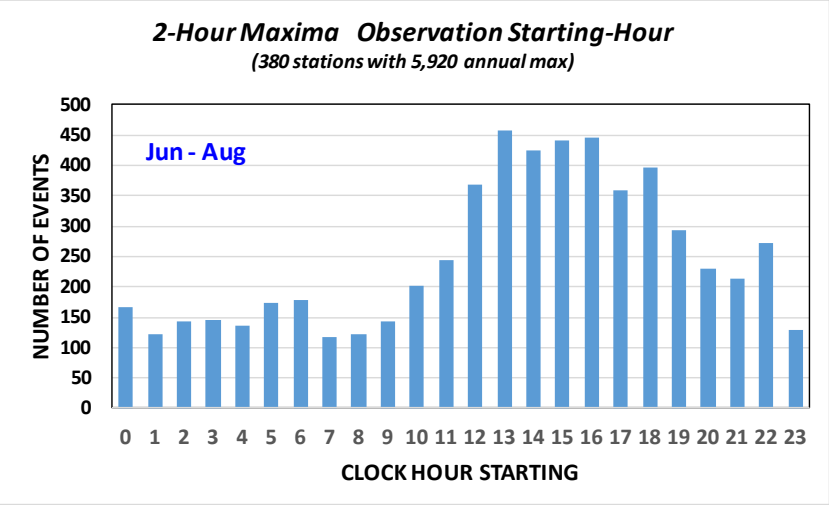


***Figure F-5 - Observed Clock-Hour Starting for 2-Hour Precipitation Maxima for TVA Study Area for the June through August Timeframe***

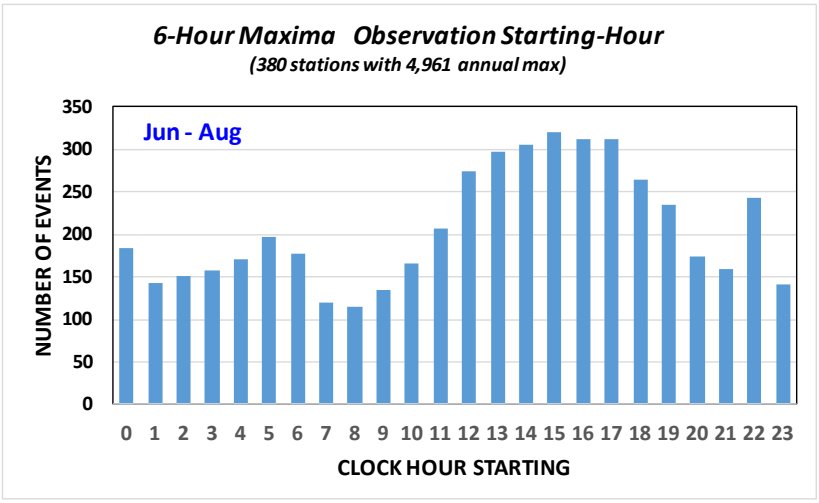


***Figure F-6 - Observed Clock-Hour Starting for 6-Hour Precipitation Maxima for TVA Study Area for the June through August Timeframe***

A review of ***Figure F-5*** and ***Figure F-6*** shows a lull in the morning hours between 7 AM and 9 AM and the maximum frequency of occurrence for initiation of storms between about 1 PM and 5 PM in the afternoon local time. This is the natural signature of the timing of the MEC and LS storm types. The results of this analysis suggest that somewhere in the 7 AM to 9 AM timeframe is a natural break for the timing of the MEC and LS storm types and a logical time for setting the start/end of the Century Network Day.

By comparison, the long-duration MLCs and TSRs with synoptic scale atmospheric conditions, do not have time-of-day tendencies. The start times for these storms are essentially uniformly distributed over the 24-hour clock without any time-of-day tendencies like those seen in ***Figure F-5*** and ***Figure F-6***.

## F.3 Reporting Time of Century Network Stations

There are about 50 long-term high-quality precipitation measurement stations in each of the western and eastern areas of the TVA Study Area (***Figure F-7***). These stations are used to provide a measure of the extent of areal coverage of daily precipitation for use in storm typing. A daily precipitation threshold of 0.50-inch was used as the indicator of precipitation sufficiently large to be considered as part of a "storm". Counts were made of the number of stations where the daily precipitation exceeds this threshold and a count was also made for the number of stations that were operational for the given day. The "percentage of active stations over the 0.50-inch threshold" was the indicator for the scale of the areal coverage of precipitation and a separate measure was computed for the TVA-West and TVA-East zones.

All of the stations in the Century Network have Observational-Day gages where precipitation is reported once a day on a fixed time schedule. Morning (7 AM, 8 AM and 9 AM) and evening (5 PM, 6 PM and 7 PM) are the most common reporting times with a few stations reporting at midnight. ***Figure F-8*** depicts the count of Century Network precipitation stations in the Tennessee and North Carolina areas and the observational times in the period from 1890 through 2010. These stations were chosen because a complete history of observational times was available. This analysis was conducted for stations reporting at decade-ending years for each decade from 1890 through 2010. An average of observation times was computed by decade and it is seen in ***Table F-1*** there has been a slow shift over the years from mostly evening reporting to primarily reporting in the morning.

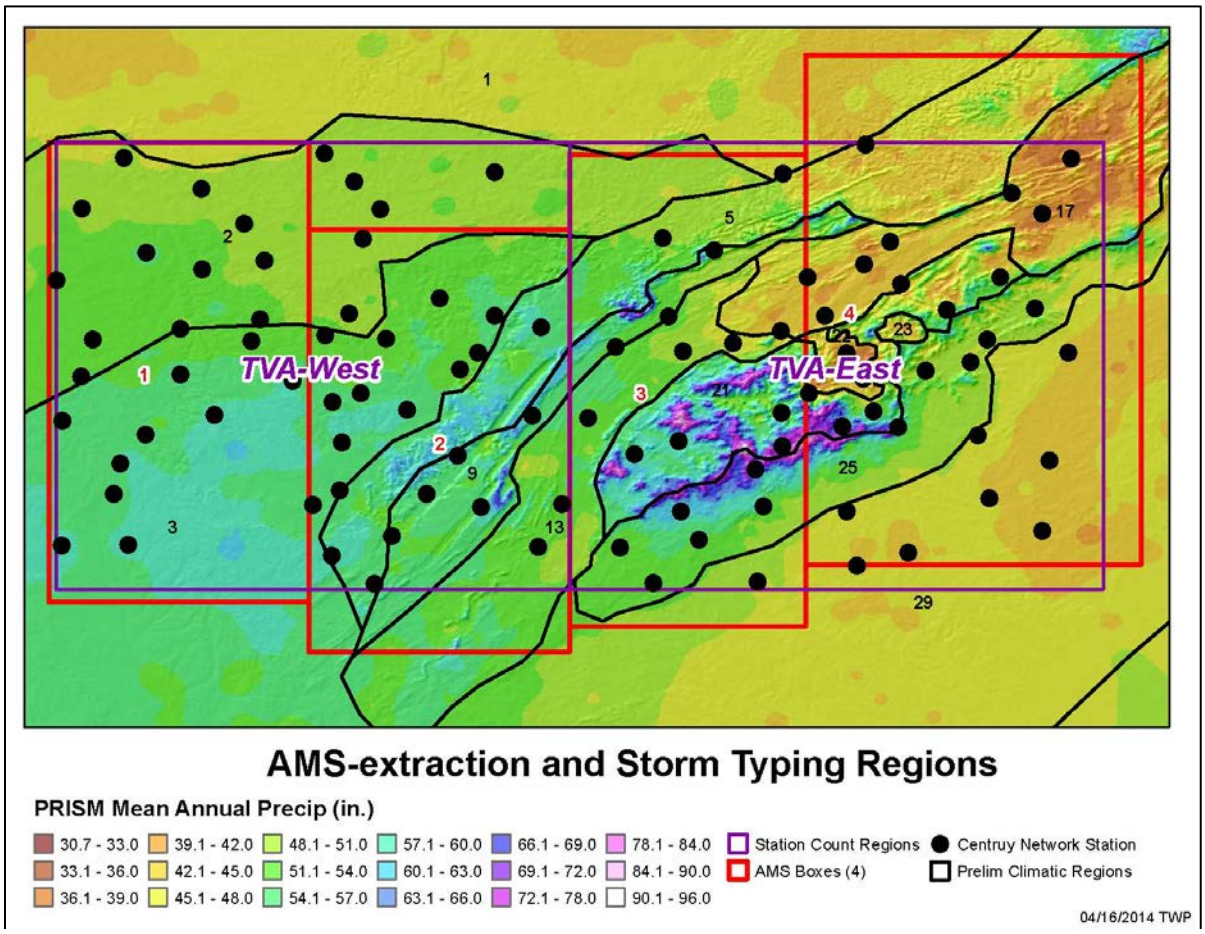


***Figure F-7 - TVA Study Area Depicting TVA-West and TVA-East Zones, Location of Precipitation Measurement Stations for the Century Network and Four Annual Maximum Series (AMS) Extraction Zones***

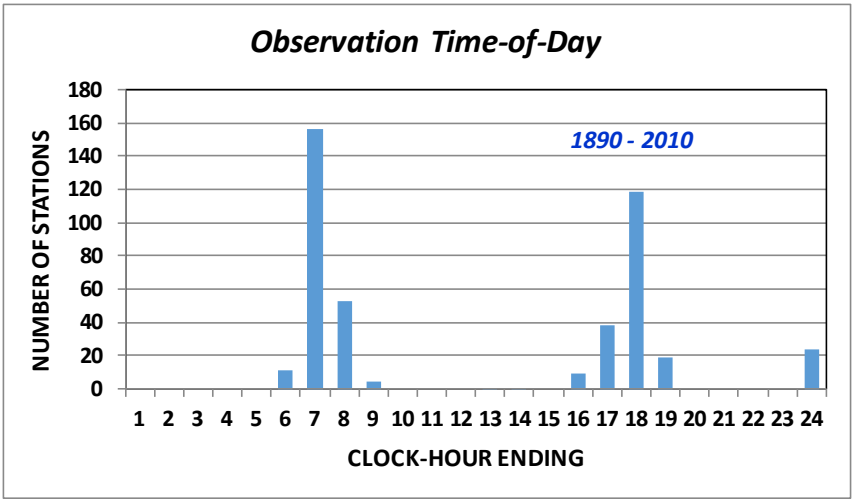


***Figure F-8 - Measure of the Frequency of Reporting Times for Daily Stations in the Century Network for the period from 1890 through 2010***

Automated precipitation gages came on-line in the 1940's and hourly data became available in electronic format in 1948 when the NCDC was assigned the responsibility for managing the climatological data. Therefore, the period of 1948 to present is of interest for the short-duration precipitation maxima for the MEC and LS storm types.

An assessment was made of how the observational timing of stations in the Century Network would affect the decision for setting the start/end timing of the Century Network Day. The analysis was conducted by considering the start/end of the Century Network Day to be at 8 AM (***Figure F-9***) which is the time of the lull in the frequency of occurrence of the start time for 2-hour and 6-hour precipitation annual maxima (***Figure F-5*** and ***Figure F-6***). This is the natural break in timing based on storm characteristics.

A review of ***Table F-1*** shows the 8 AM timing to be consistent with the morning observational time of the majority of the Century Network stations for the period from 1948 to present. The remaining stations that report in the evening (nominally 6 PM) still have about 14-hours of overlap in the reporting period with the morning stations which is typically sufficient time to register over the 0.50-inch threshold in order to be counted in the measure for storm areal coverage. Therefore, the measure of the extent of areal coverage by the Century Network is not overly sensitive to the minority number of stations reporting in the evening. This conclusion is supported by the large number of MEC and LS storms identified in the storm typing process (***Figure F-1*** and ***Figure F-2***). It was concluded the existing collection of Century Network stations and observation times are compatible with the selection of 8 AM for defining the Century Network Day.

*Table F-1 - Average of Time-of-Day of Observational Day Stations in Century Network*

| DECADE ENDING | NUMBER OF STATIONS | | | AVERAGE TIME-OF-DAY (24-Hr Clock) |
|---|---|---|---|---|
| | Morning Stations | Evening Stations | Midnight Stations | |
| 1890 | 5 | 1 | 0 | 9:51 |
| 1900 | 14 | 15 | 0 | 12:44 |
| 1910 | 13 | 24 | 0 | 14:10 |
| 1920 | 10 | 27 | 0 | 14:52 |
| 1930 | 14 | 24 | 0 | 13:54 |
| 1940 | 19 | 18 | 0 | 12:15 |
| 1950 | 23 | 16 | 2 | 12.10 |
| 1960 | 23 | 16 | 2 | 12.10 |
| 1970 | 17 | 14 | 3 | 13.05 |
| 1980 | 18 | 13 | 2 | 12.25 |
| 1990 | 18 | 11 | 4 | 12.45 |
| 2000 | 23 | 5 | 5 | 11.24 |
| 2010 | 27 | 1 | 6 | 10.32 |

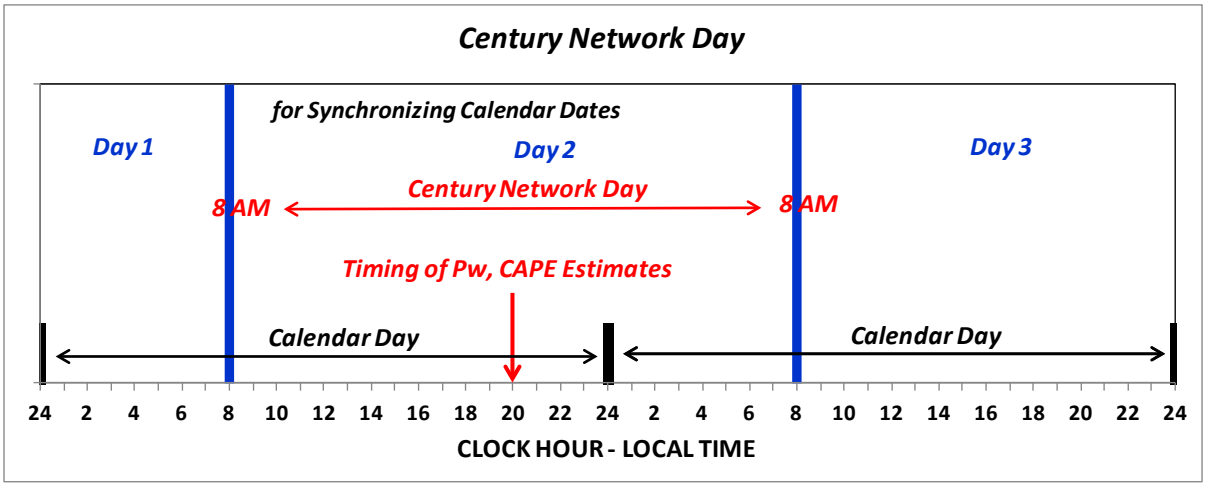


*Figure F-9 - Depiction of Century Network Day for Use in Automated Daily Storm Typing*

## F.4 Considerations for Daily Timing of Pw and CAPE

The daily values of Pw and CAPE that have been estimated for the four AMS Extraction Zones are for a time of 0:00 Z (UTC) which corresponds to 7 PM or 8 PM in the TVA Study Area, standard time and daylight savings time, respectively. This timing places the Pw and CAPE at the mid-point of the proposed 8 AM to 8 AM window for defining the Century Network Day (***Figure F-9***). Further, the 8 PM (daylight savings time) timing in the warm season is near the optimum timing of the start of historical MEC and LS storms (***Figure F-5*** and ***Figure F-6***). The proposed 8 AM start of the Century Network Day is compatible with the timing of the measures of Pw and CAPE.

## F.5 Expectations for the Frequency of Storm Typing Decisions

A logical question is – "how often will a storm typing decision be required for determining the appropriate day using the proposed 8 AM start/end time for the Century Network Day"? This situation would arise where a candidate 2-hour or 6-hour precipitation annual maxima spanned the 8 AM start/end boundary for the Century Network Day and there are two different storm types for adjacent days.

This question was answered for the 6-hour annual maxima by examining 131 noteworthy MEC and LS storms in the 1971-1980 timeframe. These are storms that were storm typed using Manual methods as part of the process of developing automated storm typing criteria and procedures. It was found that in 51% of the cases adjacent days had the same storm type and a decision on the appropriate storm type would not be required. For the other 49% of the cases, the probability of a storm spanning the 8 AM boundary is 0.17, represented by starting times from 3 AM through 7 AM (***Figure F-6***). This corresponds to a decision on storm typing to be required in about 8% of the cases for MEC storms. Similar analysis for the 2-hour duration indicates a decision on storm type was required in only about 1% of the cases for LSs.

The scripting for assembly of hourly precipitation annual maxima data series included a decision process whereby each hour of the Century Network Day was assigned a storm type for all days in the DDST (1881-2014). The precipitation total for each candidate annual maxima for each of the two storm types was computed and the annual maxima was linked with the storm type associated with the majority of the precipitation. In the case, where neither storm type had a majority of the hours, the candidate annual maxima was assigned to both storm types. This criterion reflected uncertainties inherent in timing issues associated with the storm typing process and timing and spatial variability of thunderstorm precipitation. The majority rule criterion also reflected that storms often are hybrids having characteristics of two storm types. In these cases, it was reasonable to consider the annual maxima being an element of both data series for the two storm types. It should be noted that only a small number of annual maxima are likely to be a member of the data series for two storm types, this is probably about 5%, or one annual maxima in twenty.

A similar decision process was used for stations with observational day gages for multi-day annual maxima for synoptic scale MLCs and TSRs. Specifically, if a decision was required for identifying the storm type, the storm type with the greatest precipitation total was selected. This decision was subject to the majority rule criterion discussed above.

# APPENDIX G
# Seasonality Analysis of Extreme Storms

Information on the seasonality of occurrence of extreme storms is needed for flood modeling for the four storm types. In particular, the most extreme storms of a given storm type often have a narrower season of occurrence than the seasonality of precipitation annual maxima with smaller magnitudes. Procedures have been developed for identifying the largest and most noteworthy storms in the precipitation records for conducting a seasonality analysis. The general procedure is described below, , with application of the analysis to the seasonality of PMP described in a companion Technical Memorandum (Schaefer[24]).

## G.1 Method of Analysis

The following procedures are used in conducting the seasonality analyses. Minor changes to these procedures are made for some storm types. Any differences in procedures will be described in the sections describing the results of the seasonality analyses for each storm type.

1. For a given storm type and duration, scan the annual maxima dataset for each station and identify precipitation amounts and associated storm dates that exceed a specified frequency threshold; typically exceeding a 10-year event (AEP of 0.10).
2. Sort the resultant dataset by storm date to create a list of the precipitation stations exceeding the frequency threshold, associated precipitation amounts, and estimated AEPs for each storm event. The number of stations that exceed the frequency threshold, the magnitudes of precipitation, and AEPs collectively provide a measure of the spatial extent and rarity of each storm event.
3. Rank the individual storm dates in the dataset created in Step 2 by the number of stations exceeding the frequency threshold.
4. Use the highest ranking storms/storm dates to conduct the seasonality analysis. The number of storms utilized in the seasonality analysis is a balance between retaining the most extreme storms and having a dataset sufficiently large for frequency analysis.
5. Convert the calendar storm dates to numerical storm dates, compute sample statistics and construct a probability plot to graphically depict the seasonal behavior.
6. Fit a Normal distribution or 4-parameter Beta distribution to the numerical storm data and use the fitted distribution to construct a monthly frequency histogram to describe the seasonal behavior.

## G.2 Example of Seasonality Analysis

An example probability plot and fitted 4-parameter Beta distribution is shown in ***Figure G-1*** for the 48-hour duration for the TSR storm type. The seasonality frequency of occurrence for 48-hour duration TSR storm type is depicted as a frequency histogram in ***Figure G-2*** based on the fitted 4-parameter Beta distribution.

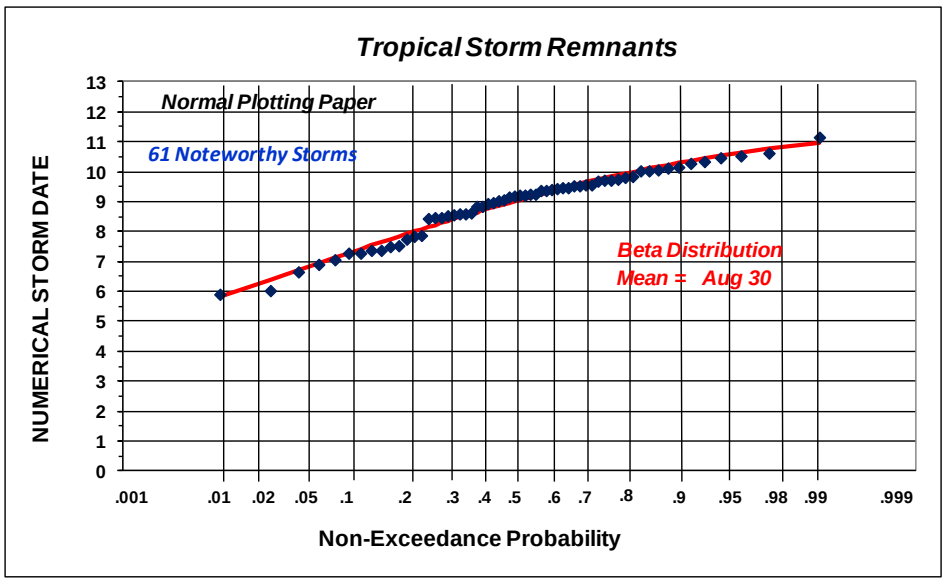


*Figure G-1 - Probability plot of Numerical Storm Dates for the Most Extreme 48-Hour Duration TSR Storms in the TVSA for the Period from 1896-2012*

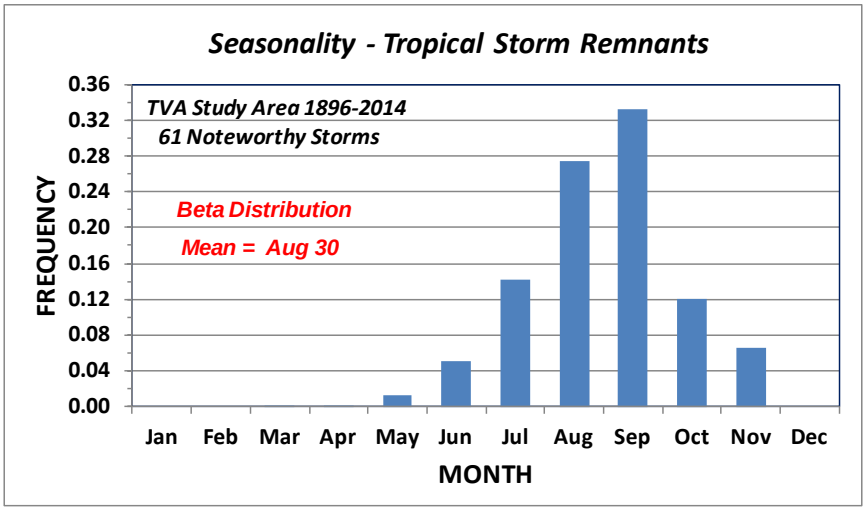


*Figure G-2 - Seasonality Histogram for the 48-Hour Duration for the TSR Storm Type in the TVSA for the Period from 1896-2014*

# APPENDIX H
# Equivalent Independent Record Length

One of the important concepts employed in a regional precipitation-frequency analysis is the concept of trading space for time sampling. This approach takes advantage of the situation that the size of the study area is much larger than the typical storm areal coverage where precipitation annual maxima are produced. Therefore, there will be many storms in the regional dataset of storms (separate storm dates) with annual exceedance probabilities rarer than indicated by the chronological length of the sampling period. The regional dataset of precipitation annual maxima for stations therefore contains many rare storms, which are of primary interest in the precipitation-frequency analysis. In particular, the large dataset of storms can greatly reduce uncertainties in estimation of regional statistical parameters by reducing the effects of sampling variability.

EIRL is a measure of the independent information contained in a regional dataset. EIRL is a function of the size of the study area, the typical areal coverage of storms and the density of precipitation measurement stations. If the storms of interest have large areal coverage relative to the density of the station network, then the EIRL will be a small fraction of the station-years of record because the large areal coverage of the storm would be expected to result in greater correlation (statistical dependence) amongst the gage records. Conversely, if the areal coverage of storms is small and the density of the station network is low, then the EIRL will be a large fraction of the station-years of record. The latter case is the situation for MECs and LS storm types where the cross-correlation between precipitation annual maxima at stations is low.

Some analysts have used the regional magnitude of station cross-correlation in the estimation of EIRL. ***Figure H-1*** through ***Figure H-4*** depict the relationship between the linear correlation coefficient between station annual maxima and distance between stations for the four storm types. The red fitted line is from a LOWESS smooth (Cleveland[1] and Helsel et al[7]) to provide perspective on the general shape of the relationship. The relative magnitudes of cross-correlation are indicative of the areal coverage of the various storm types. A review of the figures shows higher cross-correlation for the synoptic-scale MLC and TSR storm types that decays with distance between stations. The MEC storm type shows dramatic reduction in cross-correlation relative to the MLC and TSR storm types. LSs have very low cross-correlation due to the areal coverage being very limited in extent. It should be noted that these cross-correlation coefficients are for precipitation annual maxima and not for specific storms, and are therefore generally larger than what would be obtained for storm-specific cross-correlation.

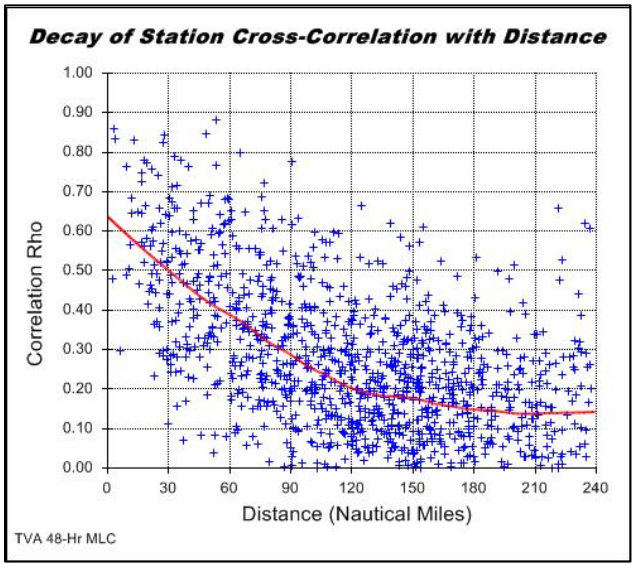


***Figure H-1 - Relationship Between Cross-Correlation Coefficients and Distance between Stations for 48-Hour Precipitation Annual Maxima for Synoptic Scale MLCs***

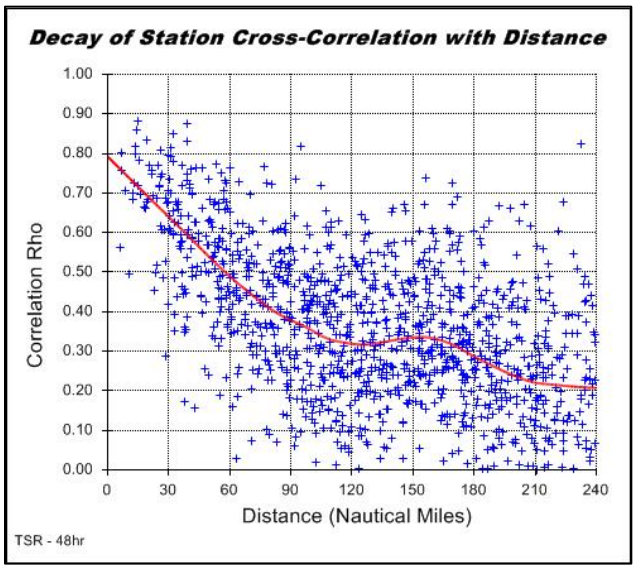


***Figure H-2 - Relationship Between Cross-Correlation Coefficients and Distance between Stations for 48-Hour Precipitation Annual Maxima for Synoptic Scale TSRS***

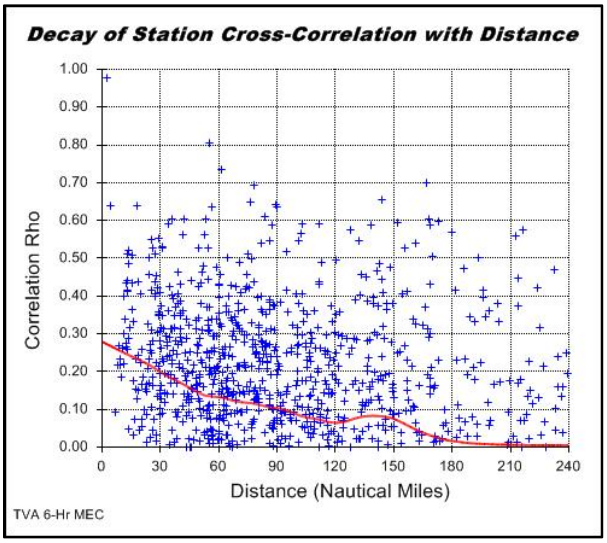


***Figure H-3 - Relationship Between Cross-Correlation Coefficients and Distance between Stations for 6-Hour Precipitation Annual Maxima for MECs***

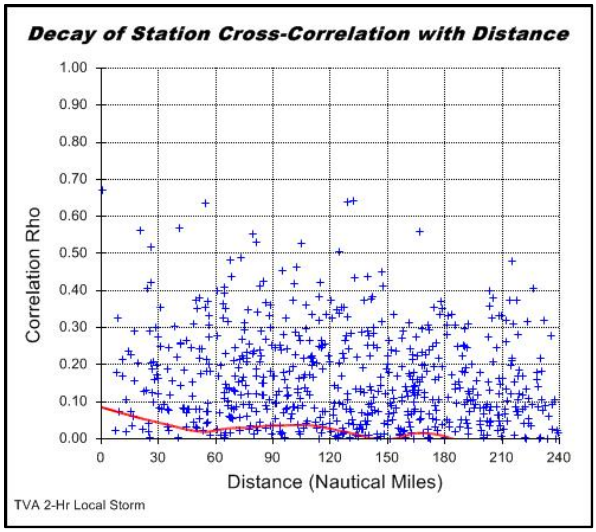


***Figure H-4 - Relationship Between Cross-Correlation Coefficients and Distance between Stations for 2-Hour Precipitation Annual Maxima for LSs***

Two methods were used to estimate EIRL. The first method is a frequency-based method that examines the behavior of the largest 10% of storm events. The second method relies on simple counting of independent storm dates for all storm events. Both methods are presented in the following sections.

## H.1 Frequency-Based EIRL

The frequency-based method for estimating EIRL (Schaefer[17]) is as follows.

1. Compute the AEP of each precipitation annual maximum at each precipitation station using the estimated at-site mean, regional values of the L-moment ratios L-Cv and L-Skewness, and the regional probability distribution.
2. Select all precipitation annual maxima/storm dates with AEPs more rare than a specified threshold (AEP of 0.10 (10-year recurrence interval) was used as the threshold in this study)
3. Sort all precipitation annual maxima from step 2 by storm date. For each storm event, retain the annual maximum with the rarest AEP (indicative of storm center) and remove all other annual maxima for that storm date. Annual maxima must be sufficiently separated by time and/or distance to be considered as separate/independent storms. An independent MLC or TSR storm was considered a storm separated by at least 1 dry day, although the typical case was separation by many days or weeks. An independent MEC or LS storm event was considered when stations were on separate days and/or separated by 100-nautical miles or more. The resultant listing of precipitation annual maxima, each with a separate storm date and an AEP associated with the storm center, is used in computing the EIRL.
4. A least-squares solution (Schaefer[17]) is used to compute the EIRL that best matches the exceedance frequencies of the storms in the dataset (from Step 4). The solution approach can be envisioned as follows. For a representative dataset of 1,000 independent annual maxima, it would be expected to have about 100 events exceed the 10-year threshold, 20 events exceed the 50-year threshold, 10 events exceed the 100-year threshold, 5-events exceed the 200-year threshold, 2 events exceed the 500-year threshold, and 1 event exceed the 1,000-year threshold. This statistical behavior is described by plotting-position formulas (Cunnane[2]) and is used in least-squares estimation of EIRL.

The red curves in ***Figure H-5*** show the exceedance characteristics expected for independent record lengths of 5,000, 7,300 and 10,000 years based on the Cunnane plotting position formula with a weighting parameter of 0.44. The data plot in ***Figure H-5*** is for the exceedance characteristics for Convective Storms at the 2-hour duration in the TVSA.

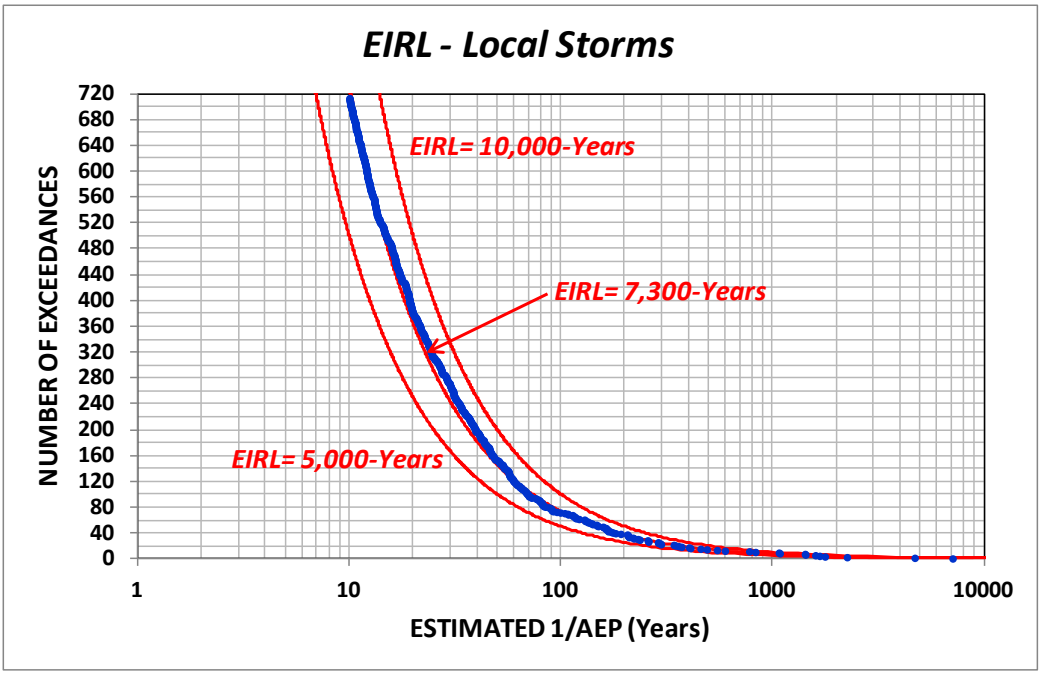


***Figure H-5 - Graphical Depiction of EIRL for 2-Hour Duration for LSs for the TVSA***

## H.2 EIRL from Storm Counts

The second method for estimating EIRL makes use of the concept of physically independent storm events. Specifically, storms in the TVSA are produced by a combination of moisture supplied via the Gulf of Mexico or Atlantic Ocean and precipitation generating mechanisms originating from weather systems over the North American continent or Caribbean tropics. A physically independent storm is considered to be a storm event (spatial and temporal precipitation pattern) that is separated from other storm events by sufficient time and/or distance to be considered physically independent. The meteorological basis for this criterion for MLC and TSR storm types is the change in air mass and synoptic conditions for concurrent storms. In the case of convective storms, stations, or clusters of stations, must be separated sufficiently such that the site-specific atmospheric and meteorological conditions are different (different thunderstorm cells). In actuality, storms were typically separated by weeks or longer, representing independent atmospheric conditions. The procedures for the EIRL storm count are listed below.

1. Sort precipitation annual maxima for all stations and years by date of the annual maxima;
2. Synoptic Scale Mid-Latitude Cyclones and TSRs - a physically independent storm is counted when there is a day or multiple contiguous days with precipitation annual maxima over the 10-year threshold and separated by one or more dry days;
3. Convective Storm Types – a physically independent storm is counted when stations, or clusters of stations, exceed the 10-year threshold and are separated longitudinally by 100 nautical-miles or more;
4. Count the number of separate storm dates.

***Table H-1*** lists the results of the EIRL analyses for the four storm types. A review of ***Table H-1*** and ***Figure H-1*** through ***Figure H-4*** portrays a consistent picture. EIRL is a smaller percentage of the station-years of record for synoptic-scale storms with larger areal coverage of precipitation. The percentage of EIRL relative to the station-years of record increases for Mesoscale and LS types as the areal coverage of the storms continue to decrease in size relative to the size of the study area.

***Table H-1 - Estimates of EIRL for Four Storm Types Using Precipitation Data for Stations with Record Lengths of 15 Years or More***

| Storm Type | Station-Years of Record | EIRL Estimates (Years) | | | EIRL Percent of Station-Years |
|---|---|---|---|---|---|
| | | Frequency Based | Storm Count | Geometric Mean | |
| MLC | 50,281 | 5,700 | 2,760 | 3,970 | 7.9% |
| TSR | 25,862 | 1,250 | 675 | 925 | 3.6% |
| MEC | 13,611 | 5,800 | 2,690 | 3,950 | 29.0% |
| LS | 9,154 | 7,300 | 4,592 | 5,790 | 63.2% |

The initial impression from review of the EIRL estimates in ***Table H-1*** is that the frequency-based and storm counting estimates are quite different. The storm counting estimates of EIRL are generally one-half to two-thirds of the frequency-based EIRL estimates. However, these two estimates need to viewed from a frequency perspective, with consideration given to the underlying procedures. In the case of the frequency-based method, several situations or a combination of situations could account for the differences. The dataset of storms may be representative of a more active period of storm magnitudes relative to the number of storm events. For example, it is not uncommon for a 50-year precipitation record to have several storms with AEPs rarer than expected in a 50-year record. The same can be true in a regional record. Much of the differences in the two EIRL estimates could also be accounted for by a change of about 5% in the maximum precipitation magnitudes for storm events. Likewise, a similar 5% change in the at-site mean used to estimate the AEP of a given storm event could account for much of the differences.

With regard to the storm counting estimate, it likely represents an undercount of the number of storms given the relatively stringent spatial separation criteria used in the procedures for counting. This is particularly true for the MEC and LS storm types with smaller areal coverage. For these reasons and acknowledging that both are estimates, it is reasonable to adopt a measure of EIRL that utilizes estimates from both the frequency-based and storm counting methods. A geometric mean of EIRL was computed (***Table H-1***), which considers both methods to have equal merit in estimating EIRL.

EIRL will be used in the uncertainty analysis in Phase 3 for determining statistical characteristics of parameters that are used in computing the basin-average precipitation-frequency relationship for watersheds and storm types in the TVSA.

# APPENDIX I
## Isopluvial Maps of 48-Hour Precipitation for Mid-Latitude Cyclones

The following isopluvial maps were generated using the gridded datasets for at-site means, regional L-Cv and regional L-Skewness for 48-hour precipitation annual maxima for MLCs. The 4-parameter Kappa distribution, as fitted by the method of L-moments (Hosking and Wallis[10]), was used for computing quantile estimates. Isopluvial maps are presented for annual exceedance probabilities of $10^{-1}$, $10^{-2}$, $10^{-3}$, $10^{-4}$ and $10^{-5}$ (***Figure I-1*** to ***Figure I-5***).

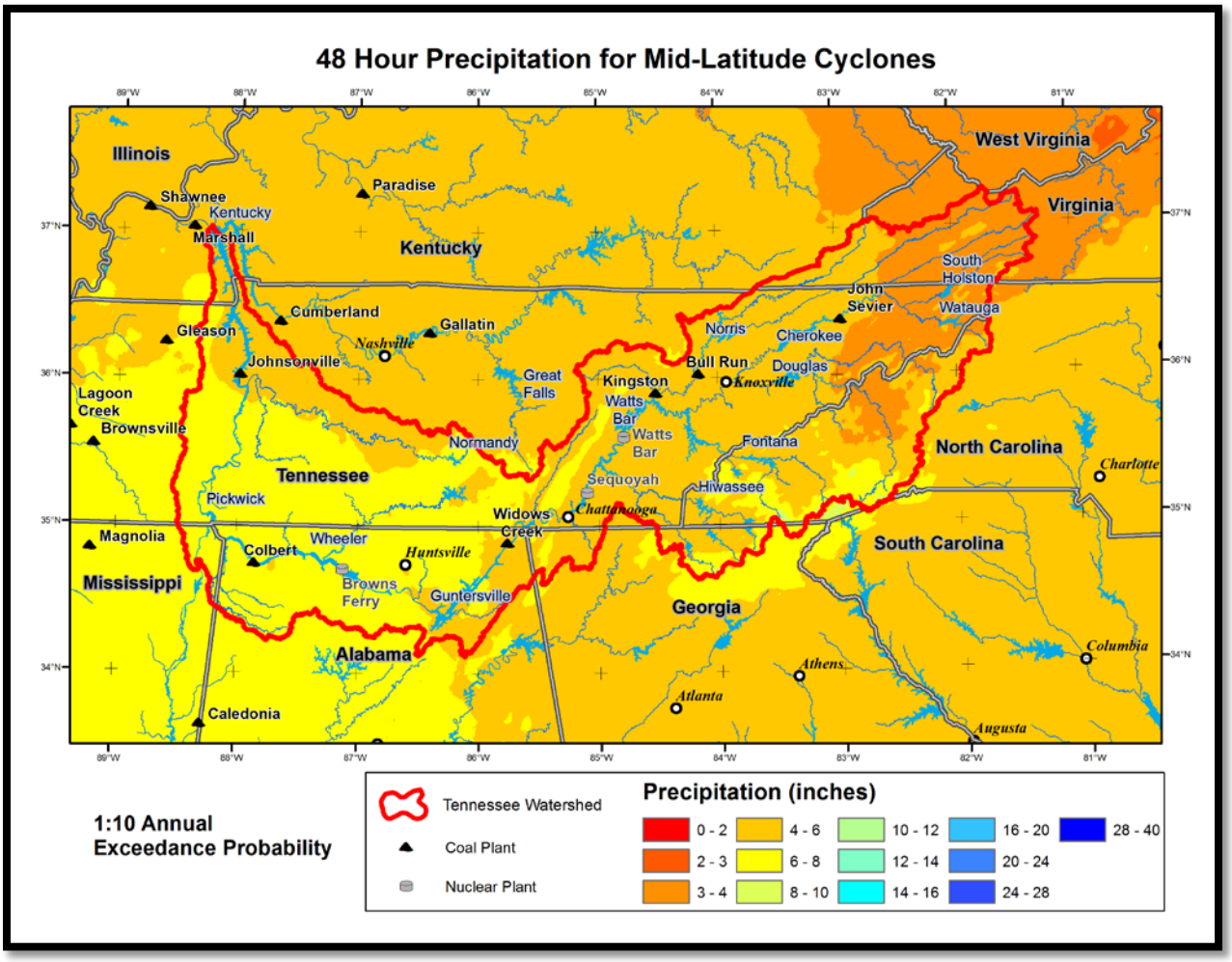


***Figure I-1 - Isopluvial Map of 48-Hour Precipitation for MLCs for AEP of 1:10***

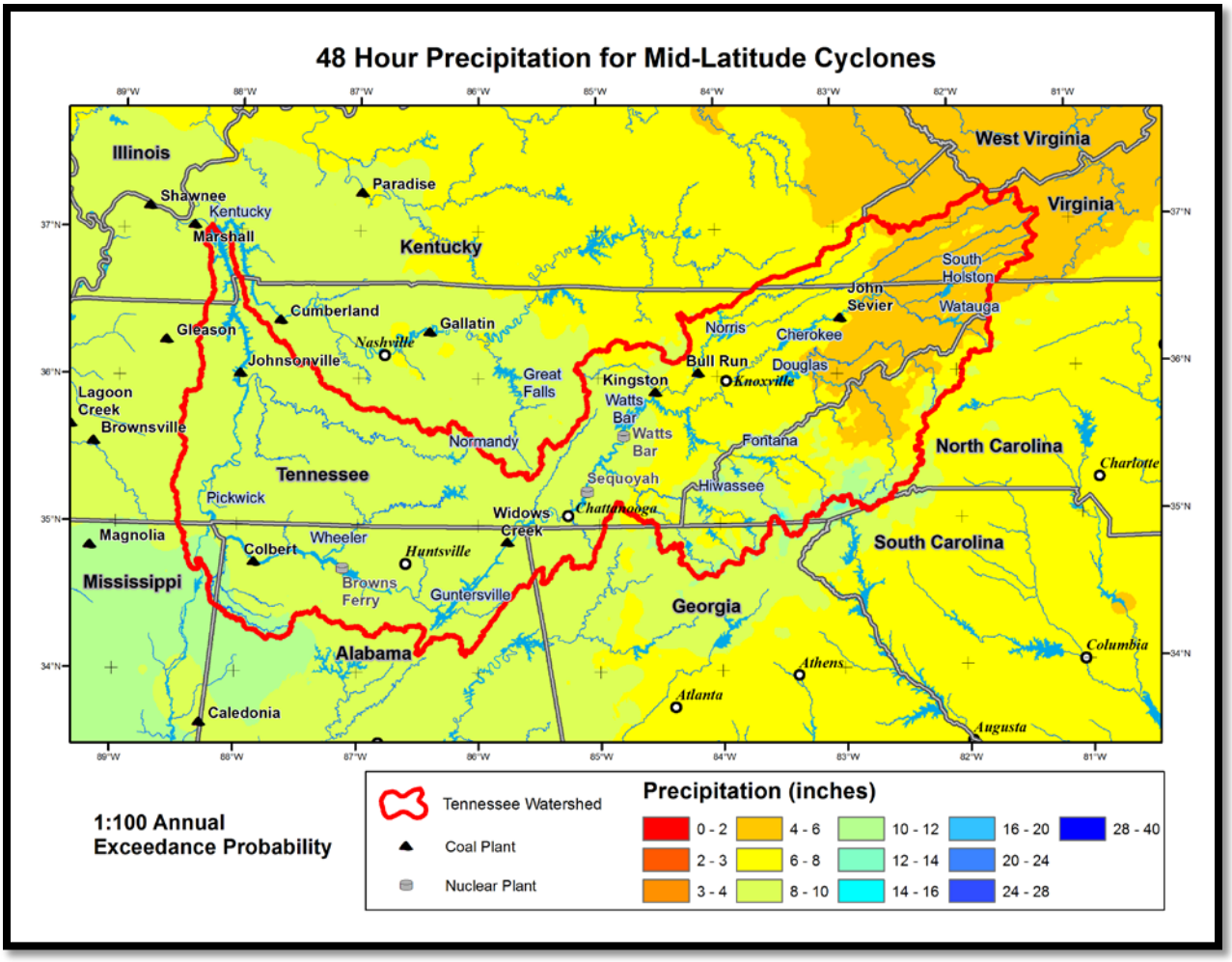


***Figure I-2 - Isopluvial Map of 48-Hour Precipitation for MLCs for AEP of 1:100***

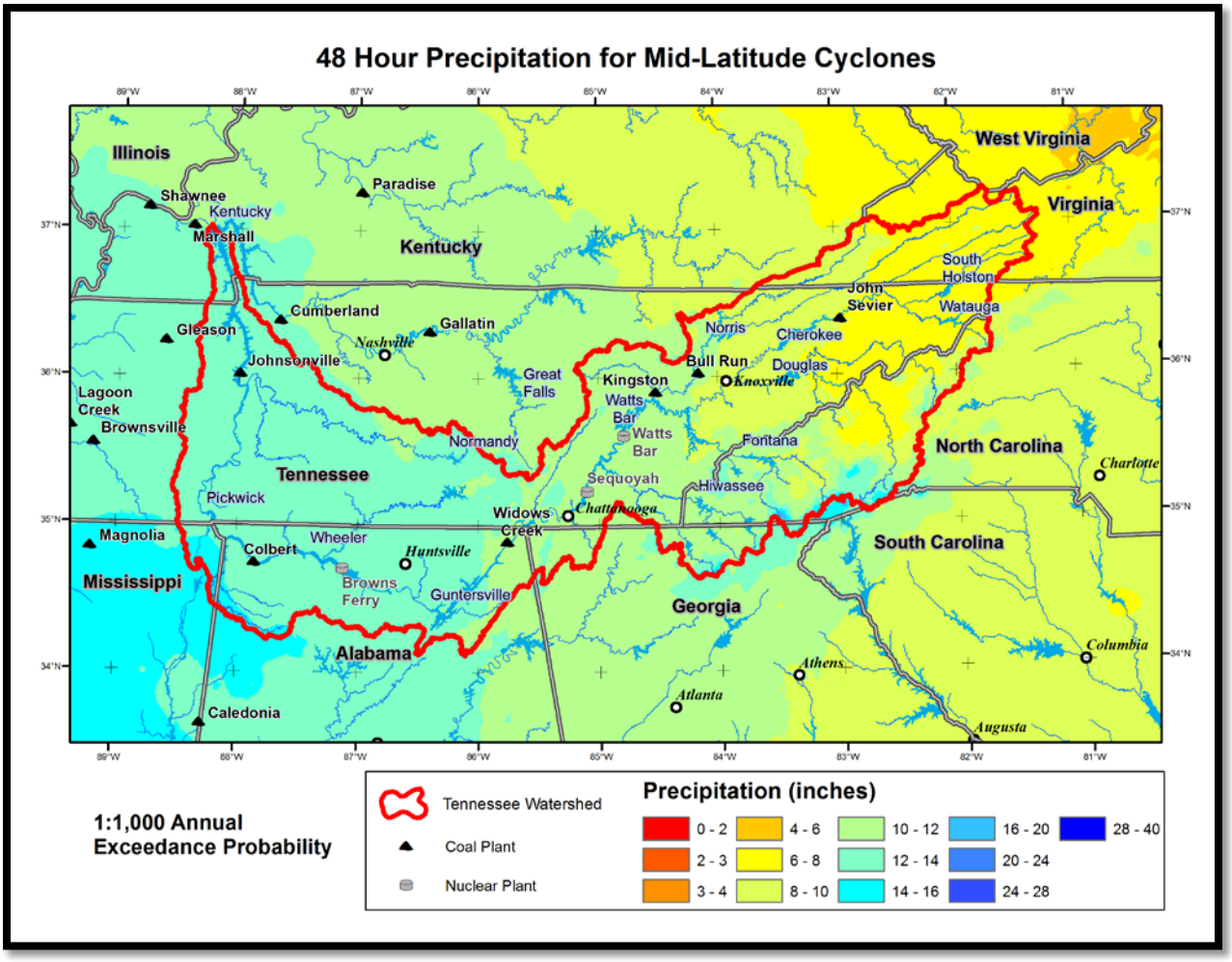


***Figure I-3 - Isopluvial Map of 48-Hour Precipitation for MLCs for AEP of 1:1,000***

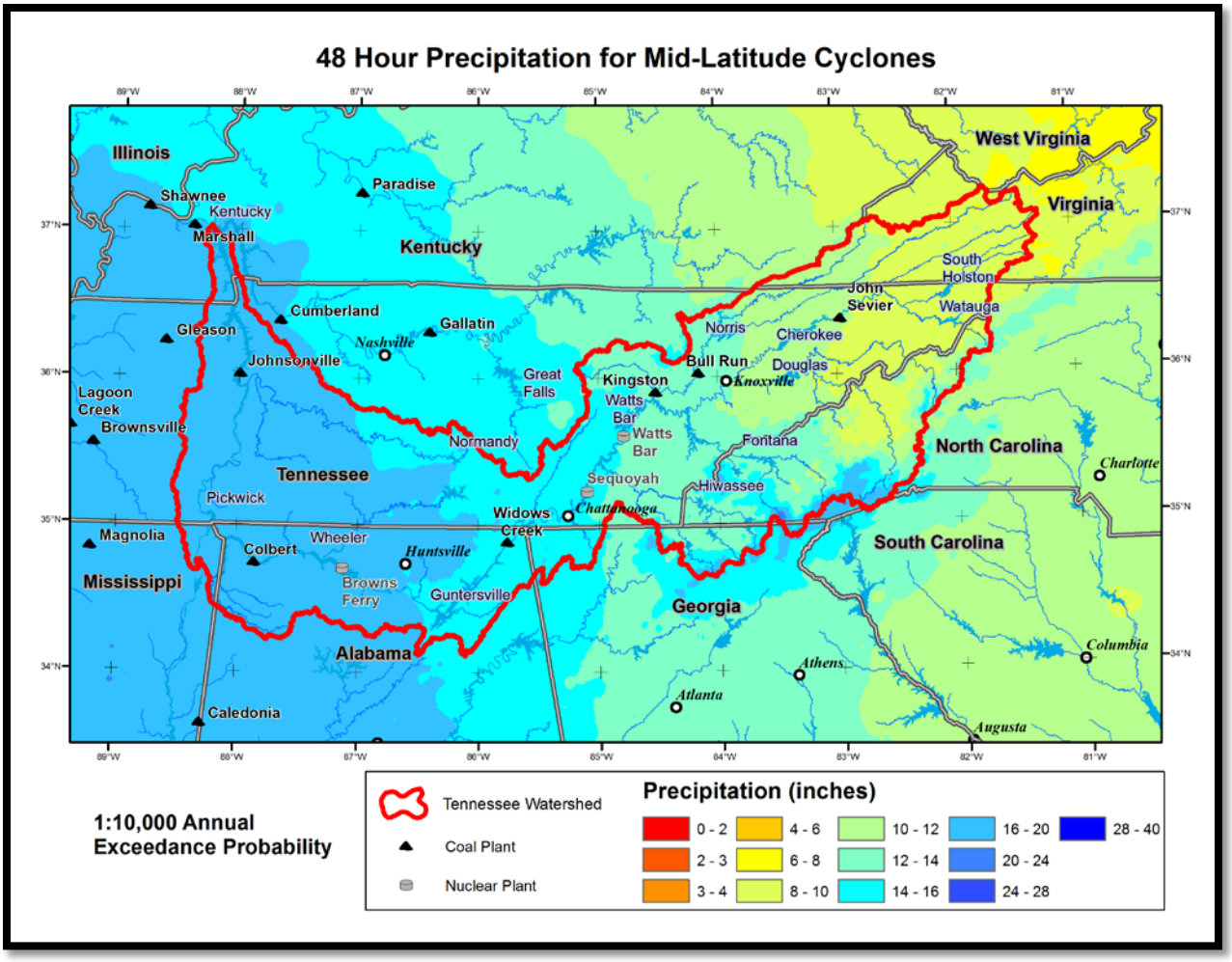


***Figure I-4 - Isopluvial Map of 48-Hour Precipitation for MLCs for AEP of 1:10,000***

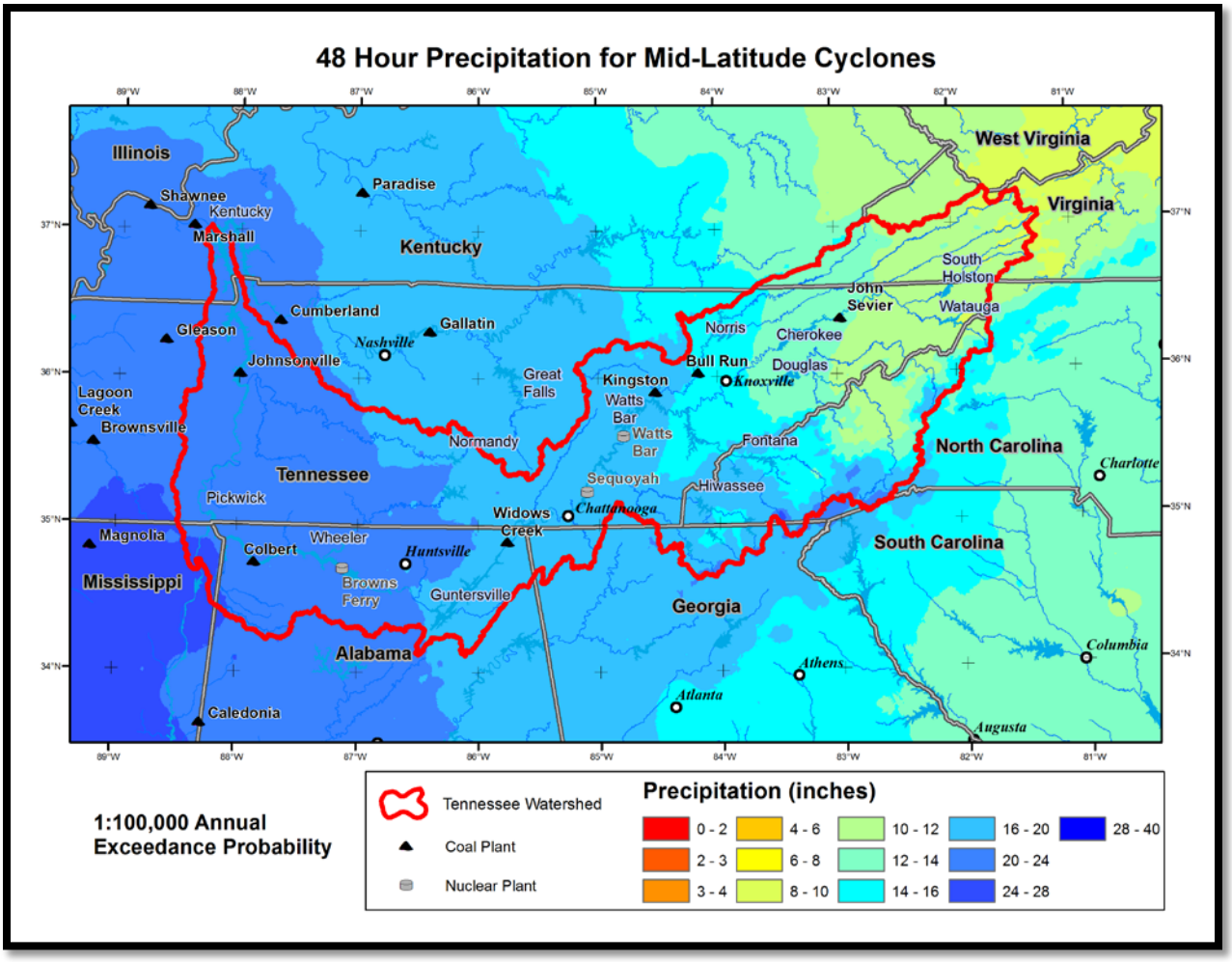


***Figure I-5 - Isopluvial Map of 48-Hour Precipitation for MLCs for AEP of 1:100,000***

# APPENDIX J
## Isopluvial Maps of 6-Hour Precipitation for Mesoscale Storms with Embedded Convection

The following isopluvial maps were generated using the gridded datasets for at-site means, regional L-Cv and regional L-Skewness for 6-hour precipitation annual maxima for MECs. The 4-parameter Kappa distribution, as fitted by the method of L-moments (Hosking and Wallis[10]), was used for computing quantile estimates. Isopluvial maps are presented for annual exceedance probabilities of $10^{-1}$, $10^{-2}$, $10^{-3}$, $10^{-4}$ and $10^{-5}$ (***Figure J-1*** to ***Figure J-5***).

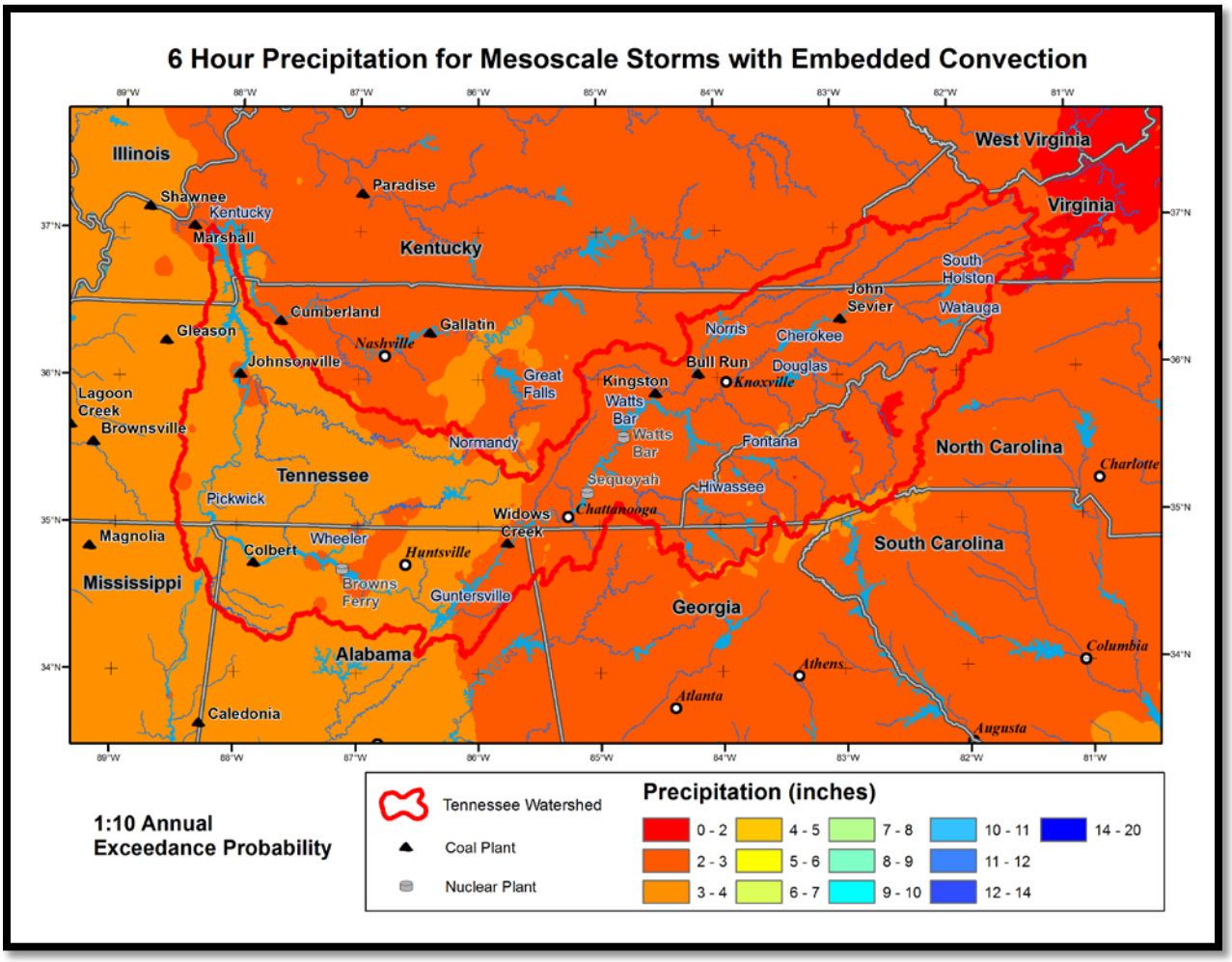


***Figure J-1 - Isopluvial Map of 6-Hour Precipitation for MECs for AEP of 1:10***

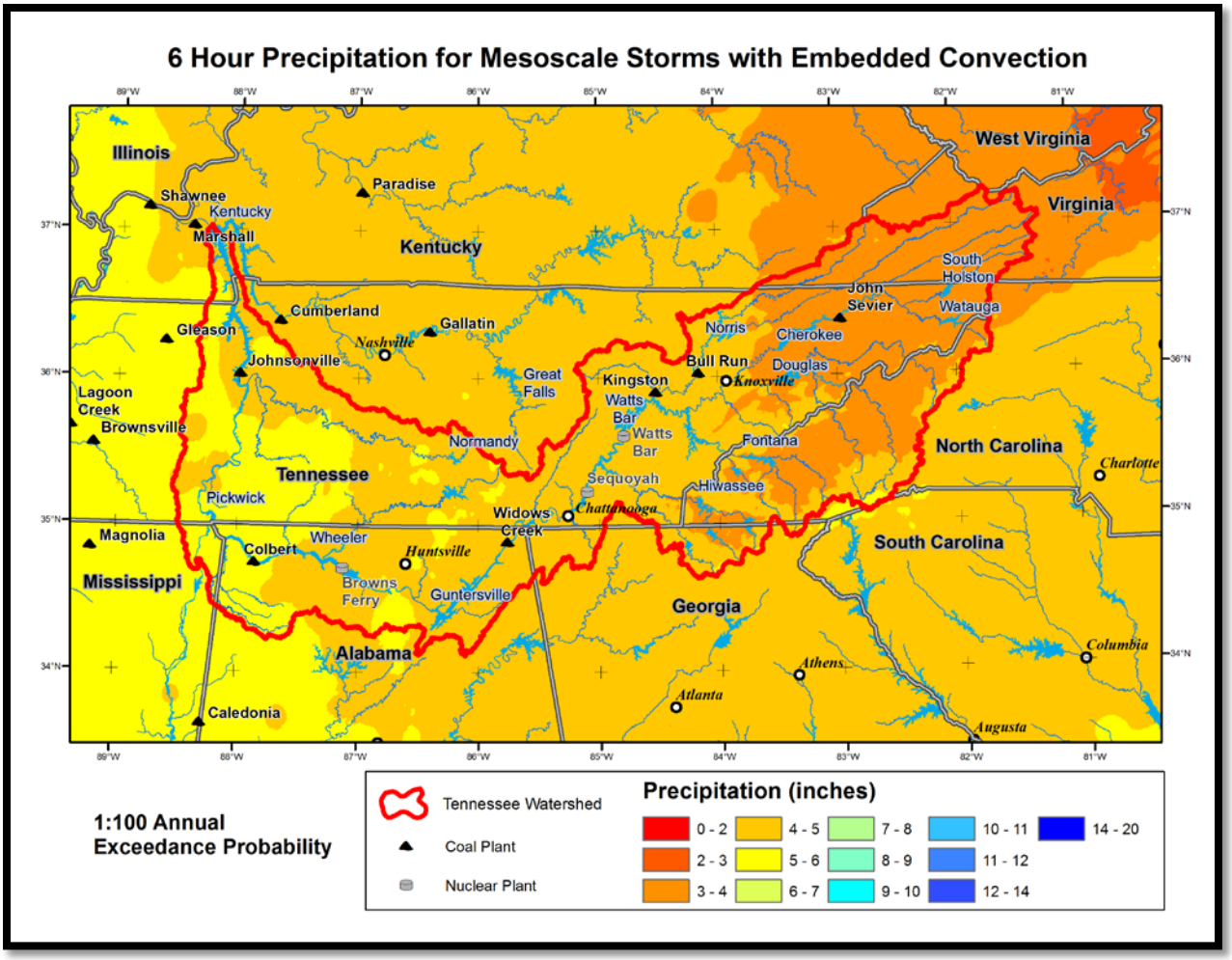


***Figure J-2 - Isopluvial Map of 6-Hour Precipitation for MECs for AEP of 1:100***

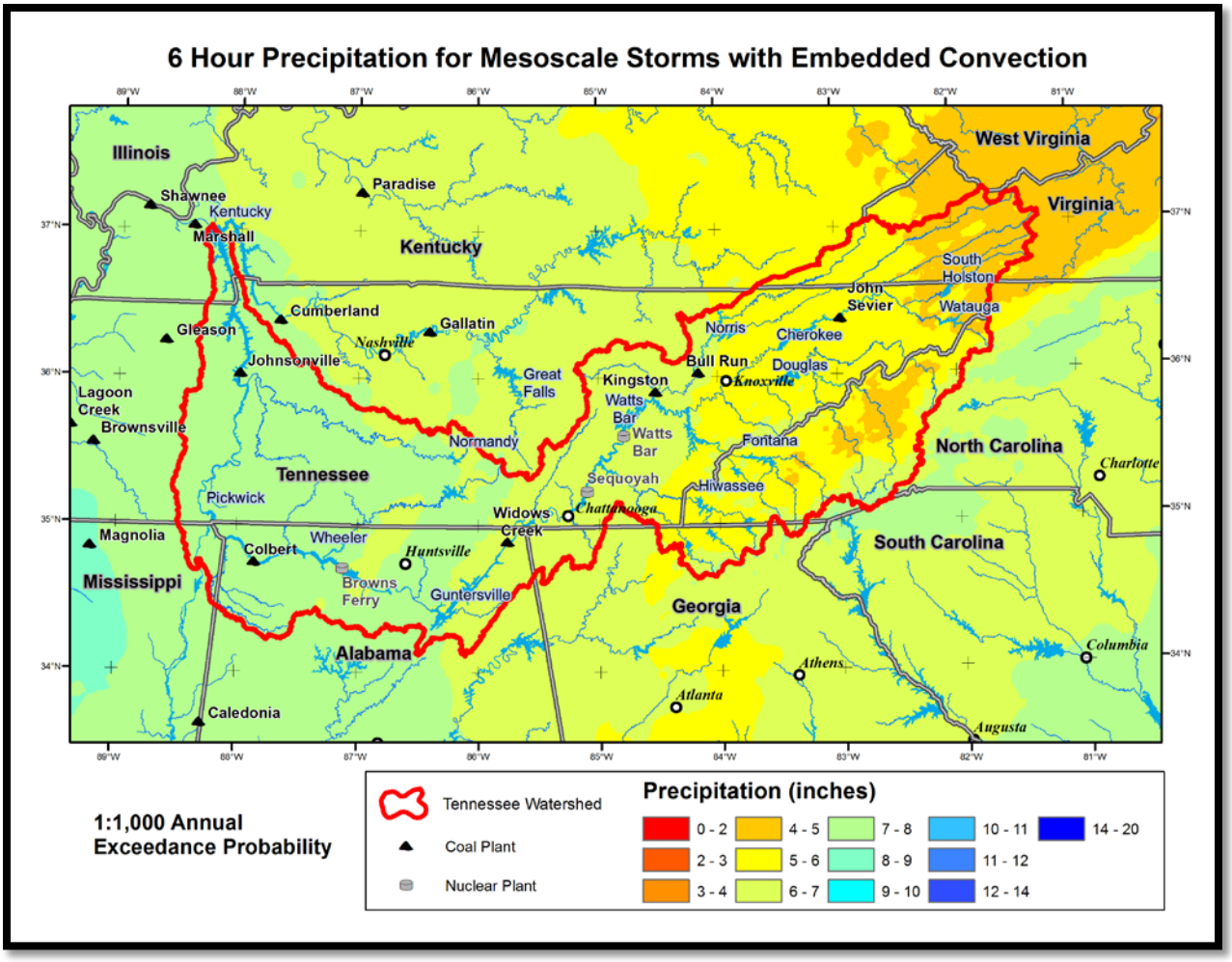


***Figure J-3 - Isopluvial Map of 6-Hour Precipitation for MECs for AEP of 1:1,000***

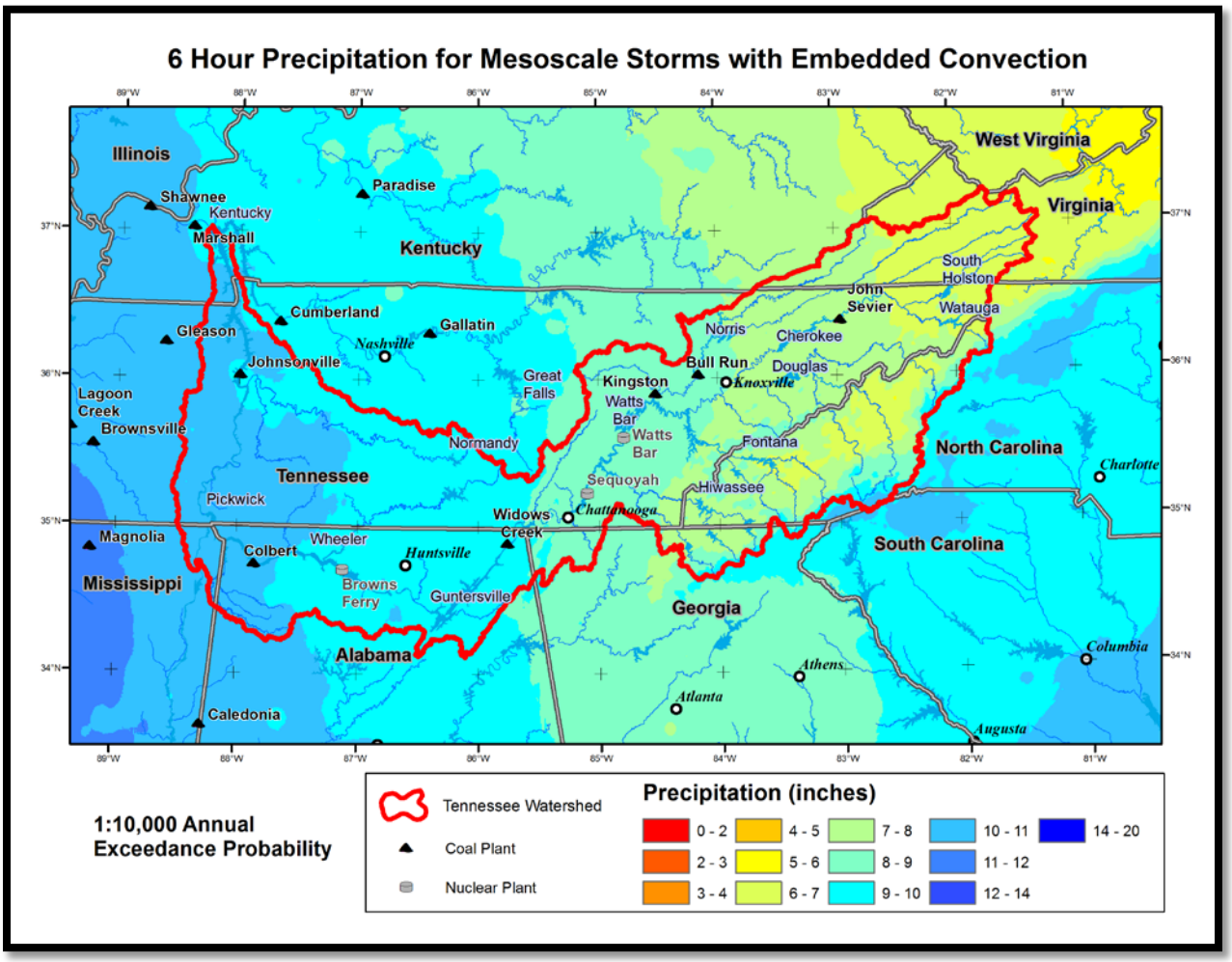


***Figure J-4 - Isopluvial Map of 6-Hour Precipitation for MECs for AEP of 1:10,000***

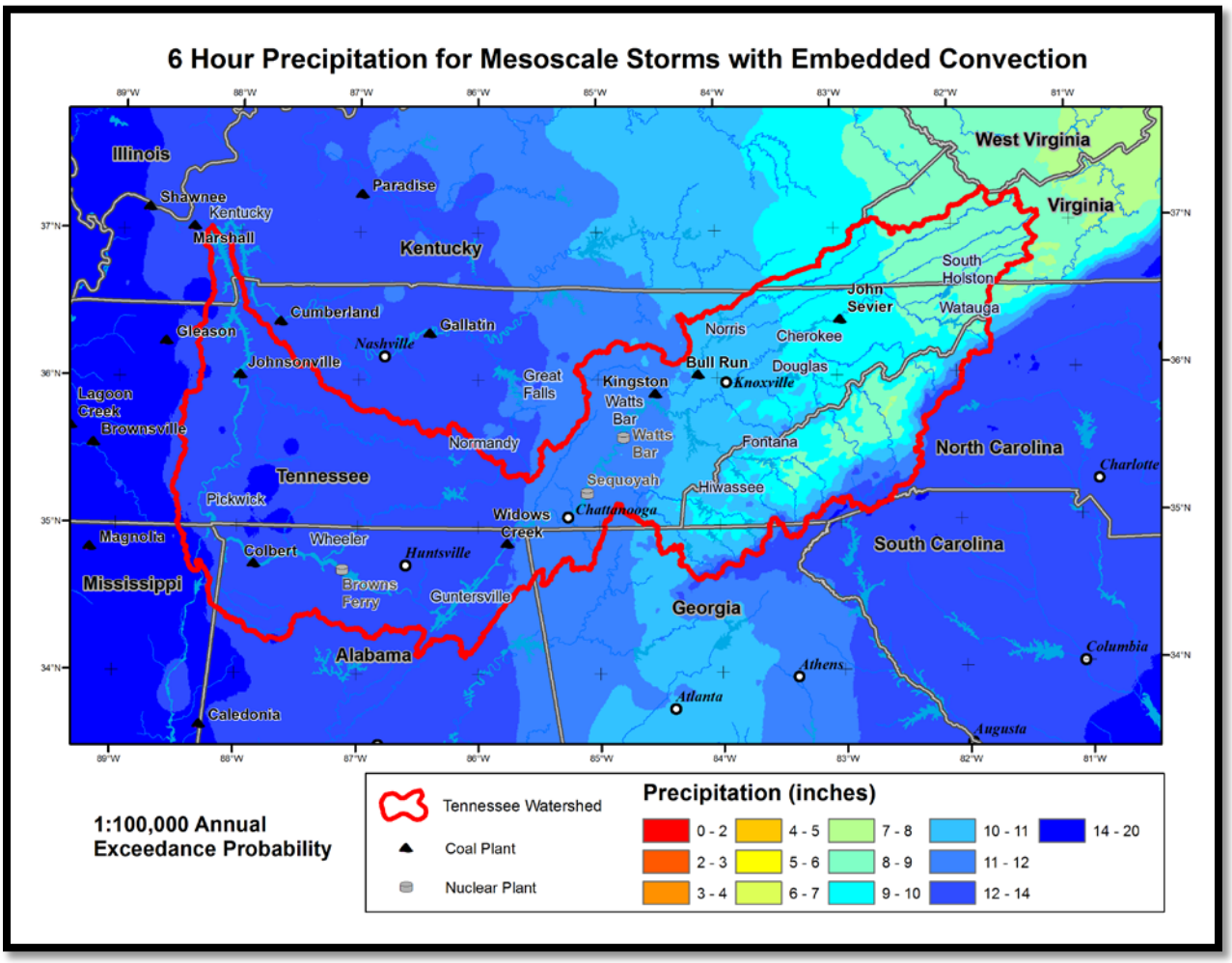


***Figure J-5 - Isopluvial Map of 6-Hour Precipitation for MECs for AEP of 1:100,000***

# APPENDIX K
## Isopluvial Maps of 1-Hour Precipitation for Convective Storms

The following isopluvial maps were generated using the gridded datasets for at-site means, regional L-Cv and regional L-Skewness for 1-hour precipitation annual maxima for LSs. The 4-parameter Kappa distribution, as fitted by the method of L-moments (Hosking and Wallis[10]), was used for computing quantile estimates. Isopluvial maps are presented for annual exceedance probabilities of $10^{-1}$, $10^{-2}$, $10^{-3}$, $10^{-4}$ and $10^{-5}$ (***Figure K-1*** to ***Figure K-5***).

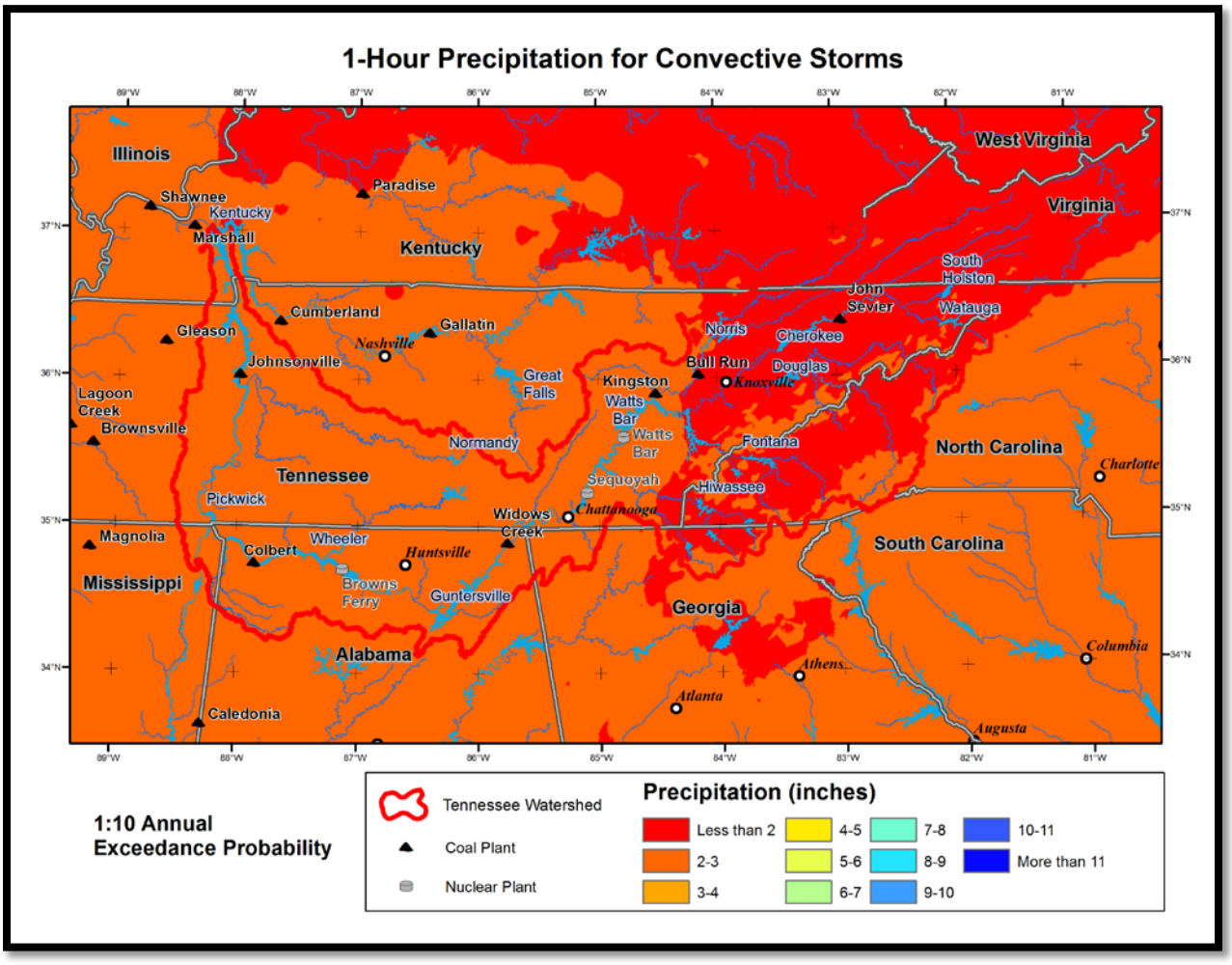


***Figure K-1 - Isopluvial Map of 1-Hour Precipitation for Convective Storms for AEP of 1:10***

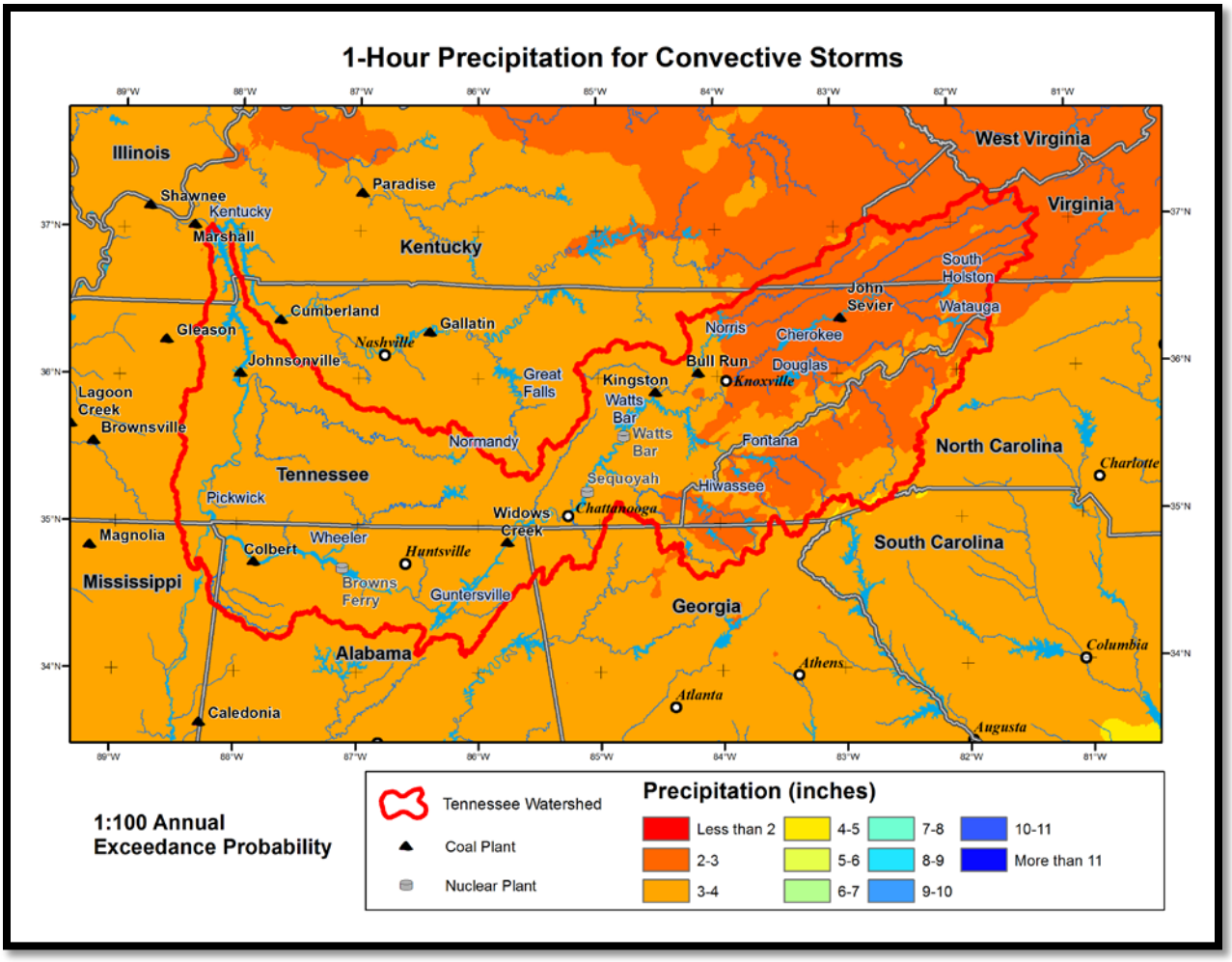


***Figure K-2 - Isopluvial Map of 1-Hour Precipitation for Convective Storms for AEP of 1:100***

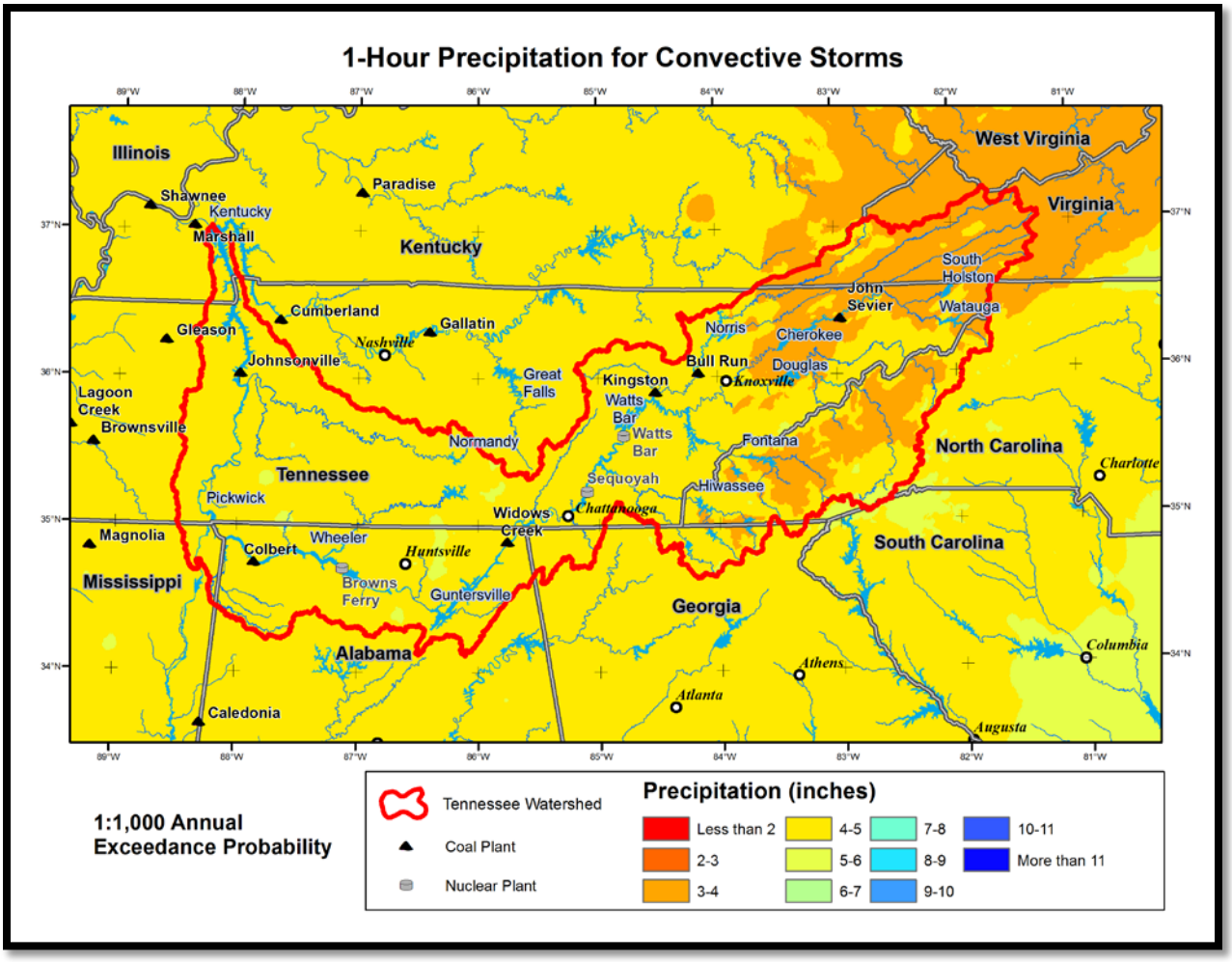


***Figure K-3 - Isopluvial Map of 1-Hour Precipitation for Convective Storms for AEP of 1:1,000***

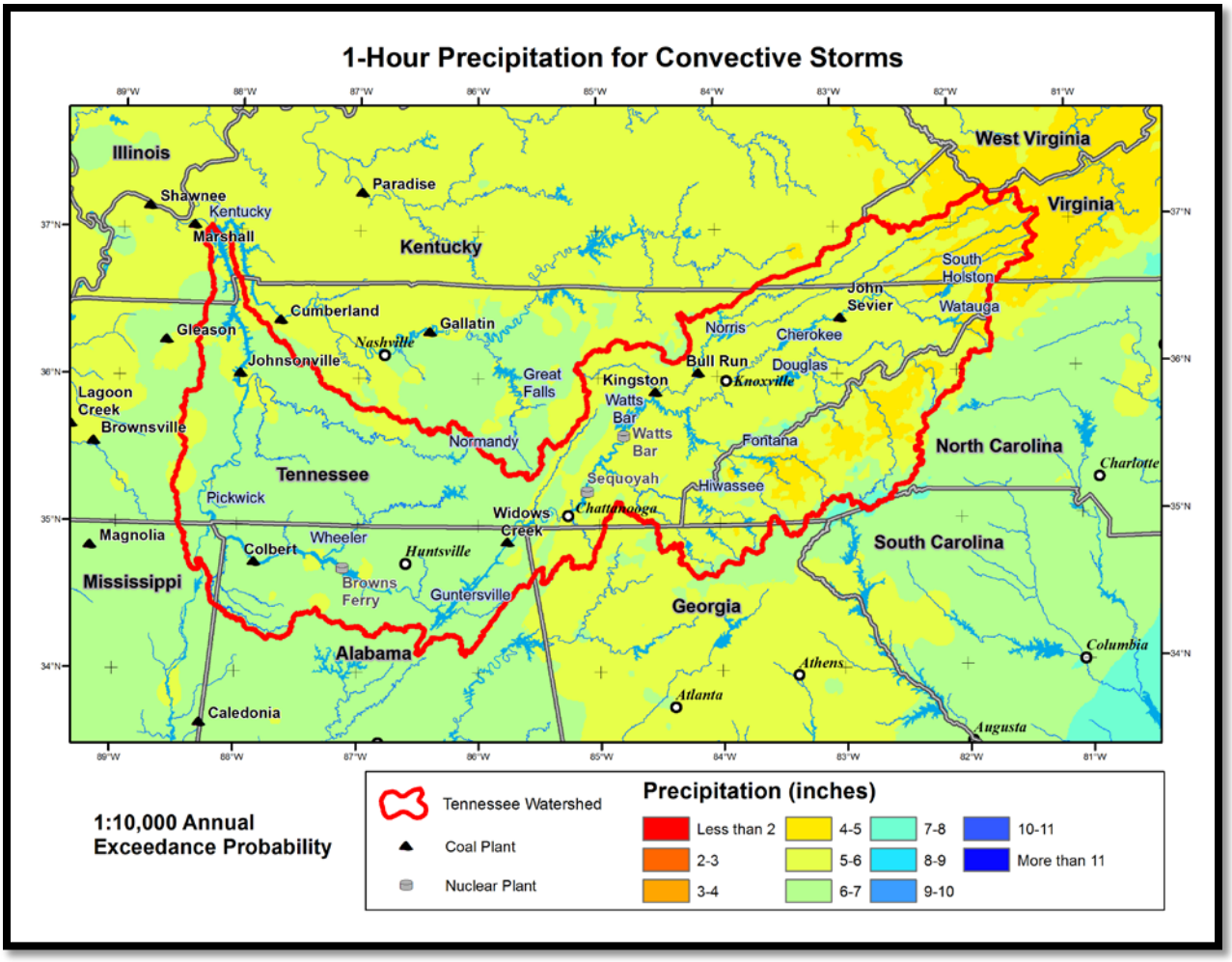


***Figure K-4 - Isopluvial Map of 1-Hour Precipitation for Convective Storms for AEP of 1:10,000***

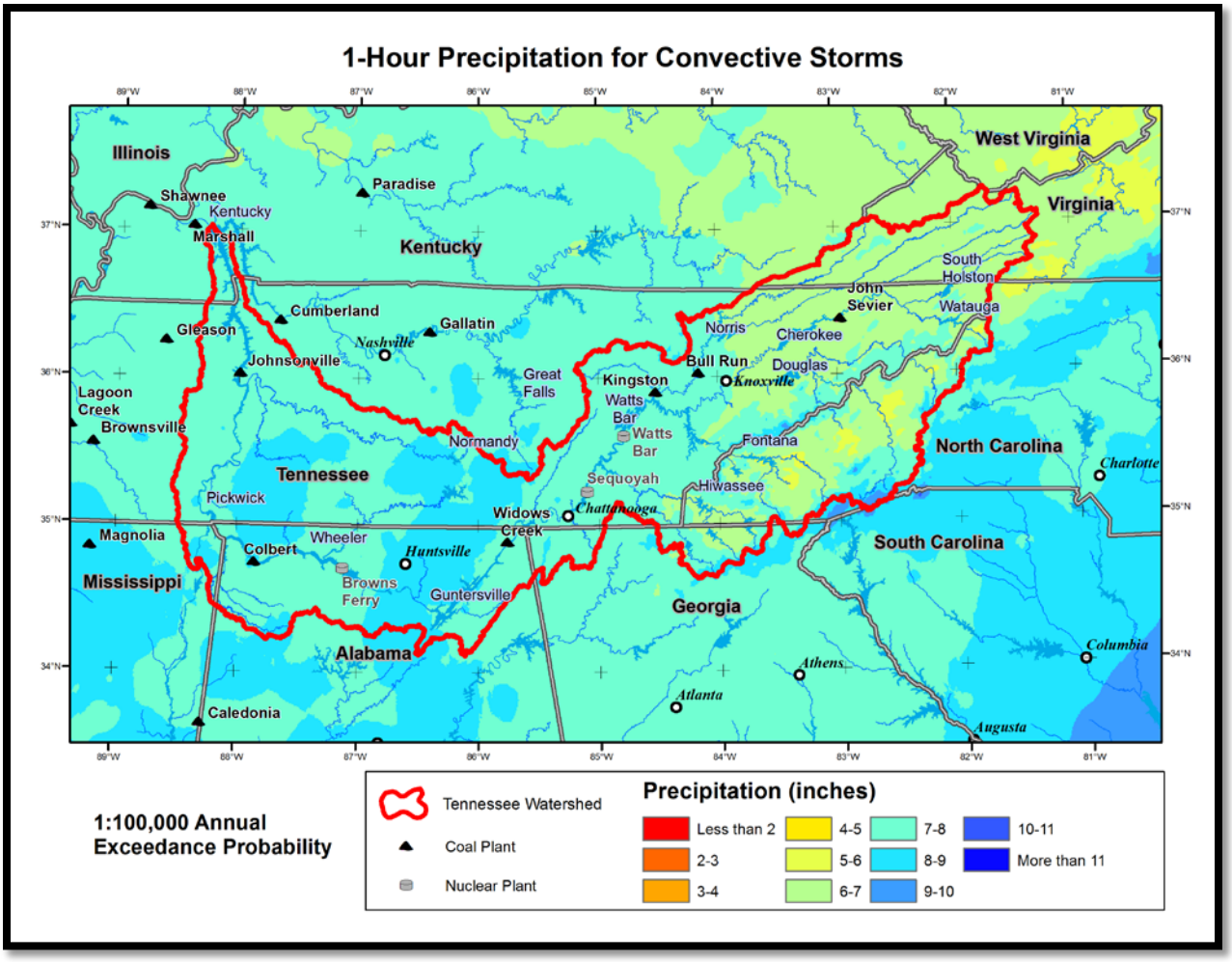


*Figure K-5 - Isopluvial Map of 1-Hour Precipitation for Convective Storms for AEP of 1:100,000*

# APPENDIX L
## Isopluvial Maps of 48-Hour Precipitation for TSRs

The following isopluvial maps were generated using the gridded datasets for at-site means, regional L-Cv and regional L-Skewness for 48-hour precipitation annual maxima for TSRs. The 4-parameter Kappa distribution, as fitted by the method of L-moments (Hosking and Wallis[10]), was used for computing quantile estimates. Isopluvial maps are presented for annual exceedance probabilities of $10^{-1}$, $10^{-2}$, $10^{-3}$, $10^{-4}$ and $10^{-5}$ (***Figure L-1*** to ***Figure L-5***)

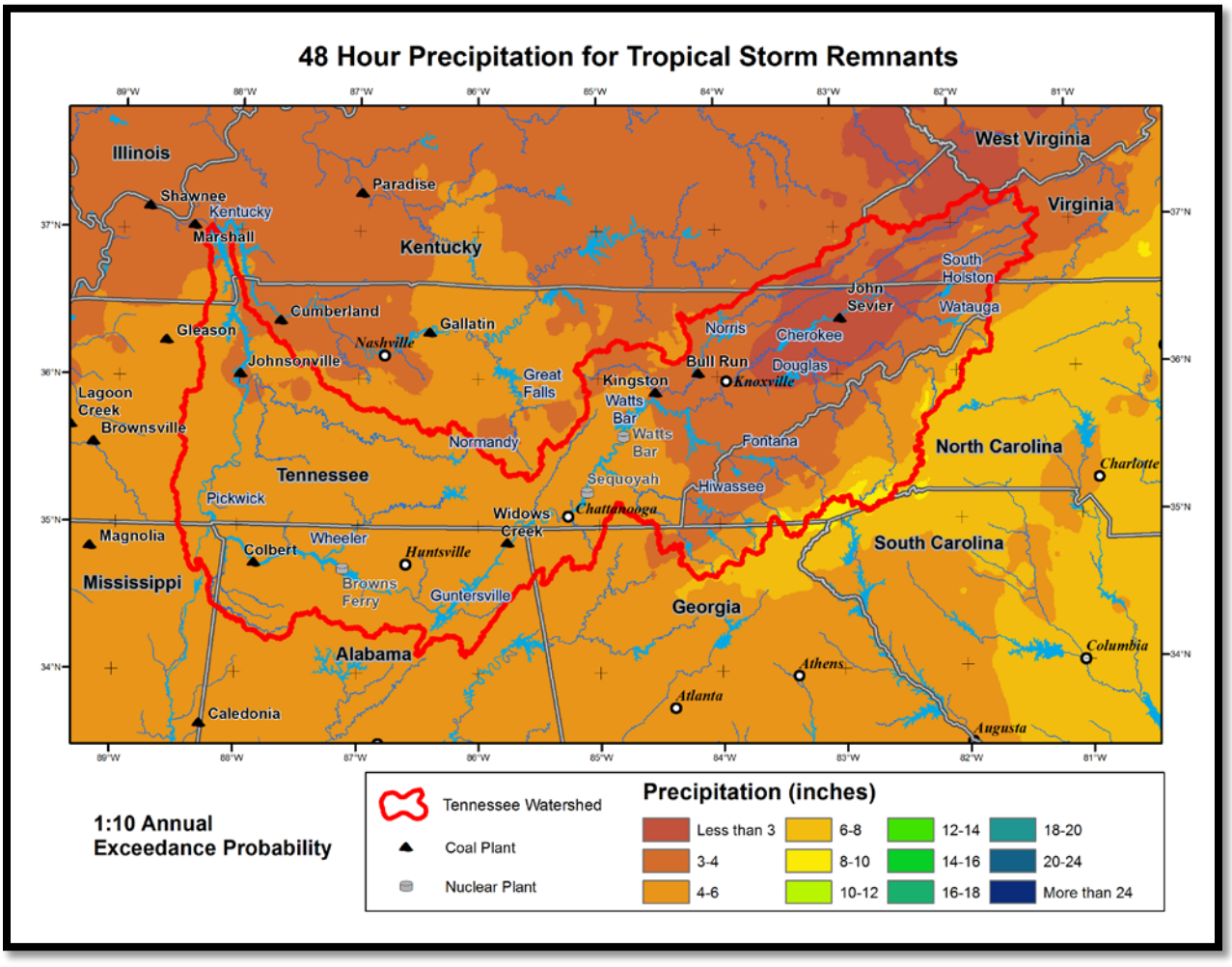


***Figure L-1 - Isopluvial Map of 48-Hour Precipitation for TSRs for AEP of 1:10***

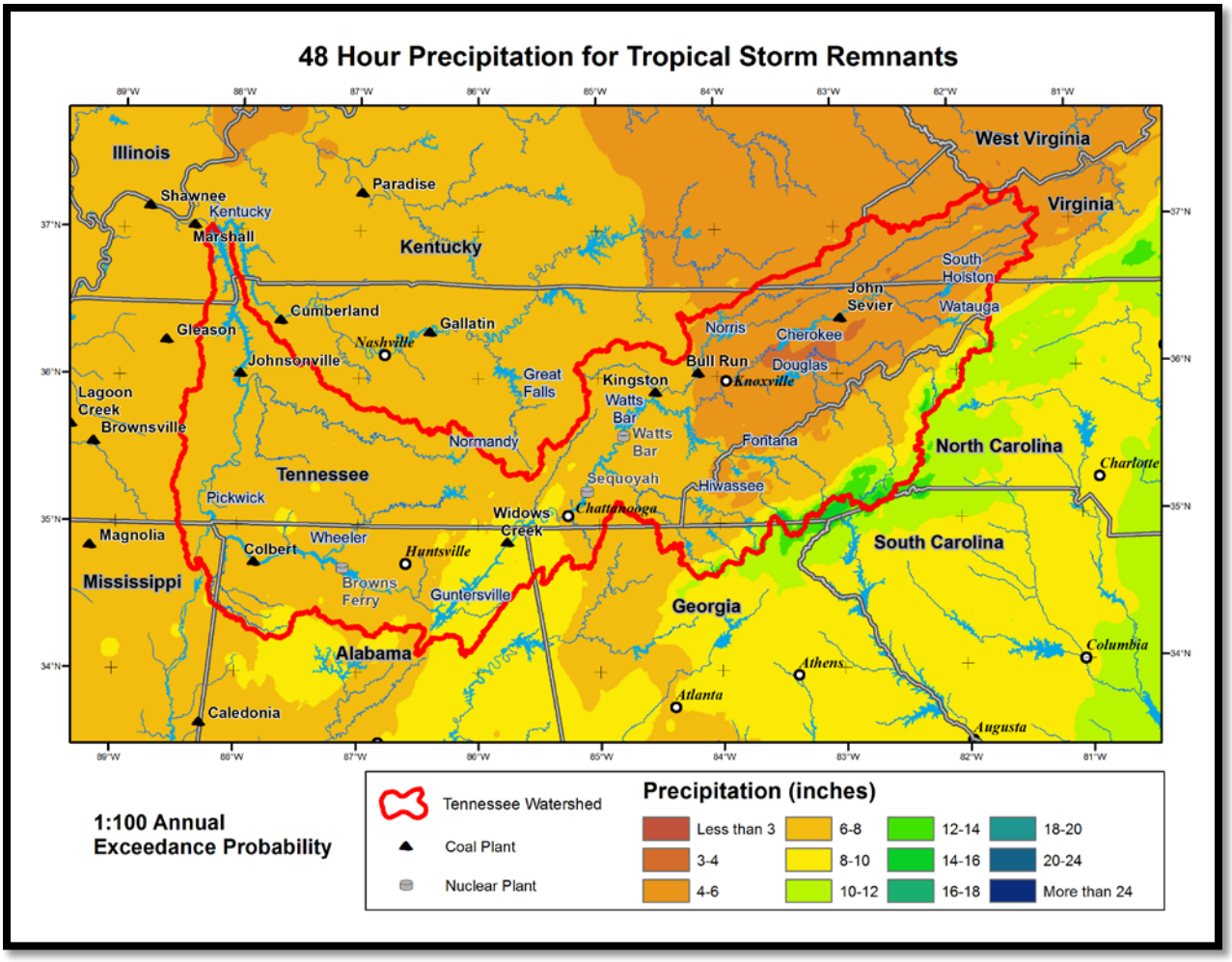


***Figure L-2 - Isopluvial Map of 48-Hour Precipitation for TSRs for AEP of 1:100***

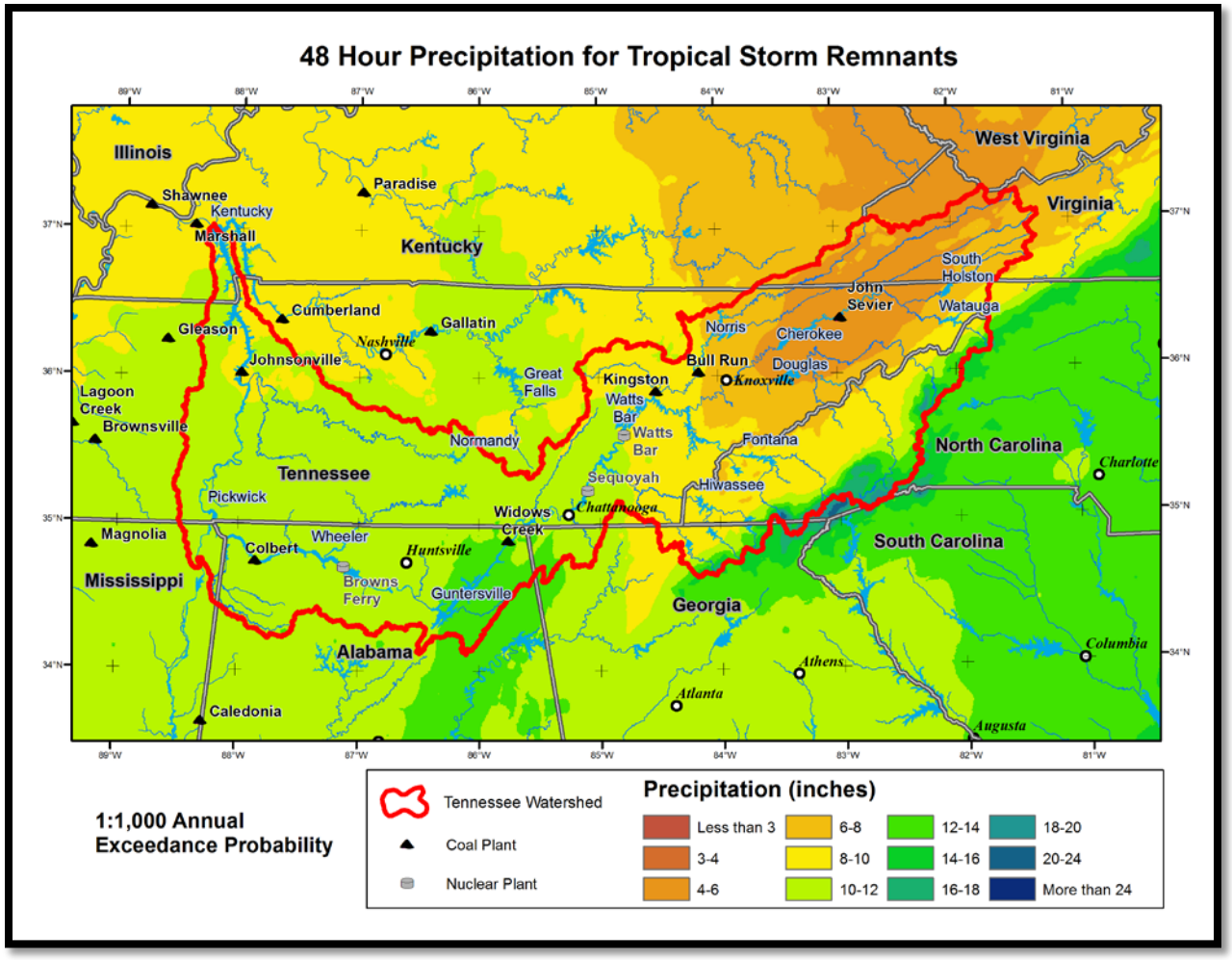


***Figure L-3 - Isopluvial Map of 48-Hour Precipitation for TSRs for AEP of 1:1,000***

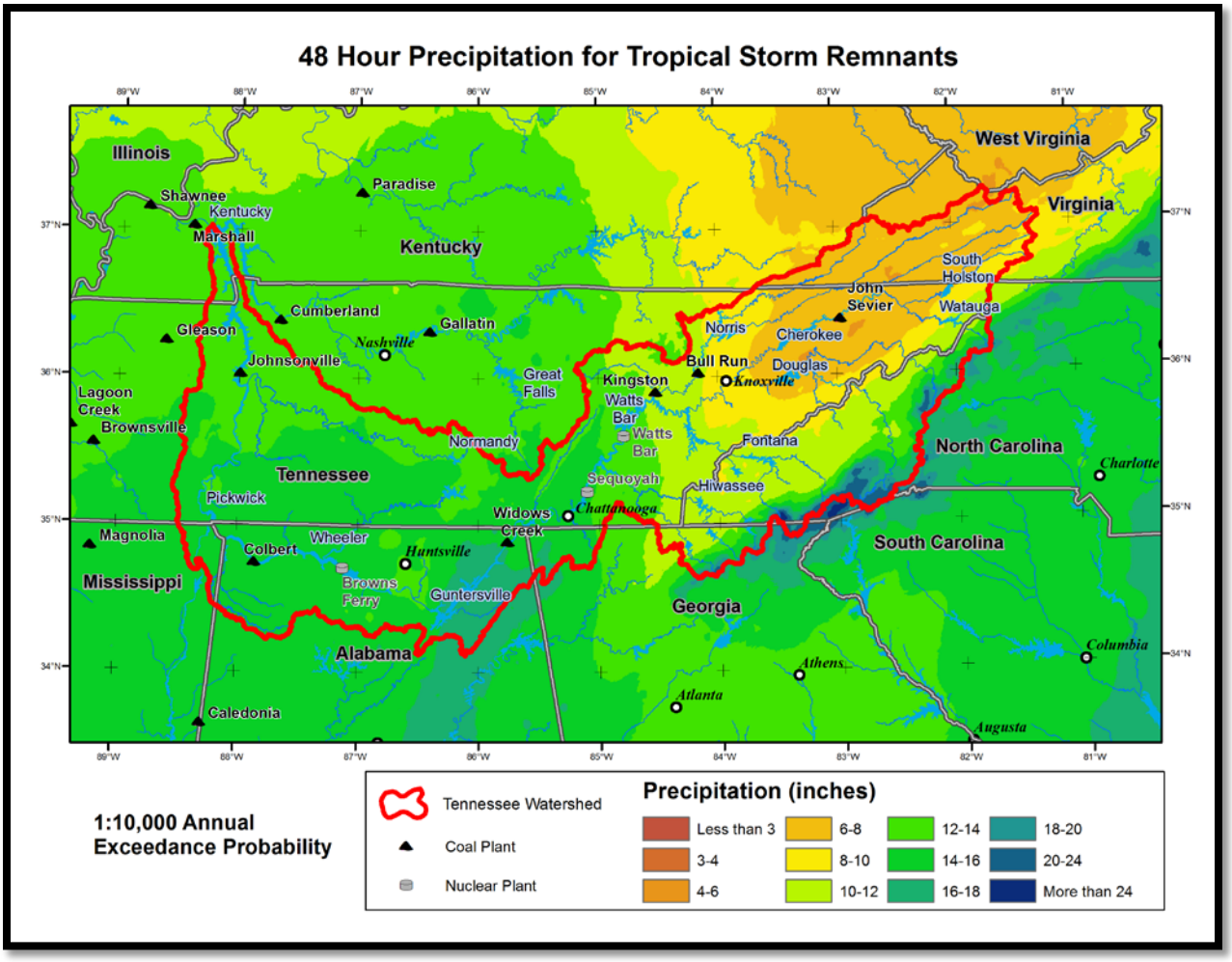


***Figure L-4 - Isopluvial Map of 48-Hour Precipitation for TSRs for AEP of 1:10,000***

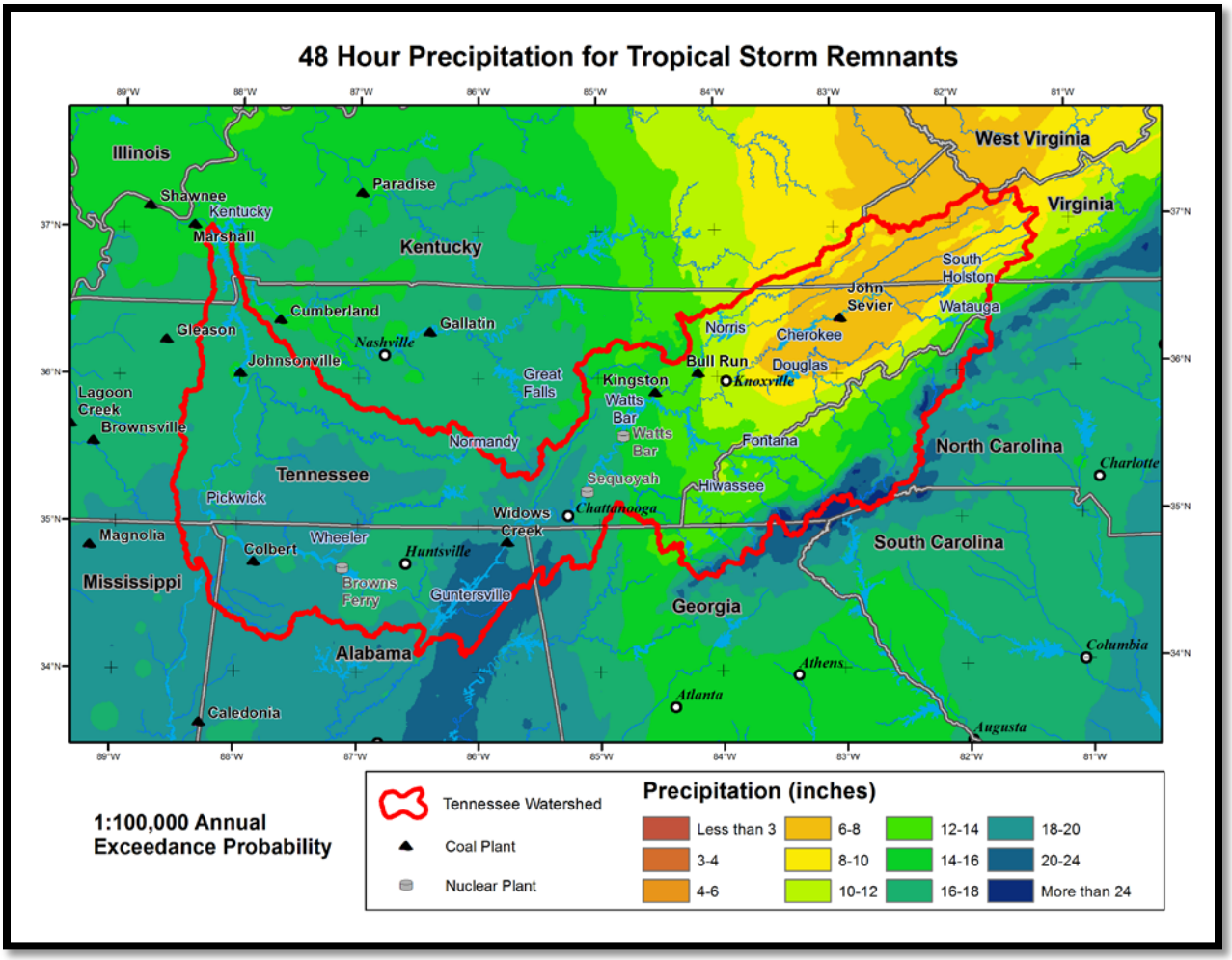


***Figure L-5 - Isopluvial Map of 48-Hour Precipitation for TSRs for AEP of 1:100,000***